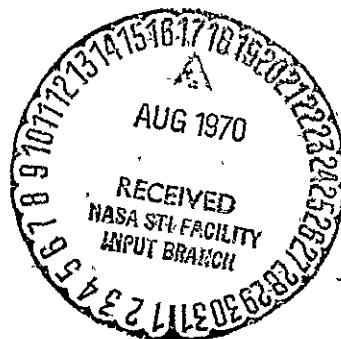


X-460-70-3
PREPRINT

NASA TMX- 63980

SMS PHASE B REPORT



FEBRUARY 1970

Reproduced by
NATIONAL TECHNICAL
INFORMATION SERVICE
Springfield, Va. 22151



GODDARD SPACE FLIGHT CENTER
GREENBELT, MARYLAND

FACILITY FORM 602	N70-34388	
	(ACCESSION NUMBER)	(THRU)
	256	1
	(PAGES)	(CODE)
	TMX-63980	31
	(NASA CR OR TMX OR AD NUMBER)	(CATEGORY)

SYNCHRONOUS METEOROLOGICAL SATELLITE

PHASE B STUDY REPORT*

Compiled by
D. V. Fordyce
M. B. Weinreb

January 1970

ATS Project Office
Goddard Space Flight Center
Greenbelt, Maryland

*This is an early release of a document which will be published under NASA
Goddard Space Flight Center number X-460-70-30.

PRECEDING PAGE BLANK NOT FILMED.

FOREWORD

This Phase B Analytical Report, which evolved into a proposed combined Phase-C and -D Project Plan, required the group efforts of many GSFC and ESSA personnel. This report is a result of the interchange of ideas, discussion, and critiques among a number of individual authors and groups. Consequently, assigning specific credit is very difficult.

Some information pertaining to the Visible Infrared Spin Scan Radiometer included in this report has been derived from material published by the Santa Barbara Research Center.

The complete document was reviewed and coordinated by the SMS Study Group members comprising:

- G. Albert - ESSA Representative
- H. Butler - Chief of the Operations Satellite Office
- J. Castellano - Test & Evaluation
- R. T. Fitzgerald - T&DS Scientist
- J. B. Flaherty - Systems Division
- D. V. Fordyce - SMS Study Manager
- M. Garbacz - NASA Headquarters
- T. A. Page - R&QA
- B. Perkins - Communications Systems
- R. M. Rados - Sensor
- W. E. Shenk - Project Scientist
- M. B. Weinreb - Assistant Study Manager

PRECEDING PAGE BLANK NOT FILMED.

TABLE OF CONTENTS

<u>Section</u>		<u>Page</u>
I	BACKGROUND	I-1
II	REQUIREMENTS AND CONSTRAINTS	II-1
	1. <u>REQUIREMENTS</u>	II-1
	1.1 EARTH IMAGING	II-1
	1.2 RETRANSMISSION OF IMAGED DATA	II-1
	1.3 DATA COLLECTION	II-1
	1.4 DATA RELAY	II-2
	1.5 SPACE ENVIRONMENT MONITOR	II-2
	2. <u>CONSTRAINTS</u>	II-2
III	SUMMARY	III-1
	1. <u>INTRODUCTION</u>	III-1
	2. <u>EARTH IMAGING</u>	III-1
	3. <u>RETRANSMISSION OF IMAGE DATA</u>	III-2
	4. <u>DATA COLLECTION</u>	III-3
	5. <u>WEFAX</u>	III-5
	6. <u>ENVIRONMENTAL MONITORING SYSTEM</u>	III-5
IV	WALLOPS ISLAND CDA STATION	IV-1
	1. <u>INTRODUCTION</u>	IV-1
	2. <u>ATS GROUND EQUIPMENT</u>	IV-1

<u>Section</u>	<u>Page</u>
2.1 SSCC PICTURE PROCESSING EQUIPMENT. . .	IV-1
2.2 COMMAND AND TELEMETRY SYSTEM	IV-5
3. <u>CDA STATION FUNCTIONS FOR SMS</u>	IV-14
4. <u>MODIFICATIONS TO CDA NECESSARY FOR SMS LAUNCH</u>	IV-15
4.1 TELEMETRY AND COMMAND (T&C)	IV-15
4.2 RADIOMETER DATA RECEPTION AND PROCESSING	IV-15
4.3 REMOTE DATA COLLECTION	IV-16
4.4 RANGING	IV-17
4.5 INTERFACE WITH SUITLAND NESC.	IV-17
4.6 SUMMARY	IV-18
V IMPLEMENTATION TO ATTAIN PROGRAM OBJECTIVES	V-1
1. <u>INTRODUCTION</u>	V-1
2. <u>TELESCOPE/RADIOMETER IMAGING SYSTEM.</u>	V-3
2.1 DESCRIPTION.	V-3
2.2 PERFORMANCE ANALYSIS.	V-21
2.3 SPACECRAFT GROUND TRANSMISSION SYSTEM	V-40
2.4 SPIN SCAN CLOUD CAMERA	V-64
3. <u>RECORDING AND RETRANSMISSION OF IMAGED DATA</u>	V-71

<u>Section</u>	<u>Page</u>
3.1 SUMMARY OF RADIOMETER PARAMETERS. . . .	V-71
3.2 DATA PROCESSING	V-72
3.3 LIMITED RESOLUTION DATA PROCESSING	V-83
3.4 STRETCHED DATA LINK CALCULATION	V-84
4. <u>DATA COLLECTION SYSTEM</u>	V-91
4.1 INTRODUCTION TO DATA COLLECTION SYSTEMS.	V-91
4.2 DATA COLLECTION SYSTEMS DESCRIPTIONS. . .	V-102
4.3 SUMMARY OF DATA COLLECTION SYSTEM TECHNIQUES.	V-167
4.4 FINAL SELECTION OF DATA COLLECTION SYSTEM; PLAN FOR PHASE C STUDY	V-169
5. <u>WEFAX</u>	V-171
5.1 GENERAL	V-171
5.2 MODULATION TECHNIQUE	V-171
5.3 S-BAND UP-LINK.	V-172
5.4 S-BAND DOWN-LINK	V-172
5.5 CONVERSION OF APT STATIONS.	V-172
6. <u>SPACE ENVIRONMENT MONITORING SUBSYSTEM.</u>	V-177
6.1 SOLAR ENERGETIC PARTICLE MONITOR.	V-177
6.2 SOLAR X-RAY MONITOR	V-179
6.3 SYNCHRONOUS SATELLITE MAGNETOMETER . .	V-181
6.4 SEMS DATA TRANSMISSION	V-183

<u>Section</u>	<u>Page</u>
7. <u>SPACECRAFT DESCRIPTION.</u>	V-185
7.1 GENERAL	V-185
7.2 STRUCTURE SUBSYSTEM	V-185
7.3 THERMAL CONTROL	V-188
7.4 ELECTRICAL POWER SUBSYSTEM.	V-188
7.5 SPACECRAFT COMMUNICATION SUBSYSTEM. . .	V-189
7.6 TELEMETRY AND COMMAND SUBSYSTEM	V-194
7.7 STABILIZATION AND CONTROL	V-202
7.8 APOGEE MOTOR	V-208
7.9 SPACECRAFT INTEGRATION AND TEST	V-208
8. <u>LAUNCH REQUIREMENTS</u>	V-209
8.1 LAUNCH VEHICLE	V-209
8.2 LAUNCH OPERATIONS	V-211
8.3 GO/NO-GO VAN.	V-213
8.4 LAUNCH PARAMETERS	V-213
8.5 LAUNCH AND TRAJECTORY.	V-213
APPENDIX A—LINK CALCULATIONS FOR VARIOUS SOMS/ GOES DATA COLLECTION CONFIGURATIONS .	A-1
APPENDIX B—CONTRIBUTION OF THE EARTH TO DCP ANTENNA NOISE	B-1
APPENDIX C—SMS FIELD INTENSITY CALCULATIONS . . .	C-1

ILLUSTRATIONS

<u>Figure</u>		<u>Page</u>
IV-1	Wallops Island ATS-I Ground Equipment	IV-2
IV-2	Earth Picture Processing System Block Diagram	IV-3
V-1	SMS Communications System Concept	V-2
V-2	VISSR Thermal Channel and Visible Channels IGFOV Arrangement	V-4
V-3	VISSR Scanner Layout Drawing	V-5
V-4	VISSR Scanner Aft Optics Detail	V-6
V-5	VISSR IGFOV and Visible Channel Sun Optics Angular Relationship	V-12
V-6	VISSR Timing Event Diagram	V-15
V-7	Radiometer Output Voltage Waveforms	V-17
V-8	VISSR Electronics Block Diagram	V-18
V-9	Sensor Redundancy	V-22
V-10	Effective Radiance N and dN/dT as a Function of Target Temperature in the 10.5- to 12.6 Micron Band	V-26
V-11	VISSR Thermal Channel S/N and $NE\Delta T$ as a Function of Target Temperature, T (For an Extended Target)	V-27
V-12	Spectral Distribution of Sun's Energy Outside the Earth's Atmosphere (From the Handbook of Geophysics)	V-28
V-13	Effective Absolute Spectral Sensitivity (PMT + Filter)	V-30
V-14	VISSR Visible Channel S/N as a Function of Albedo	V-31
V-15	Relative Frequency Response of VISSR Optics, Field Stop and Electronics	V-34

<u>Figure</u>		<u>Page</u>
V-16	VISSR V_p/V_{SS} as a Function of Target Size	V-35
V-17	VISSR Thermal Channel $NE\Delta T$ as a Function of Down-Link SNR at $T = 330^\circ K$ and $200^\circ K$	V-44
V-18	SSSC/FDM Frequency Spectrum	V-52
V-19	Radiometer Data Acquisition System	V-74
V-20	Stretched Video Timing	V-77
V-21	Retransmission of Stretched Data	V-83
V-22	Illustration of DSBSC Interrogation Spectrum for GOES/DCP.	V-106
V-23	DCP Block Diagram Developed During SOMS/GOES Study	V-107
V-24	PN Code Multiplexing Format	V-111
V-25	Cross Correlation SNR Versus DCP Stability	V-113
V-26	Cross Correlation SNR Versus DCP Bit Capacity	V-114
V-27	Example of SMS PN Data Collection System Time/Frequency Structure	V-115
V-28	Digital Cross-Correlation of Two Maximal Length Binary Sequences	V-119
V-29	Power Spectrum of the $S_3(t)$ Waveform.	V-122
V-30	PN-DCP Link SNR Versus DCP Transmit Power	V-130
V-31	Typical Implementation of PN-Transmitter and Correlation Receiver	V-131
V-32	Auto Correlation of PN Code	V-132

<u>Figure</u>		<u>Page</u>
V-33	Binary Error Probability vs. Carrier to Noise Ratio in a Matched Filter Bandwidth	V-137
V-34	Possible Techniques for Data Modulation of PN Signal . . .	V-138
V-35	DCP Bandwidth Allocation.	V-142
V-36	SMS PN Ranging Concept	V-145
V-37	Ranging Timing Diagram	V-146
V-38	Conceptual Block Diagram of CDA Station PN Ranging Requirements	V-147
V-39	PN Turn Around Ranging Station Block Diagram.	V-148
V-40	Development of Range Equation	V-150
V-41	PN-DCP Transmitter Block Diagram.	V-155
V-42	Minimum Probability of Failure Versus Systems Bandwidth.	V-164
V-43	Optimum Value of T Versus System Bandwidth	V-165
V-44	Random Access Data Collection System.	V-166
V-45	Block Diagram of APT S-Band Conversion	V-175
V-46	Conceptual Drawing of SMS Spacecraft	V-186
V-47	Electric Power System Block Diagram	V-190
V-48	Block Diagram of Spacecraft Communications Subsystem With Single SHF Transponder For DCS	V-191
V-49	Block Diagram of All S-Band Communication Transponder with Linear DCS Transmitter	V-192

TABLES

<u>Table</u>		<u>Page</u>
IV-1	SHF Link Calculation (4 GHz) Wideband Data Mode ATS-I . . .	IV-6
IV-2	Command Subsystem Link Calculation.	IV-7
IV-3	OGO/ATS Command Console Address and Execute Tone Assignments	IV-11
IV-4	Telemetry Subsystem Link Calculation	IV-13
IV-5	Retransmission Band Width Requirements for Data Link . . .	IV-18
IV-6	Summary of Station Modifications to Meet SMS Requirements	IV-19
V-1	Summary of VISSR Design and Performance Characteristics. .	V-7
V-2	Summary of VISSR Physical Characteristics	V-8
V-3	Comparison of SSSC/FDM/FM and TDM/PCM/QPSK	V-61
V-4	Narrow-Band Radiometer Bandwidth Requirements	V-63
V-5	Data Relay Present vs SMS Requirements	V-69
V-6	Radiometer Data Stretching Equipment Present Vs SMS Requirements	V-85
V-7	Stretched Data Link Calculations	V-86
V-8	Stretched Data Link Performance.	V-89
V-9	Major Constraints of Data Collection System.	V-92
V-10	Estimate of Traffic Reporting to CDA in 6 Hr. Synoptic Interval at Time of Launch.	V-93
V-11	Receiver Noise Characteristics	V-95
V-12	Noise Temperature Contribution Due Antenna and Feed	V-97

<u>Table</u>	<u>Page</u>
V-13	Down-Link Performance and System Margin V-98
V-14	B_a (Hz) and B_i/B_a (db) for $B_i = 100$ Hz V-100
V-15	Advantages and Disadvantages for the SMS Pseudo Noise Data Collection System V-110
V-16	Characteristics of Various Maximal Length PN Codes V-119
V-17	DCP 2.1 GHz Up-Link Power Budget V-127
V-18	DCP 1.7 GHz Down-Link Power Budget (to 40 foot CDA Station) V-129
V-19	PN Acquisition Parameters V-136
V-20	DCP Interrogated Down-Link Power Budget V-141
V-21	Up-Link to SMS From TRS for PN Turn Around Ranging 2.1 GHz V-152
V-22	Down-Link to 15' Turn Around Ranging Station 1.7 GHz V-152
V-23	Overall PN Ranging Link Summary V-153
V-24	Pseudo-Noise DCP Subsystem and Estimated Cost* Breakdown V-156
V-25	Comparison of Data Collection Systems V-168
V-26	Wefax Links V-173
V-27	SMS-Spacecraft Communication System Design Alternatives V-193
V-28	Telemetry Subsystem Link Calculation V-195
V-29	Command Subsystem Link Calculation V-196
V-30	SMS Spacecraft Attitude Requirements versus Resolution V-207

FREQUENTLY USED ABBREVIATIONS

APT - Automatic Picture Transmission

ASCII - American Standard Code for Information Interchange

CDA - Command and Data Acquisition

CLR - Crater Lamp Recorder

DCP - Data Collection Platform

DCS - Data Collection System

DPSK - Differentially Coherent Phase Shift Keying

DSBSC - Double Sideband Suppressed Carrier

DUS - Data Utilization Station

EBR - Electron Beam Recorder

FDM - Frequency Division Multiplex

FSK - Frequency Shift Keying

IGFOV - Instantaneous Geometric Field of View

I. T. U. - International Telecommunications Union

LBR - Laser Beam Recorder

MACE - Mechanical Antenna Control Electronics

MSSCC - Multicolor Spin Scan Cloud Camera

MTF - Modulation Transfer Function

PAM - Pulse Amplitude Modulation

PMT - Photo-Multiplier Tube

PN - Pseudo-noise

PNG - Pseudo-noise Generator

PSK - Phase Shift Keying

QPSK - Quadri-Phase Shift Keying

RDAS - Radiometer Data Acquisition System

S/C - Spacecraft

SEMS - Space Environment Monitoring Subsystem

SMS - Synchronous Meteorological Satellite

SPNR - Signal to Pseudo-noise Ratio

SSCC - Spin Scan Cloud Camera

SSSC - Single Sideband Suppressed Carrier

TCXO - Temperature Compensated Crystal Oscillator

TDM - Time Division Multiplex

TRS - Turn-around Ranging Station

TVL - Television Lines

VISSR - Visible Infrared Spin Scan Radiometer

VSB - Vestigial Sideband

WEFAX - Weather Facsimile

SECTION I

BACKGROUND

This report presents the results at the conclusion of Phase B (Project Definition) of the SMS Project. Phase B was conducted by a study team composed of GSFC, NASA Headquarters, and ESSA personnel and supported by ATS Project personnel at GSFC and personnel from ESSA.

As a point of departure for the Phase B study, reference was made to studies conducted since 1966. These studies, some of which are discussed in various sections of the report, include the topics of imaging, data collection and total spacecraft.

The Phase A study was conducted at GSFC. The final report of that study, entitled "Synchronous Operational Meteorological Satellite Feasibility Study," dated June 1966, presented the following system:

- a. Daytime earth imaging with resolution of 3 to 6 n. m.
- b. Communication system to transmit pictures to master station and to act as relay for 13 data channels.
- c. A spacecraft design of the Intelsat II class.

Additional requirements developed since 1966 (delineated in Section II) necessitated a major change of the Phase A system. The new system is presented in this report. It is based on the use of proven designs, techniques, and hardware.

Where alternate techniques are presented, a plan to arrive at a decision is also presented.

The report contains 5 sections. Sections II and III are the background, program requirements and program constraints and summary of approach. Section IV contains a discussion of the existing ESSA CDA station and its use with the SMS spacecraft. Section V indicates how the system design will meet the program requirements.

SECTION II

REQUIREMENTS & CONSTRAINTS

1. REQUIREMENTS

The SMS program requires the development and implementation of a satellite system leading to an operational ESSA observation system from geostationary altitudes. Two satellites launched 12 months apart are planned. The requirements were placed on the program by a letter from Dr. Naugle, Associate Administrator, Office of Space Science and Applications, to Dr. Clark, Director, Goddard Space Flight Center, dated 4 February 1969. The requirements of that letter and a later letter dated 9 June 1969 as expanded through discussions with NASA Headquarters and ESSA are as follows:

1.1 EARTH IMAGING

As a minimum, provide an instrument for imaging in the visible portion of the spectrum with resolution of at least 2 nautical miles at the subsatellite point.

As a goal, provide an instrument for simultaneous imaging in the visible portion of the spectrum with a resolution of 0.5 nautical mile and the IR portion of the spectrum with a resolution of at least 4 nautical miles. (The users ultimate desire is to obtain both accurate radiance measurements and high IR spatial resolution equal to that of the visible channel).

1.2 RETRANSMISSION OF IMAGED DATA

Provide the capability to "time stretch" the image data and retransmit it with reduced bandwidth through the satellite to major data user stations.

1.3 DATA COLLECTION

Provide an optimum transponding subsystem suitable for collecting data from remotely located earth-based small sensor platforms.

The minimum data collection system for a single satellite would consist of the following:

- a. Number of Stations: 3500 to be contacted in a 6-hour period.
- b. Message Lengths: variable by station class from 50 to 3000 bits.
- c. Total 6-hour Data: 350,000 to 600,000 bits depending on coding technique.

As a goal, the system should be compatible with the following maximum data collection system:

- a. Number of Stations: 10,000 to be contacted in a 6-hour period.
- b. Message Lengths: variable by station class from 50 to 3000 bits.
- c. Total 6-hour Data: 2 million bits.

If the full data collection system is not based on an interrogation—reply approach, provision must be made for special platforms which are interrogatable.

Some provision is also desirable for a few platforms which transmit continuously at 500 bps.

1.4 DATA RELAY

Provide for narrow bandwidth transmission of weather maps, satellite pictures, and other data (WEFAX) to existing small regional stations. Station modifications, if required, should be inexpensive.

1.5 SPACE ENVIRONMENT MONITOR

Provide a subsystem to measure protons, solar X-ray flux and magnetic fields at the satellite.

2. CONSTRAINTS

In planning the SMS system three major constraints were imposed. These are:

- a. Use Delta M-6 class launch vehicle.

- b. Minimize impact on ESSA Wallops Island Station.
- c. Base all designs on use of flight proven concepts.

Although each constraint impacts the system design, the underlying effect of all the constraints is to keep the program costs and schedules within budgeted limits. The technical effects of the constraints are as follows:

- a. The launch vehicle constraint limits the size and weight of the spacecraft to about 1000 pounds placed in the proper transfer orbit.
- b. The ground station constraint limits the obtainable imagery resolution. A resolution of 2 nautical miles can be achieved with little modification to the CDA station but sixteen times the data volume will add complexity, especially in the recording portion of the associated high data rate.

SECTION I I I

SUMMARY

1. INTRODUCTION

The general philosophy used in the Phase B study has been the design of a base-line system which meets the minimum requirements while being as compatible as possible with the current configuration of the ESSA CDA ground station. While so doing, an attempt has been made to keep the total system flexible so that the ultimate goals can be achieved whenever resources are available to modify the ground system, which is the principal constraint on obtaining the growth potential of the total system.

2. EARTH IMAGING

The minimum requirement, as stated in Section II, is to provide an instrument for imaging in the visible portion of the spectrum with resolution of two nautical miles at the subsatellite point.

This minimum requirement can be met by provision for flying redundant Spin Scan Cloud Cameras (SSCC). This camera system already has proven feasible through the ATS program and meets the minimum imaging requirements. It is an "off the shelf" item which can be provided by contracting for the camera no later than 12 months prior to the desired launch date. It meets the constraint of minimum impact on the ESSA Wallops Island station because in the ATS program the total ground system requirements have already been implemented. The main revision required is the conversion from a C-band carrier frequency, now in use for ATS, to the planned S-band carrier frequency for SMS.

The imaging goal (growth potential), as described in Section II, is to provide an instrument for simultaneous imaging in the visible and the infrared portion of the spectrum. Additionally, the imaging goal should be a resolution of 0.5 n.m. in the visible and 4 n.m. in the infrared, simultaneously. These goals will be met by development, in parallel with the spacecraft, of a Visible Infrared Spin Scan Radiometer (VISSR) consisting of an optical line step scanner and electronic module. A detailed description of the proposed design will be presented later in the report. In summary, it is a Ritchey-Chretien version of the classical Cassegrain telescope. As with the SSCC, horizontal scan is produced by the spacecraft spin and vertical scan by tilting the scan mirror in discrete steps.

It should be emphasized that the proposed design of the VISSR is such that the resolution measured at the subsatellite point can be chosen to be anywhere from 0.5 to 4.0 n. m. in digital steps by command logic on the spacecraft. Thus, the telescope meets the constraint of minimum impact on the ESSA ground station since that ground station already is configured for the most conservative resolution. To improve the resolution requires only that the spacecraft be so commanded. Achievement of the goal of 0.5 n. m. of resolution critically is dependent on when ESSA is able to devote the required resources to the ground station modifications discussed in Section IV.

There are two parameters that influence the system design from a standpoint of achieving the desired imaging goal. The first of these is associated with the telescope itself. The trade-off between a telescope with two mile resolution vs. 0.5 mile resolution affects mostly the optics. Optics required to achieve 0.5 n. m. resolution are within the state-of-the-art and will be emphasized first in the development of the telescope. The second effect is related to the bandwidth of the transmitting portion of the spacecraft transponder. Here again, the bandwidth required to achieve 0.5 n. m. resolution is within the state-of-the-art, is being accomplished on other NASA programs, and is not considered a significant increase in the spacecraft cost above that required to achieve 2 n. m. resolution.

The bandwidth required to transmit 2 n. m. information from the spacecraft to the ground station is 2.5 MHz. In order to maintain the option of 0.5 mile resolution an r. f. bandwidth of 25 MHz is required if the spin rate is 100 rpm. This bandwidth dictates S-band for the carrier frequency. It will be necessary for ESSA to obtain the appropriate approvals to operate at the bandwidths associated with 0.5 mile resolution. It is possible to reduce the bandwidth requirement if the spacecraft spin rate is reduced, however, the effect of the reduced spin rate on spacecraft stability must be studied.

3. RETRANSMISSION OF IMAGE DATA

As described in Section II, the requirements are to provide the capability to time stretch the image data (as discussed above) and retransmit it with reduced bandwidth through the satellite to major data user stations. The major data user stations are assumed to be regional stations such as Suitland, Kansas City, and Miami. In the remainder of this section the regional stations will be referred to as Data Utilization Stations (DUS).

The proposed spin period of the satellite is 600 ms. Because of the nature of both of the proposed spacecraft imaging sensors, the video data from these sensors require only 30 ms of the 600 ms available. It is proposed to use the

intervening time to retransmit the image data in a stretched form. Data from the eight visible and one infrared channels received during a given 30 ms interval will be retransmitted during the remainder of the spin period.

To accomplish retransmission of radiometer data requires a receiver on the spacecraft with a 3 MHz bandwidth. This receiver together with the transmitter described earlier can be used as a transponder for this purpose. Up to this point, all requirements can be met by use of S-band alone.

4. DATA COLLECTION

The two factors that affect system trade-offs in selection of a data collection system are carrier frequency and technique.

Since the communications system required for transmission and retransmission of the imaging data will be operating at S-band, the spacecraft design will be much simpler if S-band is used for data collection as well. However, it can be expected that the cost of similar ground-based platforms would be less if UHF (400 MHz) were used instead of S-band. A UHF carrier frequency would require the addition of redundant transponders and an additional despun antenna on the spacecraft, thus greatly increasing its complexity and cost. The amount of the increase to the spacecraft is a function of the design from which it evolves.

It is possible that a combined UHF/S-band capability will endanger the launch vehicle constraint. For this reason, it is planned to have all industrial bidders propose an option both in design and increased cost to add UHF capability to the S-band capability required for imaging data. In parallel with this, an in-house study will compare costs of data collection platforms for S-band versus UHF. Thus, prior to initiation of the Phase C/D prime contract, all cost data associated with carrier frequency trade-offs will be available for a decision. It should be emphasized that the end result will be affected by the number of data platforms and the number of satellite missions assumed.

Three general techniques for data collection have been considered: (a) a totally interrogatable system; (b) a pseudo-noise spread spectrum technique, and (c) a random access approach. For both (b) and (c), a partial interrogation capability will be provided as called for in the data collection requirements.

The principal advantages of a totally interrogated system stem from its sequential nature. Because of this feature, it most likely will be the most efficient from the standpoint of channel capacity and primary power consumption by the data collection platforms. A major disadvantage of a totally interrogated system is the higher cost associated with the requirement for a receive capability at each of thousands of data collection platforms. Another major disadvantage is the complexity of operating the system. It is expected that for even the minimum number of required platforms, the interrogation transmitter at the CDA station together with the computer required to select platforms will be in continuous operation.

The pseudo-noise spread spectrum technique is a semi-time synchronized system where the DCP transmissions are allowed to overlap to some degree that is dependent upon the frequency stability of the station clock oscillators. The transmissions thus are permitted to overlap in both the time and frequency domains. This leads to the principal advantage of the system in that it minimizes the time and frequency guard bands that might otherwise be required if a pure time/frequency matrix system were employed. Another advantage of this system over the random access system to be described later is that it has a lower error rate because of its inherent reduction of multi-station interference. The main disadvantages of the system are: (a) the large bandwidth requirement; (b) an up-link power budget with the least margin due to its implementation at S-band, and (c) a requirement for expensive correlation receivers at the CDA station. The only added complexity from the spacecraft point of view is that, because of the large bandwidth required, the receive capability of the spacecraft transponder would have to be extended from 3 MHz (required for image data retransmission) to 10 MHz. Also because of the required bandwidth, the technique is constrained to S-band.

The third technique is random access allowing for time and frequency overlap by retransmission of the data several times during a single 6-hour synoptic period. It shares with the pseudo-noise approach the advantages over an interrogated system of less cost for the DCP because it eliminates the need for a receive capability. Based on a particular DCP stability it is possible to predict a certain probability of obtaining an interference-free data transmission time/frequency slot. The advantages of the technique over the pseudo-noise approach is that it requires no acquisition by correlation receivers at the CDA station and less bandwidth. However, as each DCP transmits the same message to the CDA a number of times in every 6-hour period, the data handling problem at the CDA is increased significantly.

5. WEFAX

The fourth general requirement of the SMS program described in Section II is for transmission of weather facsimile (WEFAX) pictures (obtained from both synchronous and low orbiting satellites and maps) from the CDA through SMS to Automatic Picture Transmission (APT) stations. This presently is being accomplished in the ATS program by use of a VHF downlink carrier frequency. However, this carrier frequency has the disadvantage of being in a band where RFI poses a severe problem. For the SMS program, it is important to consider converting the carrier frequency required for this purpose to S-band or UHF (if UHF is selected as the data collection frequency).

It has been estimated that to convert an existing APT station to operation at S-band will cost approximately \$1600 per station and somewhat less if UHF is used. The decision for optimizing the cost for this requirement depends on the number of stations that need to be modified.

6. ENVIRONMENTAL MONITORING SYSTEM

The final requirement of the SMS system is the provision for measuring the proton, electron and magnetic fields in the vicinity of the satellite and, additionally, the solar X-ray flux integrated over the spectral region between 0.5 and 16 Angstroms.

Solar proton monitors in the desired energy range (protons from 5 to 400 MeV, integrated electron flux above 0.3, 1.4 and 4 MeV) will be flown in the ESSA ITOS program. Similar monitors have been flown in the NASA ATS, IMP and OGO programs.

Magnetic field measurements at geostationary altitudes have been made in the ATS program by Coleman (UCLA) and Heppner/Skillman (GSFC). Additionally, magnetometers have been carried aboard the IMP and OGO satellite series. It must be emphasized that the choice of instruments needs to take into account the fact the ATS magnetometers were able to provide reliable measurements in the presence of stray magnetic fields which could exist on the SMS program.

Solar X-ray monitors in the desired regions have flown on the OSO and OGO series. However, at geostationary altitudes when the instrument is immersed at all times in an energetic particle environment, account must be taken of the influence of that environment on the instrument from a scintillation point of view.

The instruments detailed in later sections of this report represent possible instruments for fulfilling the environmental monitoring requirement. It is planned that the spacecraft contractor will in his proposal have surveyed these and other possible approaches to each of the three sensor requirements. No significant additional complexity to the spacecraft for the power, telemetry and weight required to accommodate an integrated package are envisioned.

SECTION IV

WALLOPS ISLAND CDA STATION

1. INTRODUCTION

The National Environmental Satellite Center (NESC) Command and Data Acquisition (CDA) station is located on the eastern shore of Virginia along the Atlantic coast of the Delmarva peninsula, approximately 40 miles southeast of Salisbury, Maryland. The station is built on government owned land within the boundaries of the National Aeronautics and Space Administration (NASA) Wallops Island Station.

The NESC station contains electronic systems for tracking, receiving, and recording meteorological data from the ESSA meteorological satellites and the GSFC ATS satellites.

2. ATS GROUND EQUIPMENT

The capability exists at Wallops for receiving SSCC data from the ATS-I spacecraft. Command and telemetry processing functions can also be performed. Figure IV-1 is a block diagram of the ATS-I facility.

2.1 SSCC PICTURE PROCESSING EQUIPMENT

The following is a brief description of the ESSA ATS SSCC picture processing system operation.

The earth picture processing system shown in Figure IV-2 produces photographs of the earth using video information received from a satellite in synchronous orbit. A spin-scan camera located on board the spacecraft scans the earth from synchronous altitude (22,300 s. mi.). A picture is scanned by using the spin of the satellite for horizontal sweep; one line is produced for each spacecraft revolution. The camera is stepped in elevation (vertical sweep) once each revolution to produce 2017 lines per earth picture. A complete picture takes approximately 20 minutes to produce. The analog video information produced by the camera is transmitted by the spacecraft over a 4 GHz RF link which is received by a 32 ft. shaped dish antenna, cooled paramp, and down-converted to 70 MHz by the SHF receiver. The 70 MHz RF signal is demodulated by the threshold extension demodulator and sent to the digital synchronizer and line stretcher

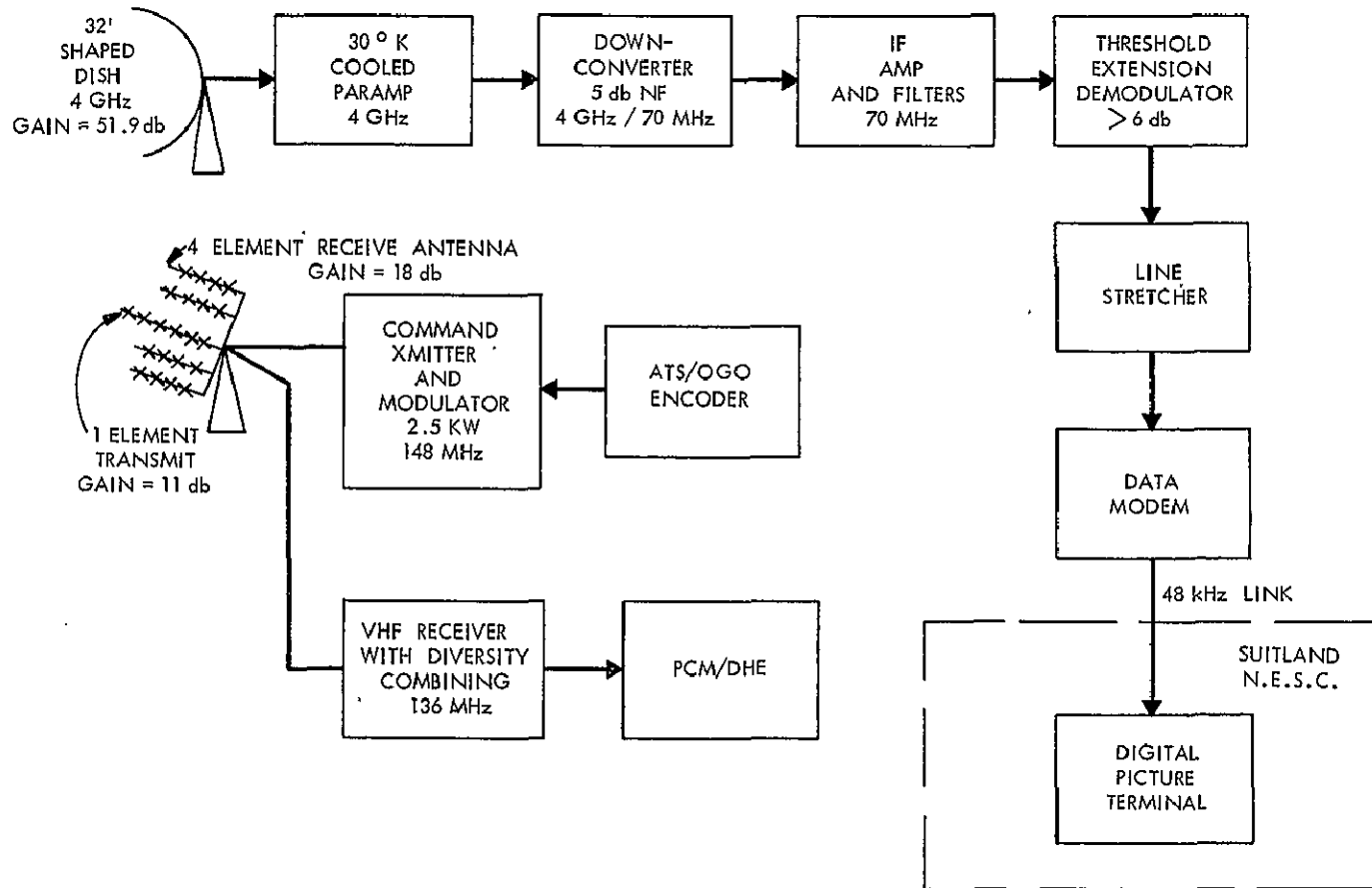


Figure IV-1. Wallops Island ATS-I Ground Equipment

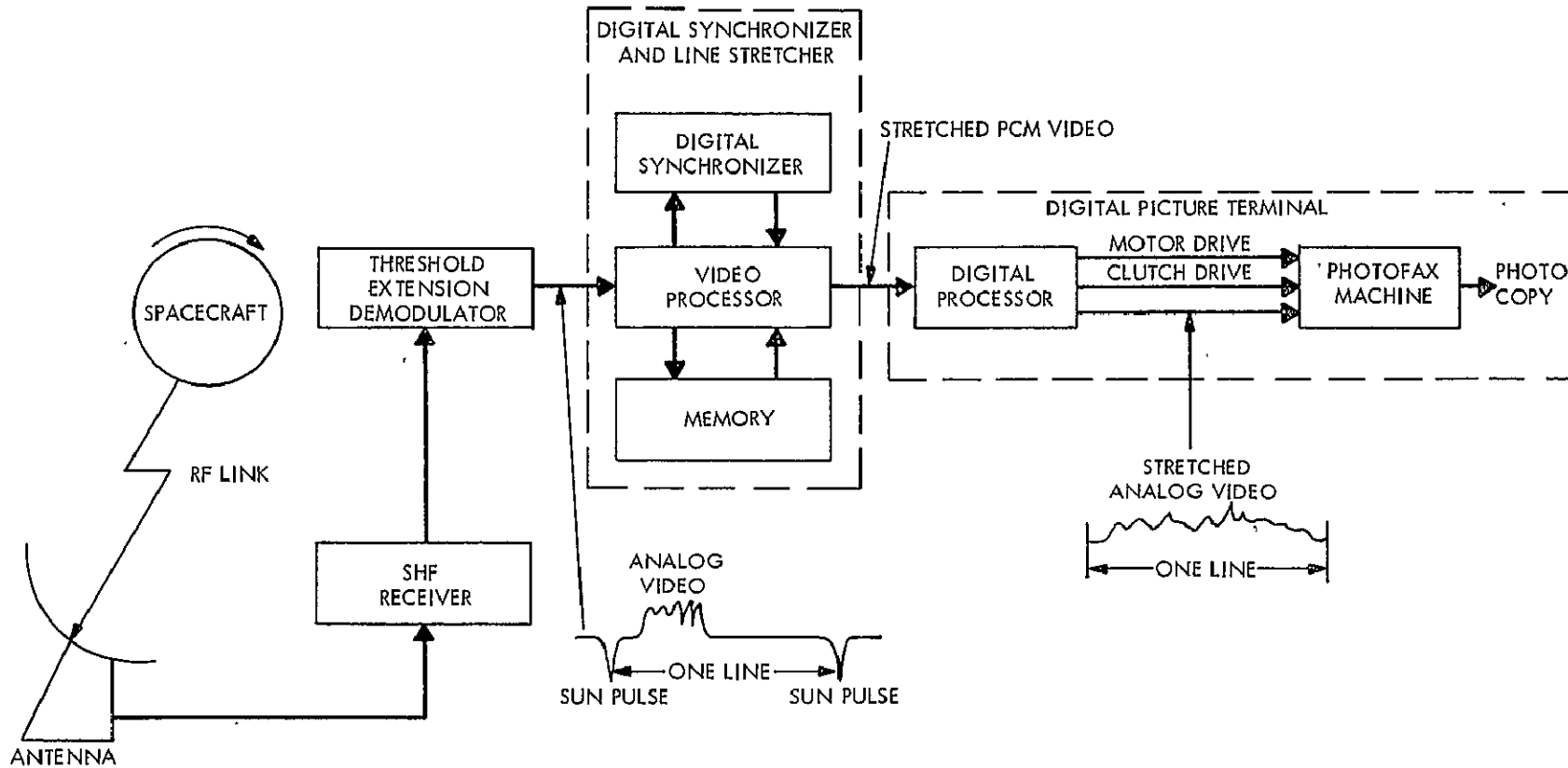


Figure IV-2. Earth Picture Processing System Block Diagram

(DS/LS) as analog video plus sun pulse. Since the satellite "sees" the earth for only a fraction of an entire rotation, the video at this point occupies only a small fraction of the total spin time.

The DS/LS stretches the video so that it occupies an entire line and produces stable earth-referenced line-sync pulses from the received sun pulses. The received video is converted from analog to digital in the video processor and is stored in a core memory. The contents of the core memory are then read out at a rate slow enough to make the data occupy an entire line. The sun pulse is detected and delayed by a different amount each revolution to account for the changing sun-earth angle due to earth rotation. The digital video and line-sync information are sent to the digital picture terminal (DPT) in a pulse-code-modulated (PCM) bit-stream over a 48 kHz bandwidth ground link. The digital processor extracts the line-sync information from the PCM and uses it to rotate the photofax drum at the same speed as the satellite speed relative to the earth. The digital processor also converts the digital video information back into analog and drives the light source in the photofax machine for exposing the film which is wrapped around the drum. Frame-sync from the bandwidth compressor is detected by the digital processor and used to start the photofax at the beginning of a picture.

The photofax machine consists of a rotating drum and a light source whose intensity is varied by the digital processor (DP). The light source is on a carriage that is geared to the drum rotation. The light source traverses the film from top to bottom as the camera in the satellite vertically scans the earth from the North Pole to South Pole. In this way, with the drum rotation providing horizontal sweep and the light source movement providing vertical sweep, a picture is produced.

The digital synchronizer consists of a precision digital phase-lock loop (PLL) and a reference converter. The phase-lock loop will lock on to input signals with periods from 1 to 0.0025 second and will quantize the period to 0.5 microsecond resolution. The input to the PLL is generated from a sun sensor mounted on a spin-stabilized synchronous orbit satellite. The PLL output is therefore phase-locked to the sun reference. The reference converter delays the PLL output to produce an earth-reference output by multiplying the quantized spin period from the PLL by an appropriate fraction equal to the angular distance from the sun to the earth as subtended by the spacecraft in its direction of rotation. The fraction is continually updated to compensate for the changing sun-satellite-earth geometry.

The picture processor is capable of handling a single channel input of 2 mi. resolution data with 8 bits per sample. The jitter on the sun pulse used for

synchronization should be held to plus or minus 64 microseconds when acquiring sync in the stretcher. Table IV-1 is the link analysis of the SHF, 4 GHz, receiving system at Wallops Island.

2.2 COMMAND AND TELEMETRY SYSTEM

Presently in service at Wallops Island is an ATS/OGO command console and a PCM DHE. This system is capable of generating all of the commands and command functions and decommutating all of the PCM telemetry of the ATS spacecraft.

2.2.1 Command System

The command system consists of the ATS/OGO command console and the VHF transmitter and antenna as indicated in Figure IV-1. The link parameters are as given in Table IV-2. Any ATS command can be easily generated and executed manually.

The command console is not limited in its output FSK frequencies. The FSK frequencies can be changed in 200 Hz steps between 7 and 11 kHz. The bit rate can also be changed along with the output format. These modifications, if required, can be implemented readily in the existing command encoders.

2.2.1.1 PURPOSE AND DESCRIPTION

The OGO/ATS Command Console provides commands required to control OGO and ATS spacecraft. The command to be transmitted to a satellite may originate at peripheral equipment (such as a control center computer or paper tape reader) or manually at the Command Console control panel. The Command Console converts a command request to the required sequence of pulse-code-modulated (PCM) frequency shifts or tone bursts, energizes the command transmitter, and transfers the command. The command is generated within the Command Console and is used to modulate the transmitter carrier.

When the Command Console receives a request to generate a command, it performs the following functions:

- Generates the command in the mode and format required for spacecraft response and compliance.
- Verifies the command externally or internally, as desired.

Table IV-1

SHF Link Calculation (4 GHz) Wideband Data Mode ATS-I

S/C Transmit Power	36.5 dbm
Diplexer and Cabling Losses	-1.8 db
Phase Shifter Loss	-1.0 db
S/C Antenna Loss	-1.5 db
S/C Antenna Gain	18.0 db
Off Beam Center Allowance	-1.5 db
Space Loss	-197.2 db
Path Losses	-0.5 db
Margin	-3.0 db
Ground Antenna Gain	50.9 db
Received Carrier Power	-101.1 dbm
System Noise Temp (50° K)	17.0 db
System Noise Power Density	-181.6 dbm/Hz
System Bandwidth (25 MHz)	74.0 db
System Noise Power	-107.6 dbm
CNR	6.5 db*

*5.5 db is required for the threshold extension demodulator

Table IV-2

Command Subsystem Link Calculation

Frequency	148.26 MHz
Transmitter Power (500 watts) (Worst Case)	57 dbm
Transmit Antenna Gain	11 db
Path Attenuation	-168 db
Spacecraft Antenna Gain	-5 db
Passive Element Losses	-2 db
Polarization Loss	-3 db
System Operating Margin	<u>-3 db</u>
Received Carrier Power	-113 dbm
Command Receiver Threshold	-118 dbm
Signal Margin Over Threshold	5 db
Bit Rate	128 bps
Modulation	FSK/AM/AM
Frequencies	7.4 kHz = 0 binary
	8.6 kHz = 1 binary
	5.79 kHz = execute tone

- Keys on the command transmitter.
- Transfers the command serially to the command transmitter.
- Transfers the command once, twice, or four times as selected.
- Generates the command address at all times.

A switch on the Command Console permits command generation to fit the requirements of OGO or ATS spacecraft.

2.2.1.2 FUNCTIONAL CHARACTERISTICS

The Command Console operates in either of two distinct modes: the digital (PCM) mode or the tone mode.

2.2.1.2.1 Digital Mode Characteristics

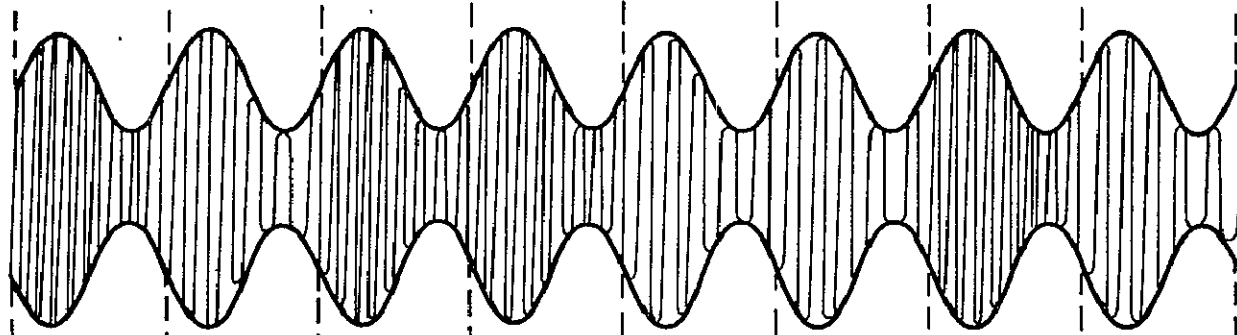
In the digital mode, 256 digital commands are available for controlling a spacecraft. A digital command is a series of PCM frequency tone shifts generated at 128 bits per second. The format of a command and the frequency representing a binary "0" are controlled by selecting the OGO or ATS program. A frequency of 8.6 kHz represents a binary "1", and a frequency of 8.0 kHz with the OGO program or 7.40 kc with the ATS program represents a binary "0". True frequency shift keying (FSK) is used in generating the PCM sub-carrier signals. The sub-carrier is derived from one oscillator that is forced to operate at one of two distinct frequencies. The shift in frequency instituted by a digital bit transition occurs in less than five oscillator periods. Bit synchronization is provided by amplitude-modulating the sub-carriers with a 128-Hz source synchronized with digital bit transition. Figure IV-3 illustrates the composite output of the Command Console operating in the digital mode: A complete digital command consists of 64 bits. A series of "0's" precedes the transmission of significant data.

Figure IV-4 illustrates the ATS digital command format in which 28 "0's" followed by two sync bits (29, 30) precede the most significant address character. The sync bit configuration is a "1" followed by a "0". The next eight bits (31 through 38) are the spacecraft address. Bits 39 through 46 form the spacecraft command.

Following the transmission of a command, a series of "0's" is transmitted to the ATS spacecraft until external equipment indicates that an execute tone of 5790 cps is to be generated. The time of initiation and period of the execute

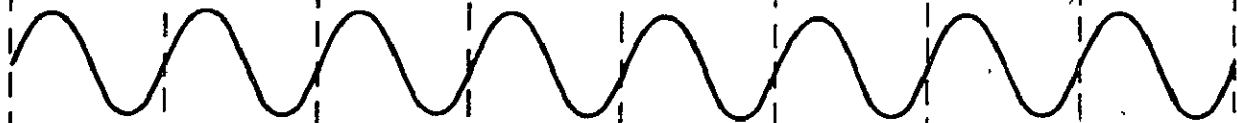
ATS PROGRAM

COMPOSITE
AUDIO
WAVEFORM
AM 50 %

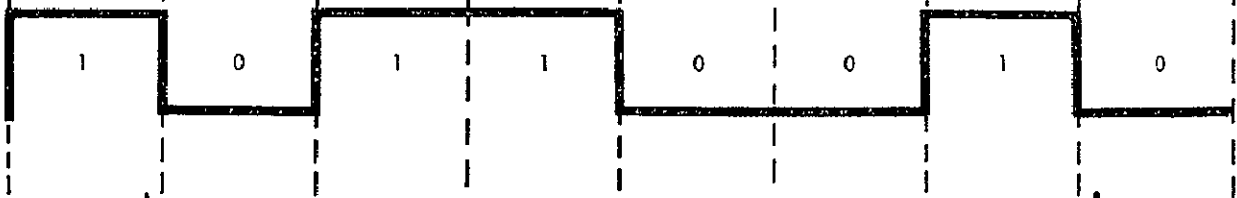


8.6 kHz 7.4 kHz 8.6 kHz 8.6 kHz 7.4 kHz 7.4 kHz 8.6 kHz 7.4 kHz

BIT SYNC
MODULATION
128 Hz



SERIAL
DIGITAL
COMMAND
128 BITS
PER SECOND



BIT CROSSOVER POINTS FOR ATS PROGRAM

Figure IV-3. Digital Command Composite Output

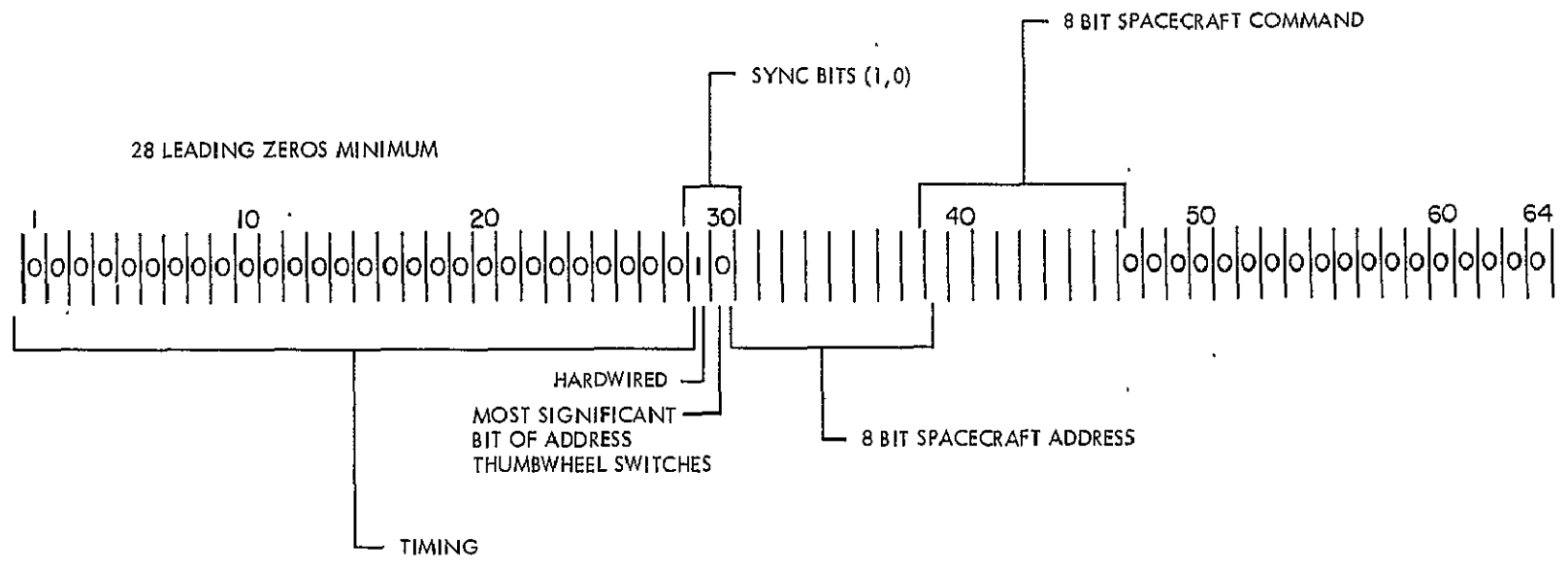


Figure IV-4. ATS Digital Command Format

tone and the number of times the tone is generated is controlled by a signal from external equipment. Between each execute tone and after the final execute tone a series of "0's" is generated until transmission is stopped by a signal from the external equipment or from the front panel controls.

2.2.1.2.2 Tone Mode Characteristics

Up to 343 tone commands are presently available for controlling a spacecraft in the tone mode. A tone command is a series of either three tone bursts or four tone bursts, with blank (no-tone) periods separating each tone burst. The duration of the tone bursts, blank periods, and the minimum time interval between successive tone commands can be controlled in 0.25-second increments. Burst periods and blank periods can range from 0.25 to 3.75 seconds. The time between tone commands can range from 0.25 to 7.75 seconds.

A tone command consists of an address tone preceding either two or three execute tones. Table IV-3 presents the address and execute tone assignments. As shown, only four of the address tones are presently assigned. Selection of a zero execute tone will produce an extended blank (no-tone) period.

Table IV-3

OGO/ATS Command Console Address and Execute Tone Assignments

OCTAL NUMBER	BINARY NUMBER	ADDRESS TONE	EXECUTE TONE
0	000	5790 ATS only	No tone
1	001	1097	2000
2	010	Not assigned	2270
3	011	1477	2650
4	100	1750	3000
5	101	1860	3305
6	110	Not assigned	3620
7	111	Not assigned	3850

2. 2. 2 PCM Telemetry Decommutation System

The PCM telemetry decommutation system is capable of synchronizing and decommutating all of the ATS PCM telemetry data. This includes, besides main frame data, subframe data also. The data is displayed on addressable displays and also printed on a printer. The unit establishes bit, main frame, and ID frame synchronization. The link parameters are as given in Table IV-4.

The PCM equipment is not limited to the current ATS PCM code, bit rate, and format. The system can be reprogrammed for various PCM codes, formats, and bit rates by means of external controls on the unit.

The following gives a general summary of the PCM DHE equipment capability:

1. Bit rates - 10 bps to 1,000,000 bps
2. PCM codes - NRZC, NRZM, NRZS, bipolar, 50% RZ, SOC, SOM, and SOS
3. Word Length - 4 to 33 bits
4. Frame length - 2 to 999 words
5. ID - Subframe synchronizer; length up to 255 frames
6. Recycle Subframe Synchronizer length up to 299 frames
7. Primary Frame Code Pattern length 4 to 33 bits

Table IV-4

Telemetry Subsystem Link Calculation

Frequency	136.47 MHz
Satellite Transmitter Power	32.0 dbm
Diplexer and Line Losses	-2.8 db
Satellite Antenna Gain	-3.2 db
Path Loss	-167.4 db
Ground Receive Antenna Gain	18.0 db
Ground Receive Losses	<u>-2.0 db</u>
Received Carrier Power	-125.4 dbm
Receiver Noise Temperature (NF = 4 db)	435° K
Sidelobe Noise Temperature	65° K
Galactic Noise Temperature	<u>1200° K</u>
Total Receiver System Noise Temperature	<u>1700° K</u>
Received Noise Power Density	-166.3 dbm/Hz
Carrier/Noise Power Density	40.9 db-Hz
Carrier/Noise Power Density Threshold	35.5 db-Hz
Margin Over Threshold	<u>5.4 db</u>

NOTE: Calculations based on using diversity reception

3. CDA STATION FUNCTIONS FOR SMS

The CDA station will function as the spacecraft control and major data collection center for the SMS operations. Its detailed functions will include:

- a. Receive and process the 25 MHz* wide (RF) data from the spacecraft telescope/radiometer system.
- b. Reduce the baseband bandwidth of this data and retransmit it with an RF bandwidth of approximately 3.0 MHz via the spacecraft to "small" data utilization stations (DUS) within the viewing area of the spacecraft.
- c. Receive and process all data from approximately 10,000 data collection platforms (DCP's).
- d. Transmit all radiometer and DCP data to Suitland NESC.
- e. Interrogate such DCP's as may be provided with receive capabilities.
- f. Perform ranging measurements utilizing the spacecraft transponder and two remote slave stations, thus providing information for picture gridding.
- g. Transmit commands to the S/C for control and utilization as instructed by the ESSA Satellite Operations Control Center (ESOCC).
- h. Receive, process and transmit spacecraft housekeeping data to ESOCC.
- i. Receive and process data from the space environment monitoring sub-system (SEMS) package.

*This may be only 10 MHz depending upon the down-link bandwidth allocation.

4. MODIFICATIONS TO CDA NECESSARY FOR SMS LAUNCH

4.1 TELEMETRY AND COMMAND (T&C)

The SMS T&C subsystems have been modeled on the corresponding ATS subsystems and therefore the existing VHF T&C system at Wallops Island will be capable of operating with the SMS at launch. There presently exists no S-band capability at Wallops; hence no use can be made of the spacecraft S-band T&C subsystem until new S-band antenna, transmitters and receivers have been installed.

At the present time Wallops Island cannot receive real-time telemetry data from ATS spacecraft due to the low gain of the VHF T&C antenna. The only way this can be received is by the use of the 85' antenna. This condition will apply also to SMS.

Another problem is that Wallops Island is not equipped with a synchronous controller (such as the units at Rosman & Mojave) and therefore have no capability for maneuvering ATS or SMS spacecraft. A suitable unit will have to be provided to control the SMS spacecraft in the future.

The antenna problem is probably not serious since maneuvers could be planned at a time when the 85' antenna was available.

4.2 RADIOMETER DATA RECEPTION AND PROCESSING

4.2.1 S-Band Reception and Transmission

To permit reception of the SMS radiometer data at launch the CDA station must be equipped with an S-band antenna equivalent to a 40' parabola, with a right hand circularly polarized feed system and having at least a limited scan capability.

In addition, a cooled parametric amplifier receiver having a total system noise temperature of not more than 100° K and a 1 db bandwidth of at least 25 MHz will be required.

A 10 watt S-band transmitter with a 1 db bandwidth of 3 MHz will be required for interrogation of DCP's, retransmission of stretched data, and commanding of the spacecraft. Switching circuits within the transmitter will be required to ensure time synchronization of the up-link stretched data and DCP interrogation transmissions and the down-link radiometer data transmission.

4. 2. 2 Demodulation/Demultiplex Equipment

The down-converted signal from the S-band receive system will be fed to demodulation/demultiplex equipment which will recover the 8 visible and 2 radiometer channels. This equipment will be required at launch if radiometer data (with any resolution between 0.5 and 4.0 n. miles) is to be received. There is presently no equipment at Wallops Island which can perform this function.

It is difficult to state at this time whether demultiplex equipment for only 2.0 n. mile resolution could be provided as a basic installation and added to later. This would depend to a large extent on the modulation/multiplex technique chosen.

4. 2. 3 Data Recording and Stretching

There is no equipment at Wallops Island at the present time suitable for recording 0.5 n. mile radiometer data, however, it is probably not required to have such a facility at SMS launch.

The existing Hughes built line stretcher could be used to receive 4.0 n. mile data and stretch it to a format and bandwidth suitable for retransmission to Suitland NESC, and via the SMS to Data Utilization Stations (DUS's). A difficulty arises in using the existing stretcher in that the stretched data format will be incompatible with the format recommended for the ultimate 0.5 n. mile stretcher and DUS receiving equipment suitable for the existing format would have to be either replaced or considerably modified to receive the new format.

The Westinghouse built line stretcher presently used at the Rosman ATS station for ATS-3 would provide stretched 2.0 n. mile resolution data but again the format would be incompatible with that of the ultimate system.

4. 3 REMOTE DATA COLLECTION

A decision on whether equipment will be provided at launch for collection of data from DCP's will depend upon many factors. Some of these are

1. The type of system selected; frequency band, totally interrogated or only partially, etc.
2. Compatibility of the selected system with sensor equipment already in the field.

3. Cost of conversion of existing field equipment and provision of new new equipment.
4. Feasibility of providing basic facilities at the CDA station and expanding gradually to the full system capability.
5. Assuming that (4) is possible, cost of such versus cost of providing full system immediately.

No statement is possible, therefore, at the present time, on what should be provided at launch.

4.4 RANGING

It has been proposed that the CDA station be equipped with ranging equipment to provide capability for determination of the sub-satellite point, mainly for gridding of pictures. A trilateration technique appears to be the most economical to implement as it requires only relatively simple equipment at two remote "slave" stations and ranging equipment located only at the CDA station.

To accomplish a trilateration measurement the CDA station will require a time interval measuring unit & a data formatter which will time annotate and identify each range measurement and output the composite data either on paper or magnetic tape or directly to a computer for real-time determination of the sub-satellite point.

Unless gridding is a definite requirement at launch there does not seem to be any real need to provide the ranging equipment at that time. The only other reason for providing this equipment would be for day-to-day stationkeeping and based on ATS experience this should not be necessary, since it has been proposed that orbit determination be conducted by the STADAN network (at VHF) on a monthly or bi-monthly basis and this should be adequate for stationkeeping purposes.

4.5 INTERFACE WITH SUITLAND NESC

There presently exists between Wallops Island and Suitland NESC a 48 kHz digital data link which could be utilized for the transmission of 2.0 n. mile data from the existing line stretching equipment assuming the link SNR is satisfactory.

The link requirements for transmitting the DCP data to Suitland are more difficult to define but it could be expected that as few as two 75 baud teletype circuits will be sufficient to handle the expected 2×10^6 data bits to be collected

over the 6 hour period. This will be dependent upon the collection system selected. A random access system would require many more than 2 circuits, possible as many as 10. These requirements are summarized in Table IV-5.

4.6 SUMMARY

Table IV-6 summarizes those modifications which are required at the CDA station both prior to SMS launch and ultimately to achieve all of the SMS goals.

Table IV-5

Retransmission Band Width Requirements for Data Link

<u>VISSR DATA</u>	<u>LINK REQUIREMENTS*</u> <u>(50% DUTY CYCLE)</u>
0.5 N. MILE RESOLUTION	DC-225 kHz
1.0 N. MILE RESOLUTION	DC-56 kHz
2.0 N. MILE RESOLUTION	DC-14 kHz
4.0 N. MILE RESOLUTION	DC-3.5 kHz

*NOTE: THIS IS THE BASEBAND RESPONSE.

REMOTE DATA COLLECTION

(1) INTERROGATION SYSTEM	2 TELETYPE CIRCUITS
(2) SPREAD SPECTRUM SYSTEM	2 TELETYPE CIRCUITS
(3) RANDOM ACCESS SYSTEM	10 TELETYPE CIRCUITS (APPROXIMATELY)

Table IV-6

Summary of Station Modifications to Meet SMS Requirements

PRIOR TO LAUNCH

- | | |
|------------------------------|--|
| 1. T & C | PROVIDE--SYNCHRONOUS CONTROLLER, REAL-TIME DATA RECEIVER
(THESE ARE REQUIRED FOR MANEUVERING) |
| 2. VISSR DATA RECEPTION | PROVIDE--S BAND ANTENNA (40 FOOT DIAMETER), 25° K COOLED
PARAMETRIC AMPLIFIER AND DEMULTIPLEXING EQUIPMENT |
| 3. VISSR DATA STRETCHING | NO MODIFICATIONS REQUIRED IF 4.0 N. MILE RESOLUTION IS
ACCEPTABLE (LOAN OF <u>W</u> STRETCHER FOR MSSCG WILL
ALLOW 2 N. MI RETRANSMISSION) |
| 4. VISSR DATA RECORDING* | PROVIDE--LASER BEAM RECORDER (VISIBLE DATA)
GRATER LAMP RECORDER (THERMAL DATA)
ANALOG RECORDER
DIGITAL RECORDER |
| 5. VISSR DATA RETRANSMISSION | VIA ATS VHF - NO MODIFICATION REQUIRED (IF TRANSMITTED AS FACSIMILE PICTURE)
VIA S BAND - PROVIDE--10 WATT S BAND TRANSMITTER
PROVIDE--40 FOOT DIAMETER S BAND ANTENNA |

ULTIMATE

- | | |
|----------------------------------|--|
| 1. RADIOMETER DATA
STRETCHING | PROVIDE; LINE STRETCHER WITH 0.5 N, MILE RESOLUTION CAPABILITY.
WIDE BAND LINK TO SUTTLAND N. E. S. C. |
| 2. DATA COLLECTION | PROVIDE; RECEIVERS (DEPENDING ON SYSTEM SELECTED)
DCP INTERROGATION GENERATOR
TELETYPE LINKS TO SUTTLAND N, E, S, C. |

*IN CASE OF SUTTLAND LINK FAILURE PROVISIONS SHOULD BE MADE TO RECORD DATA AT WALLOPS ISLAND

SECTION V

IMPLEMENTATION TO ATTAIN PROGRAM OBJECTIVES

1. INTRODUCTION

This section of the report discusses each program objective stated in Section II. Each objective is discussed separately and a complete description is given detailing how the system design will meet that objective. Where required, tradeoffs and alternatives are discussed.

The SMS system will consist of the spacecraft, ground station (CDA), and remote data collection platforms plus a satellite operations control center and a central data collecting and processing facility. The CDA station will be remote from the latter two facilities.

The spacecraft is spin stabilized and located at synchronous altitude in view of the CDA ground station. The primary spacecraft payload consists of a telescope/radiometer for both infrared and high resolution visible photography and associated communications system, for data collection and distribution, and a space environment monitor system.

The communications system (figure V-1) will utilize S-band and in addition may use UHF frequencies. It will be used to transmit radiometer data to the CDA station; retransmit stretched pictures to regional stations; collect and transmit to the CDA the data from up to 10,000 DCP's; disseminate weather facsimile data; receive and transmit command and telemetry data; and perform turn around ranging transmissions. Also, a ground communications link is required from the control center and data collecting facility to the CDA station.

The SEMS will comprise a variety of scientific sensors designed to measure on a continuous basis the solar emission activities. These sensors will be contained in an integrated flight package. The data will be transmitted to the ground via the S-band communications system.

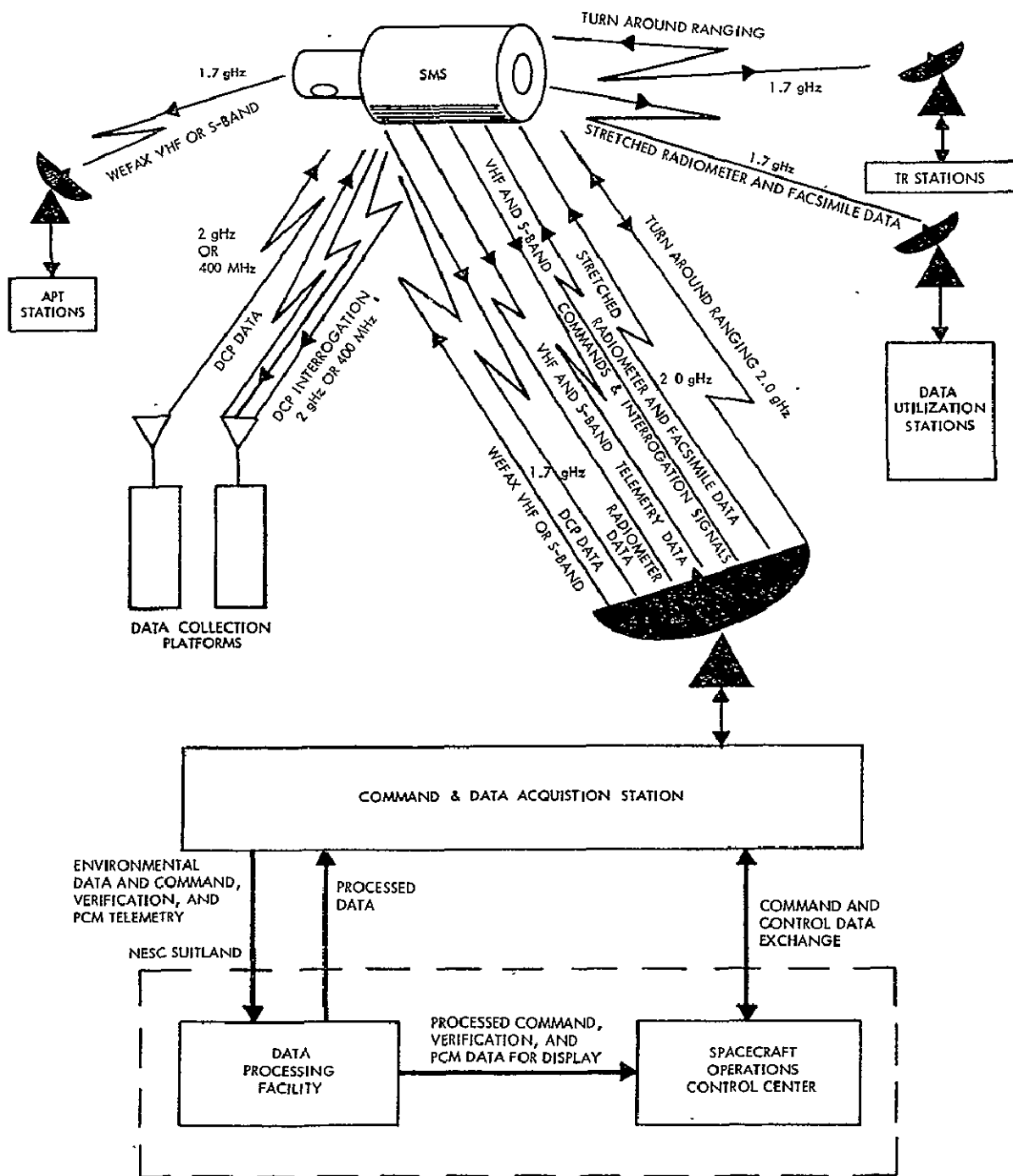


Figure V-1. SMS Communications System Concept

2. TELESCOPE/RADIOMETER IMAGING SYSTEM

2.1 DESCRIPTION

The Visible Infrared Spin-Scan Radiometer (VISSR) selected for the SMS will consist of an optical line step scanner and an electronics module. The electronics module will be separate from the scanner to facilitate performing initial gain adjustments of the radiometer when the scanner must be in a thermal-vacuum environment.

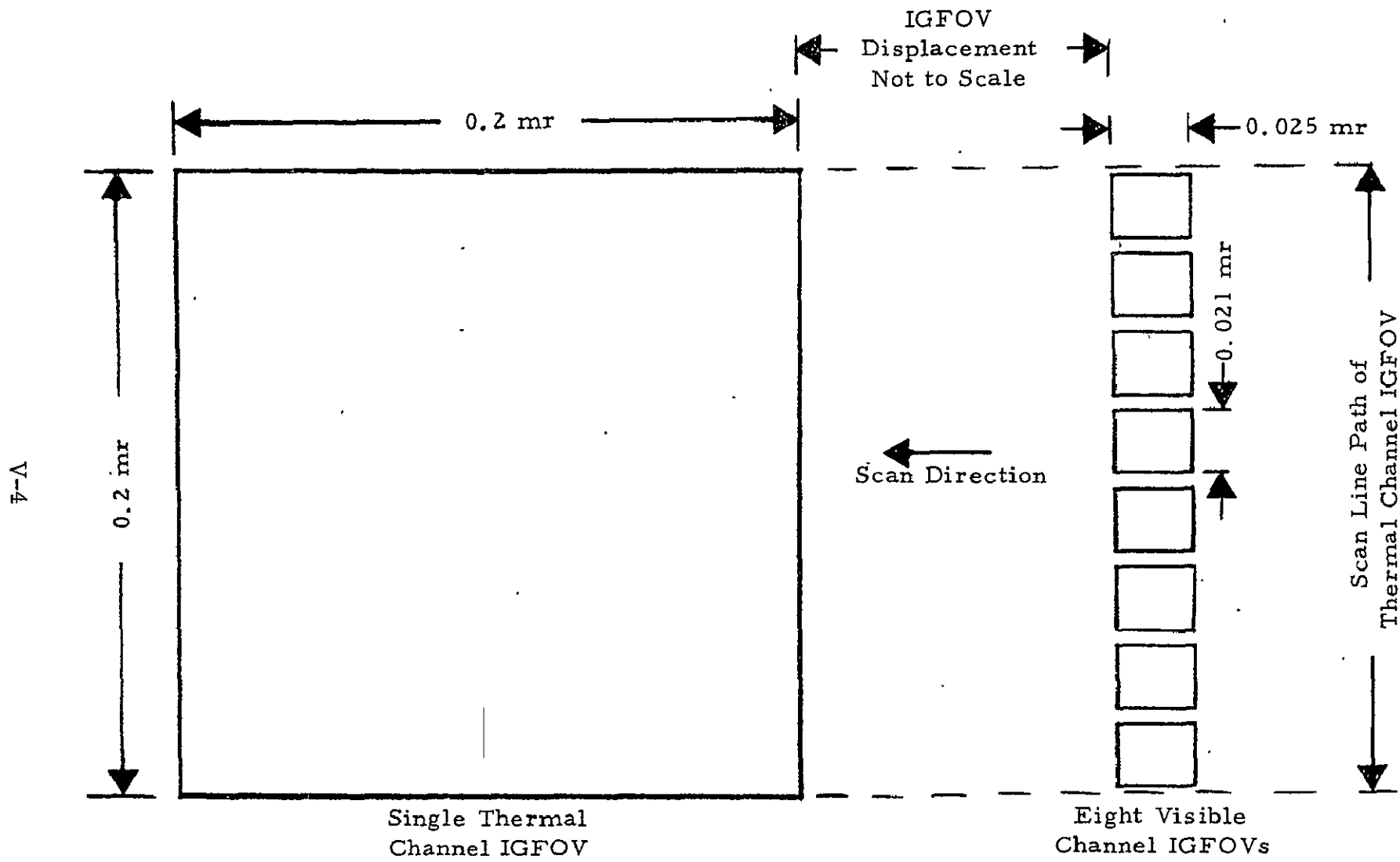
The radiometer contains eight identical visible channels which operate in the 0.55 to 0.70 micron band, and a single infrared (thermal) channel which operates in the 10.5 to 12.6 micron band. The instantaneous geometric field of view (IGFOV) of each visible channel is 0.025×0.021 mr. The IGFOV of the thermal channel is 0.2 mr square. The IGFOV's of the eight visible channels are aligned in a linear array so that they sweep out the same scan path (with a 20 percent underlap between channels) as the single (and larger, 0.2×0.2 mr) thermal channel IGFOV. (See Figure V-2.) In addition, one redundant thermal channel having equivalent performance will be provided.

Table V-1 gives a summarized list of VISSR design and performance characteristics. Table V-2 gives the physical characteristics of the VISSR.

2.1.1 Optical Design

The optical system proposed for the VISSR is shown schematically in Figures V-3 and V-4. It consists of the following.

- a. An object-space scan mirror.
- b. A Ritchey-Chretien primary-secondary mirror system.
- c. Relay optics for the thermal channel.
- d. Fiber optics light-guides and collimating optics for the visible channels.
- e. Optical filters for the thermal and visible channels.
- f. An immersed (to PMT window) optical prism in each visible channel to achieve enhanced photocathode effective quantum efficiency.



(Redundant Channel is Adjacent to the Single Channel)

Figure V-2. VISSR Thermal Channel and Visible Channels IGFOV Arrangement

9-A

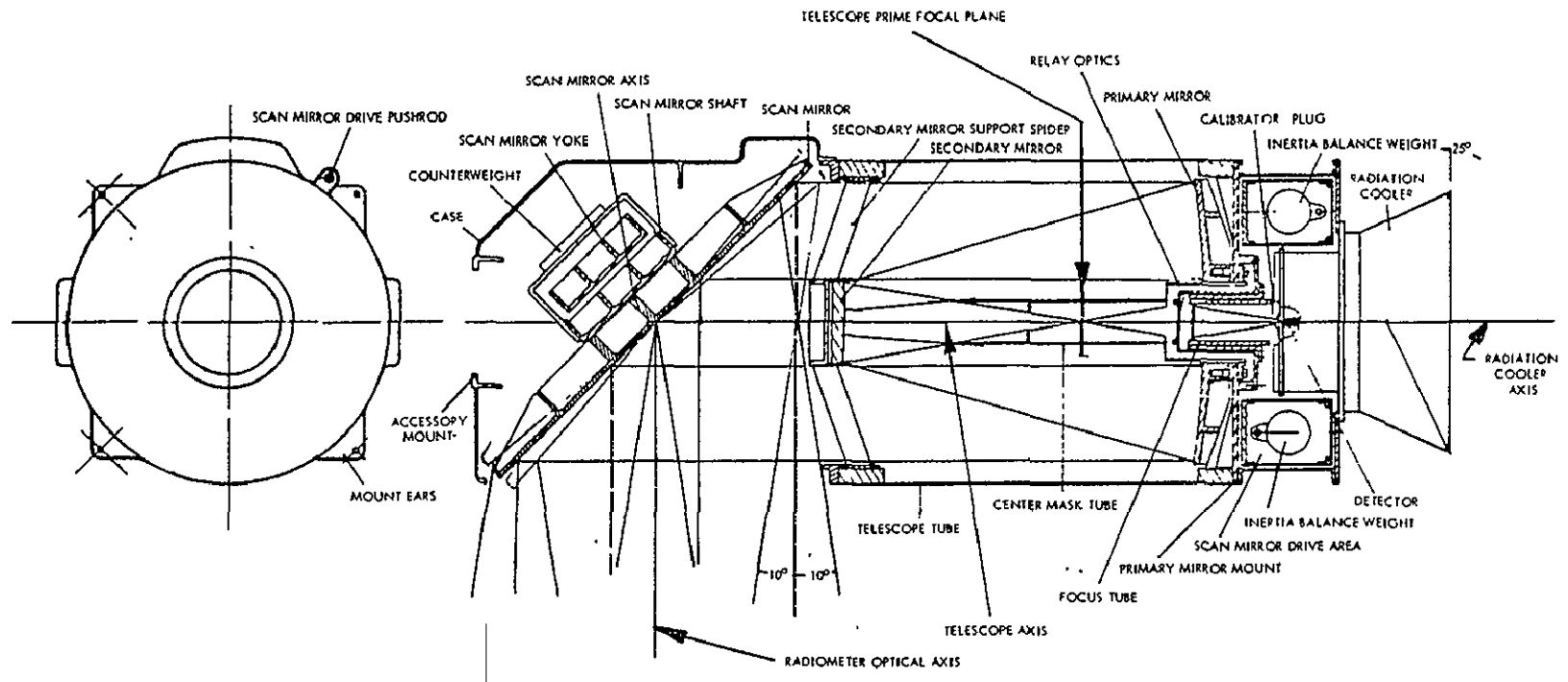


Figure V-3. VISSR Scanner Layout Drawing

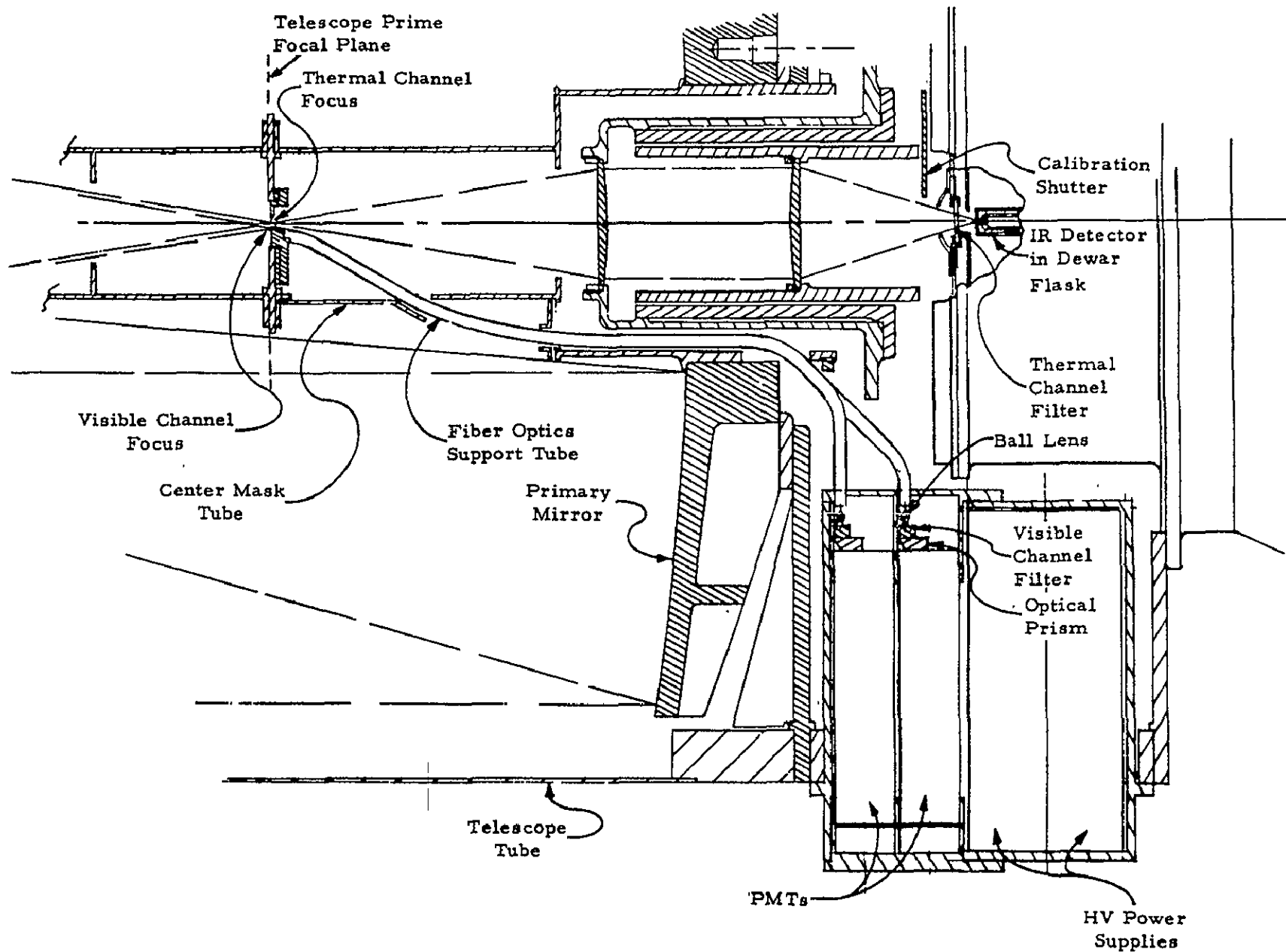


Figure V-4. VISSR Scanner Aft Optics Detail

Table V-1

Summary of VISSR Design and Performance Characteristics

Design Parameters	Visible Channel	Thermal Channel
Number of Channels	8	1 plus 1 redundant channel
Wavelength Band of Operation, Half-Power Points	0.55-0.7 microns	10.5-12.6 microns
Instantaneous Geometric Field of View	0.025 x 0.021 mr	0.2 x 0.2 mr
Collecting Aperture	1170 cm ²	1170 cm ²
Detector	RCA 8645 PMT	Intrinsic Longwave
Size	--	0.12 x 0.12 mm
Response	S-20 (enhanced)	--
Scan Period	0.6 sec	0.6 sec
Dwell Time	2.4 x 10 ⁻⁶ sec	1.9 x 10 ⁻⁵ sec
Video Bandwidth	210 kHz	26 kHz
Dynamic Range, Albedo (%); Target Temperature (°K)	0 to 80%	0 to 330° K
Performance Characteristics	Visible Channel	Thermal Channel
Noise Equivalent Radiance, NEN for an Extended Source (watt-cm ⁻² -sterad ⁻¹)	--	1 x 10 ⁻⁵
Noise Equivalent Differential Temperature for an Extended Source	--	1.5°K at 200°K 0.38°K at 300°K
S/N at 0.5% Albedo, for an Extended Source	2.8 = 9 db	
Modulation Transfer Function	0.34 at 2 x 10 ⁴ cycles/rad	0.42 at 2.5 x 10 ³ cycles/rad
V _p /V _{ss} , Target Size Equal to IGFOV's, Includes Optical Response Factors (Approximate)	0.45	0.55

Table V-2

Summary of VISSR Physical Characteristics

Physical Characteristics	Scanner	Electronics Module
Estimated Weight	120 lb	12.5 lb
Size	58 x 20 x 20 in.	450 in. ³
Power Requirements	23 watts	
Inflight Calibration Provisions	Visible Channel 1. Sun and Space Thermal Channel 1. Sun and Space 2. Calibration Blackbody and Space	

2.1.1.1 Telescope Design—A Ritchey-Chretien version of the classical Cassegrainian telescope is proposed for the VISSR. The primary mirror is an f/1.8, 16-inch aperture aspheric (nonconic section); the secondary is also aspheric and is 4.8 inches in diameter. The effective focal length is 48 inches for an overall focal ratio of f/3.

The selection of a specific telescope design involves the tradeoff of fabrication difficulty with the required optical performance.

2.1.1.2 Telescope and Scan Mirror Material—From weight considerations, the scan mirror, the primary and secondary mirrors, and the primary-secondary telescope housing will be fabricated from beryllium.

2.1.1.3 Optical Train—Radiation collected by the primary optics is imaged in a plane between the primary and secondary mirrors (see Figure V-3). At this point, the visible channels and thermal channel are optically separated as shown in detail in Figure V-4, which is an enlarged cutaway drawing of the scanner layout rotated 90° from the plane shown in Figure V-3. The ends of eight fiber optic light-guides are located on-axis in the plane shown and oriented in a linear array perpendicular to the plane of the drawing. The ends of the fiber optics light-guides, which are 0.0014 x 0.0012 inches in size (including cladding), are the defining field stop aperture for the eight visible channels. The radiation intercepted by each of the fiber optics light-guides is

conducted behind the primary mirror where it is collimated by a spherical lens and then filtered. Following filtering, the collimated radiation in each visible channel is directed into a photomultiplier tube (PMT) by means of an immersed optical prism. The immersed prism arrangement provides a means for enhancing the effective quantum efficiency of the PMT. The radiation energy in each visible channel is converted into electrical signals by the PMT photocathode and amplified by the PMT electron multiplier. The amplified output of each PMT is buffered by a low output impedance transistor circuit located on the scanner assembly. The amplified and buffered signals are then supplied as inputs to the electronics module where they are further amplified, processed, and then conditioned for the spacecraft communications system.

Radiation for the thermal channel passes the principal focal plane of the primary optics through a light baffle which is slightly off-axis. After passing through the light baffle the thermal channel radiation is reimaged by means of a relay lens system in the plane of the thermal channel detector. A 10.5 to 12.6-micron bandpass filter is located in the converging beam of the relay lens system and establishes the spectral band limits for the thermal channel. For the thermal channel, the detector element defines the channel IGFOV. The light baffle located in the principal focal plane of the primary optics is made large enough to facilitate ease in optical alignment of the thermal channel, and to ensure that a small lateral displacement of the detector (e.g., as a result of the launch environment) does not result in energy loss due to obscuration. The energy collected by the thermal channel detector is converted into an electrical signal by the detector and amplified by a low-noise preamplifier located on the scanner assembly. The amplified signal is then supplied as an input to the electronics module where the signal is further amplified, processed, and then conditioned for the spacecraft communications system.

2.1.1.4 Thermal Channel Relay Optics—The lens material used in the thermal channel relay optics is germanium. In addition to relaying the telescope's prime focal plane to the thermal channel detector plane, the relay optics also increase the optical speed of the overall thermal channel optics.

2.1.1.5 Visible Channel Aft Optics—The visible channel aft optics consist of a fiber optics light-guide assembly and collimating lens, an optical filter, and an optical prism (for PMT enhancement) for each visible channel. The fiber optics assembly consists of eight light guides. Each light-guide core has a rectangular cross section which is 0.0012 x 0.0010 inch in size. The ends of the light guides are located in a linear array at the radiometer's prime focal plane, and therefore serve as the field defining aperture for eight visible channels.

2.1.2 Rapid Frame Rate Mode

The latitude line step motion provided by the radiometer scanner can be operated in either the normal (closed-loop) or backup (open-loop) mode by a command from the ground. In the open-loop mode of operation, either of two frame rates can be selected: the normal frame rate of approximately 3 frames/hour with the normal frame height (20°), or a rapid frame rate of approximately 30 frames/hour with a reduced frame height (2°). The reduced latitude frame can be positioned at any location within the normal 20° frame at the time the open-loop line step mode is selected by ground command. The rapid frame mode, therefore, will permit the monitoring of localized high velocity cloud and storm centers in greater temporal detail than could be achieved with the normal frame rate.

2.1.3 Radiation Cooler Arrangement

A three-stage radiation cooler is used to cool an intrinsic long-wavelength detector used in the thermal channel to a temperature of approximately 75°K. As seen in Figure V-3, the axis of the radiation cooler is aligned parallel with the radiometer telescope axis, and therefore the spin axis of the spacecraft. This arrangement permits the axis of the radiation cooler to point in either the north or south direction (whichever is required for proper operation), and still allow the radiometer "latitude line step" motion in the north-south direction to be conveniently achieved. The cooler will radiate to space after the apogee motor is ejected.

2.1.4 Spin-Scan Operation

A layout drawing of the radiometer scanner is shown in Figure V-3. The scanner design uses an elliptically-shaped plane scan mirror and primary optics which are common to the radiometer visible channels and the radiometer thermal channel. The scan mirror is set at a nominal angle of 45° to the radiometer telescope (primary optics) axis which is aligned parallel to the spin axis of the spacecraft. The spinning motion of the spacecraft, therefore, provides an east-west line scan motion when the spin axis of the spacecraft is oriented parallel with the earth's axis.

Latitude line step motion of the radiometer's optical axis is accomplished by tilting the scan mirror about its minor (ellipse) axis in small steps called "latitude scan steps." The latitude scan steps occur once each spin rotation of the spacecraft when the radiometer's optical axis is at an angle of approximately 180° from the north-south earth center line. The timing pulses to initiate the latitude scan steps are provided by the spacecraft computer. Each latitude scan step tilts the scan mirror by an angle of 0.1 mr to produce an effective line

step of 0.2 mr. The total effective north-south line-step coverage provided is 20° (±10° about the nominal radiometer optical axis). Therefore, for an assumed spacecraft spin rate of 100 rpm, a complete 20° "latitude" frame (1750 thermal channel scan lines) will be accomplished in 17.5 minutes. A frame retrace is accomplished in approximately 1.8 minutes.

2.1.5 Inflight Calibration

A method for accomplishing an inflight calibration of VISSR is provided for both the visible and thermal channels.

The visible channel inflight calibration is accomplished by permitting the visible channel to scan through the sun with a reduced-size "side looking" collecting optical aperture. The sun calibration aperture is a reflecting surface that occupies a small part of the radiometer scan mirror. Its area size (each of three angular offsets) is approximately 1.1×10^{-5} that of the effective scan mirror collecting aperture (or approximately 1.0×1.0 mm) so that a 50 percent albedo calibration point is provided when the sun is scanned. The angular relationship between the radiometer IGFOV and the sun calibration optics three FOVs is illustrated in Figure V-5. The reduced size apertures are offset in angle so that the three sun calibration optics FOVs lead the radiometer's IGFOVs in scan angle (in the scan plane) by 15°. The center FOV of the sun calibration optics scans along the same scan line as the radiometer's IGFOVs. The two outside FOVs scan at elevation angles of ±20° with respect to the radiometer's IGFOV. This optical arrangement permits an inflight calibration of the visible channels to be accomplished each frame (except during solar eclipse) every day of the year. An inflight calibration of the eight visible channels, each frame against the same source, will permit normalization of the channel gains so that gray scale variation along the eight scan line band (due to any random photo-multiplier gain drift) can be eliminated during ground processing of the visible channel signals.

Two methods are provided for accomplishing an inflight calibration of the VISSR thermal channel. One method permits a calibration of the entire thermal channel. It is accomplished by placing the thermal channel preamplifier in a precision attenuate mode when the sun is scanned. Immediately when the sun is sensed by the first section of the thermal channel preamplifier, the second section of the preamplifier is placed in a precision attenuate mode of approximately 0.24×10^{-2} of normal gain. Therefore, a calibration signal of approximately 50 percent of full scale is provided. This attenuate mode lasts only while the sun is being viewed by the thermal channel. This method of inflight

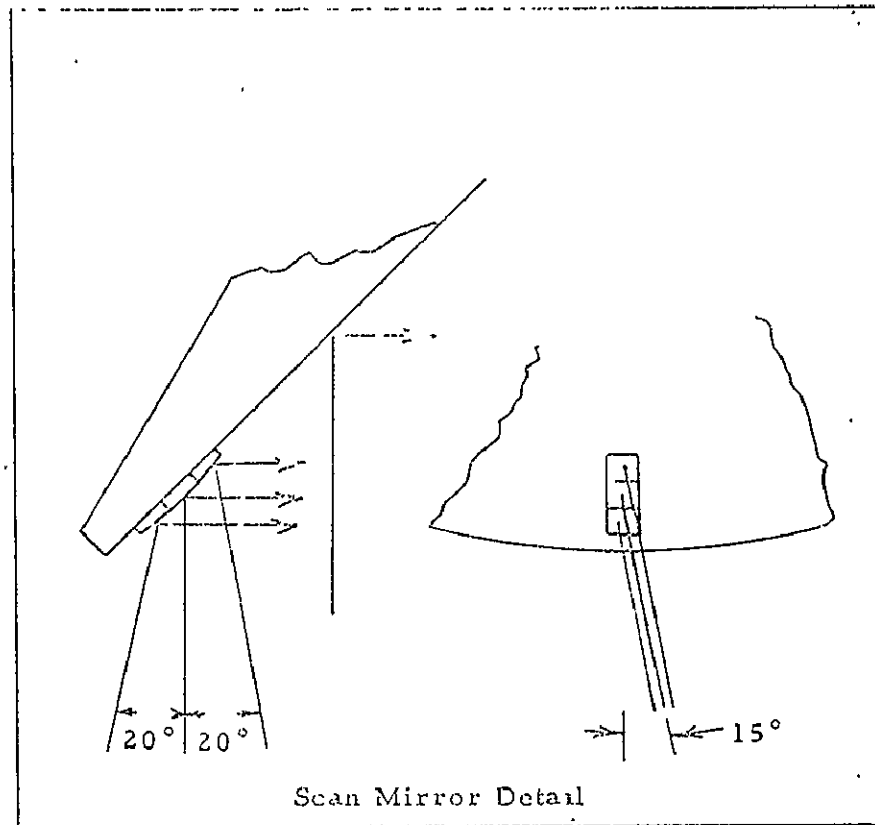
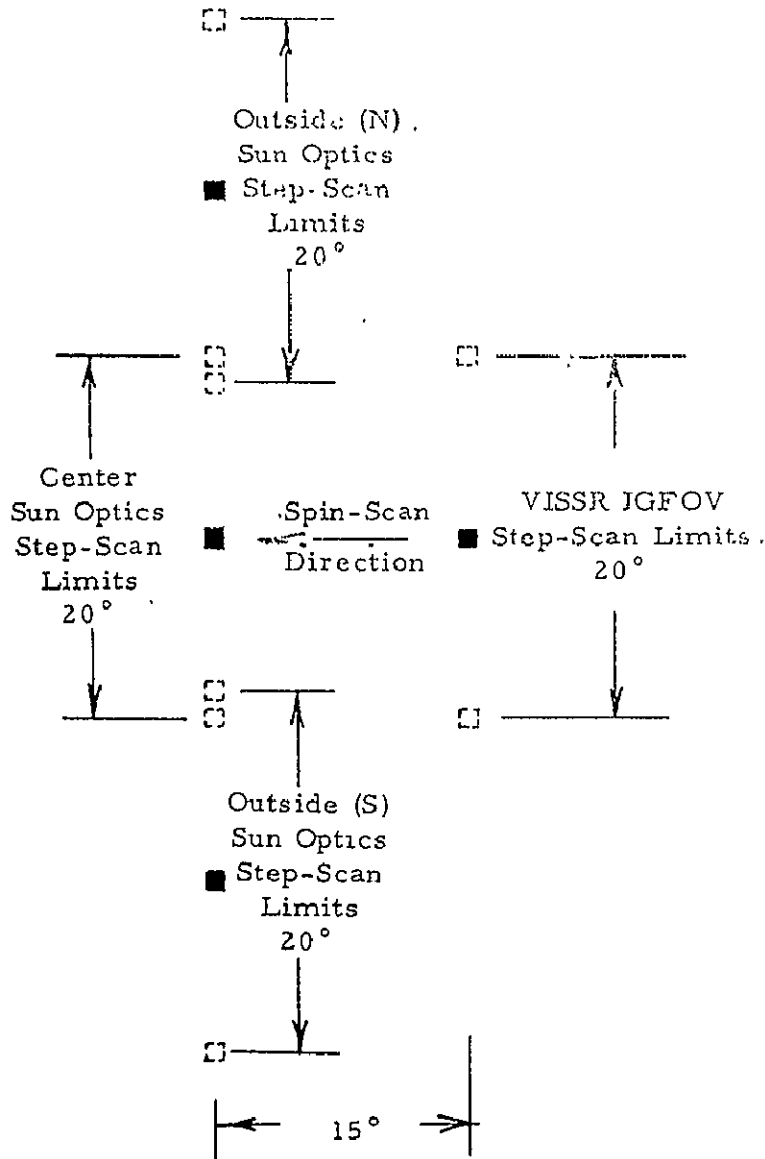


Figure V-5. VISSR IGFOV and Visible Channel Sun Optics Angular Relationship

calibration, however, is limited to being performed only during certain periods of the year* (approximately 20 days before and after both the vernal and autumnal equinox).

The second method of inflight calibration of the thermal channel provides a calibration point only for the combined optical filter-detector-electronics train. It does not include the scan mirror, primary optics or relay optics. The calibration is initiated by a ground command which places an ambient temperature blackbody shutter, whose temperature is monitored, in the optical train of the thermal channel. When the shutter-calibrate command relay is activated, the radiometer timing circuits will place the shutter in the calibrate position for a period of 0.1 second just after the earth scan has been completed. This action will be repeated each scan cycle until the shutter-calibrate command relay is deactivated by a ground command. Either a solid or slotted shutter can be commanded into position to provide two calibration points (in addition to space), therefore also permitting a check of the radiometer thermal channel linearity to be made.

2.1.6 Thermal Channel DC Restore

DC restoration (zeroing) of the thermal channel base line (when space is viewed) is performed once each scan cycle. It is initiated by a timing pulse supplied by the spacecraft computer and is performed just prior to each earth scan. Three important benefits, given in the following, are derived by the use of dc restoration in the thermal channel.

- a. Essentially zero droop of the earth radiation pulse is achieved without the attendant increase in effective noise bandwidth that would normally result when a detector having predominantly $1/f$ noise characteristics is considered and standard low-frequency cutoff filters are used. For an equivalent noise bandwidth of the VISSR using dc restoration) use of low-frequency cutoff filter having a 12-dB/octave rolloff would result in an earth radiation pulse droop of approximately 3% compared to essentially zero droop when dc restoration is used.
- b. The thermal channel output voltage corresponds to the absolute value of the target scene radiation.

*It appears that the method of inflight calibration similar to that used in the radiometer visible channels could be incorporated for the thermal channel to permit an inflight calibration of the entire thermal channel each frame every day of the year.

- c. A single polarity telemetry system can be used to transmit the thermal channel data.

DC restoration is not required for the radiometer visible channels since sufficient gain is achieved in the PMT electron multiplier to permit the use of dc amplification in the final transistor amplifier stages.

2.1.7 Scan Line Sync Pulses

Precision timing pulses are required by the VISSR from the spacecraft computer to generate coded synchronization pulses, which will be added to each of the radiometer's nine channel outputs each scan cycle. The line-to-line jitter of the spacecraft precision timing pulses must be significantly less than the dwell period of the radiometer's visible channels IGFOX (2.4×10^{-6} seconds) to ensure suitable registration of the photofacsimile produced at the ground station. The synchronization "pulse" added to the channel outputs will be a series of three 0.2-msec pulses separated by 0.2-msec spaces. It is assumed that the spacecraft precision timing pulses will occur when the radiometer IGFOV is 300° (-60°) from the north-south earth center line.

2.1.8 Radiometer Scan Sequence

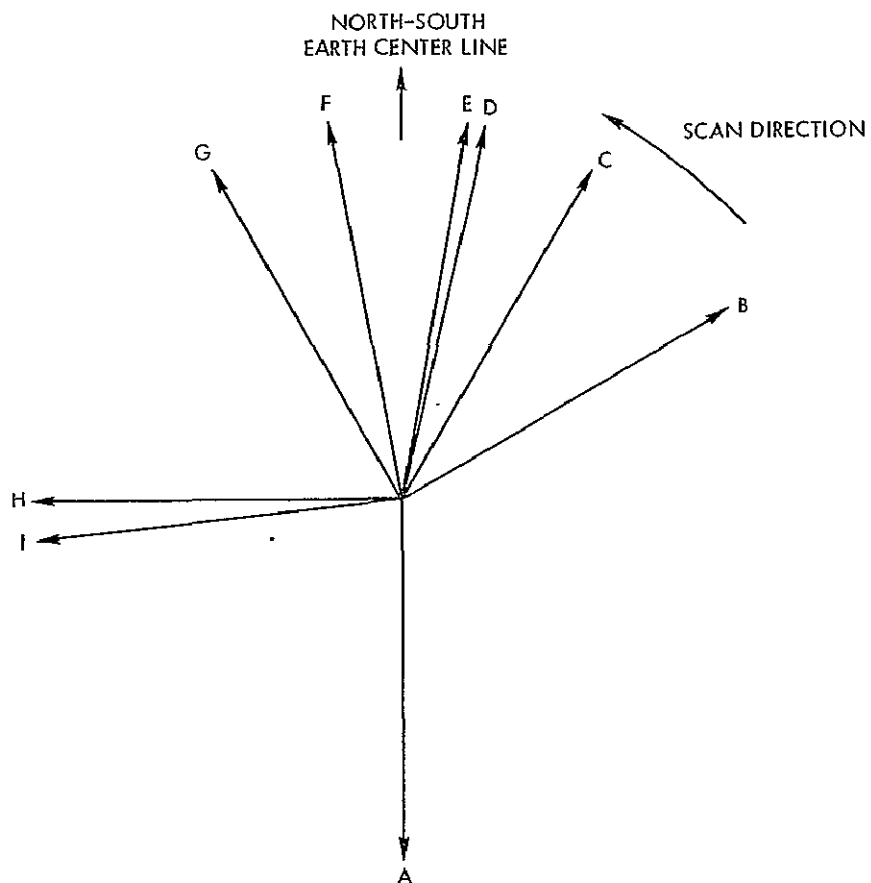
The angular position of the radiometer's optical axis at the different timing events that occur each spin-scan cycle of the spacecraft is diagrammatically illustrated in Figure V-6. Zero angle reference is defined as the north-south earth center line. Spin rotation is assumed to be counterclockwise.

At 180° (when the radiometer's optical axis is pointing away from the earth), a latitude line step is initiated.

At 300° (-60°), the radiometer scan line synchronization pulse is initiated.

At 330° (-30°), just prior to earth scan, a dc restore timing pulse is received from the spacecraft computer. Upon receipt of this pulse, dc restoration of the radiometer thermal channel base line is initiated. At 348° (-12°), dc restoration of the radiometer thermal channel is completed.

*To ensure that dc restoration of the radiometer thermal channel does not occur when the sun is being viewed, the dc restore timing pulse supplied by the spacecraft computer is programmed to occur at 305° (-55°) whenever the sun position is between -5° and -32° (0020 to 0208 hours).



<u>REFERENCE LETTER</u>	<u>ANGLE</u>	<u>LEGEND</u>	<u>EVENT</u>
A	-180°		LATITUDE LINE STEP INITIATED
B	-60°		SCAN LINE SYNC PULSE INITIATED
C	-30°		THERMAL CHANNEL DC RESTORE INITIATED
D	-12°		DC RESTORE COMPLETED
E	-9°		EARTH SCAN BEGINS
F	+9°		EARTH SCAN ENDS
G	+30°		SHUTTER CALIBRATE INITIATED (WHEN CALIBRATE RELAY IN ACTIVATE POSITION)
H	+90°		SHUTTER CALIBRATE COMPLETED AND ELECTRONICS CALIBRATE INITIATED
I	+95°		ELECTRONICS CALIBRATE COMPLETED

Figure V-6. VISSR Timing Event Diagram

At 351° (-9°), the earth scan period begins. At 9° the earth scan period ends.

At 30°, the calibration shutter will be placed into the calibrate position whenever the shutter-calibrate command relay is in the ACTIVATE position. At 90°, the calibration shutter will be removed from the calibrate position and a two-level calibration and linearity check of the complete thermal channel electronics will be initiated. At 95° the thermal channel electronics calibration will be completed.

At the end of each frame (at 180°), a 5-kHz end-of-frame tone burst is added to each of the radiometer channel outputs for 0.1 second. At the start of each frame (at 180°), a 10-kHz start-of-frame tone burst is added to each of the radiometer channel outputs for 0.1 second.

The voltage waveforms that occur at the output of the radiometer's visible and thermal channels during a scan cycle are illustrated in Figure V-7. The scan cycle represented assumes the sun is scanned, 1500 hours time-of-day, and the shutter calibration command relay in the ACTIVATE position.

2.1.9 Electronics Design

The radiometer thermal and visible channel electronics is illustrated in block diagram form in Figure V-8. Only one of eight identical visible channels is shown. The preamplifiers, PMT high-voltage supplies and telemetry functions associated with these circuits are located within the VISSR scanner. All remaining electronic circuits are packaged in a separate module. This packaging arrangement permits initial calibration to be performed with the scanner located in a vacuum-thermal chamber.

2.1.9.1 Thermal Channel Preamplifier—The thermal channel preamplifier uses an ultra-low noise, bipolar transistor input stage connected in such a way as to provide a constant current source into the low-impedance (100 to 200 ohms) detector connected to it. The preamplifier thus provides bias to the detector; therefore, the block diagram shows no separate detector bias supply. The regulation of the constant current source is provided by a high gain negative feedback loop which ensures that bias current is controlled to an accuracy dependent only on a few passive components. Any change in detector voltage is sensed by the regulating loop and appears, greatly amplified, at the preamplifier output. The gain of this stage is determined almost exclusively by wirewound and metal-film resistors, so gain stability of 0.1 percent or better may be expected. An additional advantage of the constant current input preamplifier is the high input impedance which causes no loading of the detector. Any drift in detector impedance is not translated into a change in responsivity because of loading effects.

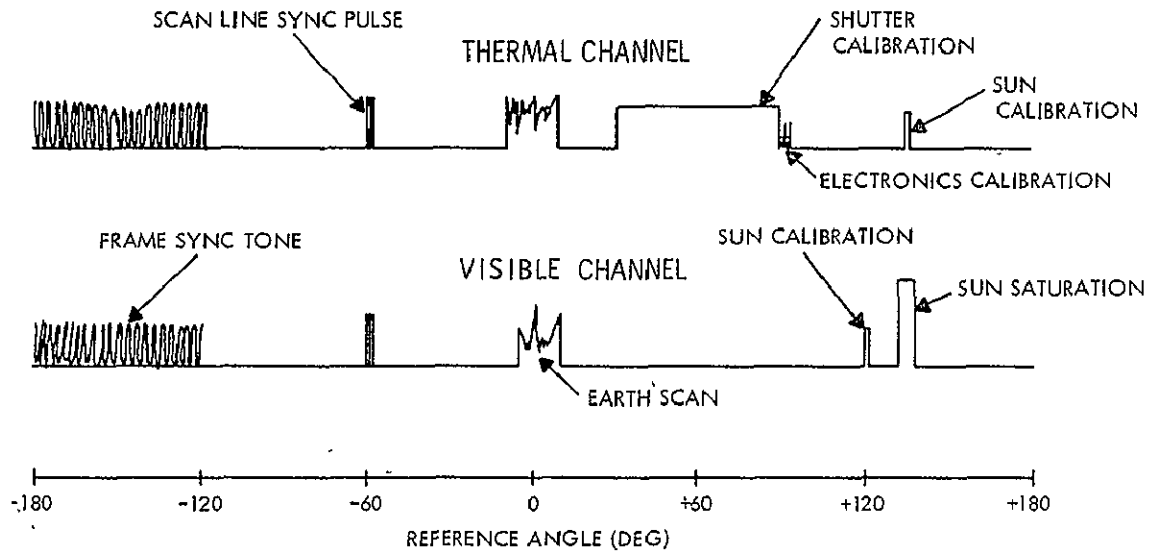


Figure V-7. Radiometer Output Voltage Waveforms

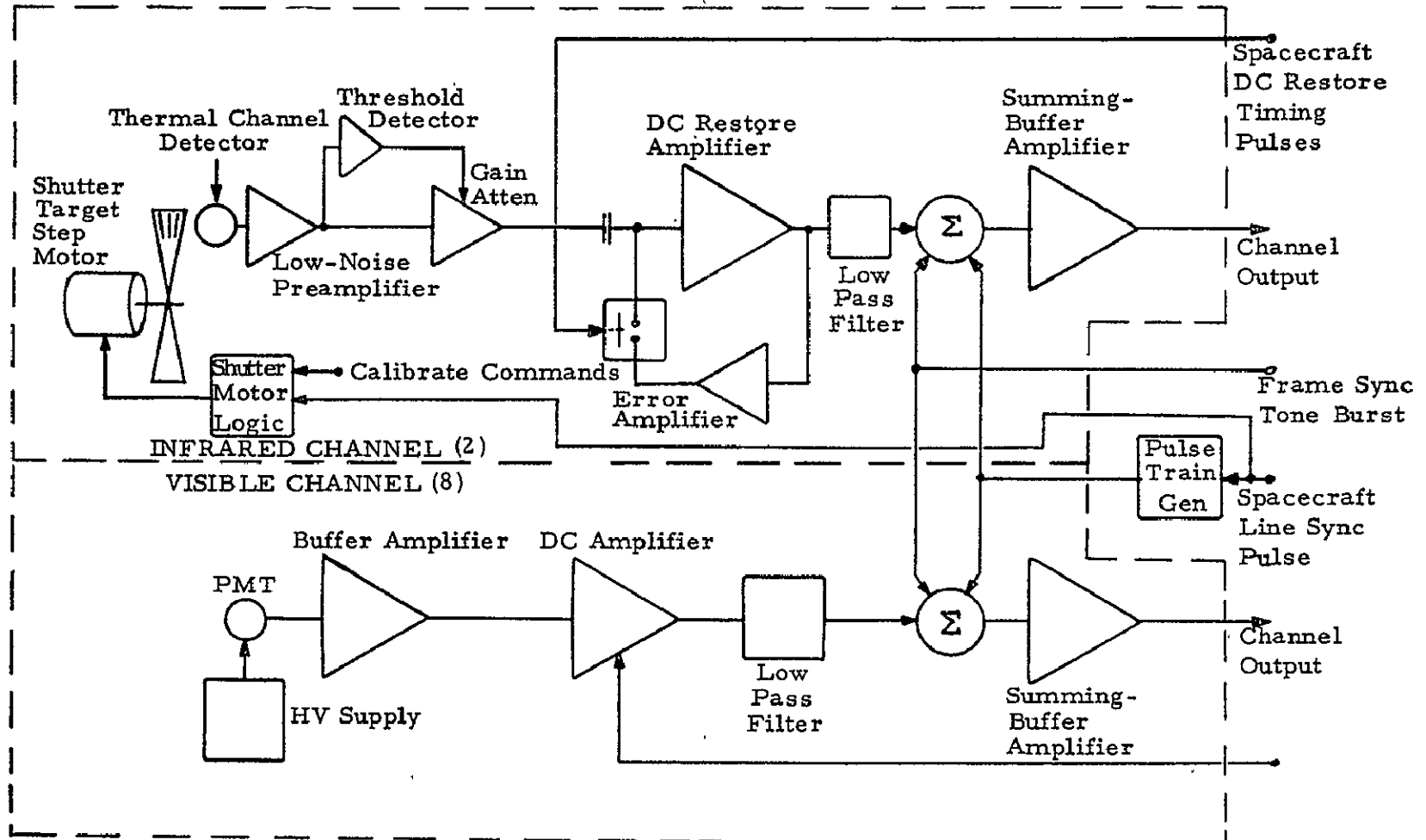


Figure V-8. VISSR Electronics Block Diagram

The noise generated by the detector is greater than Johnson noise by an amount whose amplitude and spectrum depends on the bias level. This noise, combined with that contributed by the preamplifier, results in an S/N ratio which depends on detector bias current and has an optimum value for bias currents between 0.5 and 2.0 ma depending on the detector characteristics.

Fine, low (thermal) conductivity wires will connect the detector to terminals on the ambient temperature stage of the radiation cooler. From these terminals, a low-noise shielded cable will connect to the preamplifier. The low output impedance of the preamplifier permits many feet of cable between the preamplifier and the remaining channel amplifiers in the electronics module.

The thermal channel preamplifier is composed of two sections. The total gain in the first preamplifier section is made as large as possible without causing amplifier saturation when the sun fills the field of view (FOV). At this point in the channel, a signal level detector senses the amplified signal and introduces attenuation in the second preamplifier section when the sensed signal amplitude rises to many times that which would cause saturation in the channel output if the attenuator were not used. This occurs whenever the sun enters the FOV. The precision attenuation factor permits the sun signal to be read at approximately 50% of full scale at the channel output. When the first preamplifier section output falls below the threshold of the signal level detector, the second section gain returns to normal.

2.1.9.1.1 DC Restore Amplifier—Following the preamplifier is a dc level restorer which is used to establish a dc reference level when the radiometer looks into space. This is necessary because ac coupling is required by the high channel gain. The coupling time constant is made sufficiently long so that the signal droop during each scan cycle is negligible. The dc restore stage consists of a signal amplifier having a capacitively coupled field effect transistor (FET) input, an error feedback amplifier, and an FET switch forming a loop as shown in the block diagram. Closing of the FET switch causes the feedback amplifier to charge the input coupling capacitor such that the channel output is driven to zero (or some arbitrary fixed reference level).

The dc restore command which closes the FET switch is provided by the spacecraft, and occurs only when the radiometer FOV is filled by space.

With the switch FET open, the capacitor is connected only to the amplifier FET gate, providing the extremely long coupling time constant which causes negligible signal droop between dc restoration commands.

Between commands, the signal amplifier functions as a simple amplifier having a gain between 20 and 80, the exact value determined during system test and set by selection of feedback resistors in this amplifier stage. The amplifier consists of a differential pair of FETs followed by an integrated circuit operational amplifier. At the output of the dc restore amplifier is a passive low-pass filter which is used to limit the signal bandwidth (26 MHz) and determine the transient response of the channel.

2.1.9.1.2 Output Buffer Stage—The thermal channel output stage is a summing amplifier which combines the signal from the dc restoration amplifier, with a synchronization pulse train derived from the spacecraft precision timing pulse, and frame sync tone bursts. Output current limiting is also provided in the output stage. This limiting protects the channel from damage in the event of accidental application of a supply voltage or ground line to the output terminal.

2.1.9.2 Visible Channel

2.1.9.2.1 Input Buffer Amplifier—The use of the PMTs for visible channel detectors eliminates the need for high-gain, low-noise preamplifiers on the scanner. Instead, a unity gain buffer amplifier will be used to decouple capacitance from the load resistor of the PMT. The use of bootstrapping techniques in this amplifier permits an input capacitance of approximately 5 pf, for a rolloff frequency of over 300 kHz. The output impedance of the buffer amplifier is sufficiently low to drive the cable between the scanner and electronics module. Short circuit protection is incorporated in the buffer stage.

2.1.9.2.2 High-Voltage Supply—A high-voltage bias supply is used for each PMT. These supplies are located on the scanner in close proximity to the PMTs. These supplies are separately commanded ON and OFF so that a failure in one will not disable any of the other seven tubes and supplies. A nominal operating voltage of 1500 vdc is planned. A typical modular supply at appropriate rating for this application weighs approximately 1/2 lb.

2.1.9.2.3 DC Amplifiers—The visible channel dc amplifiers are located in the VISSR electronics module. The nominal gain of each channel amplifier will be approximately 30. It will be set during initial calibration of the radiometer. To take into account the possibility that significant (greater than 10%) PMT gain drift may occur after long term operation in space, a 4-step ± 3 -db gain control will be provided in each visible channel dc amplifier. The gain steps will be controllable by ground command. This feature will permit a more effective use of channel dynamic range without incurring saturation problems.

2.1.9.2.4 Output Buffer Amplifier—The low-pass filter and buffer amplifier that follow each visible channel dc amplifier will be identical to that used in the thermal channel except that the filter will have an upper cutoff frequency of 210 kHz.

2.1.9.2.5 Channel Switching—The visible channel electronics will include switching circuits which will parallel adjacent channel outputs. This switching will be accomplished by ground command. For maximum flexibility and redundancy the eight individual channels will be capable of being switched into four groups of two, two groups of four or one group of eight. (See Figure V-9).

2.2 PERFORMANCE ANALYSIS

The two most important parameters specifying the performance characteristics of a radiometer are spatial resolution and radiance resolution. For radiometers using a thermal channel, radiance resolution is frequently expressed as temperature-differential resolution specified for a particular scene temperature. Whereas, for radiometers using a visible channel, the radiance resolution is frequently expressed as a radiometer signal-to-noise value for a specified scene albedo. When the radiometer is used to produce a two-dimensional cloud cover map, the radiometer radiance resolution can be thought of as the measure of "gray scale" resolution that can be achieved. For the VISSR thermal channel, the radiance resolution also defines the inferred cloud top altitude resolution.

The radiometer spatial resolution is a measure of the degree of detail or structure that can be observed in the two-dimensional cloud cover map. For the VISSR thermal channel, detail information of the spatial resolution characteristics also can be used to provide a means of predicting the additional temperature measurement uncertainty that can be expected when the observed map structure approaches the spatial resolution of the radiometer.

In general, the spatial resolution of a radiometer is determined by the radiometer telescope and includes the effects of diffraction, aberrations and spectral filtering; the radiometer geometrical field stop; the spectral and temporal response of the detector; the angular scanning rate of the radiometer; and the frequency response of the radiometer electronics.

Theoretically, once the spatial resolution characteristics of a radiometer have been determined they can be combined with the radiometer radiance resolution for an extended source and any given map structure to determine the temperature or albedo measurement uncertainty expected for every point on the map. However, when expressing the spatial resolution characteristics of a radiometer and the map structure in generalized two-dimensional coordinates, and then determining the radiometer response for an arbitrary scan direction, this can become very involved. Therefore, the spatial resolution characteristics of a radiometer are frequently only evaluated for easily handled map patterns. Two such patterns are 1) a sine bar pattern, from which the modulation transfer function (MTF) of the radiometer can be determined for any one-dimensional spatial

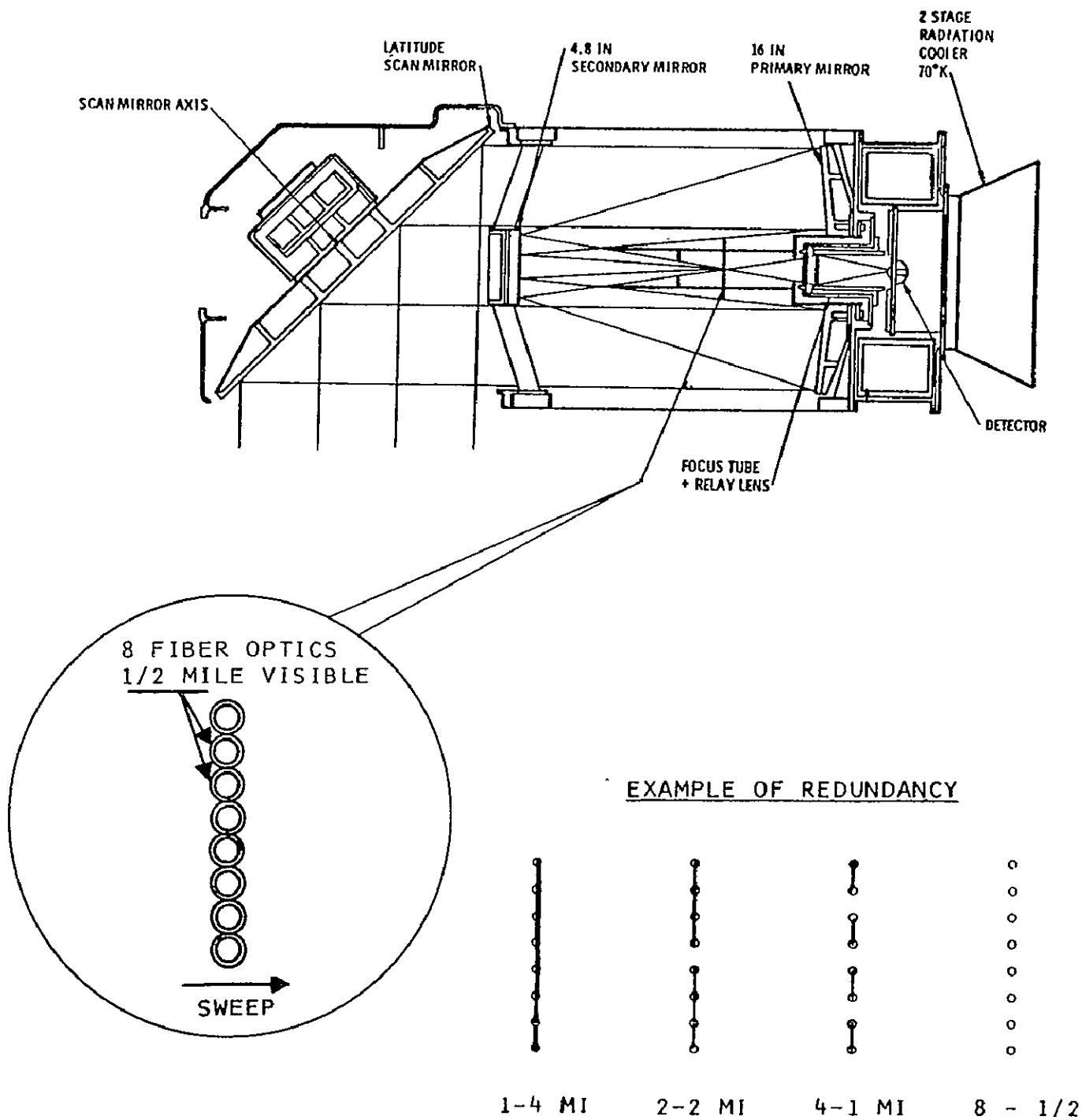


Figure V-9. Sensor Redundancy

frequency, and 2) a spot target whose angular dimension is equal to the instantaneous geometric field of view (IGFOV) of the radiometer. The ratio of radiometer peak amplitude output when scanning a spot target compared to that for an extended source is usually designated as V_p/V_{SS} .

The spatial resolution characteristics have been evaluated for the visible and thermal VISSR channels for sine bar patterns having spatial frequencies from 1 to 29,000 cycles/radian. Values of V_p/V_{SS} for the VISSR channels have been calculated for several different size square-spot targets for an assumed square FOV. The results of these calculations have been included in this section.

2.2.1 Thermal Channel

2.2.1.1 Noise Equivalent Radiance (NEN) Calculations—For a scanning (nonchopping) radiometer using a detector whose detectivity is expressed as a D^* value, the NEN of the radiometer (for an extended source) can conveniently be expressed as:

$$NEN = \frac{\sqrt{CY}\sqrt{A_d\Delta f_n}}{A_oT_o\Omega D^*} \text{ watt-cm}^{-2}\text{-sterad}^{-1} \quad (2-1)$$

- where
- C is a factor to correct for the fact that the chopping frequency at which the detector D^* was measured may be different from the frequency to which the calculated effective noise bandwidth is referred.
 - γ is the preamplifier and load resistor degradation factor which includes the effects of both preamplifier noise and signal loading.
 - A_d is the detector area in cm^2 .
 - Δf_n is the effective noise bandwidth of the radiometer in Hz.
 - A_o is the effective entrance aperture area in cm^2 .
 - T_o is the effective "transmission" factor of the radiometer optics and includes all mirrors, lenses, and filters.
 - Ω is the solid angle FOV of the radiometer in steradians.
 - D^* is the average specific detectivity of detector in the spectral band of interest in $\text{cm-Hz}^{\frac{1}{2}}\text{-watt}^{-1}$.

Listed in the following are the values for the parameters of equation 2-1 used to compute the NEN value of the VISSR thermal channel. Also listed are the VISSR design parameters and conditions on which these values are based.

- $C = 1800/2000 = 0.9$. Based on: 1) the chopping frequency used in determining the specified detector D^* being 1800 Hz, and 2) the detector frequency f_c being 2000 Hz (worst-case assumption).
- $\gamma = 1.3$. Based on experience with the type of intrinsic photoconductors proposed for the VISSR thermal channel, and preamplifier test results using low-noise transistors.
- $A_d = (D \times f / \# \times \theta)^2 = 1.44 \times 10^{-4} \text{ cm}^2$. Based on: 1) an entrance aperture diameter, D , of 16 inches (40.6 cm); 2) an effective $f/\#$ of 1.5; and 3) an IGFOV, θ , 0.2-mr square.
- $\Delta f_n = 50.4 \text{ kHz}$. Based on: 1) an information bandwidth equal to the reciprocal of twice the IGFOV dwell time, $t_{\text{dwell}} = 1.9 \times 10^{-5} \text{ sec}$; 2) a low-pass filter rolling off at 12 db/octave; 3) use of dc restoration to set the low-frequency cutoff characteristics; 4) an information gathering period, $T_1 = 0.07 \text{ sec}$; and 5) a restore network time constant, $T_2 = 0.03 \text{ sec}$.
- $A_o = (\pi/4D^2 \times 0.90) = 1170 \text{ cm}^2$. Based on: 1) an entrance aperture diameter of 16 inches (40.6 cm); and 2) central obscuration of 10% (includes secondary mirror and spider support arms).
- $T_o = (R_m^3 \times T_r \times T_f) = 0.47$. Based on: 1) three reflecting mirror surfaces with a reflectivity $R_m = 0.96$ in the 10.5- to 12.6 micron band; 2) an optical relay system with an effective transmission $T_r = 0.83$; and 3) an effective filter transmission of 0.65.
- $\Omega = \theta = 4 \times 10^{-8} \text{ steradians}$ based on an IGFOV of 0.2 mr square.
- $D^* = 1.4 \times 10^{10} \text{ cm-Hz}^{\frac{1}{2}} \text{-watt}^{-1}$. Based on: 1) an average detector D^* in the 10.5- to 12.6 micron band of $1.0 \times 10^{10} \text{ cm-Hz}^{\frac{1}{2}} \text{-watt}^{-1}$ measured under an ambient temperature background of 2π steradians; and 2) a minimum expected D^* improvement factor of 1.4 when a cold shield of approximately 1.5 $f/\#$ is used to reduce background radiation.

Using the above parameter values in equation 2-2 yields an NEN for the VISSR thermal channel of:

$$\text{NEN}_{(10.5-12.6)} = 1 \times 10^{-5} \text{ watt-cm}^{-2} \text{ sterad}^{-1} \quad (2-2)$$

2.2.1.2 Temperature Resolution and S/N—The noise equivalent temperature differentiation (NE Δ T) of a radiometer operating in the spectral band $\Delta\lambda$, and viewing a blackbody target scene at a temperature T_0 , can be expressed as:

$$NE\Delta T = NEN \left[\frac{dN(\Delta\lambda)}{dT} \right]_{T_0}^{-1} \quad (2-3)$$

where $\left[\frac{dN(\Delta\lambda)}{dT} \right]_{T_0}$ is the thermal derivative of the target scene radiance in the spectral band evaluated at the scene temperature T_0 .

The radiometer S/N output can be expressed simply as

$$S/N = N(\Delta\lambda)_{T_0} \left[NEN \right]^{-1} \quad (2-4)$$

The values of $\left[\frac{dN(\Delta\lambda)}{dT} \right]_{T_0}$ and $N(\Delta\lambda)_{T_0}$ for $\Delta\lambda = 10.5$ to 12.6 microns are plotted in Figure V-10 as a function of T.

The expected NE Δ T and S/N values for the VISSR thermal channel are shown in Figure V-11 as a function of target scene temperature for the NEN value calculated in equation 2-2.

It can be seen from Figure V-11 that for a scene temperature of 200° and 300° K, the radiometer NE Δ T values are approximately 1.5° and 0.4° K, respectively, for an extended target.

2.2.2 Visible Channel

2.2.2.1 Effective Albedo Radiance — The spectral distribution of the sun's energy outside the earth's atmosphere is shown in Figure V-12. The effective radiance value in the VISSR visible channel for an albedo of 100% is obtained by multiplying the values of Figure V-12 with the spectral response of the VISSR visible channel, integrating the resulting product over wavelength and then dividing by π . Performing these calculations yields a radiance value of

$$N_{(100\% \text{ albedo})} = 8.0 \times 10^{-3} \text{ watt-cm}^{-2}\text{-sterad}^{-1} \quad (2-5)$$

The effective irradiance at the VISSR aperture in the spectral band of a visible channel for an albedo of 0.5% can be expressed as:

$$H_{(0.5\% \text{ albedo})} = 4.0 \times 10^{-5} \times \Omega \text{ watt/cm}^2 \quad (2-6)$$

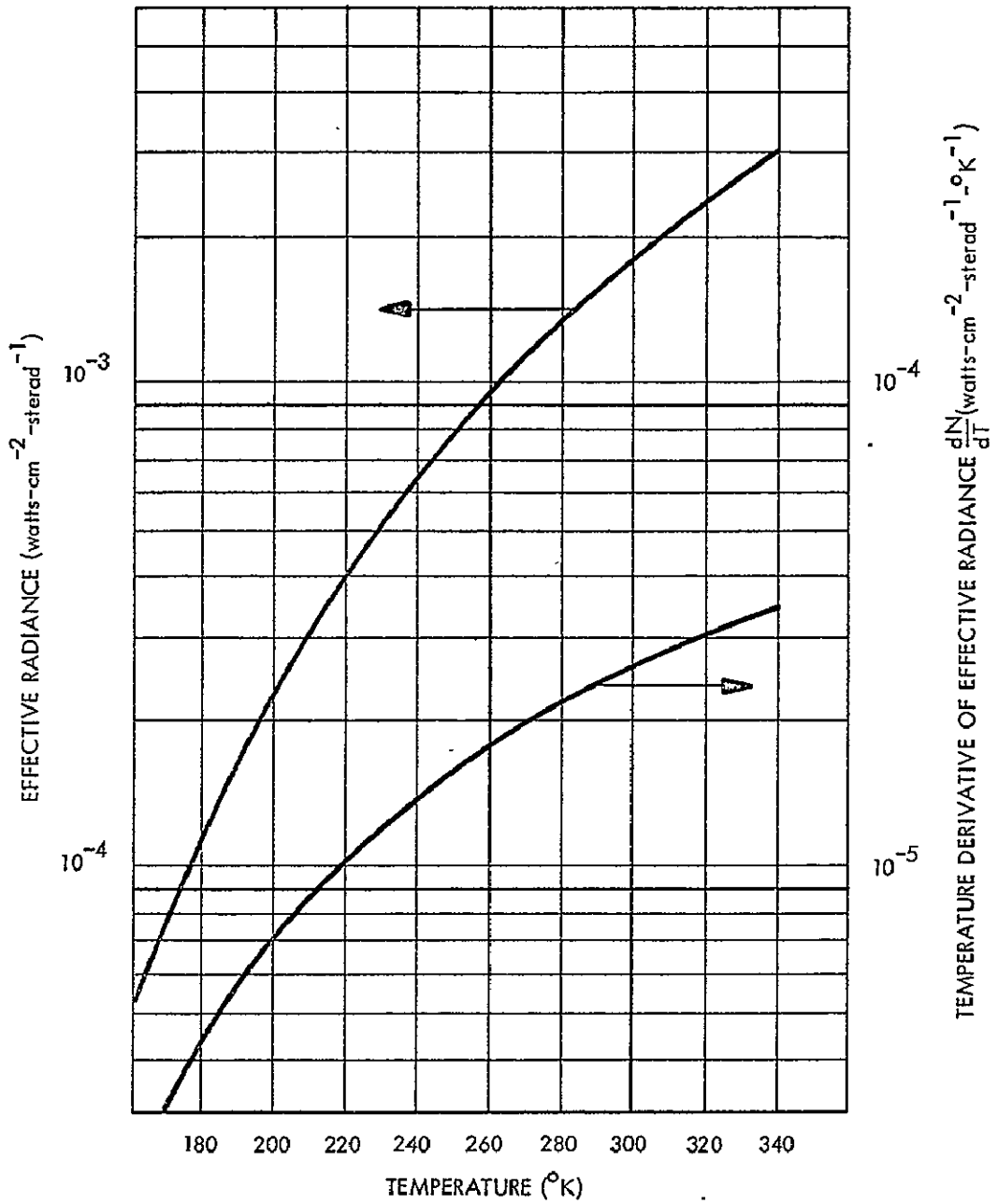


Figure V-10. Effective Radiance N and dN/dT as a Function of Target Temperature in the 10.5- to 12.6 Micron Band

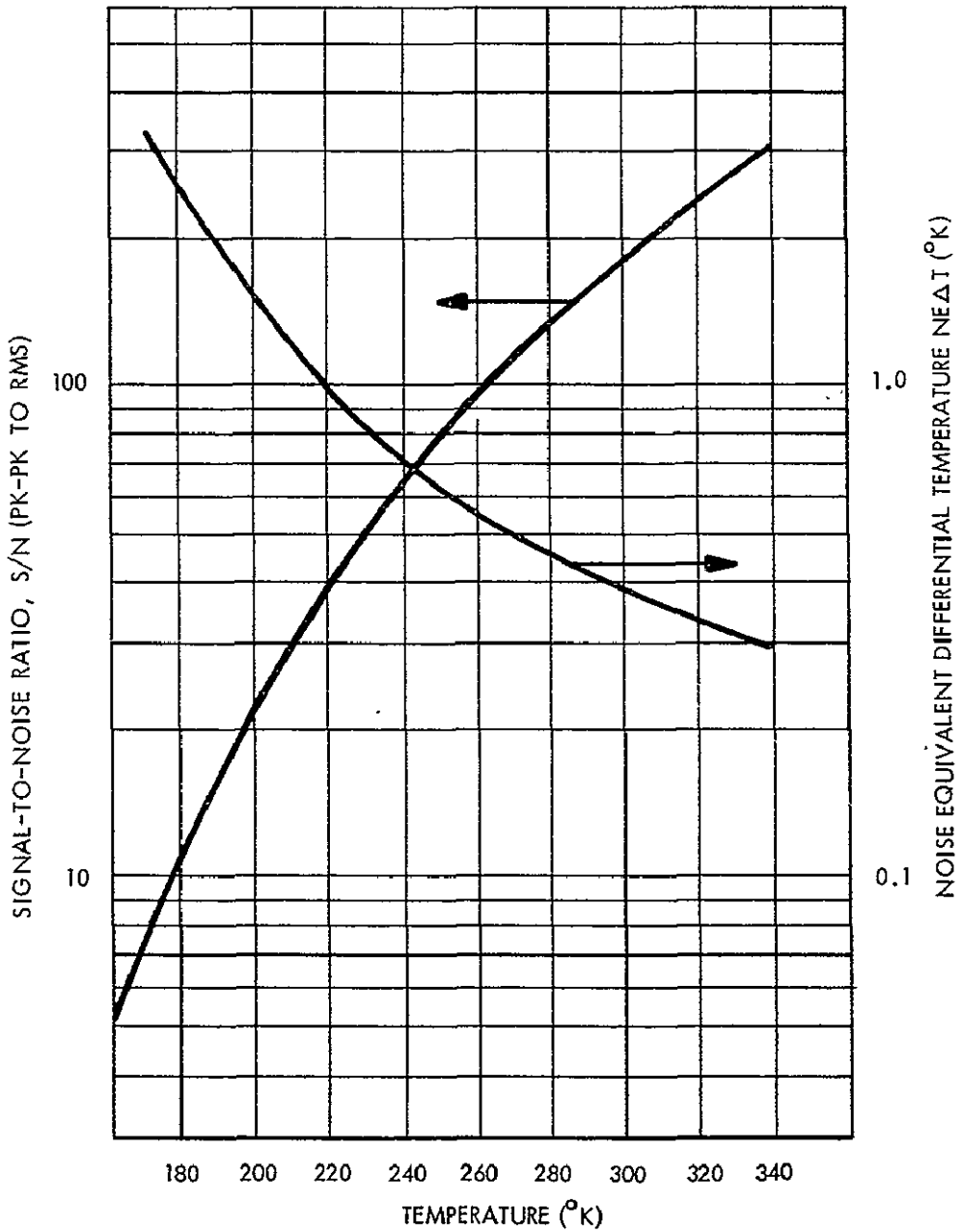


Figure V-11. VISSR Thermal Channel S/N and NEΔT as a Function of Target Temperature, T (For an Extended Target)

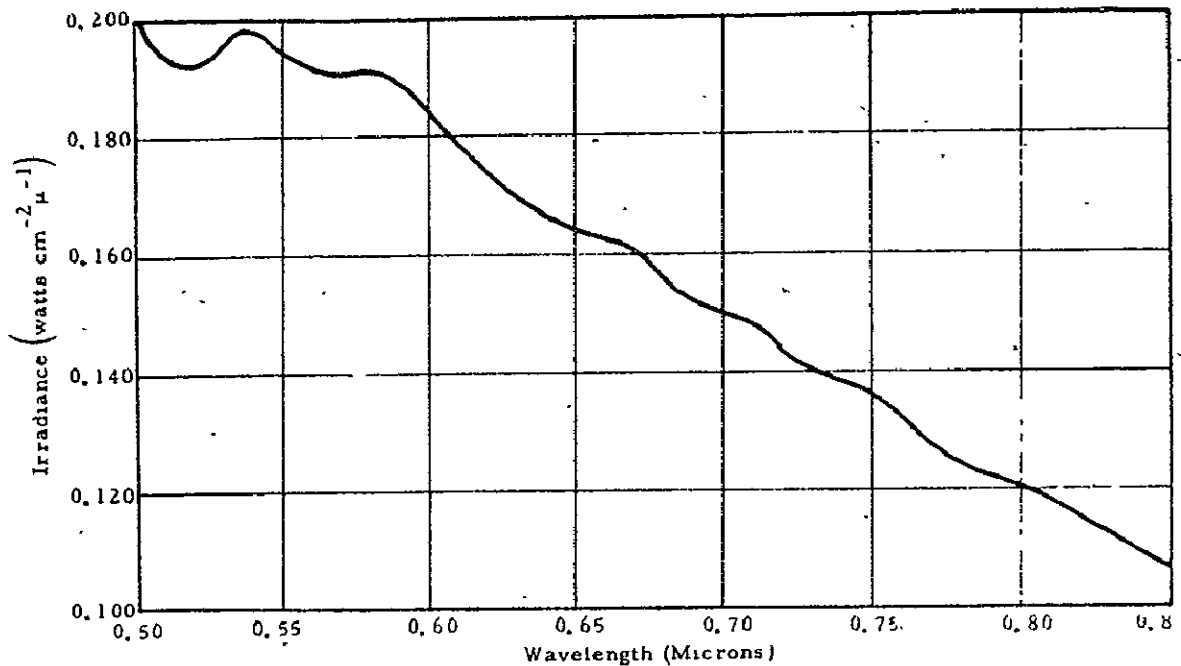


Figure V-12. Spectral Distribution of Sun's Energy Outside the Earth's Atmosphere (From the Handbook of Geophysics)

where Ω is the solid angle FOV of a VISSR visible channel in steradians.
 For $\Omega = 5 \times 10^{-10}$ steradians

$$H = 2 \times 10^{-14} \text{ watt/cm}^2 \quad (2-7)$$

2.2.2.2 Signal-to-Noise—The S/N of a VISSR visible channel can be expressed as:

$$S/N = \sqrt{\frac{HSA\tau_o(\sigma-1)}{2e\Delta f\sigma}} \quad (2-8)$$

where H is the effective irradiance at radiometer aperture (watt/cm²)

S is the peak radiant sensitivity of the photocathode surface (amps/watt)

A is the collecting aperture of the radiometer (cm²)

τ_o is the effective optical train efficiency

σ is the gain of each photomultiplier stage

e is charge of an electron (coulombs)

Δf_n is the effective noise bandwidth (Hz)

Listed in the following are the values for the parameters of equation 2-8 used to compute the S/N value of a VISSR visible channel for an albedo of 0.5%. Also listed are the VISSR design parameters and conditions on which these values were based.

$$H = 2 \times 10^{-14} \text{ watt/cm}^2. \text{ (See equation 2-6.)}$$

$$S = 0.06 \text{ amp/watt. (See Figure V-13.)}$$

$$A = 1170 \text{ cm}^2. \text{ (See Thermal Channel.)}$$

$$\tau_o = (R_m^3 \times T_{AO}) = 0.63. \text{ Based on: 1) three reflecting mirror surfaces with a reflectivity of } R_m = 0.95 \text{ in the } 0.55\text{- to } 0.70 \text{ micron band; 2) transmission of the visible channel aft optics of } 0.75; \text{ and 3) the visible channel filter transmission being included in "S" above.}$$

$$\sigma = 4. \text{ Based on a nominal PMT gain of } 10^6 \text{ for ten stages.}$$

$$\Delta f_n = 258 \text{ kHz. Based on: 1) an information bandwidth equal to the reciprocal of twice the IGFOV dwell time, } t_{\text{dwell}} = 2.4 \times 10^{-6} \text{ sec; and 2) a low-pass filter rolling off at } 12 \text{ db/octave.}$$

Using the above parameter values in equation 2-8 yields an S/N in a VISSR visible channel for an albedo of 0.5% of

$$S/N_{(0.5\% \text{ albedo})} = 2.8 = 9 \text{ db} \quad (2-9)$$

It should be noted that since the S/N only increases as the square root of the irradiance, the S/N for an albedo of 80% would be

$$S/N_{(80\% \text{ albedo})} = 36 = 31 \text{ db} \quad (2-10)$$

The S/N ratio as a function of albedo is illustrated in Figure V-14.

2.2.3 Spatial Resolution

2.2.3.1 Sine Bar Pattern Scene—The VISSR relative response*, V(f), to a given spatial frequency can be expressed as follows:

$$V(f) = O(f) \times F(f) \times E(f) \quad (2-11)$$

*Voltage output versus radiation input.

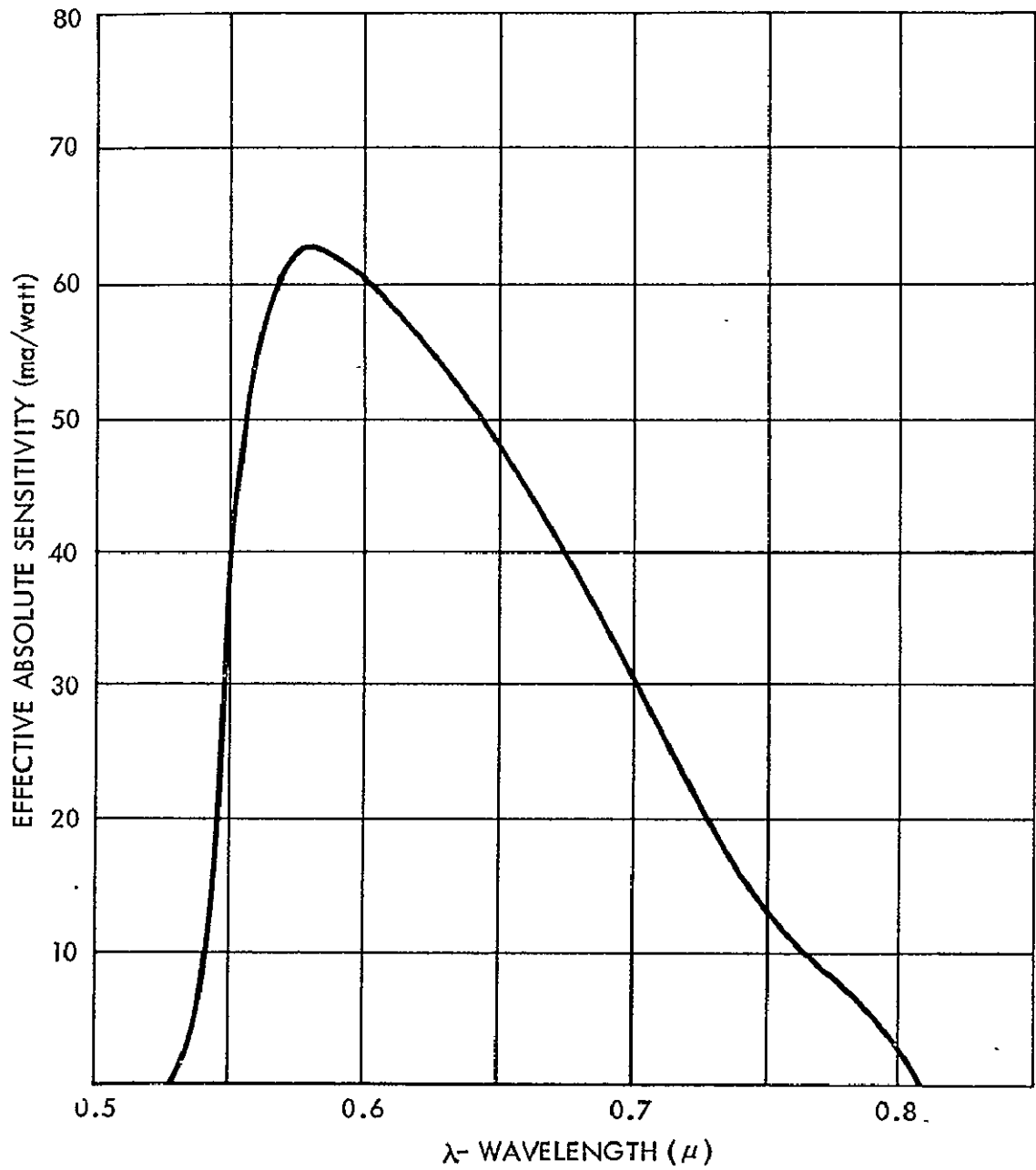


Figure V-13. Effective Absolute Spectral Sensitivity (PMT + Filter)

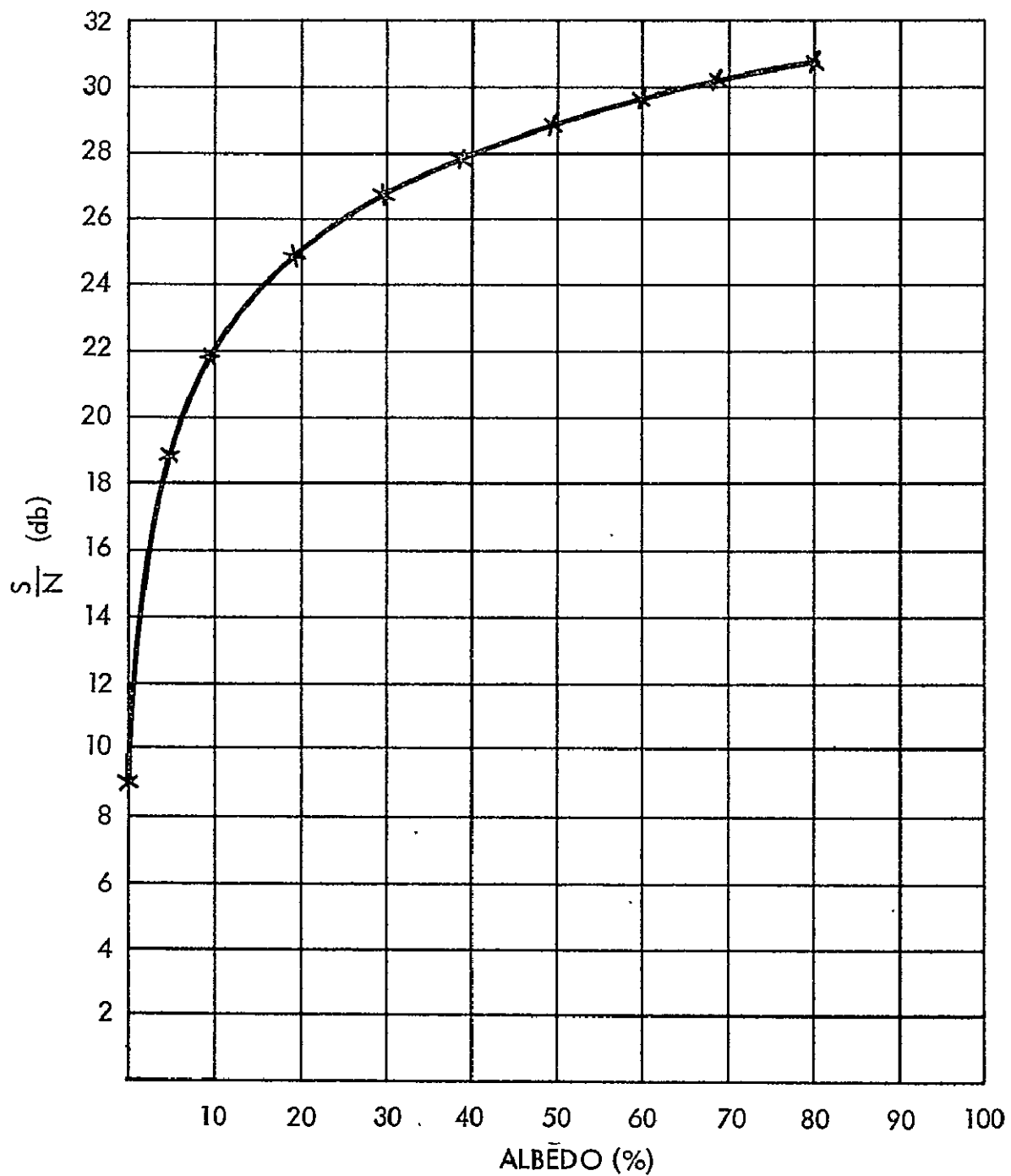


Figure V-14. VISSR Visible Channel S/N as a Function of Albedo

where $O(f)$ is the relative frequency response of the radiometer optics

$F(f)$ is the relative frequency response of the radiometer IGFOV (field stop)

$E(f)$ is the relative frequency response of the radiometer electronics

f is the frequency being considered expressed in the time domain in Hz

and the transformation of frequency from the space domain (cycles/radian) to the time domain (Hz) is accomplished by using the radiometer scan rate (radian/sec).

The diffraction pattern for the VISSR 16-inch aperture with 0.3 obscuration has been calculated by using the following equations:*

$$I(P) = \left[\frac{I_0}{(1 - \epsilon^2)^2} \frac{2J_1(Ka\omega)}{Ka\omega} - \epsilon^2 \frac{2J_1(K\epsilon a\omega)}{K\epsilon a\omega} \right]^2 \quad (2-12)$$

and

$$I_0 = \frac{H\pi^2 a^4 (1 - \epsilon^2)^2}{\lambda^2} \text{ watts sterad}^{-1} \quad (2-13)$$

where H is the uniform irradiance upon the aperture in watts cm^{-2}

a is the entrance aperture radius in cm

λ is the wavelength of the light in cm

ϵ is the ratio of obscuration radius to a

$K = \frac{2\pi}{\lambda}$

$\omega = \sin \theta$ where θ is the angular direction between point P and the geometric image point

J_1 = Bessel function of the first kind.

This diffraction pattern has been convolved with itself along a line to determine the line spread function. The angular spread of the line spread function has been converted to the time domain by using the scan rate of 10.4 radians

*M. Born and E. Wolf, "Principles of Optics," Pergamon Press, New York, N. Y. (1959).

per second (100 rpm). The resulting frequency response for a VISSR visible channel and the VISSR thermal channel is given in Figure V-15.

The effects of aberrations in the VISSR thermal channel are relatively small compared to the channel IGFOV and can be neglected. However, aberrations in the VISSR visible channels are significant compared to the IGFOV and must be taken into account. In determining the relative frequency response of the VISSR visible channel optics due to aberrations, the blur circle has been assumed to be cosine in shape.

The frequency response of a VISSR visible channel IGFOV and the VISSR thermal channel IGFOV has been determined from a $\sin x/x$ pattern converted to the time domain and the results shown in Figure V-15.

The electronic frequency response (assuming two identical isolated RC low-pass filter sections) for a 3-db cutoff frequency of 26 kHz (thermal channel) and 210 kHz (visible channel) are also plotted in Figure V-15.

The response curves shown in Figure V-15 have been appropriately combined to show the resultant frequency response for the VISSR visible and thermal channels.

For a spatial frequency having a period equal to twice the dwell time of the VISSR IGFOV (visible channel = 2×10^4 cycles/radian; thermal channel = 2.5×10^3 cycles/radian), the MTF for the VISSR visible and thermal channels are 0.34 and 0.42, respectively.

2.2.3.2 Square Source Target Scene—The value of V_p/V_{SS} (peak response to a spot target compared to that of an extended source) has been calculated for the VISSR channels for several different size square spot targets. The results of these calculations are shown in Figure V-16 for target sizes normalized to the radiometer IGFOV.

2.2.4 Bandwidth Considerations

The high frequency response requirements (Figure V-15) for both visible and thermal channels at the maximum resolution capability of each are:

- a. Visible (10 db cutoff): 225 kHz corresponding to 0.5 n. m. resolution
- b. Thermal (10 db cutoff): 30 kHz corresponding to 4.0 n. m. resolution

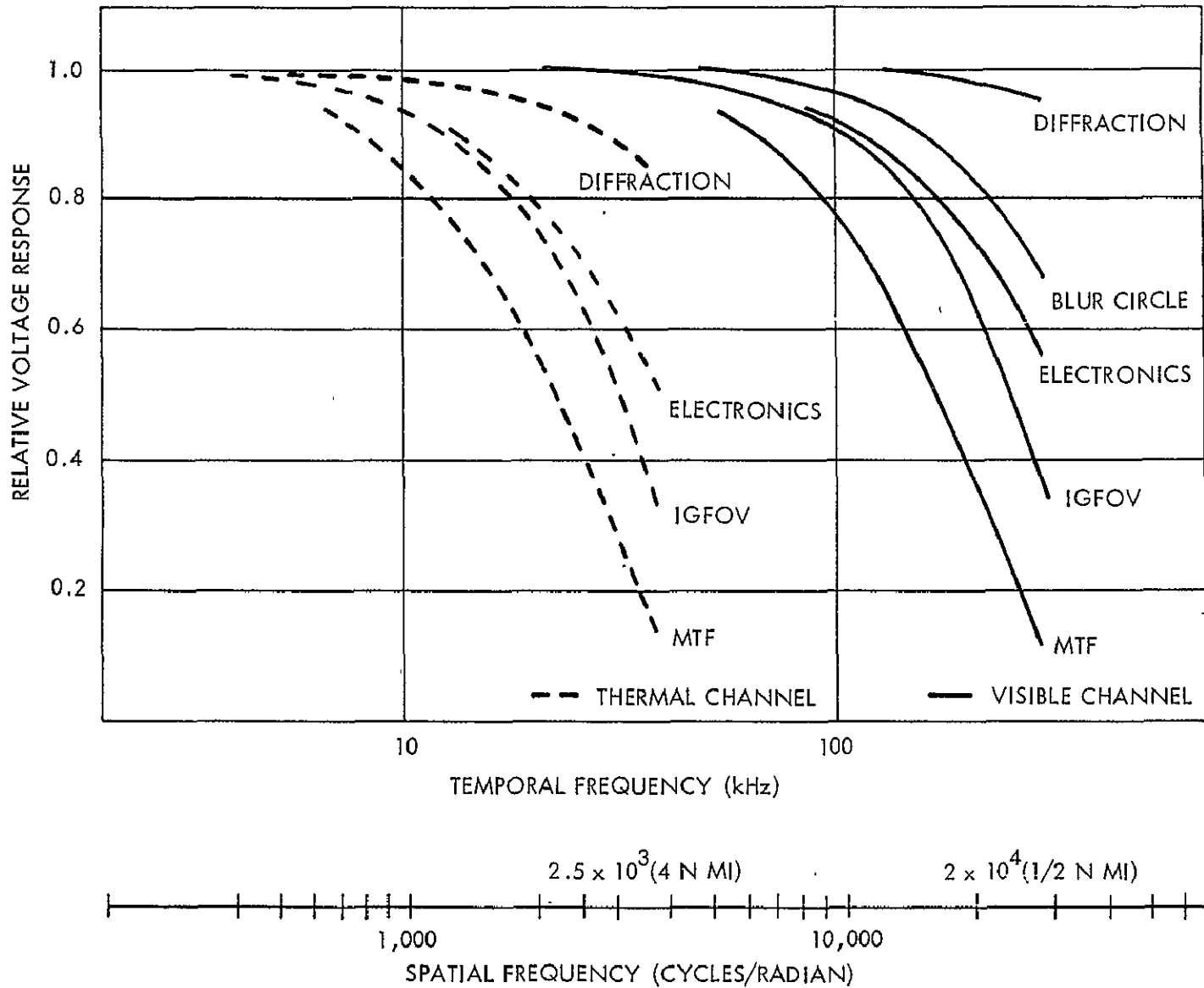


Figure V-15. Relative Frequency Response of VISSR Optics, Field Stop and Electronics

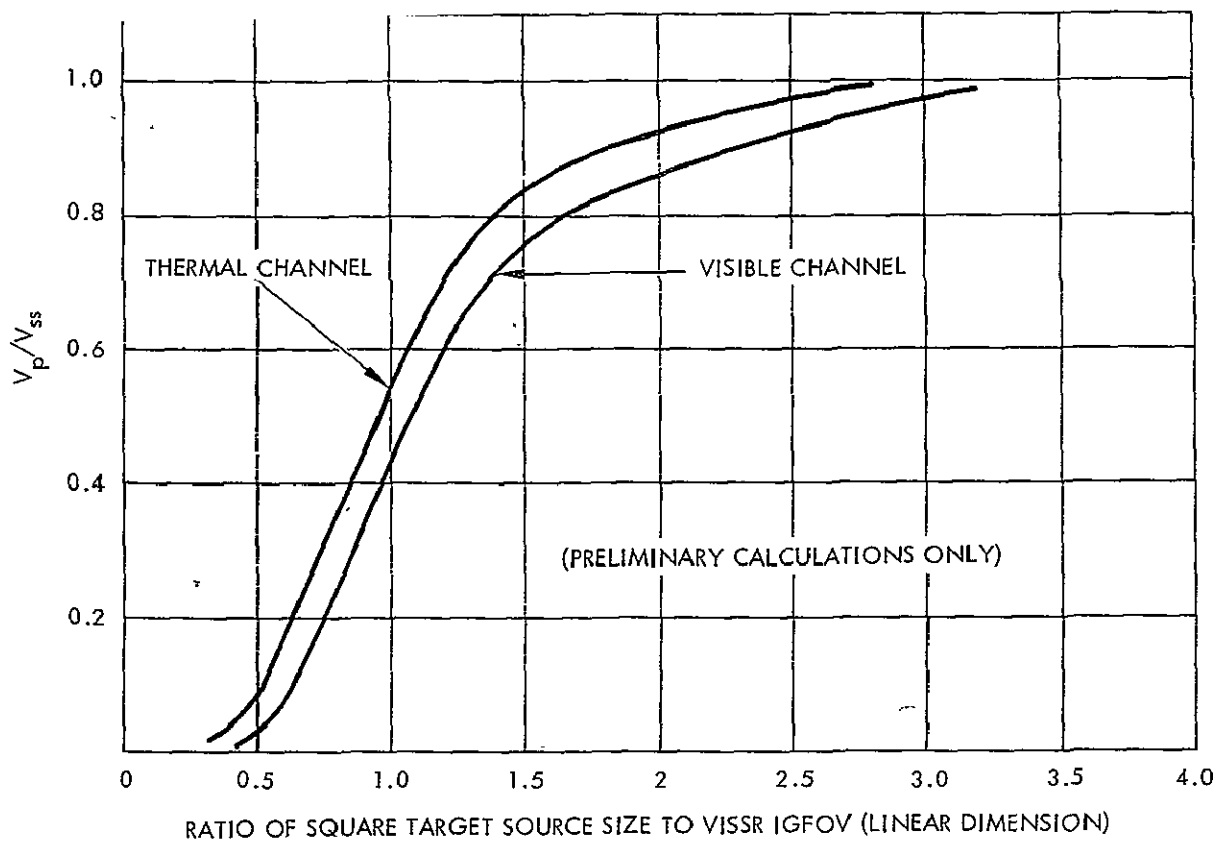


Figure V-16. VISSR V_p/V_{ss} as a Function of Target Size

Thus for maximum resolution the total baseband bandwidth (neglecting possible guard bands) will be $8 \times 225 + 2 \times 30 = 1860$ kHz.

In the SMS system it is conceivable that there will be a requirement for the capability of operating with reduced visible resolution.

The reasons for this requirement are three-fold

- a. The desire by ESSA to utilize, at least initially, their existing recording and line stretching equipment which has a capability associated with only a 2 n. mile resolution.
- b. Possible inability of ESSA to obtain approval to use an RF bandwidth sufficient to transmit the full 0.5 n. mile resolution data from the spacecraft to the ground. In this circumstance the baseband bandwidth (and the resolution) will have to be "traded off" against the required signal/noise ratio.
- c. Failure of one or more visible sensors (these are not redundant in the 0.5 n. mile mode) and/or failure of one or more of the visible down-link channels.

The technique for meeting the requirements of (1) and (2) will be to linearly sum the outputs of adjacent visible channels in various combinations upon ground command. For maximum flexibility the eight channels should be capable of being combined into four groups of two, two groups of four or one group of eight.

Since the vertical resolution of each of the visible channels is 0.5 n. mile, the above combinations will provide 1, 2 and 4 n. mile resolutions respectively.

Now it is usual and logical to always maintain the horizontal resolution equal to the vertical resolution and therefore the channel bandwidth and their corresponding resolutions will be as follows:

<u>No. of Groups</u>	<u>No. of Visible Channels per Group</u>	<u>Visible Channel Resolution</u>	<u>Group Bandwidth</u>	<u>Total Visible¹ Bandwidth</u>	<u>Total² Data Bandwidth</u>
8	1	0.5 n. miles	225 kHz	1800 kHz	1860 kHz
4	2	1.0 "	112 kHz	448 kHz	508 kHz
2	4	2.0 "	56 kHz	112 kHz	172 kHz
1	8	4.0 "	28 kHz	28 kHz	88 kHz

Operation of the scanner system in a reduced resolution mode is also appropriate under certain failure conditions. Specific equipment failures that should be considered are

- a. Failure of one or more PMT's.
- b. Failure of one or more channels in the communication link.

The following is a discussion of the reduced resolution modes to be used under these failure conditions .

2.2.4.1 PMT Failure

In the event that one or more PMT's fail, the effect is that data is no longer available for the corresponding lines in the picture. Consider, for example, the case that just one PMT fails so that data is lost for one line out of eight in the picture. Despite the fact that no real data is available for these lines, one would not wish to reproduce them as black in the final picture because of the unpleasant striping effect that would result. A better alternative is, therefore, to estimate the data values for these lines on the basis of the valid data which is available for adjacent lines. In effect, the missing data is estimated by interpolating between available data points. Various schemes for interpolation are possible. For example, first order polynomial interpolation estimates the missing data as an average of the two immediately adjacent lines of data. This is equivalent to linear interpolation. Third order polynomial interpolation uses the data from two lines on either side of the missing line and so on. Because of limitations of data storage capacity, it is

-
1. Does not include any guard bands.
 2. Includes 60 Hz for two thermal channels.

necessary to perform the interpolation in real time, so that data from at most seven lines is all that is available as inputs to the interpolation procedure. If the missing data is at the edge of the normal swath of eight lines, then the estimation procedure becomes one of extrapolation rather than interpolation. In all cases, for polynomial interpolation, the estimated data is found by a linear combination of the data from some selected group of adjacent lines, where the precise combination depends on the particular line which is missing and the order of interpolation selected. At the present time it seems that third order polynomial interpolation (or extrapolation) would be suitable but further study of other possible interpolation methods, based on scenic data models, might modify this choice.

If more than one line of data is missing, a modified interpolation scheme may be required, depending on the relative locations of the two missing lines. However, the necessary linear combinations of data to provide polynomial interpolation of any selected order are readily worked out and tabulated for all possible missing line arrangements.

The above discussion has been made on the assumption that the loss of line data is due to PMT sensor circuit failure and no associated communication link failures are assumed to exist. Interpolation of missing line data could therefore be performed either in the S/C or on the ground. However, in order to minimize S/C equipment, it is preferable to transmit the available scanner data to the ground, via the spacecraft-ground link, in the usual way, and to perform the necessary interpolation or extrapolation at the ground station prior to retransmission to the S/C. Thus it will be relatively easy to change the interpolation scheme used if experience with real data indicates a need to do so.

2.2.4.2 Communication Channel Failure

In the event that one or more channels fail in the communication link but all the PMT sensor circuits continue to operate, a reduced resolution mode is required which makes best use of the available data. If just one channel fails there is little choice other than to accept the loss of data from one sensor, and treat the available data in the same way as in the case of a PMT failure. However, taking the opposite extreme case that all but one of the channels fail, then there are clearly many alternatives possible. For example, the one remaining channel could be used to transmit an average of the output of all sensors, or alternatively the output of one sensor alone. Clearly many other such sensor combinations are possible. In general, one might consider that class of sensor signal combinations which comprises linear combinations of the sensor outputs, where each output is summed into the channel signal with its own weighting factor. Such a scheme comprises a type of spatial filtering which

is exactly analogous to the familiar transversal filter used in electric wave filters.

Because of the line scan structure, the sensor signals are in sampled form and are, in fact, sampled values of a spatial input which may or may not be band limited in a manner commensurate with the sample rate. However, once the samples (scan line data) have been taken there is no way to tell from their values whether or not the original data was suitably band limited and one may as well assume that the samples have been taken from a spatial input which is band limited at the theoretical limit of one-half the sampling rate.

In order to transmit the data over a single channel, we must effectively sample the scene at one-eighth the normal rate but, as we have seen, the available data has a bandwidth effectively eight times that which is commensurate with the lower sample rate. To avoid, or at least minimize, aliasing errors in the transmitted data one therefore wishes to filter the input so that it is as nearly as possible ideally band limited to half the new sample rate. The effective transversal filter obtained by forming a linear combination of the sensor signals can be used to accomplish just this.

The actual transversal filter available is obviously limited to 8th order by virtue of there being only 8 sensors, so that there are very definite limits on the kinds of filter responses that can be obtained. For example, a sharp cut-off filter can be only approximated, since it would take an infinite length transversal filter to achieve a sharp cut-off exactly. The frequency response of the transversal filter is periodic in the spatial frequency domain with period $2\pi/T$, where T is the inter-line spacing, and for real weighting coefficients (to which we are restricted in this application) the response is symmetric about the spatial frequency π/T . However π/T is exactly the spatial frequency to which the input data is effectively band limited. Thus the periodic nature of the response above this spatial frequency is of no consequence.

The selection of approximate weighting coefficients, with which to combine the sensor outputs, is therefore equivalent to the choice of tap weights for a transversal filter so as to approximate a band limiting filter in some convenient sense. In making such an approximation it is reasonable to consider the statistics of the actual input data. Typically the power spectral density of video data may be taken to have a $1/f^2$ character over a large part of the spatial frequency range of interest. A reasonable criterion for the filter approximation is therefore to minimize the sum of the aliased signal energy and the usable signal energy loss within the bandwidth of the original data. While such an approach is straightforward in concept, the weighting coefficients in specific cases have not yet been worked out and further study will be needed to accomplish this.

The above description has been given for the case of only one working communication channel. In the case that two communication channels were working, for example, the effective available sample rate would be twice that for one channel only and a different set of filter tap weights would be needed in order to approximate an ideal filter having twice the cut-off frequency. Similarly, if only four of the eight channels were working a different set of tap weights again would be required.

The full use of an uneven number of working channels, such as 3 or 5, is a little more difficult, since such an arrangement corresponds to a non-uniform vertical sampling rate for the picture. The number of communication channels that can be used directly in a type of reduced resolution mode described above are 1, 2, 4 or 8. If in fact some other number of channels is available, the data can be transmitted as if it were sampled at a rate corresponding to the next largest number of channels out of the set 1, 2, 4 and 8 and the missing channel or channels can then be treated in the same way as if one or more sensors had failed. (See paragraph 2.2.4.1.) In this way, maximum utilization of any number of working channels can be made.

2.3 SPACECRAFT-GROUND TRANSMISSION SYSTEM

2.3.1 Link Performance Requirements

The eight visible and two thermal channel outputs from the VISSR electronics are required to be transmitted from the spacecraft to the CDA station with minimum degradation in performance. In order to ensure that this requirement is achieved it is necessary to set minimum standards for those parameters which define the performance of the down-link.

2.3.1.1 Visible Channels

a. Signal/Noise Ratio (SNR)

Although it might seem desirable to design the down-link so that it causes negligible degradation to the VISSR SNR this is rather impractical since very high SNR's would be required (> 60 db). An acceptable compromise would be to permit the link to degrade the VISSR SNR by 1 db.

In paragraph 2.2.2.2 it is shown that, in the case of visible channels, the SNR at the VISSR output increases as the square root of albedo (irradiance) whereas the signal level at the same output point varies directly with albedo. Thus while the SNR increases by 22 db (from 9 db at 0.5% to 31 db at 80% albedo) the signal level increases by 44 db (160:1).

Now in a linear transmission link the noise level is independent of the signal level and therefore SNR varies directly with the signal.

Thus, if it was required that the down-link be linear and not degrade the VISSR SNR by more than 1 db over the full dynamic range (from 0.5 to 80% albedo) then the down-link SNR would have to be 6 db better than that of the VISSR, i. e. , $9 + 44 + 6 = 59$ db (peak-to-peak to RMS).

Now although the down-link will be only 6 db better than the VISSR at 0.5% albedo it will be $59 - 31 = 28$ db better at 80% albedo, which is unnecessary. Thus if it were possible to reproduce in the down-link channel exactly the same square root relationship as exists in the VISSR (between SNR and signal (albedo) level) then the SNR required in the down-link would be $31 + 6 = 37$ db.

Although a square root relationship may be considered to be optimum for operation with the VISSR, since this requires the lowest SNR (peak-to-peak to RMS), other relationships may be easier to implement in practice and would be acceptable provided that they did not cause more than 1 db degradation (within the 0.5 - 80% range).

b. Amplitude-Frequency Response

The next performance parameter to be considered is the amplitude-frequency response of the downlink channel. Reference to Figure V-13 indicates that the modulation transfer function (MTF) of the visible channel is such that the output signal level is 10 db below maximum at 225 kHz. It may also be seen that the frequency corresponding to a resolution of 0.5 n. miles is 210 kHz. In order to provide a small working margin it seems desirable to utilize the higher frequency (of 225 kHz) for the 3 db channel bandwidth thus ensuring that the downlink channel does not appreciably degrade the camera resolution.

The low frequency amplitude response required in the downlink channel may be evaluated in terms of the permissible "tilt" in a constant peak amplitude video signal with a duration equal to the earth scan time, that is, 30 m. secs.

The effect of "tilt" on a video signal is to cause an increasing error (with time) in the color rendition of the reproduced picture during prolonged scanning of a scene with uniform coloration. It will be apparent that for a "near black" scene even small "tilts" will have quite a significant effect on the picture coloration. Ideally it would be desirable to limit "tilt" to less than 0.1%; however, this would cause serious design problems and, therefore, a maximum tilt of 1% must be accepted as a compromise between desired performance and cost.

Now it can be shown that for tilt <0.1 (10%)

$$\text{Tilt} = \frac{t}{\tau}$$

where

t = duration of the signal

τ = circuit time constant

and

$$\tau = \frac{1}{2\pi f_c}$$

where

f_c = frequency of the 3 db cut-off point

therefore,

$$f_c = \frac{\text{Tilt}}{2\pi t} \quad .$$

Hence in the particular case of interest here

$$\text{Tilt} = 0.01 \text{ (1\%)} \quad .$$

and

$$t = 30 \times 10^{-3} \text{ secs} \quad .$$

Therefore

$$f_c(3 \text{ db}) = \frac{0.01}{2\pi \times 30 \times 10^{-3}} = 0.05 \text{ Hz} \quad .$$

This then is the frequency corresponding to the point where the amplitude/frequency response is 3 db down.

From the above then it is apparent that the low frequency response required extends down to only a few hundredths of a Hz.

c. Amplitude Linearity

Amplitude non-linearities, provided they are not excessive do not cause serious problems in the link since they can be calibrated out on the ground. It is very important however, that the linearity remain stable after calibration. Experience shows that a linearity of 1 percent (deviation from a best-fit straight line) is both attainable and acceptable.

d. Phase-Frequency Response

The last parameter to which attention must be directed is the phase-frequency response required in the baseband downlink channels. Phase distortion is most likely to occur at the extreme ends of the baseband spectrum, that is, near 200 kHz and below about 100 Hz. Phase distortion at high frequencies causes excessive "post ringing" on video signals containing sudden transitions and this results in repetitive images, following the real image, in the received picture. If the amplitude of the ringing is sufficiently large and

the frequency is below the upper cut-off frequency of the channel these images will be reproduced in the processed picture.

At the present time there do not appear to be any accepted standards for high frequency phase distortion or alternatively for ringing except to state that the ringing frequency should desirably exceed the channel cut-off frequency.

As far as low frequency phase distortion is concerned this will manifest itself in a similar way to poor low frequency amplitude response, that is, it will cause "tilt" of a constant amplitude video signal. It should therefore be practicable to combine these two parameters together and limit the amount of acceptable tilt due to both.

Now a circuit with a 3 db cut-off frequency of 0.05 Hz will, in fact, have a phase shift of 0.1 degrees at 30 Hz. It will be assumed therefore that the permissible phase shift is 0.1 degrees at 30 Hz and therefore the total acceptable tilt, due to both amplitude and phase effects, will be 1 percent.

2.3.1.2 Thermal Channel

a. Signal/Noise Ratio

Figure V-11 gives the values of thermal channel SNR corresponding to various target temperatures.

For design purposes the maximum target temperature will be taken to be 330°K and the minimum to 180°K. The corresponding SNR's will be 48 db $\frac{P-P}{RMS}$ and 21 db $\frac{P-P}{RMS}$ respectively.

In the thermal radiometer the SNR is directly proportional to signal level (i. e., the output noise level is constant and independent of signal level); therefore, it is desirable for the downlink channel to have the same characteristic.

For the same reasons discussed under visible channels it will be an acceptable compromise for the down-link to degrade the VISSR SNR's by 1 db. The SNR's required of the link will be therefore 54 db $\frac{P-P}{RMS}$ at 330°K and 27 db $\frac{P-P}{RMS}$ at 180°K.

Reference to equations 2-3 and 2-4 shows that at any given temperature, T, the temperature resolution $NE\Delta T$ is inversely proportional to SNR (voltage ratio) hence the overall resolution (VISSR plus link) will be 0.35°K at 330°K and 2.8°K at 180°K. (By comparison the VISSR resolution is 0.31°K at 330°K and 2.5°K at 180°K).

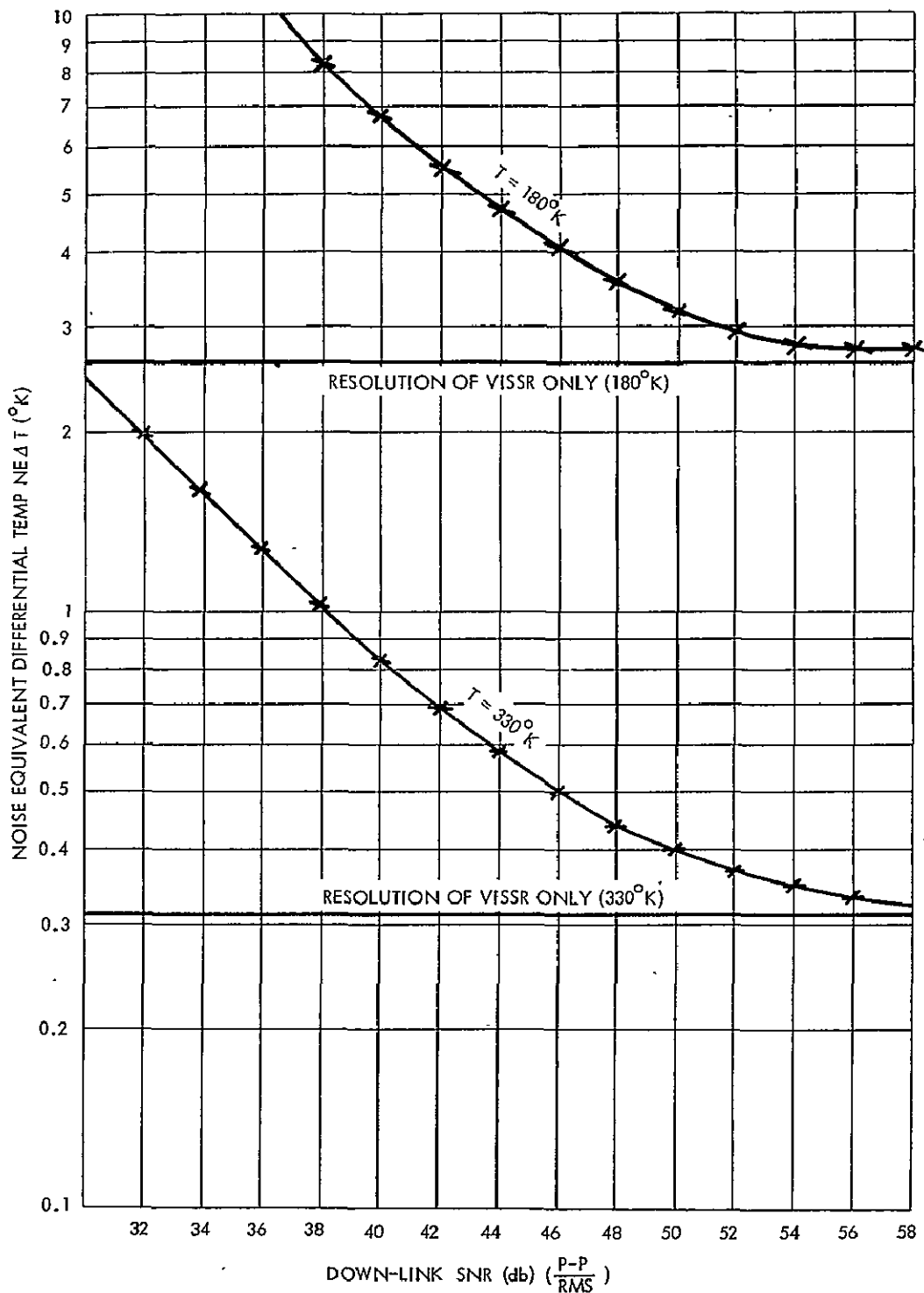


Figure V-17. VISSR Thermal Channel NEΔT as a Function of Down-Link SNR at T = 330°K and 180°K (assuming link noise is constant)

Figure V-15 shows a graph of noise equivalent differential temperature (resolution), $NE\Delta T$, versus downlink SNR, at $T = 330^\circ K$ and $T = 180^\circ K$ from which the effect of utilizing various downlink SNR's may be assessed.

b. Amplitude-Frequency Response

Having established the SNR required in the thermal downlink channel the next parameter to be discussed is the amplitude-frequency response necessary to transmit the thermal data without significant degradation. Figure V-15 shows the MTF of the thermal channel and indicates that the signal level is 10 db below maximum at very nearly 30 kHz. It may also be seen that the frequency associated with a resolution of 4 n.m. is 26 kHz. In order to insure that the downlink channel does not significantly degrade the radiometer resolution, the higher frequency (of 30 kHz) will be utilized as the upper 3 db cut-off point.

The evaluation of the required low frequency response may be based on the same type of analysis as was used for the visible channels. However, the amount of acceptable "tilt" in a constant amplitude video signal must be reassessed for the thermal situation.

From Figure V-10 it can be seen that, for all practical purposes, the change in the logarithm of Effective Radiance, $N(\Delta\lambda)_T$, is directly proportional to the change in target temperature for small temperature changes, say, $\Delta T < 5^\circ K$ i. e., $\Delta \log [N(\Delta\lambda)_{T_0}] \propto \Delta T$ for $\Delta T < 5^\circ$

$$\therefore \Delta \log [N(\Delta\lambda)_{T_0}] = \beta \Delta T \text{ for } \Delta T < 5^\circ .$$

By graphical methods it can be shown that at $T_0 = 330^\circ K$, $\beta \approx 0.006$ and $N(\Delta\lambda)_{T_0} = 2.5 \times 10^{-3}$.

Now at $330^\circ K$ the temperature resolution ($NE\Delta T$) of the VISSR will be $0.31^\circ K$ and it would be desirable therefore to restrict the "tilt" to this same amount (that is, hold the error due to tilt equal to one resolution element). For $T_0 = 330^\circ K$ & $\Delta T = 0.31^\circ K$, $\Delta \log [N(\Delta\lambda)_{330}] = 0.0019$

$$\text{Now } N(\Delta\lambda)_{330} = 2.5 \times 10^{-3}$$

$$\text{and } \log [N(\Delta\lambda)_{330}] = -2.6021$$

therefore, $\log \left[N (\Delta \lambda)_{330} - \Delta T \right] = -2.6040$

$$\text{and } N (\Delta \lambda)_{330} - \Delta T = 2.49 \times 10^{-3}$$

From equation 2-37 it is apparent that since NEN is a constant then the signal at T_o is proportional to $N (\Delta \lambda)_{T_o}$

$$\text{i. e., } S_{T_o} \propto N (\Delta \lambda)_{T_o}$$

therefore, $S_{T_o} = \gamma \left[N (\Delta \lambda)_{T_o} \right]$ (since it may be assumed that $S = 0$ when $N (\Delta \lambda) = 0$).

$$\text{Now Tilt}_{T_o} = \frac{S_{T_o} - S_{T_o} - \Delta T}{S_{T_o}} = \frac{N (\Delta \lambda)_{T_o} - N (\Delta \lambda)_{T_o} - \Delta T}{N (\Delta \lambda)_{T_o}}$$

$$\begin{aligned} \text{therefore, Tilt}_{330} &= \frac{(2.5 \times 10^{-3}) - (2.49 \times 10^{-3})}{2.5 \times 10^{-3}} \\ &= \frac{0.01 \times 100 \%}{2.5} \\ &= 0.4\% \end{aligned}$$

Therefore from the above analysis it is proposed that the tilt be limited to 0.4%.

By the same analysis as was used in the case of visible channels (see paragraph 2.3.1.1) it can be shown that this corresponds to a 3 db cut-off frequency of 0.02 Hz.

c. Amplitude Linearity

For the same reasons given in the discussion of visible channels the amplitude linearity should be at least 1% and stable.

d. Phase-Frequency Response

The last parameter of concern is the phase-frequency response and again at the higher frequencies the thermal channels have similar requirements to the visible channels except that the frequency of any ringing, due to phase distortion in the vicinity of the high frequency cut-off point, should exceed 30 kHz.

The phase shift at 30 Hz should not exceed 0.08 degrees to ensure that the "tilt" on a 30 m. sec. constant amplitude signal will not exceed 0.8%.

2.3.2 Link Testing

Before launch it will be essential to carry out a series of tests on simulated down-link channels to ensure that the performance requirements of paragraph 2.3.1 have been achieved in all respects.

In view of the very considerable amount of work done in the field of performance testing of standard commercial television transmission channels it is strongly recommended that similar techniques be utilized for SMS testing.

Thus it is considered that the following tests should be performed on each channel:

- a. Signal/noise ratio (including inter-channel crosstalk and intermodulation distortion with signals on all channels).
- b. Amplitude-frequency response (to sine wave signals).
- c. Low frequency waveform distortion (tilt on a 30 m. sec. constant amplitude signal).
- d. Amplitude linearity
- e. Short-time linear waveform distortion (response to a transition of maximum peak-peak amplitude and a rise time

$T_1 = 2.2 \mu\text{sec.}$ for visible channels and $T_2 = 16.7 \mu\text{sec.}$ for thermal channels).

- f. Pulse distortion (response to a sine-squared pulse with a half-amplitude duration of $T_1 = 2.2 \mu\text{sec.}$ for visible channels and $T_2 = 16.7 \mu\text{sec.}$ for thermal channels).
- g. Gain stability (over a period of 12 hr).

2.3.3 Selection of Down-Link RF Frequency and Bandwidth

2.3.3.1 Bands Available—The frequency bands for down-links from meteorological satellites have been allocated as follows:

<u>I. T. U.</u>	<u>U. S. A. (IRAC)</u>
137-138 MHz	137-138 MHz
400.05-402 MHz	400.05-402 MHz
—	417-419 MHz
1690-1700 MHz	1670-1700 MHz
—	2025-2120 MHz
7300-7750 (any 100 MHz)	7450-7550 MHz
8025-8400 MHz	8175-8215 MHz

2.3.3.2 Bandwidth Limitations—Later in this report it is shown that the RF bandwidth requirements are on the order of 25 MHz. This will have a most significant effect on the choice of the down-link frequency.

Apart from crowding in existing bands, particularly at 136 and 400 MHz, there is a limitation resulting from differential phase shift through the ionosphere.

It has been shown* that for transmission through the ionosphere, the coherence half-bandwidth near the equator is:

$$\Delta F = \frac{F^2 (1 - 0.928 \cos^2 \phi)^{\frac{1}{2}}}{1.69 \times 10^5} \Delta \theta$$

* "OPLE Satellite Transponder Study Report," Hughes Aircraft Co., Contract NAS-5-10174, July 1966.

where ΔF = half-bandwidth in MHz

F = carrier frequency in MHz

ϕ = elevation angle at the ground

$\Delta\theta$ = allowable phase difference between sidebands

$$\therefore F = \sqrt{\frac{\Delta F \times 1.69 \times 10^5}{(1 - 0.928 \cos^2 \phi)^{\frac{1}{2}} \Delta\theta}} \quad \text{MHz} .$$

Assuming that SMS is located between 90° and 110° W longitude, the elevation at Wallops Island will be between approximately 35° and 45° .

Taking $\Delta\theta = \frac{\pi}{2}$ the value of F will then be between 1210 and 1320 MHz.

Thus, on this consideration alone the possible use of the 137 and 400 MHz bands is eliminated.

The next higher available band is therefore 1690 - 1700 MHz. Although this band is only 10 MHz wide, it is reasonable to assume at this time that approval might be obtained for a 25 MHz bandwidth. At 1690 MHz the coherence half-bandwidth is between 16.3 and 19.4 MHz. This is adequate for the radiometer down-link.

Naturally, at even higher frequencies there would be no real bandwidth limitation, however, there does not seem to be anything in favor of going higher. Spacecraft antenna design would be more complicated, the spacecraft transmitter would have to use travelling wave tubes in lieu of solid state devices and the requirements on the ground antenna and receiver would become more stringent.

It is therefore recommended that the radiometer data down-link transmitter system utilize a frequency in the vicinity of 1690 MHz.

2.3.4 RF Link Calculation at 1690 MHz

Before making this calculation it is necessary to discuss briefly reasons for selecting the parameters involved.

(1) Spacecraft Transmitter Power

Considering the desirability of utilizing solid state devices in the output stages of the transmitter both from reliability and dc power economy aspects, the RF output power will be limited to 20 watts by the present state-of-the-art and available spacecraft power.

(2) Spacecraft Antenna Gain

Since the antenna is required to provide earth coverage, the half-power beamwidth must be at least 17.3° . From previous experience with electronically phased arrays (similar to that proposed for SMS) it is estimated that the efficiency is somewhat less than can be obtained from a parabola, probably on the order of 10 percent less. On this basis the achievable gain will therefore be about 18 db excluding feed losses.

(3) Ground Antenna Gain

For economic reasons it is desired that the antenna not exceed 40 feet diameter. This will provide a gain of 44.2 db at 1690 MHz.

(4) Ground Receive System Temperature

The ground receiver will be assumed to be a cooled parametric amplifier with a noise temperature of about 25° K. Based on this it should not be too difficult to realize a total system temperature of 100° K at SMS elevations.

Down-Link Calculation (1690 MHz)

Spacecraft transmitter power (dbm)	+ 43.0
Feed losses (db)	- 1.5
Spacecraft antenna gain (db)	+ 18.0
Off-beam-center loss	- 3.0
Path loss (to Wallops Island) (db)	-189.0
Ground antenna gain (db)	+ 44.2
Receiver losses (db)	- 1.0
Received signal level (dbm)	- 89.3
Receiver noise power density (dbm/Hz)	-178.6
Carrier/noise power density (db-Hz)	+ 89.3

Carrier/noise (20 MHz) (db)	<u>16.3</u>
Carrier/noise (25 MHz) (db)	<u>15.3</u>
Margin (db)	<u>2-3</u>

NOTE: The margin shown is that available for digital transmission with approximately 1×10^{-5} error rate. This will also maintain an analog FM transmission above threshold.

2.3.5 Comparison of Multiplexing & Modulation Techniques

The multiplexing/modulation techniques which it is considered should be evaluated for the radiometer down-link transmissions are;

- a. SSSC/FDM/FM
- b. DSB/FDM/FM
- c. VSB/FDM/FM
- d. TDM/PAM/FM
- e. TDM/PCM/PSK

Each of these will be evaluated to determine its ability to provide the performance required. (See para. 2.3.1.1. and 2.3.1.2.)

From discussions with responsible persons in NASA and ESSA it is assumed that the maximum RF bandwidth available in the 1690 MHz band will be 25 MHz. Even this will require a special approach to the I. T. U. as the existing allocation is only 10 MHz and a number of meteorological satellites already occupy this band.

2.3.5.1 SSSC/FDM/FM—This technique would frequency multiplex all 8 visible and 2 (redundant) thermal channels and then allow the composite signal to frequency modulate the down-link carrier.

The individual channel sub-carriers would be suppressed in the up-conversion process.

Figure V-18 shows a suitable arrangement of an FDM spectrum containing 2 thermal and 8 visible channels.

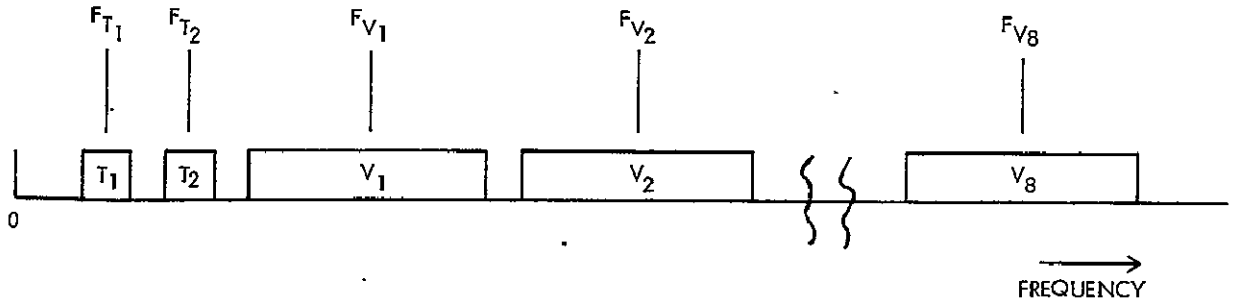


Figure V-18. SSSC/FDM Frequency Spectrum

Frequencies f_{T_1} , f_{T_2} , f_{V_1} - f_{V_8} are the center frequencies of channels T_1 , T_2 , V_1 - V_8 respectively.

For FM modulation the signal/noise ratio SNR at the output of the demodulator is given by

$$SNR = \left(\frac{C}{N_0} \right) \left[\frac{3 (\Delta f)^2}{2(f_2^3 - f_1^3)} \right] \quad (2-14)$$

where ΔF = peak deviation

f_2 = upper frequency

f_1 = low frequency

and C/N_0 = carrier/noise power density at the demodulator input.

$$\text{Now } f_2^3 - f_1^3 = (3 f^2 + \frac{B^2}{4}) B$$

where $f = \frac{f_2 + f_1}{2}$ = channel center frequency

and $B = f_2 - f_1$ = channel bandwidth

$$\text{Also in general } 3f^2 \gg \frac{B^2}{4} \quad (\text{even as } f \rightarrow B) \quad (2-15)$$

$$\therefore f_2^3 - f_1^3 \approx 3 f^2 B .$$

Inserting this result in equation 2-14 it becomes;

$$\text{SNR} = \left(\frac{C}{N_0} \right) \left(\frac{(\Delta f)^2}{2 f^2 B} \right) \quad (2-16)$$

In paragraphs 2.3.1.1 and 2.3.1.2 it was shown that for linear channels, i. e. SNR proportional to signal level, the SNR required for visible channels is 59 db (peak-peak to RMS) and that for thermal channels is 54 db (peak-peak to RMS). However, the bandwidth ratio difference is 9 db in favor of the thermal channel. Therefore the modulation indices, $M = \frac{\Delta f}{f}$, for the visible channels must be equal and 5 times (14 db) those of the thermal channels since $\text{SNR} \propto M^2$.

$$\text{That is, } M_{V_N} = 5M_{T_n} .$$

$$\text{Now if } M_{V_1} = M_{V_2} = M_{V_N} = 5M_{T_1} = 5M_{T_2}$$

$$\text{then } \frac{\Delta f_{V_1}}{f_{V_1}} = \frac{\Delta f_{V_2}}{f_{V_2}} = \frac{\Delta f_{V_N}}{f_{V_N}} = \frac{5 (\Delta f_{T_1})}{f_{T_1}} = \frac{5 (\Delta f_{T_2})}{f_{T_2}}$$

where Δf = peak deviation.

From inspection of Figure V-18 it may be seen that it is feasible to arrange the spectrum so that $f_{T_2} = 2 f_{T_1}$, $f_{V_2} = 2 f_{V_1}$, and $f_{V_N} = Nf_{V_1}$, since the bandwidth of the thermal channels is 30 kHz and that of the visible channels is 225 kHz.

It is also possible to arrange that $f_{V_1} = 7.5 f_{T_1} = 3.75 f_{T_2}$ and hence $f_{V_N} = 7.5 Nf_{T_1}$.

$$\text{Now since } \frac{\Delta f_{V_N}}{f_{V_N}} = \frac{5 (\Delta f_{T_1})}{f_{T_1}}$$

$$\text{therefore } \Delta f_{V_N} = 37.5 N (\Delta f_{T_1})$$

and similarly $\Delta f_{T_2} = 2 (\Delta f_{T_1})$.

Now in the extreme all of the signals in the 10 channels will add in phase and the total peak deviation will be the sum of all the individual peak deviations.

$$\begin{aligned} \text{Hence } \Delta f_{\text{peak}} &= \sum_{n=1}^2 \left[n (\Delta f_{T_1}) \right] + \sum_{N=1}^8 \left[37.5 N (\Delta f_{T_1}) \right] \\ &= 3 (\Delta f_{T_1}) + 1250 (\Delta f_{T_1}) \\ &= 1253 (\Delta f_{T_1}) . \end{aligned}$$

Before proceeding it is necessary to structure the FDM spectrum in accordance with the assumptions made in the analysis above.

Firstly the bandwidth of the thermal channels $B_T = 1.2 \times 30 = 36$ kHz allowing 20 percent for guard bands and that of the visible channels is $B_V = 1.2 \times 225 = 270$ kHz.

These rather wide guard bands will obviate the need for sharp cut-off filters (with poor phase response) since phase distortion requirements are quite stringent.

Thus, the spectrum should be arranged so that,

$$f_{T_1} = 36 \text{ kHz}$$

$$f_{T_2} = 2 \times 36 = 72 \text{ kHz}$$

$$f_{T_2} = 270 \text{ kHz } (=7.5 f_{T_1})$$

$$f_{T_8} = 2160 \text{ kHz } (=7.5 \times 8 \times f_{T_1}) .$$

Based on these center frequencies the total composite baseband bandwidth, B_{BB} , will be $2160 + \frac{225}{2} = 2,273$ kHz.

Now assuming that the absolute maximum available RF bandwidth, B_{RF} , is 25 MHz the permissible deviation, by Carson's rule, is

$$\begin{aligned}\Delta f_{\text{peak}} &= \frac{B_{RF}}{2} - B_{BB} \\ &= 12.5 - 2.27 = 10.23 \text{ MHz}\end{aligned}$$

$$\begin{aligned}\Delta f_{T_1} &= \frac{10.23 \times 10^3}{1253} \text{ kHz} \\ &= \underline{8.2 \text{ kHz}}\end{aligned}$$

Hence $\Delta f_{V_1} = \underline{307 \text{ kHz}}$

We can now proceed to calculate the SNR's in both the thermal and visible channels remembering that the thermal SNR's will be equal and some 5 db less than the visible channel SNR (which will also be equal).

Thus the first thermal channel signal/noise ratio,

$$(\text{SNR})_{T_1} = \left(\frac{C}{N_o}\right) \frac{(8.2 \times 10^3)^2}{2 \times (36 \times 10^3)^2 \times 30 \times 10^3}$$

(note that the information bandwidth is only 30 kHz)

$$= \left(\frac{C}{N_o}\right) - 60.6 \text{ db} .$$

In paragraph 2.3.4 it was calculated that $C/N_o = 90.3 \text{ db-Hz}$.

$$\begin{aligned}\text{Therefore } (\text{SNR})_{T_1} &= 29.7 \text{ db} \left(\frac{\text{RMS}}{\text{RMS}}\right) \\ &= \underline{38.7 \text{ db} \left(\frac{\text{P-P}}{\text{RMS}}\right)}\end{aligned}$$

The first visible channel signal/noise ratio,

$$\begin{aligned}(\text{SNR})_{V_1} &= \left(\frac{C}{N_o}\right) \frac{(307 \times 10^3)^2}{2 \times (270 \times 10^3)^2 \times 225 \times 10^3} \\ &= \left(\frac{C}{N_o}\right) - 55.4 \text{ db}\end{aligned}$$

$$\begin{aligned} \text{therefore, } (\text{SNR})_{V_1} &= 34.9 \text{ db } \left(\frac{\text{RMS}}{\text{RMS}} \right) \\ &= 43.9 \left(\frac{\text{P-P}}{\text{RMS}} \right) \end{aligned}$$

It will be seen that both of these values are 15 db less than required. Now it is true that the percentage of the time that all 10 signals will add in phase is probably quite small, even though adjacent visible channels are highly correlated; however it is estimated that the SNR's would be improved by no more than 4-5 db by allowing the system to over-deviate say 1% of the time.

The only other device which might improve the SNR's would be to use non-linear companding as discussed in paragraphs 2.3.1.1 and 2.3.1.2. The analysis of the effect of channel companders on the analog video data is very complicated and will not be attempted here. Suffice to say that instantaneous companding will generate harmonics and intermodulation products which will considerably widen the transmission bandwidth*. Since this increased bandwidth will necessarily result in a reduction in the total peak deviation (since the RF bandwidth is limited) the SNR's will not be increased by companding as much as might be expected, in fact they might not be improved at all.

In view of this it is recommended that companding not be considered for SSSC/FDM/FM without a rigorous analysis of the intermodulation problems which might arise.

Considering the SSSC/FDM/FM multiplexing technique in general there are a number of other difficulties which are apparent.

One of these is the extreme difficulty of obtaining good low frequency amplitude and phase response to near dc, since the carrier must be suppressed. This can be alleviated by using vestigial or double sideband multiplexing and this will be discussed later. Another difficulty will be the reduction of inter-channel crosstalk to a level below thermal noise. Although a signal/crosstalk ratio of 40 db (RMS/RMS) is attainable, this is near the limit of practical multiplexer design. Certainly a requirement of better than 50 db (RMS/RMS) would present a tremendous problem to an FDM designer.

The next problem which will be mentioned is intermodulation distortion noise due to linearity and group delay deviations in the IF/RF sections of the downlink. It may not be too difficult to keep this noise to a low level however its contribution must be recognized and minimized.

Finally it must be noted that the implementation of SSSC/FDM necessitates the provision of highly stable frequency sources both in the spacecraft and on

*"Communications Systems and Techniques," by Schwartz, Bennett and Stein, McGraw Hill, 1966

the ground since frequency differences between these are transferred directly to the video channel spectra.

2.3.5.2 DSB/FDM/FM and VSB/FDM/FM—Both of these multiplexing techniques offer the advantage (over SSSC/FDM) of improved low frequency response and either could be made to meet the amplitude and phase requirements.

However it is readily apparent that both require a greater baseband bandwidth than SSSC/FDM and therefore the permissible peak channel deviations and consequently the attainable SNR's must be less than for SSSC/FDM. Since the latter is already deficient in this respect there seems to be no reason to pursue the analysis of these techniques further.

2.3.5.3 TDM/PAM/FM—This technique for multiplexing the 10 radiometer channels would require the channels to be sampled sequentially and then allow these samples to frequency modulate the downlink carrier.

Since the highest visible channel modulating frequency is 225 kHz the sampling rate would have to be at least 4.5×10^5 samples/sec. To allow a reasonable margin (to prevent aliasing) we might take the rate to be 5×10^5 samples/sec. Although this sampling rate is considerably in excess of that required for the thermal channels it may not be easy to use a lower rate for these.

Therefore the total system sampling rate would be 5×10^6 samples/sec. and the bandwidth required to transmit the PAM signals with acceptable distortion would be on the order of 5 MHz.

Since this spectrum is more than twice that of the SSSC/FDM it is obvious that the attainable SNR will be very much less than for SSSC/FDM.

This factor alone precludes any need for further analysis of this technique.

2.3.5.4 TDM/PCM/PSK—As a logical progression from TDM/PAM multiplexing the concept of digitization of the PAM signals into PCM by means of analog/digital conversion must also be considered.

One of the major benefits of digital transmission is the independence of the channel SNR on the link carrier/noise (for error rates $< 1 \times 10^{-5}$) and the very reduced effect of transmission deviations on channel SNR. Furthermore, as a consequence of digitizing the analog signals, it is possible to employ non-linear digitization and thus effect companding without introducing non-linear distortion.

From paragraphs 2.3.1.1 and 2.3.1.2 it is recalled that an acceptable value of link SNR for the visible channels is 59 db (P-P/RMS) without companding or 37 db (P-P/RMS) with square root companding and for thermal channels 54 db (P-P/RMS) (without companding).

Now in PCM, the SNR due to quantization noise only is*

$$\text{SNR} = \frac{3}{2} \times 2^{2N} \left(\frac{\text{RMS}}{\text{RMS}} \right)$$

where

N = No. of bits

Therefore, for 8 bit PCM;

$$\begin{aligned} \text{SNR} &= \frac{3}{2} \times 2^{16} = 50 \text{ db} \left(\frac{\text{RMS}}{\text{RMS}} \right) \\ &= \underline{59 \text{ db} \left(\frac{\text{P-P}}{\text{RMS}} \right)} \end{aligned}$$

and, for 5 bit PCM;

$$\begin{aligned} \text{SNR} &= \frac{3}{2} \times 2^{10} = 32 \text{ db} \left(\frac{\text{RMS}}{\text{RMS}} \right) \\ &= \underline{41 \text{ db} \left(\frac{\text{P-P}}{\text{RMS}} \right)} \end{aligned}$$

Thus, for visible channels 5 bit PCM with square root digitization will meet the link requirements and 8 bit PCM with linear digitization will be adequate for thermal channels.

The sampling rate for visible channels should be approximately 5×10^5 samples/sec and the sampling rate for thermal channels should be 6.25×10^3 samples/sec.

However, implementing a TDM with differing sampling rates for visible and thermal channels may pose real problems and it may be easier to "over-sample" the thermal channels.

In this situation the total bit rate would be;

$$(8 \times 5 \times 10^5 \times 5) + (2 \times 5 \times 10^5 \times 8) = \underline{28 \times 10^6 \text{ bits/sec.}}$$

*"Modulation Systems and Noise," by J. J. Downing, Prentice Hall, Inc. ; 1964

It is apparent that to maintain an error rate not worse than 1×10^{-5} would require an RF bandwidth well in excess of the available 25 MHz however the requirement still can be met by utilizing quadrature PSK transmission instead of biphase PSK. The symbol rate will then be 14.0×10^6 symbols/sec. i. e., half the bit rate, and the RF bandwidth of 25 MHz will then be adequate. With this bandwidth/symbol rate ratio the system performance should be within 2 db of theoretical, allowing for inter-symbol interference and energy loss.*

It can be assumed that differentially coherent PSK would be utilized and the C/N required, for an error rate of 1×10^{-5} , would be therefore, 10.5 db. (See Figure V-33.) Allowing the 2 db margin already mentioned the required C/N would be 12.5 db which when compared with the link calculations in paragraph 2.3.4 gives a margin of nearly 3 db. This is both adequate and desirable.

From the foregoing it may be seen that TDM/PCM/QPSK can provide the SNR required for both visible and thermal channels.

There are other advantages to this technique also. Firstly, the low frequency response of the channel extends down to dc thus fulfilling another important requirement. Secondly, as already mentioned, the channel SNR is essentially independent of C/N for all values above 12.5 - 13 db and thirdly, PCM/QPSK is less adversely affected by IF/RF linearity and group delay deviations than analog FM.

There are however some disadvantages to using TDM/PCM/QPSK which must be discussed.

The primary difficulty appears to be the analog/digital (A/D) converters required in the spacecraft. Two methods of A/D conversion are possible, viz, conversion before or after commutation. Conversion before commutation would require the A/D converters to operate at speeds up to 2.5×10^6 bits/sec, however, 10 converters would be required. Conversion after commutation would require one A/D converter operating at 20×10^6 bits/sec for visible channels and another at 8×10^6 bits/sec for thermal channels.

A/D converters for these bit rates are not off-the-shelf items and certainly are not flight proven so that a good deal of research and development will be required to produce equipment with demonstrable reliability adequate for an operational spacecraft sub-system.

Another consideration is the power requirement for these high bit rate A/D converters which may place too great a burden on the spacecraft power system. Obviously detailed studies will be required to determine whether these problems can be overcome.

*"Filter Distortion and Intersymbol Interference Effects on QPSK," by J. J. Jones, Philco-Ford, Palo Alto, California, Unpublished Paper.

2.3.5.5 Recommended Technique—Reviewing the foregoing analysis it is apparent that only two techniques seem worthy of further consideration. These are SSSC/FDM/FM and TDM/PCM/QPSK. Each, at the present time, has problems associated with its implementation. SSSC/FDM/FM cannot meet the SNR requirements, unless it can be demonstrated that analog companding is feasible and will provide the necessary improvement, and the low frequency response and inter-channel crosstalk requirements will present a severe problem to the FDM designer. On the other hand TDM/PCM/QPSK can provide acceptable performance but will require A/D converters operating at bit rates maybe as high as 20 MB/S and these must be regarded as being state-of-the-art certainly as far as spacecraft hardware is concerned. Table V-3 summarizes the advantages and disadvantages of each technique.

All things considered, however, it seems much more probable that, at the present time, the latter problems can be solved more easily than the former and therefore TDM/PCM/QPSK is the multiplexing/modulation technique recommended for the downlink radiometer transmission system from the SMS.

For the benefit of designers of future spacecraft communications systems, however, it is also recommended that a study be undertaken of instantaneous analog companding of television signals since the information available in this area seems to be very limited.

2.3.5.6 Narrow-band Radiometer Operation—As discussed in paragraph 2.2.4 provision is required for operation of the radiometer at reduced bandwidths and resolutions.

In these circumstances it may be assumed that the sampling rate would be reduced appropriately, however, the degree of digitization would remain unchanged. Table V-4 shows the parameters in these alternate configurations. (The normal mode is included for comparison purposes.)

It will be seen from this table that, if the RF bandwidth is limited to 10 MHz, the visible resolution will be restricted to 1.0 n. miles (the thermal will be unchanged), however the channel SNR's will not be degraded.

Under these conditions the C/N will be 20:3 db which is unnecessarily high so that a reduction in spacecraft transmitter power by up to 4 db could be effected, by ground command.

An important aspect of reducing the sampling rate is the need to correspondingly reduce the bandwidth of the video signals prior to sampling otherwise aliasing may result in the production of false images. Thus, baseband filter switching must accompany any changes in the sampling rate.

Table V-3

Comparison of SSSC/FDM/FM and TDM/PCM/QPSK

ITEM	SSSC/FDM/FM	TDM/PCM/QPSK	REMARKS
1. $SNR \left(\frac{P-P}{RMS} \right)$ Visible Channels Thermal Channels	43.9 db (no companding) 38.7 db	41 db (with companding) 59 db	Requirement is 59 db without companding or 37 db with companding. Requirement is 54 db.
2. Low Frequency Amplitude and Phase Response	Impossible to attain good response to near dc	Response down to dc	Response is required to extend down to approx. 0.02 Hz (3 db point) for 1% tilt.
3. Effect of transmission deviations	Production of inter-modulation noise which will further degrade SNR	Causes inter-symbol interference and increased error rate. Margin of 2 db already allowed for this and further 4 db available if required.	These deviations are not expected to cause significant problems with either technique.
4. Inter-Channel Crosstalk	Will degrade SNR. Attainment of at least 50 db $\left(\frac{RMS}{RMS} \right)$ extremely doubtful due to problems with phase response of sharp cut-off filters	Good design will attain required level. No filter problems.	

Table V-3 (Continued)

Comparison of SSSC/FDM/FM and TDM/PCM/QPSK

ITEM	SSSC/FDM/FM	TDM/PCM/QPSK	REMARKS
5. Hardware Design and Reliability	Probably not state-of-the-art but a number of design problems to be solved (in relation to low frequency response and crosstalk). Reliability should be good.	A/D converter would be state-of-the-art and reliability yet to be demonstrated.	TDM/PCM/QPSK development costs would probably be higher but has a greater likelihood of success.
6. Spacecraft Power Drain	Should not be any problem.	A/D converter may increase spacecraft power requirement depending on speed of operation.	This area requires study.

SSSC - Single side band suppressed carrier

QPSK - Quadrature phase shift keyed

Table V-4

Parameters of Alternate VISSR Configurations

Configuration	No. of Groups	No. of Channels Per Group	Resolution	Group Bandwidth	Sampling Rate
<u>Visible Channels</u>					
Normal	8	1	0.5 n. m.	225 kHz	5.0×10^5 samples/sec.
Alt. A.	4	2	1.0 n. m.	112 kHz	2.5×10^5 samples/sec.
Alt. B.	2	4	2.0 n. m.	56 kHz	1.25×10^5 samples/sec.
Alt. C.	1	8	4.0 n. m.	28 kHz	6.25×10^4 samples/sec.
<u>Thermal Channels</u>					
All Configurations	2	1	4.0 n. m.	28 kHz	6.25×10^4 samples/sec.
Configuration	Total Symbol Rate (Half bit rate)		Total RF Bandwidth (Bandwidth/symbol rate = 1.8)		
Normal	14×10^6 symbols/sec		25 MHz		
Alternate A	4.5×10^6 symbols/sec		8 MHz		
Alternate B	1.6×10^6 symbols/sec		2.9 MHz		
Alternate C	6.5×10^5 symbols/sec		1.2 MHz		

NOTE: In all configurations the visible channel SNR = 32 db $\left(\frac{\text{RMS}}{\text{RMS}}\right) = 41$ db $\left(\frac{\text{P-P}}{\text{RMS}}\right)$
and thermal channel SNR = 50 db $\left(\frac{\text{RMS}}{\text{RMS}}\right) = 59$ db $\left(\frac{\text{P-P}}{\text{RMS}}\right)$

Alternatively the sampling rate could be maintained at 5×10^5 samples/sec. and the bit rate would then be 18×10^6 bits/sec. Using quadrature PSK this would be 9×10^6 symbols/sec. In a 10 MHz bandwidth with a C/N of 20.3 db the error rate should not exceed 1×10^{-5} and thus the channel SNR's would be maintained.

2.4 SPIN SCAN CLOUD CAMERA

This section contains a description of the classical spin scan cloud camera as used in ATS-I and -III. The ATS-I camera provided black and white pictures while the ATS-III camera contained three channels and provided color photographs.

The spin scan cloud camera will meet the minimum requirement spelled out in Section II. For the SMS application, the three channel ATS-III multi-color spin scan cloud camera (MSSCC) would be used. However, it would be modified so each channel would provide black and white pictures, thus providing redundancy. The description which follows is that of the MSSCC and Table V-5 gives the ATS-III camera specifications as modified to include the SMS black and white specifications.

2.4.1 General Description

The MSSCC Camera consists of a high resolution telescope, three photomultiplier light detectors, and a precision latitude step mechanism. The latitude step motion, combined with the spinning motion of the ATS synchronous satellite, provides a scan of the complete earth disc.

The camera is housed in the ATS-III Spin-Stabilized Synchronous Satellite and generates three signals for three different regions of the solar spectrum. A high resolution reflective telescope with a set of three 0.0015 inch diameter field defining apertures gathers the energy from three visible wavelength bands and floods three respective photo-multiplier tube cathodes. The camera telescope latitude step following each spacecraft revolution (or every 3 spacecraft revolutions) will provide pole-to-pole coverage in 2400 (west to east) scan lines. Ground resolution at the sub-satellite point is 2.2 statute miles (0.1 milli-radian). The camera generates 100 scan lines per minute (nominal 100 rpm spacecraft spin) for a total frame time of 24 minutes for full earth coverage.

The latitude step mechanism is caused to advance south in one step increments by a command from the spacecraft Mechanical Antenna Control Electronics (MACE) system for each spacecraft revolution. When the step

mechanism has completed the required 2400 steps (24 minutes for nominal 100 rpm spacecraft spin rate) a limit switch initiates retrace. The substitution of a 17 Hz oscillator output for the MACE command combined with a reversal in the step motor phase sequencing causes the telescope to return to the north latitude position in approximately 2.4 minutes. At this point another limit switch signals the return to normal north-south stepping in synchronism with the spacecraft rotation.

2.4.2 Optical Design

Specifications required that the MSSCC provide full earth disk coverage with a resolution of approximately 20 seconds of arc in three spectral intervals in the visible spectrum.

To achieve maximum light throughout, separate field stops are used for color. The field stops are arranged in a line in the direction of satellite spin (east-west) so that on any one scan the signals from the same earth position are displaced slightly in time. Displacement is approximately 6.25×10^{-5} seconds for nominal 100-rpm satellite rotation. The green channel leads or will see an object first, red second, and blue third. This phase shift must be corrected in the ground equipment.

As the three field stops could not all occupy the same position at the center of focal plane, it became necessary to design an optical system with good off-axis imagery. A Wynn-Rosin design was chosen. All optical elements are made of fused silica. Its low temperature expansion together with the invar mount provide a system insensitive to temperature change. The primary and secondary mirror are coated with aluminum and overcoated with magnesium fluoride. The corrector lenses are made of UV Grade fused silica which is virtually free of bubbles or inclusions and shown to be virtually unaffected by heavy radiation doses. The corrector lenses are coated with a high efficiency antireflection coating to reduce any effect of surface reflections. A flexible fiber optic assembly was designed to convey energy from the movable telescope to the fixed photomultiplier assemble.

2.4.3 Mechanical Design

The MSSCC major mechanical components are the frame, telescope, precision step mechanism, multiplexer housing, and the electronics housing. The telescope assembly, fabricated from Invar 36 steel alloy to provide temperature compatibility in association with the quartz optics, is supported in the frame by two Bendix flexural pivots, which allow for the limited $\pm 9.0^\circ$ telescope motion.

The camera telescope moves an angular distance of 27 seconds of arc, in a single step, for each rotation of the spacecraft. This precision angular step is accomplished in approximately 10 msec (1/60 of a spacecraft rotation period). The step drive sequence starts with rotary motion from a 90° stepper motor. This motor (IMC Magnetics Model 0 15-802, Size 15) has four windings energized sequentially by the camera electronics. A 90° rotation of the stepper motor shaft produces a 0.0005-inch linear motion along the axis of the lead screw which is coupled to the telescope as an angular motion by a rectangular frame, drive bands, and drive sector arms.

Two electrical limit switches signal the ends of the drive mechanism travel. Two positive mechanical stops act as a backup should the switches fail. If these mechanical stops are encountered they cause a non-binding mechanism stall, and manual commands can perform the limit switch functions. The telescope with the rectangular drive frame, sector arms and lead screw, i. e., all parts that move with the telescope, are statically balanced to introduce little if any effect on spacecraft spin rate.

Theodolite measurement of the telescope step positions recorded during final testing indicate a repetitive nonlinear effect. This non-linearity is the result of a minimal nutation of the step drive lead screw. The deviation from linearity of the camera step mechanism shows two components, one slowly changing component with maximum error of approximately 50 seconds of arc and another component related to the nutation of the step drive lead screw. The second term shows a 40 step periodicity, corresponding to one revolution of the drive shaft. The maximum deviation from linearity is approximately 1 step.

2.4.4 Electronic Design

The MSCC electronics provide four basic functions as follows:

- a. Circuitry for generation and processing of picture information or video.
- b. Circuitry to produce and control mechanical motion of the optical telescope (step scanning)
- c. Circuitry for housekeeping functions such as temperature monitoring, etc

The light in the three spectral regions is detected by three separate photomultiplier tubes. The gains of the tube multiplier sections are controlled by the value of high voltage applied. The high-voltage power supplies or converters used (one for each tube) have provision to externally control their

outputs over a range of 500 volts. This is done by changing the value of a resistance between a converter terminal and converter ground. Four steps of gain for each color channel are available by ground command.

The camera gain change feature provides:

- a. A camera video level adjustment to ensure that the camera output signal range always matches the spacecraft microwave repeater, and preserves maximum signal-to-noise at the ground receivers.
- b. High gain capability for low light level pictures with no downlink degradation.
- c. Increased gain capability should camera output tend to degrade with time in orbit.

High-voltage telemetry modules are connected to each converter to provide a telemetry voltage proportional to the high-voltage output. This information is used to: 1) determine the gain step position and 2) to verify that the high voltage is correct in flight.

The output of each photomultiplier tube is connected to the time division multiplexer. The tube termination resistors are located in the multiplexer.

The motor step logic provides the necessary electronics to control motion of the camera telescope. The telescope must be stepped with each spacecraft revolution during the normal down scan picture making operation. The step command is provided by the spacecraft MACE system, buffered at the camera input and directed to the proper motor phase driver by the motor sequencing flip-flop. Combined with this circuitry is a step start/stop flip-flop and shunt switch that can be ground commanded. A step rate flip-flop allows for ground commanding to a step/3 revolution mode, and a north-south flip-flop controls step direction at the scan frame ends. Retrace of the frame (return of the telescope to the northernmost, earth reference, position) can be fast when the scan mode is ground commanded to normal or slow (MACE rate) when the scan mode is selected to be back-to-back. The retrace oscillator is freerunning with a frequency of approximately 17 Hz.

2.4.5 Multiplexer

The MSSCC camera requires the transmission of three nearly simultaneous video signals to the ground station. Since only one modulator is

available in the spacecraft, some type of multiplexing scheme is required. A time division multiplexing scheme was selected because of equipment simplicity, good linearity, and low crosstalk.

The time-division multiplexing system switches each of the three camera signals in sequence to a summing amplifier at a 500 kHz rate. A fourth channel, a known dc voltage, is also sampled and summed with the three camera signals. This channel is used for synchronization and dc restoration in the ground equipment.

The green, red, and blue camera signals are amplified and filtered to remove unwanted components above 200 kHz. A positive-going sun pulse (obtained from a spacecraft sun sensor) is passed through a threshold circuit to eliminate the earth pulse and then summed with the green and red signals. The sun pulse is added in with scale factor of $2/5$ relative to the maximum camera video so that it can be distinguished from the reference pulse of the same polarity. A tone signal is summed with the +0.5 volt reference in the fourth or calibration channel. This signal, at a frequency of 20 kHz, occurs each time the camera steps. The signal is added at an amplitude such that its peak to peak value is approximately 10 percent of the reference voltage when demultiplexed.

Electronic shunt switches in each channel ground that channel except when it is being sampled. The signals from all channels are combined in a summing amplifier which drives the spacecraft VCO. Because of the channel sampling rate (2 MHz) at least a 5 MHz bandwidth is required for the spacecraft VCO in order to preserve the rise time of the sampler and to minimize crosstalk between channels. The electronic commutator is driven by logic signals obtained from an electronic conversion unit powered by the -24 volt dc supply in the spacecraft.

2.4.6 Interface with Transmitter

The video signal interface is at a subcarrier oscillator whose output modulates the transmitter.

Table V-5

SPIN SCAN CLOUD CAMERA

OPTICAL SYSTEM

Type	Wynn-Rosin
Focal Length	15 inches
Primary Mirror	5-inch Diameter Elliptical (Fused Silica)
Secondary Mirror	1.8-inch Diameter Spherical (Fused Silica)
Corrector Lenses	Ultraviolet Grade Fused Silica (Coated)
Instantaneous Field of View	0.1 ± 0.02-mrad Diameter (50% Modulation)
Field Stops	0.0015-inch Diameter
Field Stop Separation	0.010 inch Between Centers
Spectral Bandpass (Defined by Optical Filters and Photocathodes)	480 to 580 nanometers
Optical Fibers	F2-R6 Glass, 0.005-inch Diameter 12.5-inch long

PHOTOMULTIPLIER TUBES

Type	EMR Model 541A-01-14 (S-11)
Multiplier Gain Control	2:1 2.49 3:1 3.23 4:1 6.03

SCAN SYSTEM

Line Scan	Spacecraft Rotation (100 rpm Nominal)
Latitude or Step Scan (18° Total)	One Step of 27 seconds-of-arc per Spacecraft Rotation
Lines per Frame	2407 Lines
Frame Time	24 Minutes
Retrace Time	2.4 Minutes
Dwell Period (Time for Instantaneous Field to Scan a Point Source)	9.56 μsec (100 rpm s/c Spin Rate)

Table V-5 (continued)

SPIN SCAN CLOUD CAMERA

Scan Commands	Start Step, Stop Step, Normal Scan, Back-to-Back Scan, North Override Limit, South Override Limit, Step/Revolution
SIZE	12 x 11 x 17 inches
WEIGHT	23.5 lb
POWER (Maximum)	500 ma at -24 vdc
OPERATING TEMPERATURE	+40° to +100°F

3. RECORDING AND RETRANSMISSION OF IMAGED DATA

3.1 SUMMARY OF RADIOMETER PARAMETERS

The radiometer contains eight identical visible channels and two redundant infrared channels. The field of view of the infrared channels is 0.2 mr square; the eight visible channels are 0.025 mr (in the line scan direction) by 0.021 mr "vertically." The visible channels are aligned in a vertical linear array so that they sweep out the same scan line as the infrared channels. Horizontal scan is produced by the S/C spin. The nominal spin period is 600 ms (100 rpm) but may be as low as 480 ms (125 rpm) or as high as 800 ms (75 rpm). Vertical scan is accomplished by tilting the scan mirror in increments to produce an effective line step of 0.2 mr. The number of north-south line steps provided is 1750 for a total angular coverage of 0.35 radians or very nearly 20 degrees. At synchronous altitude the earth subtends an angle of 17.3 degrees.

During normal scanning the steps occur once each spin rotation when the radiometer is at a spin angle of 180 degrees from the north-south earth center line. In the normal mode the limits of scan step are controlled by two limit switches. Frame retrace (south-north stepping) is not synchronized with the spin motion and requires about 1.8 minutes to complete.

In the back-up (open-loop) mode a full frame scan of either 1750 or 175 steps can be commanded. Frame retrace is synchronized with the spin motion at one step per rotation so that image data may be collected during this time.

Inflight calibration of all channels is possible. The eight visible channels view the sun once per revolution using a special small section of the scan mirror. The received energy corresponds to 50 percent albedo; the normal maximum input signal from clouds is estimated to be 80 percent albedo.

Two methods are provided for inflight calibration of the infrared channels. Whenever the infrared channels scan the sun the sensor amplifier gain is reduced by a factor of about 400; this provides a signal of approximately 50% of full scale. The second calibration is initiated by a ground command. Upon such command a temperature monitored shutter is placed in the path of the infrared channel for 60 degrees of S/C rotation just after the earth scan is completed. This is followed (for 5 degrees of rotation) by a two level check of the infrared electronics. This action is repeated each scan until commanded to stop.

In addition to such normal video and calibrate signals there are line and frame synchronization signals. The scan line sync pulses are a sequence of

three 0.2 msec pulses separated by 0.2 msec spaces occurring 60 degrees before the north-south earth center line. Start of frame is indicated by a 10 kHz tone for 0.1 seconds; end of frame is indicated by a 5 kHz tone for 0.1 seconds. These tones occur when the radiometer is pointed 180 degrees from the north-south earth center line. These signals are shown in Figure V-7.

Let us now consider the S/N ratio and required bandwidth for this system at the nominal spin period of 600 ms. If the spin period is decreased the S/N ratio decreases and the required bandwidth (for a given spatial resolution) increases.

For the visible channels the peak-peak signal to rms noise ratio is 36 (31 db) at 80% albedo; note that the noise decreases as the square root of the albedo. The S/N ratio decreases to 2.8 (9 db) at 0.5% albedo. For the infrared channel the peak-peak signal to rms noise is about 240 (48 db) for a black-body source at 330°K. The noise is independent of the signal; however the infrared radiometer output is not proportional to the source temperature. For example at 240°K the signal is lower by a factor of over 4.

The required bandwidth of the visible channel can be computed from the 0.025 mr field of view of the radiometer. The modulation transfer function (MTF) decreases to zero for a spatial frequency of $\frac{10^3}{0.025} = 40,000$ cycles/radian. Since the S/C has a spin rate of $\frac{2\pi}{0.6}$ radians/sec this corresponds to a frequency of 420 kHz. At a frequency of 210 kHz the MTF equals 0.34; this latter figure includes limitations introduced by the optics and the S/C electronics. Without the effect of the S/C electronics the MTF would equal 0.45 at 210 kHz.

For the infrared channel the MTF equals 0.42 at 26 kHz. Without the effect of the S/C electronics the MTF would equal 0.58 at 26 kHz.

Additional study to seek means to make more effective use of this resolution by wider bandwidth video data communications to the ground or increase of the field of view to improve the S/N ratio is warranted.

3.2 DATA PROCESSING

The primary functions of the radiometer data acquisition system (RDAS) at the CDA station involves recording and retransmission of this data in a suitable form. For purposes of this discussion it is assumed that the 8 visible and 2 infrared channels are made available in parallel at the output of a radiometer demultiplexer at the CDA station. Since the 2 infrared channels are

redundant, only 1 will be utilized for processing making a total of 9 channels to be recorded and retransmitted. (The RDAS block diagram is shown in Figure V-19.)

3.2.1 Recording Equipment

The operations that take place on the video signals are, of course, directly related to the system output. The most important, and critical, output is the high resolution visible channel picture. To produce an adequate 14000 line picture only three types of film recorders seem promising: electron beam recorder (EBR), laser beam recorder (LBR), and crater lamp recorder (CLR). Many facsimile recorders, such as manufactured by Muirhead, are of the CLR type.

Before considering the recorders let us compute the resolution requirements for the film recorder. We previously noted that the radiometer field of view produced a limiting resolution of 40,000 cycles/frame. Expressed in TV lines this becomes 28,000 TVL limiting resolution. Although it may be desirable to obtain a film recorder better than the S/C sensor it is probably not warranted since the radiometer signal is significantly degraded by other factors including the limited communications bandwidth.

Use of the CLR would require film larger than 28" across because of the minimum 0.001 inch spot size. While this size would be convenient for many users it would probably have to be reduced to a 9 1/2" film for general dissemination.

The LBR equipment provides 120 cycles/mm at 40% response over a full 4 1/2" scan on 5" film. This corresponds to about 28,000 TVL and exceeds the specification above. To minimize problems of enlargement and reproduction use of 9 1/2" film is desirable.

Since the CLR and LBR have high precision mechanical scanning, excellent linearity and size stability is achieved. The use of such mechanical scanning introduces system constraints to be discussed later.

The EBR unit does not meet the resolution or raster stability requirements at this time. It is further doubtful that an adequate improvement is possible in this type recorder in which the deflection system is electronic. To date a resolution of only 60 linepairs/mm has been achieved in the NASA EBR on 70 mm film. The linearity achieved to date is about 1 part in 2000 compared to one part in 50,000 for the LBR.

The other properties of both the LBR and EBR are adequate. They both have a dynamic range of over 250:1 but the LBR has a S/N ratio of 80 db compared to 42 db for the EBR.

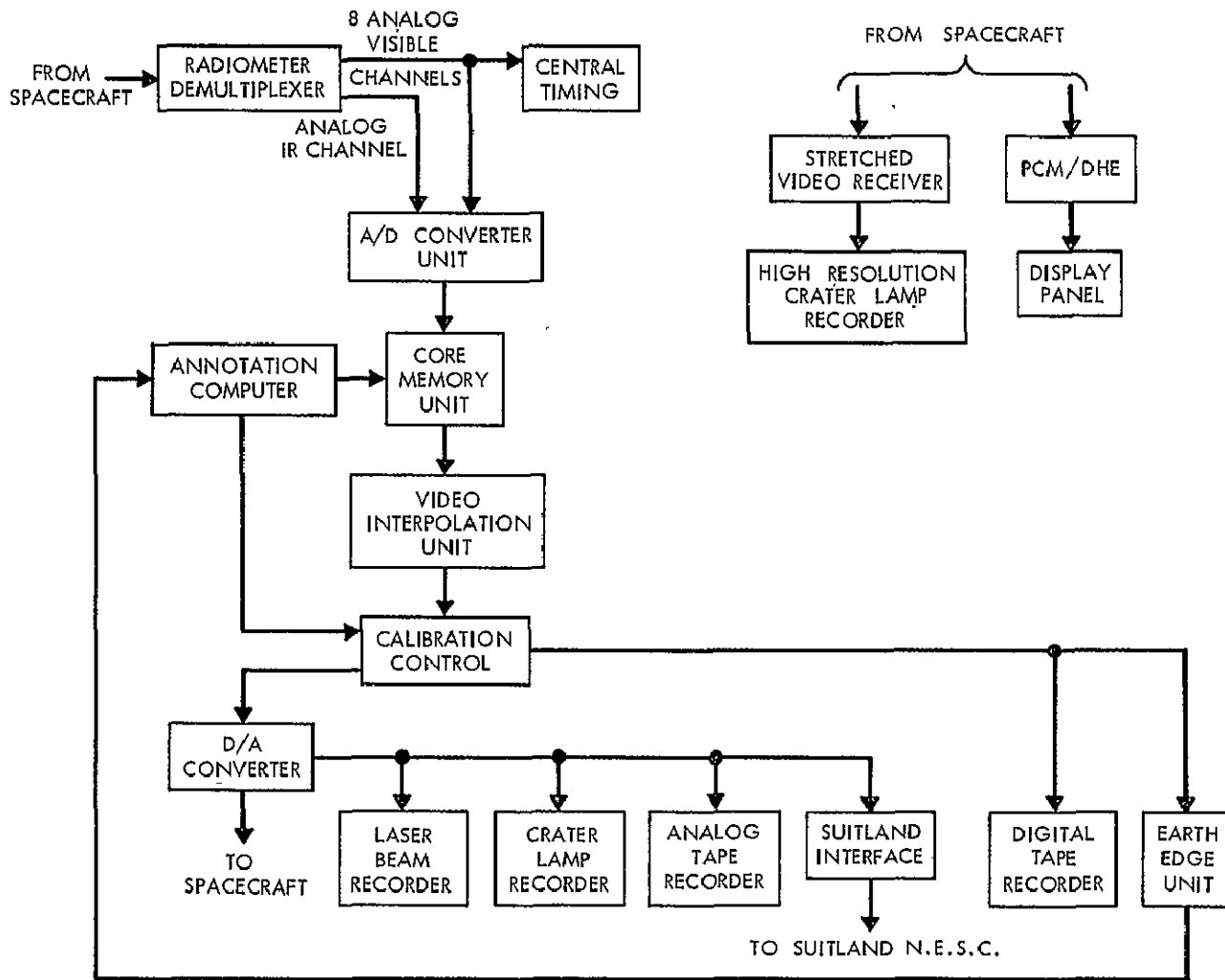


Figure V-19. Radiometer Data Acquisition System

3.2.2 Stretched Data Retransmission To Remote Users

The video data to mechanically scanned recorders is preferably arranged so that one line at a time is formed and that the period and duty cycle of each line of video is fixed. In this system although it is possible to meet these conditions certain alternatives are present. One involves image generation at the CDA RDAS from real-time data (eight lines at a time input). The LBR can incorporate a beam deflector and form the image as a sequence of dots rather than lines. Sample 1 of lines 1-8 are formed as 8 dots before sample 2 is processed.

A second alternative involves use of video data one line at a time in a group of eight lines. The dead or retrace time between lines in a group will be less than the time between groups. With such data normal lines are formed but some means must be used to avoid forming blank lines between groups. The LBR can use the same beam deflector and the CLR can use some mechanical deflection technique. Typical time between deflections would be from 30 to 60 milliseconds. Slight misadjustment of such a beam deflector would produce horizontal stripes every 8 lines. This second alternative corresponds to stretching the data as a contiguous burst.

Before commencing discussion of the fixed duty cycle approach some of the more significant parameters of the burst method will be computed. First the video should be collected by the S/C for a spin rotation of 20° instead of 18° . The latter angle leaves an inadequate tolerance of $\pm 0.35^\circ$ for errors associated with S/C position, drift rate, attitude, actual earth-sun orbit and equipment tolerances. Use of 20° increases the tolerance by a factor of almost 4 to $\pm 1.35^\circ$.

At a S/C spin rate of 125 rpm (spin period = 480 ms.) the 120 ms. transmission delay between the S/C and CDA corresponds to a S/C rotation of 90° . If retransmission of the stretched video is started immediately after the direct video has been acquired it will appear at the S/C $200^\circ (20^\circ + 90^\circ + 90^\circ)$ after the start of earth scan. The remaining 160° of S/C spin rotation is just enough to permit an 8 times stretch ($8 \times 20^\circ = 160^\circ$).

To increase the stretch factor to 16, we can store all 8 lines of data in a buffer and commence the stretch transmission immediately after receipt of the earth video. However the data is unloaded from the buffer at half the rate of the 8 times stretch. Thus when the S/C commences its next earth scan only

half the data (lines 1-4) has been transmitted. Then after a S/C rotation of 40 degrees the second half of the data (lines 5-8) is transmitted. This prevents interference with the direct transmission of earth video from the S/C and permits stretch transmission of the first four lines of data from the next scan to commence without further delay. Thus each burst of eight lines is composed of the last four lines of one scan followed by the first four lines of the next scan. Note that half of the 40 degree gap is available for other uses such as platform interrogation or sensor calibration. If this approach were to be used some stretch factor less than 16 should be selected to allow more time for these other functions.

The fixed duty cycle approach - which is recommended - provides a stretch factor up to 10. Each line of stretched data is outputted at 45 degree intervals of the S/C rotation for a total of 8 equally spaced lines per rotation. Of the 45 degrees at least 20 degrees must be made available for direct earth video transmission leaving 25 degrees for stretched video. The maximum stretch factor is then $\frac{8 \times 25}{20} = 10$. Reduction of this factor to 8 by allocating 22.5 degrees for the stretched video provides a tolerance of $\pm 1.25^\circ$ on the 20° direct earth video transmission. Simplification of the RDAS and remote user stations also appears likely through use of the stretch factor of 8.

The timing at the S/C and at CDA is shown in Figure V-20 for a stretch factor of 10 (to avoid showing tolerances) and a 480 ms. spin period. No essential difference in timing occurs for different spin periods except that, in general, the transmission of stretched video line 8 (SV8) overlaps the acquisition of the earth scan. Of the eight gaps between transmission of stretched video one is for the earth scan and one can be used for infrared (IR) data. Note that the IR data has a fixed duty cycle and thus can also be recorded using a electromechanical scan.

3.2.3 Transmission of Other Radiometer Signals (control and calibration)

The other radiometer signals (see Figure V-17) can be transmitted as follows. The scan line sync pulse should be transmitted at the beginning of the period allocated for earth scan. The frame sync tones can be transmitted during any free period such as shown in Figure V-20. The shutter and electronics calibration can similarly be appropriately placed (not shown). The sun calibration will appear at an arbitrary place and cannot be synchronized with these other signals. However since calibration is not necessary during every data frame it is feasible to receive the sun calibration signals whenever they appear in a selected gap. For example, a sun calibration signal appears between SV5 and SV6. The remaining time can be used for interrogation of remote platforms.

V-77

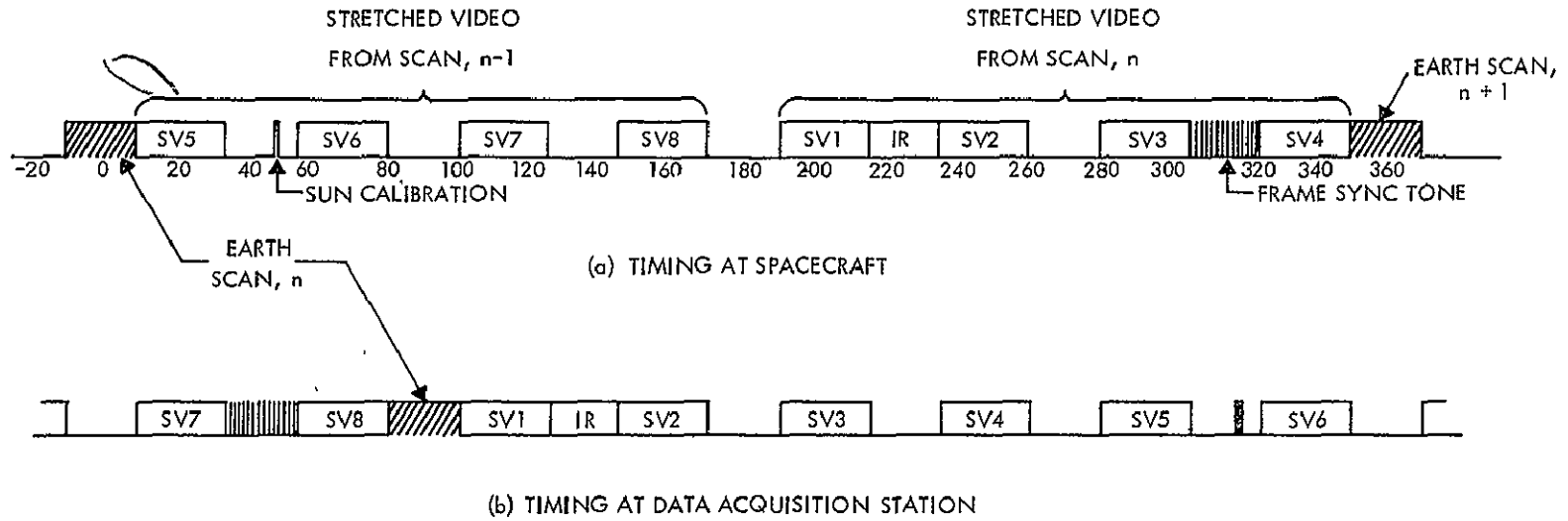


Figure V-20. Stretched Video Timing

Control of the various elements of the RDAS is provided by central timing. This unit extracts line and frame sync data from the visible channel signals; a manually set input corrects for fixed and rate errors in the S/C generated line sync. Central timing smooths these inputs and divides the S/C rotation into a large number of angular increments. All communications to the S/C for the purpose of retransmission are under control of this unit.

3.2.4 Data Storage

Storage of radiometer data at the CDA is most conveniently done using a digital core memory. The nine analog signals must first be converted to digital form using the A/D converter unit. For the IR channel the rms sensor noise at 330°K is $\frac{1}{240}$ or 0.42% of the peak-peak signal. If we assume that the communications channel does not significantly degrade the signal and we permit the A/D converter to introduce one-fourth as much noise, an 8 bit converter is required (rms noise = 0.1% of full scale).

For the visible channels the noise is not fixed but decreases with signal. At a signal level of about $\left(\frac{1}{36}\right)^2 \approx 1/1000$ of full scale the signal to noise ratio is one. Use of an 8 bit A/D converter would thus introduce negligible errors except for very low level signals; even at an albedo of 0.1% the added noise would be less than 3 db.

Thus the A/D converter unit consists of nine 8 bit A/D converters (or equivalent). A convenient sampling rate corresponds to 2^{14} or 16384 samples per visible channel for the 20° scan or 21 uR between samples. Note that this is slightly less than the 25 uR between lines. It corresponds to 2.3 samples per cycle of 210 kHz at a spin period of 600 ms. The infrared sampling rate could be as low as 2048 samples per 20° scan but should be set to 4096 to assure retention of the full resolution of this data. Likewise, at little cost, the bandwidth of this channel should be increased from 26 kHz to 52 kHz.

The time between samples for the visible channel for a spin period of 0.48 seconds is 1.63 microseconds; the A/D converters and associated equipment must be able to support this rate.

The visible data part of the core memory unit must consist of 16384 words with each word composed of eight 8 bit samples for a total of 64 bits per word or about 10^6 bits overall. As noted before, the SV8 data unload may not be completed before the new earth scan data is received at RDAS. Thus an additional 8 bits of data per word must be stored. The need for "simultaneous"

load and unload of core may require that the SV8 data be loaded in a separate core rather than increasing the word length as implied above.

Storage for the infrared data can consist of 4096 words of 8 bits each. It may however be cheaper to increase the word length of the large core memory by 8 bits rather than obtain a second small memory.

The core memory unit also receives data from a small computer used for annotation. This annotation computer can place identification data, grids and picture control data on the final picture by altering the contents of the core memory. Typical information which could be presented by the annotation computer is S/C position and attitude, time of day and date, grid and/or fiducial marks, gray scale, resolution test charts and special comments.

3.2.5 Bandwidth Reduction

Up to this point we have discussed generation of the full visible channel pictures at the CDA or via data stretch transmission. There is some question whether it is advisable to retransmit the full data detail since this increases the communications problem to the user stations by requiring a larger user receive antenna than would otherwise be necessary. Secondly most of these stations may not be able to afford the high resolution film recorder. Reduction of the spatial resolution by a factor of two decreases the stretch video bandwidth by a factor of four. Thus the video bandwidth is reduced from 210 kHz to about 53 kHz. If this signal were to be used only for direct transmission via land lines from Wallops Island to Suitland, Maryland N. E. S. C. the bandwidth could be reduced by an additional factor of about two since the S/C timing constraints (50 percent duty cycle) are not applicable. To achieve this resolution reduction, modification of the core memory unit is required to output four lines of data per S/C rotation. In addition, controlled reduction of the image vertical resolution may be accomplished by the video interpolation unit. This unit combines the video from the eight line data and is also useful in case of a failure of one or more of the PMT sensors in the S/C; the failed channel is formed from the remaining channels. In this manner a high resolution picture may be formed without black lines caused by failed data sources. This video interpolation unit is clearly optional based on the need for its function. The interpolation function is mechanized by forming the weighted sum of two or more of the eight line data. The capability of digital addition is thus the major element of this unit.

3.2.6 Calibration Control Unit

The input to the calibration control unit is a sequence of 8 bit samples. It consists of a digital look-up table divided into nine sections; one

for each visible channel and the infrared channel. This unit can correct for differences in the eight visible channels and correct for dc offsets and non-linearities in the sensor and communications system. It can be used for deliberate introduction of a non-linearity to present the data more satisfactorily. For example the infrared sensor data can be modified so that equal temperature increments produce equal density changes in the final film product. A 4096 word by 8 bit/word core memory is sufficiently large to perform this task. Loading of the look-up table can be performed by the annotation computer.

The output of the calibration control is in a form suitable for the major uses. It is assumed that the 8:1 stretched data is suitable for these various uses. If, as discussed before, other formats are required, the timing becomes more complex and additional core storage will be needed.

3.2.7 Data Utilization

There are six major uses of this data. Included are transmission to Suitland NESG, high and low resolution film recording, tape recording, retransmission of stretched data and horizon detection for S/C attitude determination.

Transmission to Suitland is discussed separately in paragraph 3.2.9.

We shall consider the high and low resolution film recording together since it is desirable that the visible and infrared images be capable of being placed in register to form composite pseudo-color images. Several approaches are possible

- a. Use of an LBR for high resolution visible channel film recording and a CLR for low resolution infrared channel film recording. Both would use 9-1/2 inch film fed from continuous rolls and would record the data in parallel. Color printing would be subsequently done after the black and white films were developed and cut. Holes would be punched at two or more appropriate fiducial marks on each sheet of film. A 9-1/2 inch color master would be formed by sequentially contact printing each of the two black and white originals with selected colored light. The punched holes would be used with pins to ensure accurate registration of the two images. One advantage of this approach is that the two film records are independent; at night only the CLR need be used for the infrared pictures. Of course the use of independent film recorders generates the problem of maintaining accurate film size of each to permit good registration.
- b. Use of an LBR for recording of both images on the same film. Thus each image could be 4-1/2 inches wide. The infrared image would have as many lines as the visible image; these would be generated by

repeating each line eight times or by a similar technique. The key disadvantage here is the use of a relatively small image compared to the 9-1/2 inch film width.

- c. Same as approach b. but use of 19 inch film width on a drum. Film would not be automatically fed into position and would require a manual operation at the beginning and end of each frame.
- d. Same as approach b. but visible and infrared frames would be placed sequentially on film rather than side by side. This requires that the infrared data be stored first on digital tape and subsequently played back when data is not being acquired.

Of these various approaches the most appealing one is item a.; the following discussion assumes use of this technique. Thus the calibration control output goes via the D/A converter to the LBR and to the CLR. Signals from central timing to these recorders and to other units are not shown in this block diagram (Figure V-18) but are implied. Such signals are required by the various output devices for proper synchronization.

The next output device is the analog tape recorder. The bandwidth of the signal is about the same as each sensor channel from the S/C or about 210 kHz. A typical recorder suitable for this task is the Ampex FR 1900. When operating with FM wideband group II electronics at 60 ips the frequency response is down less than 4 db at the high frequency end of 200 kHz with a peak-peak signal to rms noise ratio of 41 db. With a standard 7200 foot reel the record time per track is 23 minutes; thus 1 picture per track can be recorded or 14 pictures on one inch 14 track tape.

(At the expense of additional core memory the stretch factor can be increased to 16 for input to the analog tape recorder and for data transmission to the NESC at Suitland, Maryland. This added memory (not shown) would reduce the bandwidth to about 100 kHz and permit recording two pictures per track at 30 ips and 40 db S/N ratio.)

Playback of the analog tape recorder data would require careful synchronization and tape speed control to produce high quality pictures on the LBR and CLR.

Two other output units are digital in nature. One is the digital tape recorder. Use of conventional 800 BPI digital tape requires large quantities of tape. Each visible channel picture contains about 1.8×10^9 bits. Standard 800 BPI tape can store less than 0.14×10^9 bits on a 2400 foot reel. Two

other techniques are available which have much higher capacity. One uses a video tape recorder with a rotary head. Such recorders normally have a 4-6 MHz bandwidth at a tape speed of 15 ips and record for one hour. With suitable modification (bandwidth and speed reduction) the record time can be increased to 4 hours.

A second technique uses a newly developed digital film recorder produced by Synergistics. At 15 ips the recorder will function with an input data rate of 2.5×10^6 bits/sec. Data is placed on 8mm photographic film and requires development prior to playback. Total record time is 26 minutes. A close review of such digital recording techniques is necessary prior to selecting a particular one.

The second digital output unit provides the raw data required for precision attitude estimation. The earth edge unit defines the left and right edge points for each line of visible channel video. This data is transferred to the annotation computer where it is stored on magnetic tape or directly combined with the other necessary information to compute S/C attitude.

3.2.8 Monitoring of Stretched Transmissions

Provision should be made to monitor the down-link reception of stretched video. This is done using the stretched video receiver and high resolution CLR. This recorder can alternately be used for visible and infrared channel reception. Finally, the S/C status of radiometer components is to be displayed and monitored. The data source at the CDA is the PCM/DHE with the data displayed on the monitor panel.

3.2.9 Data Transmission to Suitland

Another major output is the Suitland Interface. As shown here this assumes the existence of an analog data channel from Wallops Island to Suitland, Maryland, capable of transmission of a dc-to-225 kHz signal. As noted previously, by increase of the stretch factor to 16 (100% duty cycle) and reduction of the resolution by a factor of 2 the required frequency response can be as low as dc to 28 kHz.

If such analog data transmission is not considered suitable, digital transmission can be implemented. To transmit 10^6 bits in 600 ms. we must have a data rate capability of at least 1.7×10^6 bits/sec. Using 2 level PCM with non-return-to-zero (NRZ) coding a channel of 1 MHz bandwidth may be sufficient. The use of multi-level PCM can be used to reduce this bandwidth requirement

however. This line is best generated by forming the analog weighted sum of the eight line data per scan. Further study is required to determine the optimum weighting factors. This composite line is stored in the magnetic core during the 20 degrees of earth data acquisition. It is then read-out at one-eighth the input rate. At the maximum spin rate of 125 RPM the stretched video will arrive at the S/C 200 degrees of rotation after the start of earth scan. This stretched video will terminate after an additional 160 degrees (8×20); thus no overlap of stretched and direct earth video at the S/C will occur.

With the W3 equipment two lines of data per S/C rotation can be handled. The first of these two lines would be processed in a manner identical to that previously discussed and would be stretched out for 160 degrees of S/C rotation. After a 20 degree delay the second line would be transmitted to the S/C at the same rate as the first. In this manner a fixed duty cycle of $\frac{160}{180}$ is achieved. The third section of core memory available in W3 would be needed in general to accept data while the second section is stretching data for transmission to the S/C. Table V-6 gives details of existing and required line stretching equipment.

Of the various systems discussed for handling limited resolution data the W3 is best since it outputs twice as much data at the same bandwidth as W1. The H1 system uses less bandwidth but at a further loss of horizontal resolution; if desired horizontal resolution may be reduced for the W1 or W3 systems.

Unfortunately, the W1/H1 one line stretch, the W3 two line stretch and the full eight line stretch systems are not directly compatible. That is, electro-mechanical and circuit changes would probably be required at the user stations to change from one format to another. Since it is unlikely that the users would instrument for a format without assurances that it would not change we must recognize that the format initially selected may also be the final one.

3.4 STRETCHED DATA LINK CALCULATION

The stretched visible and IR data will be D/A converted at the CDA station to a single 225 kHz channel. This analog signal will contain the 8 visible and a single IR channels in a serial format. The up and down links to the Data Utilization Stations (DUS's) will be configured as an FM transmission signal spectrum utilizing a 3 MHz transmission bandwidth at S-band.

The complete power budget calculations for the stretched data links are presented in Table V-7. These calculations are based on the reception of full 1/2 n. m. resolution with a 15 foot antenna at the DUS. Figure V-21 shows the essential elements which would comprise a typical link.

slightly. Of course resolution reduction is also effective with digital transmission; a factor of four reduction permits use of a 70 kHz channel. Such digital data would come directly from the calibration control unit rather than the A/D converter.

3.3 LIMITED RESOLUTION DATA PROCESSING

The general arrangement of a full resolution radiometer data acquisition system is discussed in the preceding paragraphs. Such a system involves an expense which can be deferred for some time after S/C launch. To minimize the initial data acquisition costs there is interest in employing equipment built to acquire data from the spin scan experiment aboard ATS-I and/or ATS-III. It is recognized that the full resolution capability of SMS cannot be achieved in this manner.

Three units were constructed for the spin scan acquisition task and will be designated by the manufacturer name and ATS S/C number: Hughes-1, Westinghouse-1 and Westinghouse-3 (H1, W1 and W3). The H1 unit is now at Wallops Island and plans have been made to deliver the W1 unit to Wallops Island. The W3 equipment is currently at Rosman, North Carolina but may become available for SMS prior to launch. The core memory part of W1 required to perform the line stretch task is now employed at Rosman with W3 for data stretch and WEFAX transmissions and is not currently planned to be delivered to Wallops Island. In the following discussion of the W1 equipment it will however be assumed to be at Wallops Island in a complete form.

There are two essential differences between the H1 and W1 units. The H1 equipment timing subsystem uses a fixed frequency clock independent of spin rate; thus the number of clock pulses per S/C rotation is not fixed. By using a variable frequency clock the Westinghouse unit divides the S/C rotation into 294,912 parts independent of spin rate. The latter approach is more suitable for line stretch since the stretched video duty cycle remains fixed; this is particularly desirable with electromechanical scanners such as employed with most facsimile systems. Of course for a fixed S/C spin rate both systems are equally satisfactory.

The second difference lies in the size of the core memory. H1 uses 4,096 samples per line while W1 employs 8,192 samples per line. Thus the horizontal resolution with the W1 equipment will be twice as good as with the H1 unit. The W3 equipment is very similar to the W1 equipment except that it can process three lines of scan data in parallel.

Either the H1 or W1 equipment can be used with SMS to acquire and stretch the visible video data. Only one line of data per S/C rotation can be handled

Table V-6

Radiometer Data Stretching Equipment Present Vs SMS Requirements

<u>EXISTING-</u>	<u>WALLOPS ISLAND</u>
	<u>ATS-1 LINE STRETCHER (BY HUGHES)</u>
	RESOLUTION CAPABILITY—4 N. MILE VERTICAL, 2 N. MILE HORIZONTAL
	MEMORY—32,768 BITS (4096 EIGHT BIT WORDS)
	FIXED FREQUENCY CLOCK—DUTY CYCLE DEPENDENT ON SPACECRAFT SPIN RATE
	<u>ROSMAN ATS</u>
	<u>ATS-1 LINE STRETCHER (BY WESTINGHOUSE)</u>
	RESOLUTION CAPABILITY—4 N. MILE VERTICAL, 1 N. MILE HORIZONTAL
	MEMORY—65,536 BITS (8192 EIGHT BIT WORDS)
	FIXED DUTY CYCLE—88.8%
	<u>ATS-3 LINE STRETCHER (BY WESTINGHOUSE)</u>
	RESOLUTION CAPABILITY—2 N. MILE VERTICAL, 1 N. MILE HORIZONTAL
	MEMORY—196,608 BITS (24,576 EIGHT BIT WORDS)
	FIXED DUTY CYCLE—88.8%
<u>ULTIMATE-</u>	<u>WALLOPS ISLAND—SMS LINE STRETCHER</u>
	RESOLUTION CAPABILITY—0.5 N. MILES VERTICAL AND HORIZONTAL
	MEMORY— 1.25×10^6 BITS (156,250 EIGHT BIT WORDS)
	FIXED DUTY CYCLE—50%

Table V-7

Stretched Data Link Calculations

<u>Up-Link (2.0 GHz)</u>	
RF Transmission Bandwidth (MHz)	3.0
Total Analog Baseband (kHz)	225.0
	<u>Single Hard-Limited Transponder</u>
CDA Ground Transmitter Power (dbm)	+140
Transmit Losses (db)	-1.0
Ground Antenna Gain (40') (db)	+45.5
Path Loss (db)	-190.7
S/C Off-Beam Center Allowance (db)	-2.0
S/C Receive Antenna Gain (db)	+18.5
S/C Receive Losses (db)	-1.0
S/C Received Signal Level (dbm)	<u>-91.0</u>
S/C Receiver Noise Density (dbm/Hz) (Based on 580°K)	<u>-171.0</u>
Carrier/Noise Power Density (db-Hz)	<u>+80.0</u>
CNR in 3.0 MHz Bandwidth (db)	<u>+15.5</u>
<u>Down-Link (1.7 GHz)</u>	
S/C Transmitter Power (dbm)	+143.0
S/C Transmit Losses (db)	-1.5
S/C Antenna Gain (db)	<u>+18.0</u>
S/C EIRP (dbm)	+59.5
Path Loss (db)	-189.0
S/C Off-Beam Center Allowance (db)	-1.5
Ground Receive Antenna Gain (15') (db)	+35.6
Ground Receive Losses (db)	-1.5
Ground Received Signal Level (dbm)	<u>-96.9</u>
Receiver Noise Power Density (dbm/Hz) (Based on 300°K Temp)	<u>-173.8</u>
Carrier/Noise Power Density (db-Hz)	<u>+76.9</u>
CNR in 3 MHz Bandwidth (db)	<u>12.1</u>
<u>Overall Link</u>	
CNR Up-Link (db)	15.5
CNR Down-Link (db)	12.1
Overall Link (db)	+10.3
FM Improvement, $3/2 m^2$ (m=5, 6) (db)	+16.9
Bandwidth Improvement $\left(\frac{3.0}{0.225}\right)$ (db)	+11.3
Total SNR (RMS/RMS) (db)	<u>+38.5</u>
Total SNR $\left(\frac{\text{Peak-Peak}}{\text{RMS}}\right)$ (db)	<u>+47.5</u>

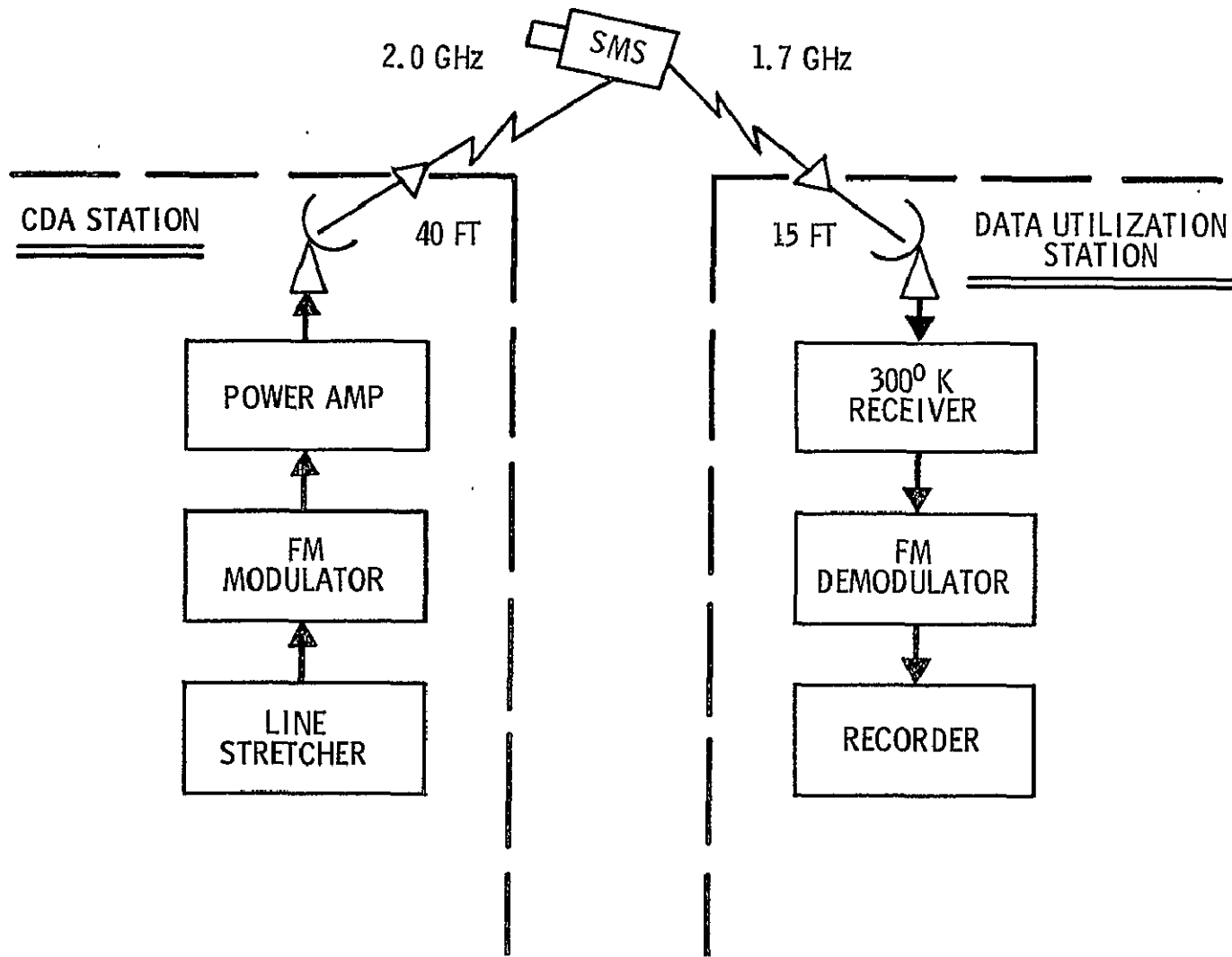


Figure V-21. Retransmission of Stretched Data

It is interesting to note the effect of the single transponder system on the performance of the stretched data up-link. Since the downlink must be power shared with the DCS, there is a restriction on the stretched data up-link power level that can enter the S/C receiver. This limitation therefore limits the attainable stretched data up-link CNR. If on the other hand, a second S/C transponder were used exclusively for the DCS, or at least a separate power amplifier, the stretched data up-link CNR can be considerably improved by increasing the CDA transmitter level. From Table V-7, for an 80 watt CDA transmitter level, the up-link is improved by 10 db resulting in an overall stretched data link improvement of 1.5 db.

It may be of additional interest to note that a much higher SNR could be realized if the resolution were increased to 1.0 n. m. This would allow a 4 to 1 reduction of the 225 kHz analog baseband to about 56 kHz. This bandwidth reduction will permit an improvement to be realized in the overall SNR of 19 db by allowing an increase in deviation ratio with the same transmission bandwidth. Perhaps, however, a more significant advantage can be gained by reducing the transmission bandwidth to 750 kHz. From Table V-7, therefore, it can be seen that the overall link CNR will increase by 6 db. This will permit the DUS to operate with a 7-1/2 foot antenna with the same CNR and SNR as that indicated for the 15 foot station. Table V-8 shows the attainable SNR's for various DUS antenna sizes.

Table V-8

Stretched Data Link Performance

Visible Data Resolution (n. miles)	No. of Visible Lines Transmitted Per Spin Cycle	Baseband Bandwidth	RF Bandwidth	DUS Antenna Size	Video SNR $\left(\frac{P-P}{RMS}\right)^{1,2}$
					1 Transponder
0.5	8	225 kHz	3 MHz	15 ft.	47.5 db
1.0	4	56 kHz	3 MHz	15 ft.	66.6 db
1.0	4	56 kHz	750 kHz	7.5 ft.	47.5 db
2.0	2	14 kHz	750 kHz	7.5 ft.	66.6 db
2.0	2	14 kHz	188 kHz	3.75 ft.	47.5 db
4.0	1	3.5 kHz	188 kHz	3.75 ft.	66.6 db
4.0	1	3.5 kHz	47 kHz	1.9 ft.	47.5 db

NOTE: 1. DUS receiver temperature taken as 300°K in all cases.

2. Visible radiometer SNR = 53 db $\left(\frac{P-P}{RMS}\right)$ (for comparison with above figures)

4. DATA COLLECTION SYSTEM

4.1 INTRODUCTION TO DATA COLLECTION SYSTEMS

The data collection and distribution system will consist of a number of remotely located data collection platforms, the spacecraft transponder, the portion of the CDA station devoted to data functions and the data relay communications link whereby the data is relayed from the CDA to Suitland N. E. S. C. and other user stations. The data relay function is not discussed in this section.

The discussion of data collection is as follows. A list of constraints for the system is stated and an attempt made to justify each. Then a few of the major alternatives of the data collection system are reviewed. The work in the Phase C study will be concentrated in this area. The function of the Phase C study is to perform the tradeoffs between the alternatives which will allow selection of optimized parameters which in turn become additional constraints. Next a few candidate systems for data collection will be described. These systems are presented to illustrate their feasibility and should not be considered as necessarily being optimized. Finally, a plan for the Phase C study is presented in which the most important alternatives are evaluated.

4.1.1 Constraints

There are certain factors which bear on the design of the data collection system which are limited to a range of values through cost and state-of-the-art considerations. These constraints are listed in Table V-9.

4.1.1.1 Data Speed and Format—To achieve compatibility with the equipment of present sources and users of data which may be relayed through the spacecraft, it is reasonable to assume that most or all traffic will be in the teletype (ASCII) code which is 100 WPM, seven bits per character or about 75 bits per second. A character error rate on the order of $1P^*$ in 10^4 seems to be a reasonable design goal for this type of service.

4.1.1.2 Traffic—Table V-10 summarizes the traffic reporting to the CDA during one six hour synoptic interval. A pessimistically high data rate has been assumed for simplicity in computing the data flow in that the class I and II stations were assumed to have reported in the 7 bits per character teletype code rather than in the more efficient binary equivalent of the thousand level analog signals or even BCD. The result is an initial system comprising about 3500 stations to report in 6 hours with a data flow of about 600K bits. Now adding an allowance

*P hereafter refers to part, i. e. , read as 1 part in 10^4 .

Table V-9

Major Constraints of Data Collection System

Item	Limits	Justification
1. DCP Battery Energy Capacity	400 Watt-Hrs.	From Magnavox Corp.
2. DCP Frequency Stability	0.5 PPM/Year	State-of-the-art of TCXO's -40 to + 70°C Arvin and Bulova Corp.
3. Total Data Collection Time	21,600 sec	6 hour synoptic period
4. Total Traffic	2M bits	Extrapolation of present traffic estimate over a 15 year period
5. Total number of DCP's	10,000	Same as 4
6. Probability of Character Errors	7×10^{-5}	Based on a 10^{-5} bit error rate and 7 bits per character ASCII code
7. DCP Antenna Gain	3dB	From considerations of cost and/or ease of installation on unstabilized platform
8. Minimum number of Interrogatable DCP's	300	ESSA requirement
9. Bit Rate and Format	75 Bits/SEC 7 BIT ASCII Code	Compatibility with present user equipment
10. Max. DCP G/T_g	-20db/°K	Required antenna coverage, cost and state- of-the-art of low noise receivers
11. Max. spacecraft EIRP at 5° elevation circle	+55dbm	State-of-the-art of spacecraft antenna gains, cost and booster payload capability

of about 30% to the data to cover synchronization and parity check bits yields a data flow of about 780K bits. Assuming a very vigorous system growth rate of 10% per year over the original system the traffic at the end of 15 years would be 1.95M bits from about 8700 sensors. At this point the system should be considered saturated and a spacecraft with a larger power-bandwidth product would be required to accommodate additional system growth. For the purpose of all following analysis, a system of 10,000 sensors reporting 2M bits of data in each six hour intervals will be considered.

Now if the sensors reported sequentially over the entire six hour interval, the data rate would be

$$\frac{2 \times 10^6 \text{ bits}}{21,600 \text{ sec}} = 92.6 \text{ bits/sec.}$$

The 100 WPM teletype transmits 75 bits/sec. which requires about 100 Hz of double sideband transmission bandwidth. Thus to clear all the traffic in six hours at teletype transmission speed will require at least two 100 Hz channels between the DCP's, the spacecraft, and the CDA.

Table V-10

Estimate of Traffic Reporting to CDA in 6 Hr.
Synoptic Interval at Time of Launch

Class of Station	No. of Observations Per Transmission	Message Length Per Observation	No. of ID Characters per Transmission	No. of Bits Per Transmission (TTY Code, 7 Bits/Char.)	No. of Stations Reporting Per 6 Hrs.	Total Bits
I	One	3 decimal digits	4 decimal digits	49	2,500	122,500
II	Four	3 decimal digits	4 decimal digits	112	500	56,000
III	One	60 decimal digits or alphanumerics	—	420	400	168,000
IV	One	405 decimal digits or alphanumerics	—	2,835	85	240,975
Grand Total: No. of Stations Reporting per 6 hours					3,485	
Grand Total: Traffic Reporting in bits per 6 hours						587,475

In addition there is a desire on the part of ESSA that the DCS support a number (undetermined at the present time) of continuous 500 bits/sec channels. Such information would originate from threshold type sensors used in warning systems to signal excessive wind velocities, high water levels or earth tremors.

While this subject will be dealt with in detail during the Phase C study, it is believed, at this time, that the major impact of these continuous transmissions will be to reduce the margin in the data reporting link between the spacecraft and CDA due to power sharing and, in the case where the up and down links share the same transponder, reduce the margin in the interrogation link.

Since little is known about this particular requirement at this time, it is not planned to include a detailed discussion in this report.

4.1.1.3 State-of-the-Art Constraints—The items in Table V-9 which are listed as cost and/or state-of-the-art constraints are the best estimates based on today's developed bandware.

4.1.1.4 DCP Antenna Coverage—It is desirable that the DCP antenna have hemispherical coverage since many DCP's will be on floating platforms subject to pitch and rotations in azimuth. The polarization of the DCP antenna is not considered a constraint at this point. The down-link transmission will likely be circularly polarized but a circularly polarized DCP antenna will be more expensive than one with linear polarization. Since a linearly polarized receiving antenna with a circularly polarized transmitter produces a 3 db loss, the decision as to whether or not the system can afford the 3 db loss will depend on the margin left after considering all system variables.

4.1.2 Design Variables

4.1.2.1 Number of Spacecraft Transponders—Among the most important design variables to be resolved during Phase C is the general configuration of the spacecraft RF system. The use of single or multiple transponders determines the flexibility allowed in selecting the data collection system frequency. From a consideration of the large bandwidths required for the radiometer downlink and both stretched-data links, a microwave carrier appears to be mandatory. If a single transponder is used, this forces the DCP's to operate at microwave also which raises the cost and, as will be shown later, results in a reduced receiver margin. If two spacecraft transponders are used, one would likely be dedicated to the camera and stretch links and the other to the data collection system. In this case the data collection system might be mechanized at VHF or UHF.

4.1.2.2 Method of Timing DCP Reports—In both single and multiple transponder spacecraft systems a possibility exists for greatly simplifying most of the DCP's by eliminating the need for an interrogation receiver. This would be particularly attractive when the receiving equipment is expensive as it would be at a microwave frequency. Another advantage in addition to the DCP consideration is that the spacecraft power consumption would be reduced by the amount required for the interrogation link transmitter.

Interrogation of the DCP's is just one method of multiplexing many signals through the spacecraft. In interrogation-multiple-access methods highly efficient use is made of the available time-bandwidth signal space allocation since the reporting times and frequencies of the DCP's being under the control of the interrogation signal enables the DCP reports to follow through the spacecraft in close time sequence and very closely spaced in frequency with only minimum guard zones. In non-interrogated-multiple-access methods the same time-bandwidth economy cannot be realized since instead of the reports all being synchronized by one clock each report time and frequency is controlled by the independent DCP clocks. The method of timing the DCP reports remains one of the major issues to be decided in Phase C. Examples of an interrogated DCP and two distinctly different non-interrogated systems are described below to serve as a point of departure in the future study phase.

4.1.2.3 Influence of Carrier Frequency on Data Collection System—The choice of the DCP interrogation and reporting frequency impacts on the cost of the data collection system. To illustrate this the downlink is examined for three frequencies of interest for possible DCP operation.

Let the spacecraft transmitter power and antenna gain be P_t and G_t respectively. Their product is the effective isotropically radiated power, EIRP. The so-called free space loss is

$$L_s = \left(\frac{4\pi R_f}{C}\right)^2$$

where R is the slant range, C the velocity of light and f the carrier frequency. The DCP receiver is characterized by a figure of merit, G/T_s where G is the receiver antenna gain and T_s is the effective receiving system noise temperature. The carrier to noise density, C/N_o , is expressed by the equation,

$$C/N_o \text{ (db-Hz)} = \text{EIRP (dbm)} + G/T_s \text{ (db/}^\circ\text{K)} - L_s \text{ (db)} + 198.6 \text{ (dbm-Hz-}^\circ\text{K)}$$

Due to the fact that full earth coverage precludes using a spacecraft antenna beam-width less than about 17 degrees and since the spacecraft transmitter power is limited by the power source, the maximum attainable EIRP can be considered independent of frequency. The receiver noise characteristics at the frequencies of interest are summarized in Table V-11. *

Table V-11

Receiver Noise Characteristics

Frequency	RF Amplifier type	T_1 , Noise Temp of RF Amp	T_s , System Noise Temp	G/T_s
150 MHz	Bipolar Transistor	100°K	504°K	-24.0 db/°K
400 MHz	Bipolar Transistor	150°K	386°K	-22.8 db/°K
1700 MHz	Tunnel Diode Amp.	400°K	610°K	-24.8 db/°K
1700 MHz	Uncooled Paramp.	100°K	310°K	-21.9 db/°K

The system noise temperature referred to the input of the preamplifier is given by,

$$T_s = \alpha T_a + T_o (1-\alpha) + T_1$$

where

α = Attenuation factor of transmission line between the preamplifier and antenna

T_a = Antenna effective noise temperature

T_o = Physical temperature of transmission line

T_1 = Noise temperature of preamplifier

*N. E. Feldman, "Syllabus on Low Noise Microwave Devices" The Microwave Journal, July 1969 pp. 59-69

T_a consists of two components, the earth temperature which will undoubtedly fall within the main beam of a hemispherical coverage antenna and a contribution from solar noise. The noise temperature contributions due to the earth, sun and transmission line loss are given in Table V-12. Adding these results to the estimated RF amplifier noise temperatures yields the system noise temperature, T_s . The antenna gain is assumed to be 3 db for a hemispherical coverage. Based on this, the receiver G/T_s is computed and is given for each case in Table V-11. It is seen from that table, even assuming the unlikely case of an uncooled paramp on the DCP, that the range of G/T_s from VHF through 1.7 GHz varies only about 3 db. This range is narrowed to only 2 db if the use of a paramp in a practical DCP receiver is discounted.

The spacecraft antenna gain is also somewhat influenced by frequency. For example, if the spacecraft antenna beamwidth was exactly earth coverage at its 3 db points, the DCP's seeing the satellite at the horizon would experience a 3 db loss relative to the beam center. Based on the Hughes HS-303B satellite however, the electricity despun antenna at VHF has a net gain of only 10.5 db (11.5 db gain and 1.0 db loss) and for such a broad beam the off-beam center loss is only about 0.5 db. The same antenna characteristics will be assumed at UHF. On the other hand, at 1700 MHz the antenna gain is 18.0 db with 1.5 db loss and 4.5 db off-beam center loss (at 5° satellite elevation) which yields a net gain of 12.0 db. Now to hold the requirements on spacecraft prime power constant the assumption is made that the transmitter power and efficiency at all the frequencies under consideration is constant. The RF power input to the antenna system is assumed to be 20 watts.

The down-link carrier to noise density and energy to noise density ratio in 100 Hz can now be calculated as shown in Table V-13.

One constraint imposed on the data collection system is a bit error probability not to exceed 10^{-5} . To a small extent the energy to noise density ratio required to meet this performance depends on the modulation type. As is well known, for binary modulation the required carrier to noise ratio for 10^{-5} error rate varies from about 9.5 db for coherent PSK to about 13.5 db for non-coherent FSK. Since the modulation type is presently not determined the pessimistic value of 13.5 db will be assumed to be the required E/N_0 for the data collection system.

4.1.2.4 Other System Variables—Other important factors to be considered in the generalized downlink calculation are RFI, multipath fading, short term stability and field aging degradation of receiver sensitivity and spacecraft power. No RFI estimate can be made at present since to a large extent it will be dependent upon the exact frequency chosen and will be one subject of study in the next phase. The multipath fading is also difficult to estimate. For a stationary DCP at 1700 MHz and a relatively high satellite angle fading will be the least. For floating

Table V-12

Noise Temperature Contribution Due Antenna and Feed

Freq.	T_a		$-10 \log \alpha$	$(1-\alpha) T_o$	$\alpha T_a + T_o (1-\alpha)$
	Noise Temp. Contribution of Earth**	Noise Temp. Contribution of Disturbed Sun*	Attenuation (db) of Antenna Transmission Line (6 feet of 1/2" Styroflex Cable)	Noise Contribution of Transmission Line (Assumed to be at 290°K)	Noise Temp. Due to Antenna and RF Lines Referred to Input of RF Amp.
150MHz	205°K	200°	0.06	4°K	404°K
400MHz	205°K	30°	0.1	7°K	236°K
1700MHz	205°K	1°	0.2	13°K	210°K

*Extrapolated from curves in Figure B-1, "Technical and Cost Factors that affect Television Reception from a Synchronous Satellite"

Jansky and Bailey Systems Engineering Dept. June 30, 1966 (N67-36665)

**See Appendix B, this report.

Table V-13

Down-Link Performance and System Margin

Freq. (MHz)	8.5° Off-Beam Center S/C EIRP (dbm)	DCP Revr. Type	DCP G/Ts (db/°K)	Max-Range* Free Space Loss (db)	Boltzmann's Constant (dbm/Hz-°K)	Carrier to Noise Density (db-Hz)	Energy to Noise Density for a 13.4 ms** Pulse (db)	Field Aging Degradation (db)	Required E/No (db)	Estimated System Margin (db)
150	53.0	Bipolar Transistor	-24.0	168.5	-198.6	59.1	40.4	2.0	13.5	24.9
400	53.0	Bipolar Transistor	-22.8	177.0	-193.6	51.8	33.1	2.0	13.5	17.6
1700	55.0	Tunnel Diode Amp.	-24.8	189.5	-198.6	39.3	20.6	2.0	13.5	5.1
1700	55.0	Uncooled Paramp.	-21.9	189.5	-198.6	42.2	23.5	2.0	13.5	8.0
$E/N_o \text{ (db)} = \frac{C}{N_o} \text{ (db-Hz)} \times T \text{ (SEC) where } T = \text{bit length}$										

*Range at point where satellite is seen at 5° elevation is 25,700 smt.

**Period of a 75 bits/sec pulse.

platforms at VHF with low angles to the satellite very severe fades may be encountered. In order to determine the fade margin allowed for the system, the probability distribution of fades must be known for each environment.

Field aging degradation of 1 db each for increase in receiver noise figure and reduction of spacecraft transmitter power will be assumed. The resulting margin for each system is indicated in Table V-13.

The receiver oscillator stabilities are the last major considerations in the DCP interrogation link. An interrogated DCP will lock its local oscillator to the spacecraft downlink transmission to remove any uncertainty in its reporting frequency. The DCP's must acquire the spacecraft signal in a bandwidth, B_A , where

$$B_A = \left[2S f_o + B_i \right]$$

and S is the long term stability factor of the DCP oscillator, f_o is the downlink carrier frequency and B_i is the IF information bandwidth required by the modulated signal. The information is demodulated in a bandwidth B_i following acquisition. It is assumed that all DCP's acquire the downlink signal at the beginning of the synoptic period thus the acquisition time is not of material importance.

It is conceivable that to avoid the relatively trivial complexity of a phase locked receiver and its acquisition circuits the signal might be demodulated in the bandwidth B_A . In this case, however, the detection bandwidth is no longer matched to the information bandwidth and the effective E/N_o is degraded on the order of magnitude of the ratio between the matched and unmatched bandwidths.

The DCP local oscillator will likely be a temperature compensated crystal oscillator (TCXO) since it is a good compromise between the desirable high stability and undesirable power consumption of oven controlled crystal oscillators. TCXO stabilities of $5P$ in 10^7 are state-of-the-art while $1P$ in 10^5 are off-the-shelf. Table V-14 shows the acquisition bandwidth and B_i/B_A ratio at each frequency of interest for various TCXO stabilities. Referring back to the system margins shown in Table V-13 and comparing the system margins to the degradation of E/N_o in an unmatched bandwidth, certain conclusions can be drawn immediately:

- Even for the best TCXO stability, for the system to have a positive margin at 1700 MHz a phase locked receiver is required.
- Non-phase locked receivers might possibly be used at UHF and VHF. The oscillator stability required will be determined by the amount of system margin used up by RFI and multipath considerations.

Table V-14

 B_A (Hz) and B_i/B_A (db) for $B_i = 100$ Hz

TCXO Long Term Stability (per Year)	f_o (MHz)			
	150	400	1,700	
1P in 10^5	B_A	3,100 Hz	8,100 Hz	34,100 Hz
	B_i/B_A	-14.9 db	-19.1 db	-25.4 db
1P in 10^6	B_A	400 Hz	900 Hz	3,500 Hz
	B_i/B_A	-6.0 db	-9.5 db	-15.4 db
5P in 10^7	B_A	250 Hz	500 Hz	1,800 Hz
	B_i/B_A	-4.0 db	-7.0 db	-12.5 db

The DCP oscillator short term stability is of particular concern due to the low, 75 bit per second data rate envisioned for the system. The effect of long term instability of the receiver (VCO) oscillator is completely eliminated by locking to the down-link signal. The short term instability is not so easily dismissed. The bandwidth of the DCP phase lock loop must be very narrow since its function is to track only the phase of the down-link carrier and not phase changes due to the 75 bit/sec. modulation. Assuming the down-link signal is noiseless and the spacecraft oscillator is perfectly stable (short term) the DCP VCO will produce noise on the demodulated data due to deviations in the VCO phase which occur in time intervals shorter than the reciprocal of the phase lock loop bandwidth. If the phase noise is Gaussian the noise power due to short term instabilities can be computed by weighting the sideband-noise power spectral density by the matched filter bandwidth and integrating the weighted spectrum. Since the sidebands follow a $1/f$ spectral density a dramatic increase in the noise due to short term instabilities can be expected as the bit rate is reduced.

All the points discussed in this section must be the subject of detailed investigation during Phase C.

4.1.3 Data Collection System Concepts

In considering the selection of a data collection system design for the SMS many trade-off factors must be weighed to arrive at an operational concept that offers the greatest possibility of fulfilling the overall goals and constraints as discussed earlier. Primary among these objectives is the minimization of overall system cost including both the DCP stations as well as the CDA station. An additional objective is to provide a system that will minimize the cost at launch and provide for expansion to complete system capabilities at some later date as the need arises.

The next section will describe three different modulation structures for achieving the overall data collection task for the SMS. This is not to say that other techniques are not adaptable but rather to indicate the immense flexibility involved in arriving at an optimum selection. In general the data collection system (DCS) plan can be divided into the two major categories of interrogated and non-interrogated systems. The interrogated system by its very nature is synchronous and will be more than likely the most efficient from the standpoint of channel capacity which can be defined in this case as:

$$\eta = \frac{T_0 B_0 m}{T W_0}$$

where T_0 is the average data time per DCP
 B_0 is the average data bandwidth
 m is the number of DCP's
 T is the total time available for data collection which is the 6 hour synoptic period in this system
 W_0 is the total bandwidth used by the DCS

The interrogated system, however, requires a DCP receive capability which can conceivably increase the DCP cost over a non-interrogated DCP design. It is important, therefore, that the channel efficiency, η , only be considered to a degree that is consistent with minimizing total system cost.

Two non-interrogatable systems will be considered. One of these, the pseudo-noise spread spectrum technique is a semi-time synchronized system where the DCP transmissions are allowed to time overlap by some degree that is dependent upon the allowable frequency stability of the DCP stations. The principle feature

of this technique is that the DCP transmissions can now overlap in both the time and frequency domains thus minimizing the time and frequency guard bands that might otherwise be required if a pure time/frequency matrix system were employed. As will be seen later, however, the effectiveness of this approach becomes less as the frequency stability of the DCP station increases.

The third system which will be briefly examined is also a non-interrogatable concept that allows for time and frequency overlap by retransmission of the data several times during a single 6 hour synoptic period. Based on a particular DCP stability it is possible to predict a certain probability of obtaining an interference free data transmission time/frequency slot. As with the spread spectrum system the advantage of this technique also becomes less attractive as the DCP stability increases. The principle advantage of the non-interrogatable system is that no receiver is required for the DCP and since a 10,000 DCP system is being considered this can have a measurable effect on the total DCP system cost. It is therefore, within this framework that the ultimate selection of the DCS must be made.

4.2 DATA COLLECTION SYSTEMS DESCRIPTIONS

This section will describe three distinct approaches to the design of a DCS for the SMS. The difficulty involved in arriving at an optimum selection is compounded largely due to the lack of sufficient system constraints around which an optimization plan could otherwise be established. The only real system constraint, as stated earlier, is a minimization of the total system cost. All other design parameters should ideally be selected with this factor in mind.

The DCS that will be discussed in this section will therefore be structured largely around the self-imposed constraints as discussed earlier in section 4.1.1. It will become more apparent as the development of this section progresses that the two design parameters having the most serious impact on the structure of the DCS will be the selection of the operating frequency (UHF versus S band) and the attainable frequency stability of the DCP.

4.2.1 SOMS/GOES Data Collection System

4.2.1.1 Introduction—Data collection systems based on UHF/VHF frequencies have been under study by ESSA/NESC since 1966.^{1, 2}

Three configurations of this data collection system which were investigated are as follows:

- a. All UHF/VHF that is either 149 MHz up/ 137 MHz down or 402 MHz up/418 MHz down.
- b. A "cross strapped" system whereby one or the other of the above bands are converted to 1.7 GHz down and 2 GHz up for communication with the CDA stations or other master terminals.
- c. All S-band, 1.7 GHz down/2 GHz up.

All the above employ an interrogation system, an ASC II Code information format and a DCP designed to lock onto the interrogation signal thereby deriving its transmitted frequency. This allows the data collection system to operate in a minimum bandwidth (100 Hz). The link calculations for these configurations are given in Appendix A.

4.2.1.2 UHF/VHF System—In this configuration, the spacecraft would have two separate transponders, one UHF/VHF and one at S-band. S-band would be used to transmit cloud data, telemetry and command, and the UHF/VHF would be used solely for data collection.

4.2.1.3 UHF/VHF-S-band System— The combined UHF/VHF S-band system would use either UHF or VHF cross coupled with the S-band transponder (see SOMS/GOES system studies). Such a system would operate as follows:

- a. An interrogation signal would be transmitted to the spacecraft at 2 GHz
- b. At the spacecraft, this signal would be converted to 418 MHz or 137 MHz depending on the band selected

¹Multiple Access Relaying for a Synchronous Operational Meteorological Satellite (SOMS). Prepared for ESSA/NESC by Telecom Inc., Arlington, Va. 14 Sept. 1966.

²Geostationary Operational Environmental Satellite (GOES) Data Collection System. Prepared for ESSA/NESC by Telecom Inc., Arlington, Va. Task 1 Nov. 1967, Task 2 Dec. 1967, Task 3 and 4 Dec. 1968

- c. The DCP would receive its interrogation on this frequency and generate its report frequency locked to this signal and communicate its data plus station identifier back to the spacecraft at 402 MHz or 149 MHz.
- d. At the spacecraft the signal is converted to 1.7 GHz and transmitted to the CDA station.
- e. Signals are received at the CDA station on the same 40-foot antenna used to receive the spin scan picture data.

Operation of this system would require a separate transmitter at 418/137 and either an additional transmitter at 1.7 MHz or the DCP reports could be transmitted only during the space scan portion of the spacecraft spin period. The DCP reports would share the transponder simultaneously with the stretch link transmission.

4.2.1.4 All S-band System—The data collection system could be configured to operate completely at S-band frequencies 1700 MHz down and 2025 MHz up. This concept would either require a separate transponder or sharing the transponder with the stretch link transmission. For continuous operation with a separate transponder, a completely dedicated band (200 Hz) of frequencies would have to be allocated in the 1700 MHz and 2025 MHz bands. The spacecraft primary power would likewise need to be increased to allow a continuous transmission of DCP interrogations and reports.

4.2.1.5 GOES/DCP—The GOES data collection platform will accept data from a variety of sensors, buoys, automatic weather stations, river gauges, etc. In this concept these platforms will be interrogated, derive the transmitted frequency from the received interrogation signal, and operate with digital data inputs. As the system expands and additional channels are added the system will operate in a frequency division multiple access mode with course time division keyed to the six-hour synoptic cycle. The more perishable data, (severe weather observations, upper air data, etc.) will be interrogated in the first two hours of the synoptic cycle and less perishable data during the last four hours (river gauges, tide gauges, etc.) A platform which meets these requirements will now be described.

The interrogated subsystem is the part of the DCP electronics package which determines when a sensor data transmission should be initiated. There are basically two types of DCP's, those which have self-contained preprogrammed timers or are actuated by an emergency condition and those which use an externally actuated command receiver system.

The internally actuated system is simply a timer which initiates data transmissions at a preset interval or a switch which initiates a transmission during emergency conditions (high winds, flood stages, earthquakes, etc.) The externally actuated subsystem consists of three basic elements: a command receiver which receives and demodulates the RF carrier, a command detector which accepts the receiver output and produces command data, and a command decoder which decodes the command and initiates appropriate action.

Since the internally actuated system is discussed elsewhere in this study, only the externally actuated system will be discussed here, although a hybrid system may be designed to include an internally actuated emergency mode such as in the Tsunami warning system.

To allow for system expansion, replacement of platforms, and spoilage during manufacture, it is assumed that an interrogation system be designed to handle 100,000 platforms. Because analog decoder techniques will only handle a limited number of platforms in a given bandwidth, the interrogation system would be digital.

The command format to be used here is 17 bits of address followed by two bits of command. This provides for 131,071 platform addresses and four commands.

The sensor data format is assumed to be the American Standard Code for Information Interchange (ASCII), which is transmitted at 75 bits per second. This code was selected because it is the standard data code for government use and it is computer compatible. However, other formats or bit rates may be used since formats and bit rates can be changed at the CDA station. It is further assumed that the 75 bps rate would require a bandwidth of 100 Hz.

Since both the interrogation and response from the platform are digital, some form of shift keying is indicated, such as phase shift keying, where a one and zero cause a plus or minus 90° shift in phase or frequency shift keying which causes a subcarrier to shift between two predetermined frequencies.

The error probabilities for a differentially coherent phase shift keyed system (DPSK) and non-coherent frequency shift keying have been compared previously, where it was stated that the same error probability can be obtained with 3 db less C/N in the DPSK system. For this reason it is assumed that a DPSK modulation will be used. However, the equipment to operate this system may be complex and therefore more expensive than the FSK technique.

Since these DCP's operate in a FDMA mode the DPSK modulation will be placed on a subcarrier (perhaps as many as six independently keyed tones spaced 170 Hz apart (150 Hz baseband plus 20 Hz guard) (see Figure V-22). This composite modulation will be Double Sideband Supressed Carrier (DSBSC) modulated onto the carrier resulting in the transmission of a DPSK/DSBSC signal.

The GOES data collection platform which is capable of being interrogated, deriving the transmit frequency from the receive frequency (thus allowing operation in a minimum of bandwidth) and operating with the digital data and modulation previously discussed is shown in the DCP Block Diagram (Figure V-23). This platform may be divided into three parts; the receiver, the synthesizer and the transmitter. The ASCII encoder and the interrogation decoder operates into the baseband unit. The antenna system is assumed to have a minimum gain of 3 db. While the system shown was designed to operate at VHF, the techniques employed could be used at any of the frequencies under consideration (i. e., VHF, UHF, and S-band).

The receiver centers the DSBSC spectrum with AFC, the range of which is adequate to cover the sensors local oscillator drift for a year or more plus the anticipated doppler shift. Once the signal is centered, the demodulator locks to the symmetrical subcarrier sidebands for coherent demodulation of the DSBSC. The subcarrier assigned to the particular sensor platform is then demodulated to recover the interrogation code.

The IF reconstructed at the baseband demodulator may be mixed with the local oscillator to reconstruct a "clean" version of the suppressed down-link carrier. This may be converted in another mixer to derive the up-link carrier frequency. By this means, the local oscillator at the platform needs only to be within perhaps 1 kHz (7 parts in 10^6) for acquisition.

If the uplink carrier is generated by a divide and multiply operation e. g. , $137.6 \times 13/12 = 149.050$ MHz, then the platform operates as a coherent transponder and the only frequency error is introduced by the spacecraft doppler shift which enters into the frequency error at the CDA demodulator. The doppler error is largely predictable so that the CDA computer could calculate an appropriate frequency offset to compensate for doppler and long-term spacecraft conversion oscillator drift.

The sensor data is applied to the transmitter modulator which consists of a double balance mixer with the baseband feeding one input and the transmitter carrier frequency from the synthesizer feeding the other to obtain at the output the desired DSBSC signal which drives the power amplifier.

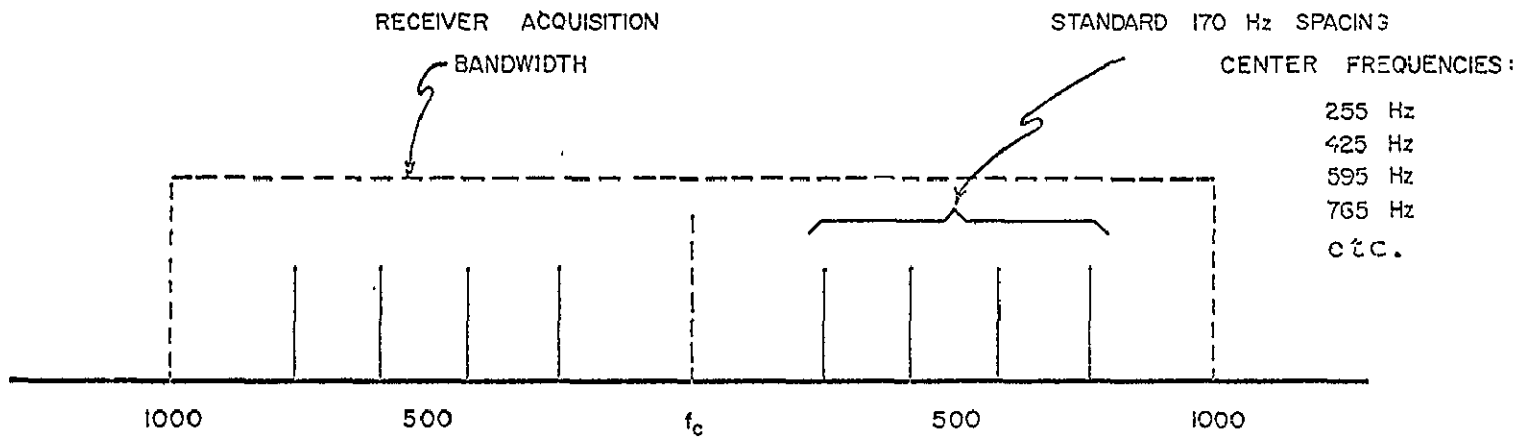


Figure V-22. Illustration of DSBSC Interrogation Spectrum for GEOS/DCP

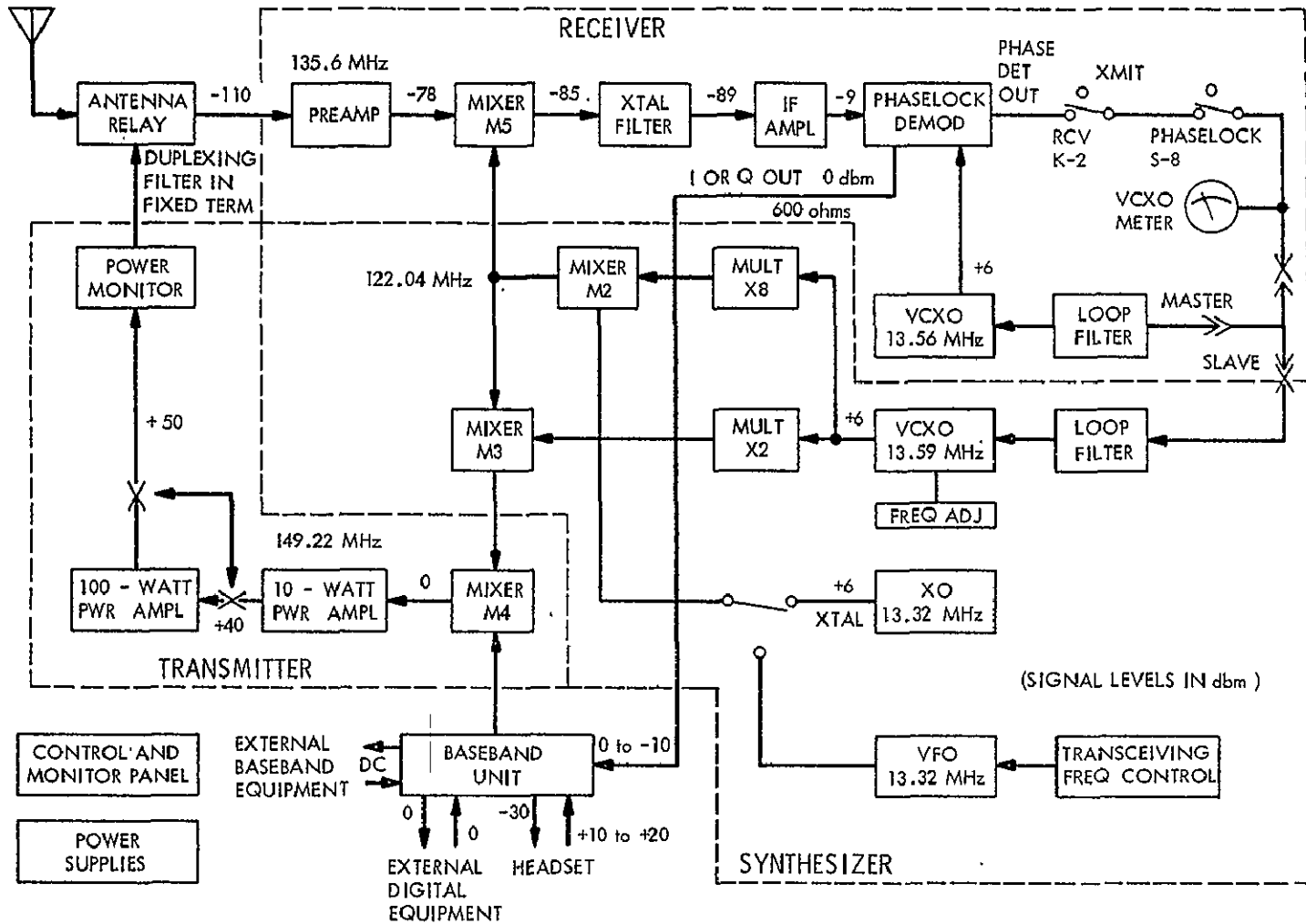


Figure V-23. DCP Block Diagram Developed During SOMS/GEOS Study

4.2.2 Spread Spectrum Data Collection System

The use of pseudo-noise spread spectrum techniques as a means for random access multiplexing is well documented in the literature [1][2][4][5][6][8][9][10][11][12][13][20]. Basically pseudo-noise spread spectrum is a quasiorthogonal code multiplexing technique which permits a determinable number of signal spectra to coexist in the same time and frequency slot. Discrimination among the various signals is then accomplished by assigning each signal a unique pseudo-noise code.

As will be shown later, PN mutliplexing is particularly well suited to a non-interrogatable system where the DCP stability is poor. The otherwise unusable spectrum that must be allowed due to frequency instability can now be used to advantage by increasing the processing gain of the spread spectrum system. It is also for this reason that the PN system will be more desirable at the S-band frequencies for a given DCP stability than at UHF or VHF.

A list of advantages and disadvantages for the pseudo-noise data collection system are presented in Table V-15.

4.2.2.1 Optimization of Time/Frequency Plan—It will be of interest here to develop a procedure for selecting an optimum arrangement of the time/frequency plan that will accommodate the DCS data flow that was discussed earlier in section 4.1.1.

It will be shown later (see section 4.2.2.2.1) equation 60, that the signal to pseudo-noise ratio (SPNR) is given by

$$\text{SPNR} = \frac{L R}{(N-1) (L+R)} \quad (38)$$

where L is the sequence length of the pseudo-noise code

N is the number of frequency and time overlapping DCP transmissions and the processing gain R can be defined as

$$R = \frac{f_c}{f_b} \quad (39)$$

where f_c is the clock rate or chip rate of the PN code and

f_b is the data bit rate

Table V-15

Advantages and Disadvantages for the SMS Pseudo Noise Data Collection System

Advantages

1. Channel efficiency is good when DCP stability is 1×10^{-5} or more
2. Addressing is accomplished with PN code
3. Offers discrimination against multipath and R. F. interference
4. Compatible with hard-limited S/C transponder
5. Reduces RF Power Density at ground
6. High resolution and non-ambiguous ranging is possible
7. No receiver required at DCP station

Disadvantages

1. Channel capacity is poor compared to interrogatable system
2. Less desirable at UHF or VHF
3. Requires code acquisition
4. In general correlation receivers at the CDA station will be more complex than conventional FDM methods

Now assuming that the correlation receiver at the CDA station must time sequentially acquire and read out all N channels in the presence of the DCP time drift, $\pm K_0 S$, where K_0 is the number of seconds per year = 3.16×10^7 , and S is the long term drift of the DCP station timer over one year then

$$N = \frac{2 K_0 S}{t_d + t_a} + 1 \quad (40)$$

where t_d is the specified data readout time and

t_a is the acquisition time of the PN code

One can further see how equation 40 is developed by reference to Figure V-24. It is assumed here that each DCP will be on for a time equal to $2 K_0 S + (t_a + t_d)$ so that the DCP is certain to be on at the time the particular DCP code is programmed into the correlation receiver at the CDA station. The correlation receiver will now sequentially turn-on the N codes each delayed a time $(t_a + t_d)$ and each code will remain on until the data is collected on that particular DCP, at which time it can proceed to the next DCP code. This procedure will progress until all N DCP's are read, and then repeated again until all DCP's are read over the six hour synoptic period.

It will be of further interest to note that under a worst case DCP time drift condition, it will be possible to have 2 N time overlapping DCP transmissions. This can only occur when adjacent DCP groups drift in opposite directions. Under normal conditions where the time drifts are random or all in a monotonic pattern, the expected number of overlap will be N as defined by equation 40.

On substitution of 40 into 38 therefore the SPNR becomes

$$\text{SPNR} = \frac{LR (t_d + t_a)}{(L+R) 2 K_0 S} \quad (41)$$

If the DCP channel capacity C is defined as

$$C = f_b t_d \quad (42)$$

and the PN code acquisition time is given by

$$t_a = \frac{L}{R_s} = \frac{L}{f_b} \quad (43)$$

where R_s is the PN search rate. Then equation 41 can be rewritten as

$$\text{SPNR} = \frac{L R C (1 + L/C)}{f_b (L+R) 2 K_0 S} \quad (44)$$

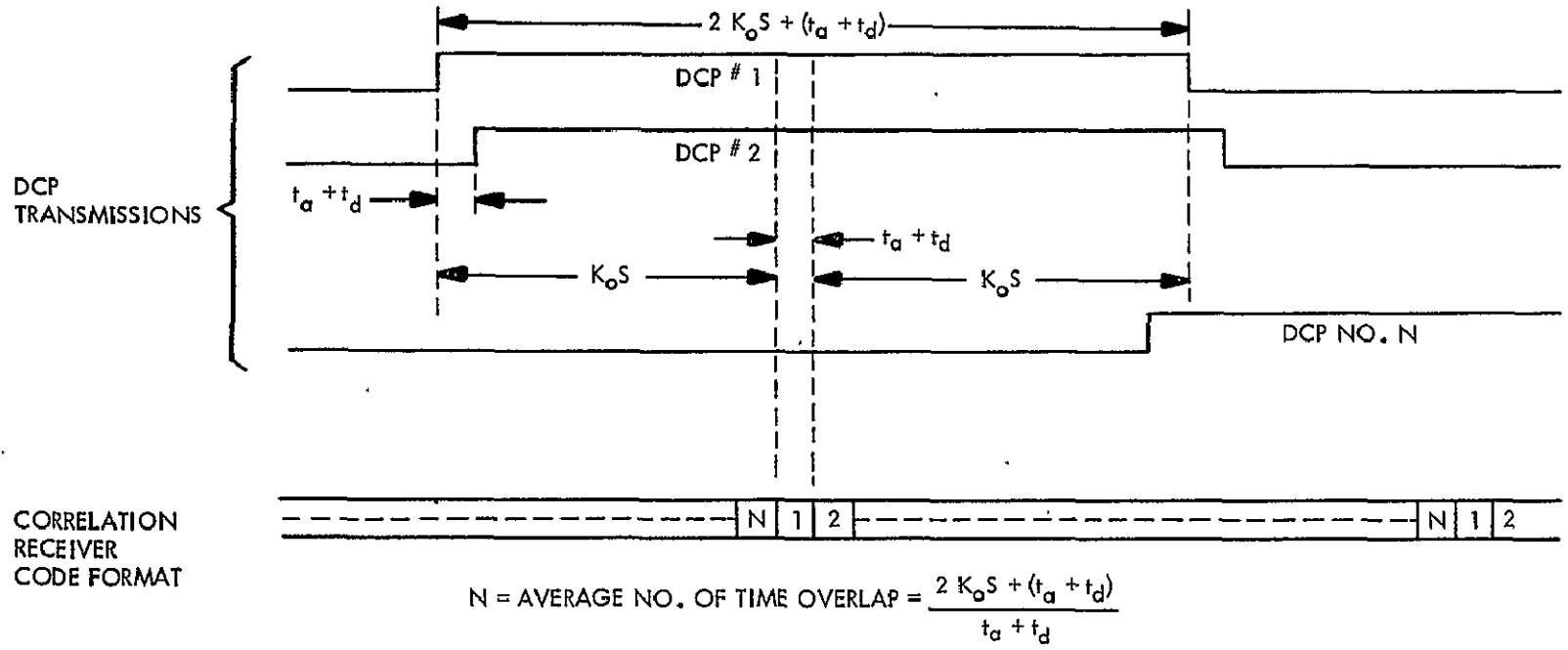


Figure V-24. PN Code Multiplexing Format

This equation is plotted in Figures V-25 and V-26 for $L = 2047$, $R = 2000$ and $K_0 = 3.16 \times 10^7$. In Figure V-25 for a stability of 1×10^{-5} , a bit rate of 75 bits/second and an average DCP channel capacity of 2000* bits, the SPNR is better than 19 db. The data time will be $C/f_b = 27$ seconds and the acquisition time $L/f_b = 27$ seconds. The number of overlapping DCP's from equation (38) or (40) will be about 13. The DCP sensor on-time $2 K_0 S + (t_a + t_d)$ will be 686 seconds and there will be 400 DCP's read in one correlation receiver over the 6 hour synoptic period. Since there are 10,000 DCP's to be considered, the required number of correlation receivers m_f will be

$$m_f = \frac{10^4}{400} = 25 \quad (45)$$

It should be obvious from the above development that the best time/frequency arrangement can only be established after all the design parameters are specified and this will change each time one or more of the variables in equation (44) is altered.

In particular it will be noted that each time the bit rate is changed there will be a corresponding change in the data collection time ($t_d + t_a$) and thus for the same DCP capacity there will be more time slots in the T_0 period and less frequency slots or

$$m_t = \frac{T_0}{t_a + t_d} \quad (46)$$

and

$$m_f = \frac{10^4}{m_t} \quad (47)$$

In the example given above $f_b = 75$ bps and $R = 2000$, therefore, the chip rate $f_c = Rf_b = 150$ kHz. This also represents the minimum transmission bandwidth for the PN channel and since there are 25 channels, the minimum transmission bandwidth will be 3.75 MHz. A pictorial representation of the time/frequency structure for this example is shown in Figure V-27.

4.2.2.2 DCP Link Calculations—This section will discuss in detail both the up and down link power budget situation for the proposed pseudo-noise DCS. All of the derivations and link calculations that follow will be based on the assumption that the spacecraft repeater and transmitter will have a linear gain transfer characteristic. The effect of a hard limited power shared spacecraft repeater will be discussed separately in section 4.2.2.2.2.2. In addition,

* For the 10,000 DCP system this represents a total system capacity of 20 million bits.

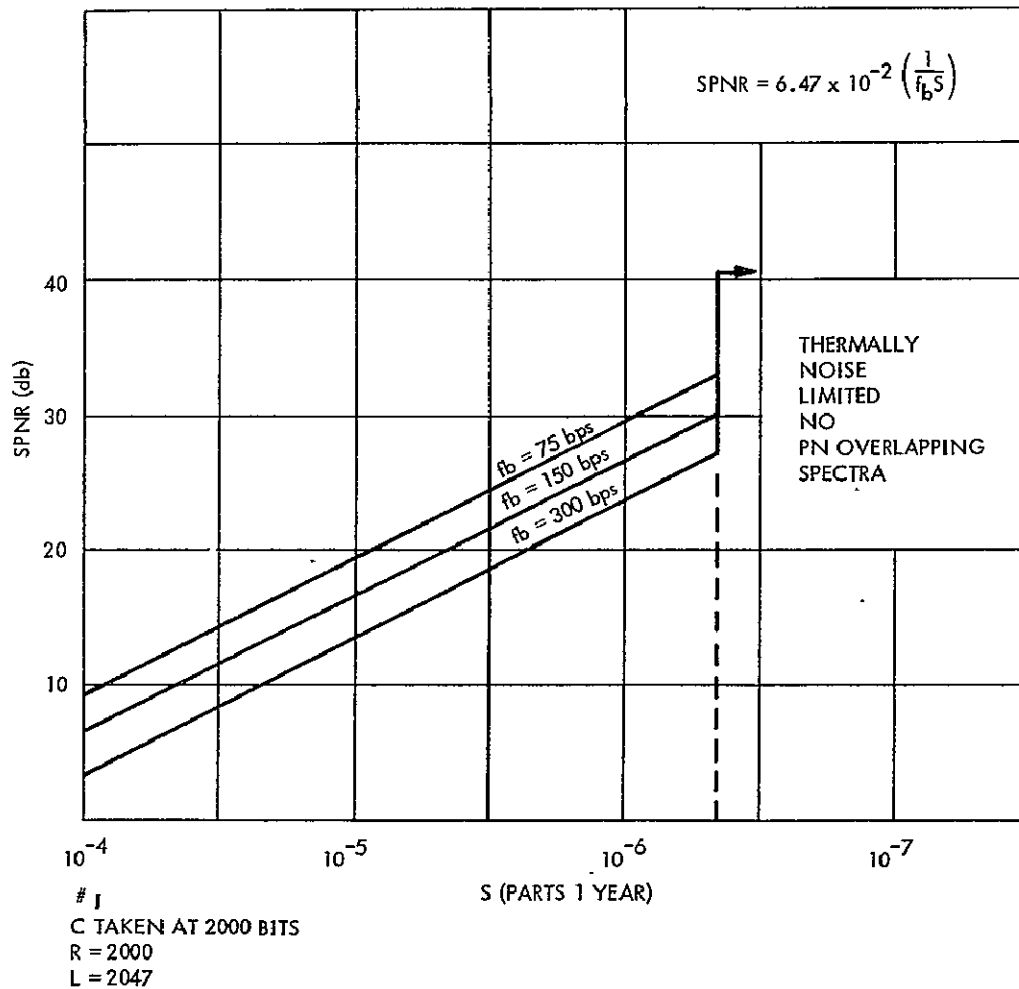


Figure V-25. Cross Correlation SNR versus DCP Stability

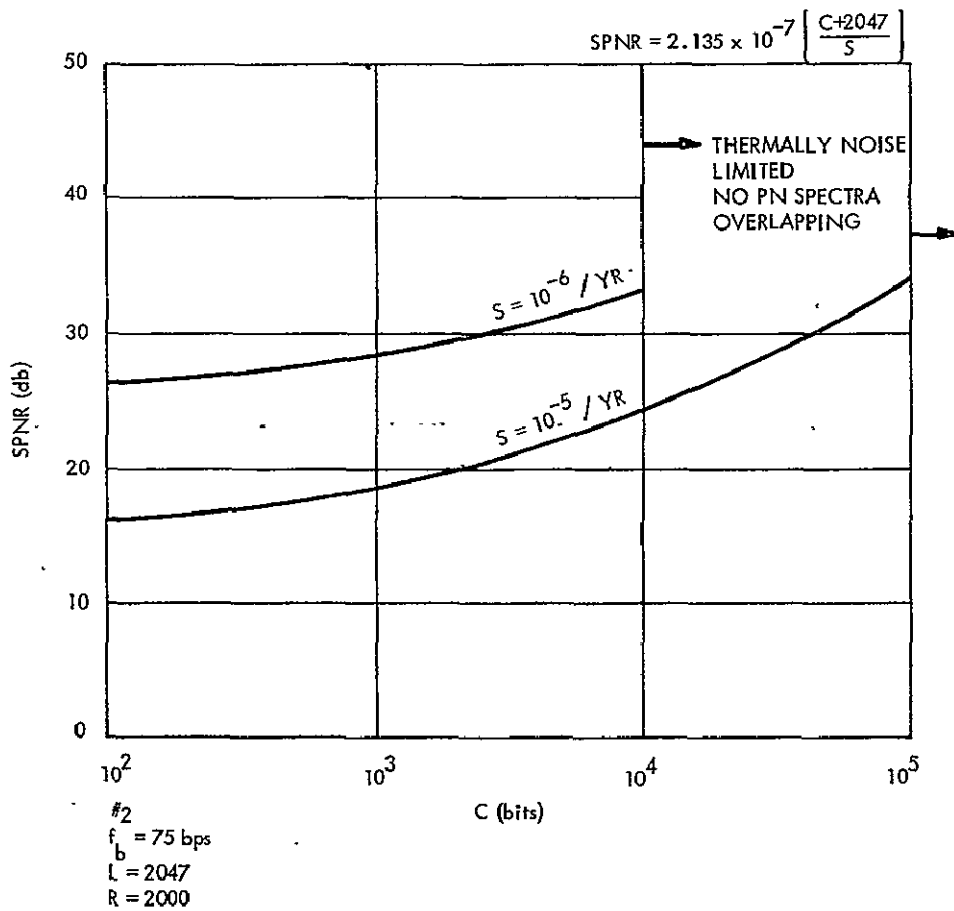


Figure V-26. Cross Correlation SNR versus DCP Bit Capacity

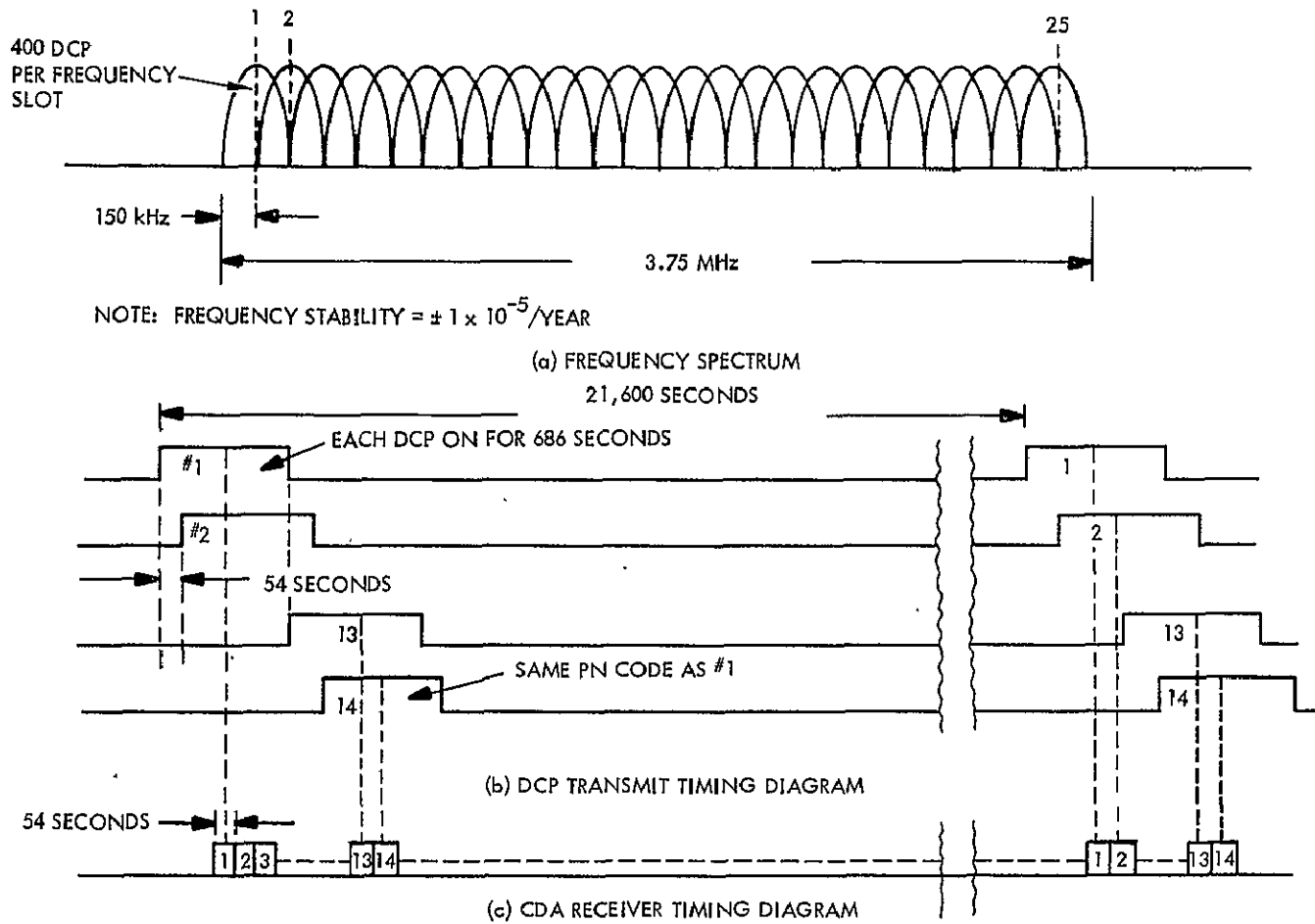


Figure V-27. Example of SMS PN Data Collection System Time/Frequency Structure

the link calculations that follow will be based on S-band operation since if a UHF or VHF system is adopted, PN is less attractive because of the additional bandwidth requirements of the PN technique.

4.2.2.2.1 Derivation of the Cross Correlation Signal-to-Noise Ratio—The proposed pseudo-noise multiplexing technique for the SMS data collection system makes use of the orthogonality properties of a particular class of pseudo-noise codes known as linear maximal length sequences. These codes, as will be shown, however are not completely orthogonal and therefore there is a limit to the number of signals that can simultaneously occupy the same time and frequency slots for a specific signal to cross-correlated noise ratio (SPNR).

4.2.2.2.1.1 Cross Correlation Properties of Linear Maximal Length Pseudo-Noise Sequences. A linear maximal length pseudo-noise sequence^[6], [14], [17], [18] is a special type of binary sequence which is characterized by the following properties:

- a. The linear maximal length binary sequence exhibits the best auto-correlation properties, that is

$$R(\tau) = \frac{1}{T} \int_0^{T=L\tau} S(t)S(t+\tau) dt = \begin{cases} 1 & \text{if } \tau = 0 \\ -\frac{1}{L} & \text{if } 1 < |\tau| < L-1 \end{cases} \quad (48)$$

In other words, the auto-correlation function is two valued having a normalized value of unity when $t = 0$ and having a maximum out of phase value ($t \neq 0$) of $1/L$. For an 11 stage PNG (pseudo-noise generator) of length $L = 2047$ bits, the out of phase correlation will be 66 db down from the peak at $t = 0$.

- b. The linear maximal length sequence has the property that the total number of "ones" will differ from the number of "zeros" by only unity when measured over one sequence length, L .
- c. The linear maximal length PN sequence exhibits a normal run-length distribution, that is, the occurrences of singles, pairs, triples, etc. of 1's and 0's must be descending powers of $1/2$.
- d. Linear maximal length PN sequences also exhibit the shift and add property, the sequence shifted and added back on itself (mod-2) produces the same sequence.

For an n stage PNG there are a total number of 2^{2^n} possibly binary codes; however, out of this number, there exists only a relatively small number that meet the qualifications of a linear maximal length PN code. These are tabulated in Table V-16 for PNGs of 3 through 25 stages. In particular, for an 11 stage PNG of length 2047 bits, there will exist 176 linear maximal length PN sequences.

It will be of interest now to examine the cross-correlation properties of these 176 sequences, which can be defined in the general case as

$$R(\tau)X = \frac{1}{T} \int_0^{T=L\tau} S_1(t) S_2(t+\tau) dt \quad (49)$$


For the case where $S_1(t)$ and $S_2(t)$ are binary (± 1) sequences, the multiplication can be viewed as a binary sum where the operation is accomplished by modulo-2 addition of $S_1(t)$ with $S_2(t)$. This operation will result in a new sequence $S_3(t)$ which will be of the same length as $S_1(t)$ and $S_2(t)$. It will also be observed that as $S_2(t+\tau)$ is shifted through each $(2^n - 1)$ bit positions, a new $S_3(t)$ sequence will be generated. This new sequence may or may not be maximal length depending on the particular τ bit position considered, that is to say, the net difference between - "1" and + "1" of the new sequence when averaged over the total sequence length of $(2^n - 1)$ bits, will be a function of τ . This operation is shown in Figure V-28.

If one now examines the cross-correlation as shown in Figure V-28, several interesting things can be concluded. First, one can expect a different value of Δ/L for each bit position of $S_2(t)$ and this value plus the distribution can be expected to vary widely depending on the particular sequences selected out of the total ensemble of 176 sequences available for $n = 11$ stages. This operation has been carried out ^[15] by a digital computer for $n = 11$ where a particular $S_1(t)$ was selected as the stationary sequence and all 175 other sequences, $S_2(t)$, were cross-correlated with it. The tabulations that result show values of Δ/L varying from a minimum of $\pm 1/L$ to a maximum of $\pm 287/L$. This is a range of from -66 db to -17 db, respectively. Not all sequences cross-correlated have this range, however; in fact, over 90 percent have a maximum peak of $\pm 129/L$ or -24 db and 22 of the 175 will have a maximum cross-correlation peak of only $65/L$ or -30 db.

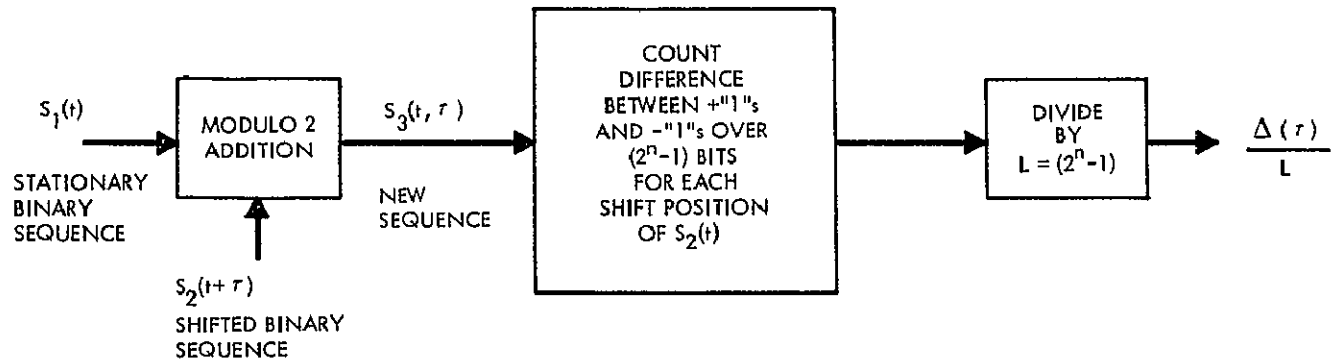
Table V-16

Characteristics of Various Maximal Length PN Codes

Generator Length (n)	Number of Possible Linear Maximal Length Codes	Code Length L ($2^n - 1$)	Maximum Cross-Correlation Between Two Codes	
			Peak(db)	RMS(db)
3	2	7	-3.0	-8.5
4	2	15	-6.6	-12
5	6	31	-10.8	-15
6	6	63		-18
7	18	127	-17.5	-21
8	16	255		-24
9	42	511		-27
10	60	1023		-30
11	176	2047	-26.6	-33
12	144	4095	-22.2	-36
13	630	8191	-36.0	-39
14	1000	16383		-42
15	1800	32767		
16	2100	65535		
17	7600	131071		
18	8000	262143		
19	19000	524287		
20	17000	1048575		
21	84000	2097151		
22	120000	4194303		
23	360000	8388607		
24	280000	16777215		
25	10^6	33554431		



-10 log L



BOTH $S_1(t)$ AND $S_2(t+\tau)$ ARE LINEAR-MAX-LENGTH OF LENGTH (2^n-1) BITS

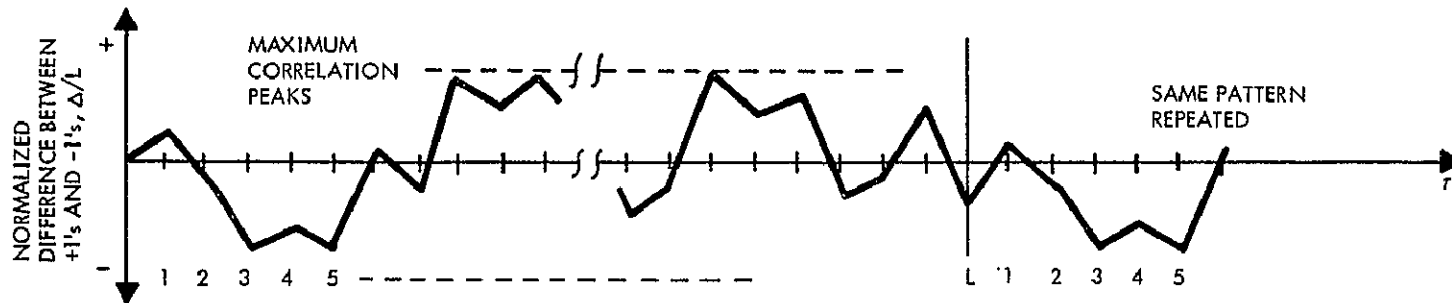


Figure V-28. Digital Cross-Correlation of Two Maximal Length Binary Sequences

4.2.2.2.1.2 Computation of the RMS Cross-Correlation. Perhaps of more importance from the standpoint of multiplexing many PN codes simultaneously in a single channel is the concept of the RMS cross-correlation value between sequences.^[19] This is a particularly valid concept when the number, N, of users in the system is large and the clock frequencies of the PNG's are not coherently related. This is to say, when N is large, from the central limit theorem, the distribution will tend toward normal and the total RMS cross-correlation noise will increase as $(N - 1) R(\tau)X$, where

$$\overline{R(\tau)X} = \frac{1}{L} \sum_{n=1}^{n=L} \left(\frac{\Delta n}{L} \right)^2 \quad (50)$$

and $\overline{R(\tau)X}$ denotes the RMS power value of the cross-correlation function as depicted in Figure V-28. This operation was performed for several sequence pairs of widely differing correlation peaks, and it was found that for the 2047 bit sequence

$$\overline{R(\tau)X} = \frac{1}{L} \quad (51)$$

and is independent of which two sequences are selected. Anderson^[16] also indicates that

$$\overline{R(\tau)X} = \frac{1 + 1/L - 1/L^2}{L} \quad (52)$$

which also converges to $1/L$ for large L.

If the number of system users, N, is large, the normalized RMS cross-correlation noise power will be $(N - 1) / L$ or the signal to total RMS noise power will be given by

$$\text{SNR (RMS cross-correlation)} = \frac{L}{N - 1} \quad (53)$$

4.2.2.2.1.3 Computation of Partial Cross-Correlation Noise. The foregoing analysis has dealt only with computation of the RMS or DC value of the cross-correlation noise. In fact, it can be seen that this only represents the DC value of the $S_3(t)$ sequence as it is convolved by shifting $S_1(t)$ with respect to $S_2(t)$.

It is of interest now to examine the additional spectral energy that is added when the integration bandwidth is increased beyond the reciprocal sequence period. This is the same as saying we wish to count the differences between

+ "1"s and - "1" over some period less than $L\tau$. This operation could indeed be done in a rigorous manner with the use of a digital computer, thus giving a detailed plot of the partial cross-correlation peaks; however, for the application at hand where one is only interested in the RMS value of the partial cross-correlation for large numbers of users, it is only necessary to examine the characteristic power spectrum of the $S_3(t)$ waveform over the bandwidth of interest. The typical power spectrum of the $S_3(t)$ binary sequence is shown in Figure V-29. It is seen that $S_3(t)$ has the $\sin x/x$ envelope with line spacing equal to the reciprocal sequence period = f_c/L , where f_c is the sequence clock frequency. The DC term is simply the power due to the RMS cross-correlation, which was determined in paragraph 4.2.2.2.1.2 to have a value of $1/L$. Noise due to partial cross-correlation can now be taken into account by integration over larger bandwidths and can be defined as

$$\hat{R}(\tau)X \text{ part} = \frac{1 - 1/L}{L} \sum_{n=1}^k \frac{\sin^2 n\pi/L}{(n\pi/L)^2} \quad (54)$$

where $\hat{R}(\tau)X \text{ part}$ denotes the partial cross-correlation power and k is the number of lines that are encompassed by the integration bandwidth, B_a , such that

$$k \frac{f_c}{L} = B_a \quad (55)$$

or

$$k = \frac{B_a L}{f_c} \quad (56)$$

The $1/L$ -term in the numerator of (54) accounts for the power loss in the $\sin x/x$ envelope due to the DC term, since the total power of the $S_3(t)$ waveform must remain constant.

At this point, it will be of interest to introduce the concept of spread spectrum ratio or processing gain which is the same as defined earlier in Equation 39 as

$$R = \frac{f_c}{f_b} \quad (57)$$

where f_b is the data bit rate which is matched to the integration bandwidth B_a such that $f_b = B_a$. f_c is the clock frequency or chip rate of the PN signal. Therefore, k in (55) becomes L/R and for small integration bandwidths equation (54) will reduce to

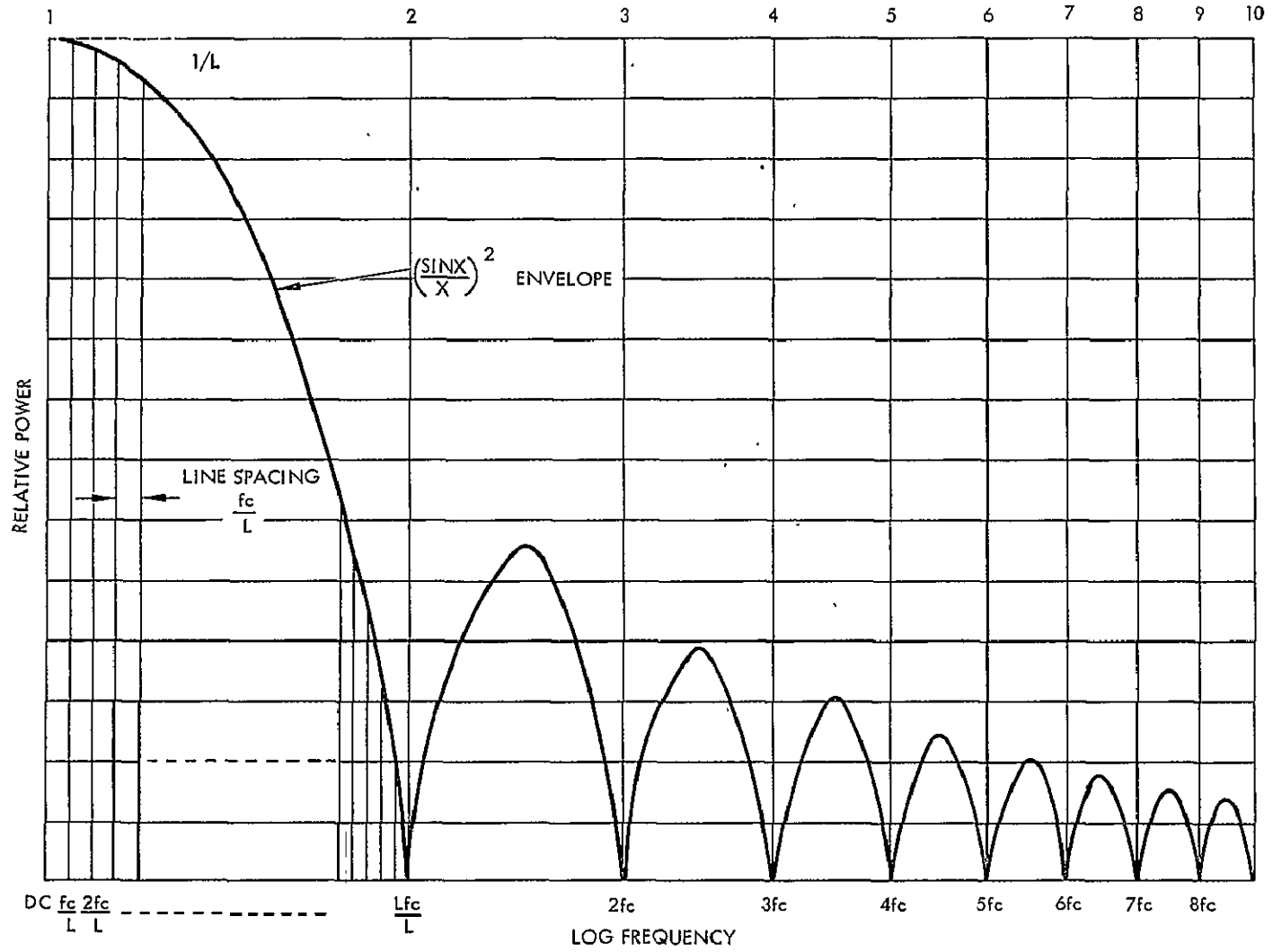


Figure V-29. Power Spectrum of the $S_3(t)$ Waveform

$$R(\tau)X \text{ part} = \frac{1 - 1/L}{L} \left(\frac{L}{R} \right)$$

or (58)

$$R(\tau)X \text{ part} = \frac{1}{R} - \frac{1}{LR}$$

and for N simultaneous users the total normalized cross-correlation noise power due to partial correlation will be approximately (N - 1)/R for R and L large, or the signal to noise power will be given by

$$\text{SNR (partial cross-correlation)} = \frac{R}{N - 1} \quad (59)$$

The total cross-correlation SNR can now be readily determined by summing equations (53) and (59), which represents the RMS and partial cross-correlation SNR, respectively, to yield

$$\text{SNR (total cross-correlation)} = \frac{LR}{(L + R)(N - 1)} = \text{SPNR} \quad (60)$$

4.2.2.2.2 Derivation of the Total Link Signal to Noise Ratio. It will be of interest here to derive a general expression for determination of the total up and down link SNR that can be applied to the SMS-PN data collection system parameters. The SNR equations will be derived for the case of a linear S/C repeater and discounted later for the effects of a hard limited repeater if that approach should be adapted.

There will be three principal sources of noise that contribute to the overall DCS SNR - the CDA or ground station thermal noise, the spacecraft thermal noise and the PN noise due to time/frequency overlapping DCP transmissions. The general equation for the total system SNR can therefore be written as

$$\text{SNR} = \frac{P_{rg}}{\left[KT_g + \alpha P_{rg} + P_{rg} (N-1) \left(\frac{1}{LB_a} + \frac{1}{f_c} \right) \right] B_a} \quad (61)$$

where

P_{rg} is the ground received power level of a particular
DCP signal

KT_g is the ground thermal noise density

B_ξ is the matched filter bandwidth equal to the data bit
rate f_b

$$\text{and } \alpha = \frac{KT_s}{P_{rs}} \quad (62)$$

where

KT_s is spacecraft thermal noise density and

P_{rs} is the DCP power level at the S/C receiver input

The denominator of equation 61 contains the three separate noise terms respectively as listed above.

It can also be seen that the total SNR is determined as a result of three separate SNR calculations. The up-link SNR, the down-link SNR and the PN cross-correlation SNR as given by equation 60. These can be separately written as follows:

$$\left. \begin{array}{l} \text{SNR} \\ \text{up} \\ \text{link} \end{array} \right| = \frac{P_{rs}}{KT_s B_a} \quad (63)$$

$$\left. \begin{array}{l} \text{SNR} \\ \text{down} \\ \text{link} \end{array} \right| = \frac{P_{rs}}{KT_g B_a} \quad (64)$$

and

$$\text{SPNR} = \frac{RL}{(N-1)(L+R)} \quad (65)$$

The task now at hand is to evaluate equation 61 in terms of the expected SMS data collection system parameters.

4.2.2.2.1 Up-link Power Budget Determination. As will be seen in the development of the up-link numbers this is the most critical link for the SMS - DCS. This is due primarily to the limitations imposed on the design of the DCP itself. Since DCP cost is critical it is highly desirable to operate at low transmitter power levels. Also since full earth coverage is a fundamental requirement the spacecraft antenna gain is limited to about 18 db and this is even less

at the earth fringe. Similarly the DCP antenna gain for omni-directional coverage can be degraded by 3 db or more at the fringe over the beam center value. Indeed it can be concluded that the composite losses at the fringe can approach 10 db over the total system losses calculated at the sub-satellite point. These total earth fringe losses can be summarized as:

Spacecraft off-beam loss at 5° EL	6.0 db
DCP off-beam loss (omni-directional coverage)	3.0 db
Additional free space loss at 5° EL	<u>1.0 db</u>
TOTAL fringe loss	10.0 db

The importance of this exercise is to point out the justification for providing a range of DCP designs that will be matched to their geographical location relative to the satellite. This points to the design of a much less expensive DCP at the sub-satellite point. It may also be advantageous to use a less expensive linearly polarized antenna at the sub-satellite location.

The up-link calculation is presented in Table V-17 for the DCP at the sub-satellite point and also at the 5° elevation point. It will be noted, at the sub-satellite point a 1 watt transmitter is sufficient to realize an E/N_0 of 15.2 db in the 75 bps matched filter bandwidth.

The cross correlation E/N_0 has already been determined from equation 44 to be better than 19 db in the same 75 bps bandwidth, therefore the total PN plus spacecraft E/N_0 will be about 13.7 db.

4.2.2.2.2 Effect of a Hard Limited Repeater on the DCS-SNR. It is beyond the intent of this presentation to give a rigorous derivation of the spacecraft limiter suppression effects on the expected system SNR. This has been well treated in the literature [3] [4] [7] [10] [13] [19] for the case of both thermally noise limited and pseudo-noise limited transponders.

In the case of the SMS-DCS there is a distinct possibility that a single hard limited transponder may be used for transmission of both the stretch data and DCP downlinks. In particular, Jones, [3] has shown that in the case where the limiter is captured by a single signal which is much greater than the sum of all other signals, there will be a suppression of the smaller signals by a factor of some 6 db. Also, in the case where the smaller signals are modeled as broadband-noise there is a suppression of 3 db of that noise term.

Table V-17

DCP 2.1 GHz Up-Link Power Budget

	<u>Sub-Satellite</u>	<u>5° EL Fringe</u>
DCP Transmitter Power (dbm)	+ 30.0	+ 40.0
DCP Transmit Loss (db)	- 0.5	- 0.5
DCP Off-Beam-Center Loss (db)	.0	- 3.0
DCP Antenna Gain (db)	+ 6.0	+ 6.0
DCP EIRP (dbm)	<u>+ 35.5</u>	<u>+ 42.5</u>
Free Space Loss at 2.0 GHz (db)	-190.0	-191.0
Spacecraft Antenna Gain (db)	+ 18.5	+ 18.5
Spacecraft Off-Beam Loss (db)	0.0	- 6.0
Spacecraft Receiver Loss (db)	- 1.0	- 1.0
Spacecraft Received Signal Level (dbm)	<u>-137.0</u>	<u>-137.0</u>
Spacecraft Noise Density, KTG (dbm/Hz)	-171.0	-171.0
Based on Receiver Temp = 290°K		
Feed Temp } = 290°K		
Ant Temp } = 290°K		
Total Temp = 580°K		
Total Up-Link (SNR) ₀ (db-Hz)	+ 34.0	+ 34.0
E/N ₀ in 75Hz Bandwidth (db)	+ 15.2	+ 15.2
Spread Spectrum SNR	<u>+ 19.2</u>	<u>+ 19.2</u>
Total Up-Link SNR	+ 13.7	+ 13.7

For the SMS system, the spacecraft transponder will be captured by this larger out-of-band stretch signal that enters the spacecraft well above the sum of all the PN signals. However, all other (N-1) in-band PN signals will appear as broadband noise and will be suppressed by 3 db. Therefore, the maximum degradation in SNR due to the spacecraft hard-limiter will be only 3 db. In this case, the worst expected SNR will be degraded to 10.7 db in the 75 bit/second match filter bandwidth.

4.2.2.2.3 DCP Down Link Power Budget. The down link power budget may change drastically depending on whether a separate spacecraft transmitter is assigned to the DCS and/or if that spacecraft repeater is a hard limited device. It can be readily shown that the worst case down link will exist in the case of the hard limited repeater that is power shared with a high power out of band signal. In this analysis the high power signal is the stretch data transmission from the CDA station and this enters the spacecraft at a power level of -91 dbm. Referring to Table V-17 a single DCP transmission enters the spacecraft at a level of -137 dbm. Therefore, the DCP output power from the spacecraft transmitter, P_{ts} , will be related to the total available power, P_T , as

$$P_{ts} = P_T \frac{P_{rs}}{P_{Ls}}$$

where P_{Ls} is the spacecraft input power level of the stretch signal. For the case in point,

Spacecraft transmitter power, P_T	+43 dbm
DCP spacecraft received signal level, P_{rs}	-137 dbm
Stretch signal at spacecraft input, P_{Ls}	-91 dbm
DCP spacecraft transmitter power, P_{ts}	<u>-3 dbm</u>

The complete down link power budget is presented in Table V-18 for the case of a hard limited transponder to the 40 foot CDA station. For the case of a 75 bps matched filter data bandwidth the down link SNR will be +25.3 db. When this is combined with the 10.7 db SNR calculated previously for the hard limited situation the net DCP system SNR or E/N_0 will be 10.5 db.

If the spacecraft were configured with a non-saturating transponder or at least a non-limiting low power transmitter devoted to the DCS, no spacecraft

Table V-18

DCP 1.7 GHz Down-Link Power Budget
(To 40 Foot CDA Station)

S/C Transmit Power (dbm)*	- 3.0
S/C Transmit Loss (db)	- 1.5
S/C Off-Beam Loss (db) @ 35° EI	- 1.5
S/C Antenna Gain (db)	+18.0
DCP-S/C EIRP (dbm)	<u>+ 12.0</u>
Free Space Loss (db)	-189.0
Ground Receiver Loss (db)	- 1.5
Ground Antenna Gain (40 Foot Dish) (db)	+ 44.0
DCP Ground Receiver Signal Level (dbm)	-134.5
Ground Receiver Noise Density (dbm/Hz) Based on 100°K Noise Temp	-178.6
Total Down-Link (SNR) _O (db-Hz)	+ 44.1
E/N _O in 75 Hz Bandwidth (db)	+ 25.3
Total Up-Link (From V-16) (db)	+ 13.7
Up-Link After S/C Limiting (db)	+ 10.7
Total Link SNR with S/C Limiting (db)	+ 10.5
Total Link SNR No S/C Limiting (db)	+ 13.4

*Only that portion of the total S/C Power devoted to a single data collection station

limiter suppression must be considered and in this case the total DCP link SNR will be the db sum of the 13.7 db up-link + PN SNR and the 25.3 db down-link or 13.4 db. Figure V-30 shows the basic SNR or E/N_0 for various DCP transmitter power levels as a function of both the saturated and non-saturated spacecraft repeaters.

4.2.2.3 Pseudo-Noise Acquisition Considerations—A model of the pseudo-noise system is shown in Figure V-31. As already indicated from previous discussion of the proposed PN system the signal will be channelized into one of 25 -150 KHz slots by selection of the DCP operating frequency. The correlation receiver must now perform the additional functions of:

- a. Resolving the ± 20 kHz of frequency uncertainty due to the 1×10^{-5} long term stability of the 2 GHz DCP source. This must be resolved to within the frequency acquisition range of the narrow band PLL.
- b. Frequency and phase acquisition within the PLL bandwidth constraints. The following procedure can generally be accepted as a requirement for achieving final acquisition of the PN signal.

Assuming a pseudo-noise generator (PNG) length, L , of 2047 chips and a search rate of 100 bps the entire PN code will be searched in a time $2047/100 = 20$ seconds, and the time to search one chip will be 10 milliseconds. At some period during this 20 second search the signal will correlate as shown in Figure V-32. The video bandwidth required to accept this pulse will be about $1/2$ the reciprocal rise time or 50 Hz. A 75 Hz acquisition bandwidth will be allowed for purposes of this discussion. The receiver must now recognize the presence of this correlation peak and resolve the course frequency uncertainty into a particular frequency cell which will be determined by the filter spacing within the ± 20 kHz band of uncertainty. Depending on the actual filter spacing and the centroiding logic employed a digital word will be sent to the PLL reference synthesizer to establish the fine frequency position to within the acquisition range of the AFC.

The filter bank search then performs two functions. First it will give an initial acquisition indication which will stop the PN code search and this condition will be held until the AFC can acquire in frequency and the PLL in phase. Its second function is to program the PLL initial conditions. If a false acquisition is made a verification signal will not be generated and after the verification time, delay, the code search will continue. Therefore each time the threshold is

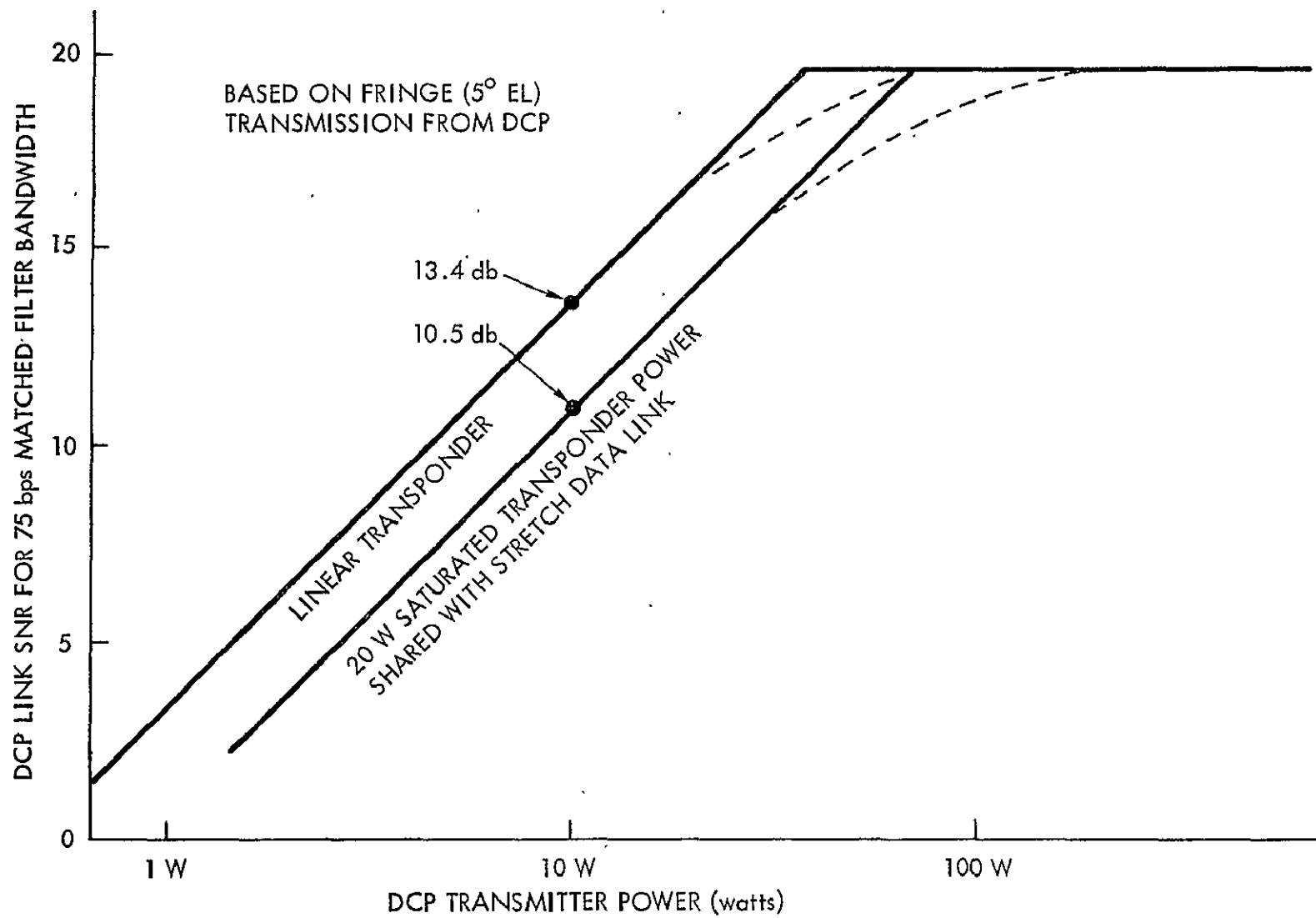


Figure V-30. PN-DCP Link SNR Versus DCP Transmit Power

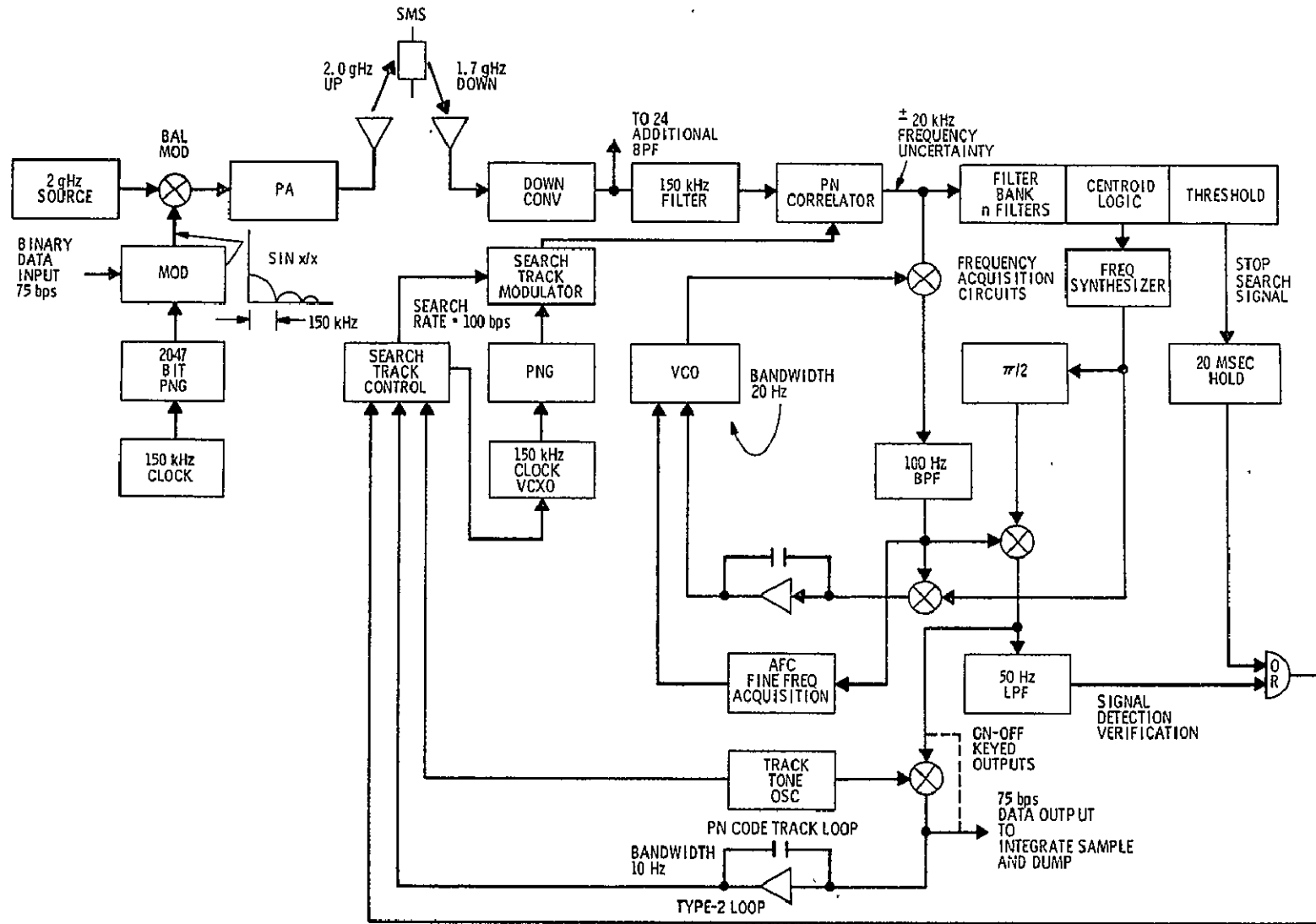


Figure V-31. Typical Implementation of PN-Transmitter and Correlation Receiver

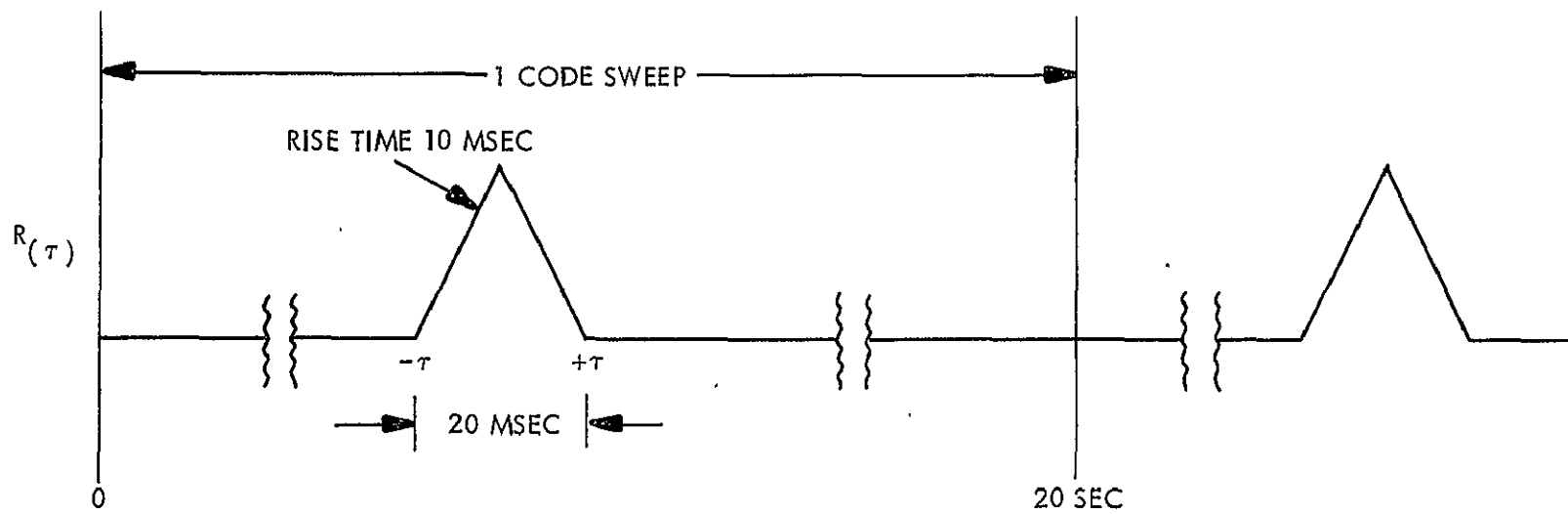


Figure V-32. Auto Correlation of PN Code

exceeded on noise a false alarm is generated and a verification delay is inserted into the overall PN acquisition time. This can be written as

$$t_a = t_0 + N_F t_r \quad (66)$$

where t_a is the total acquisition time

t_0 is the maximum noise free acquisition time ($t_0 = 20$ seconds)

N_F is the total expected number of false alarms in one search time

t_r is the verification time for PN acquisition.

It will now be of interest to determine the expected number of false alarms N_F as a function of the following parameters:

- a. SNR in the 75 Hz detection bandwidth
- b. Number of filters M in the filter bank
- c. Probability of detection on one code sweep
- d. The probability that a single filter output exceeds the threshold given that correlation is not present, α .

This is a typical pulse doppler radar problem which has already been solved in many forms [22]. Skolnik [21] shows that for a CNR of 13 db in the acquisition bandwidth, the probability of detection will be about 99 percent for a 10^{-3} false alarm probability, α , in a single filter. It is important to note for this system that the situation of ambiguous detection does not exist. Ambiguous detection can be defined as the situation where a false detection is made in a particular filter at the same instant a true correlation exists in a different filter. When this occurs the normal verification delay is incurred, after which the filter bank logic rapidly renews its search and centroids on the correct filter which has already built to its value. The time required to switch between frequency cells is independent of the filter acquisition time and therefore can occur before the PN search can be reinitiated.

Now based on a given α

$$\alpha_T = 1 - (1 - \alpha)^M \quad (67)$$

where α_T is the false alarm probability of the total filter bank of M filters.

The 40-kHz band of frequency uncertainty can be resolved with 100-400 Hz predetection filters. Based on a 13.4 db SNR in the 75 Hz acquisition bandwidth the predetection CNR in the 400 Hz filter will be about +6 db. This is far enough above the AM detector threshold to give less than a 1 db loss in the net acquisition SNR which, for purposes of this discussion, will therefore be about 12.5 db.

Now solving equation (67) for $\alpha = 10^{-3}$ and $M = 100$ yields a system false alarm probability $\alpha_T = 0.1$. The number of expected false alarms will now be this probability times the number of time cells examined which can be up to 2047 (the number of chips in the PN code). Equation 66 can therefore be rewritten as

$$t_a = L \left(\frac{1}{R_s} + \alpha_T t_v \right) \quad (68)$$

Now t_v is the time required for fine frequency acquisition and finally phase acquisition by the narrow band PLL. Fine frequency acquisition is accomplished with the aid of the 100 Hz bandwidth AFC circuit which will bring the frequency to within the ± 20 Hz bandwidth of the PLL in less than 10 milliseconds (1/Bandwidth of the AFC loop). For a phase lock loop damped to 0.707 of critical the acquisition time will be given approximately as

$$t_{PLL} = \frac{0.7 (\Delta\omega)^2}{(\omega_n)^3} \quad (69)$$

where $\Delta\omega$ is the initial frequency offset (20 Hz in this case) and ω_n is the natural resonant frequency which is the 3 db frequency for critical damping.

For $\omega_n \doteq \Delta\omega$

$$t_{PLL} = \frac{0.7}{\Delta\omega} = \frac{0.7}{2\pi(20)} \quad (70)$$

or $t_{PLL} \doteq 6$ milliseconds

and the total verification time will be $t(\text{fine}) + t_{PLL}$ or about 16 milliseconds for each false alarm.

Referring again to Figure V-31, a 20 millisecond hold will be initiated each time the acquisition threshold is exceeded. For the system false alarm probability of 0.1, 200 false alarms can be anticipated over the 2047 bit search. This will yield a total verification time of $200 \times 20 \times 10^{-3} = 4$ seconds. Therefore, from equation 66 or 68, the total expected acquisition time will be about 24 seconds. A list of the acquisition parameters is shown in Table V-19.

It has been the intent of this discussion to give some insight into the considerations involved in establishing a procedure for design of the PN acquisition circuits. This is not to indicate that the parameters listed in Table V-19 are precisely optimized for the PN system as proposed. In fact, a procedure can be established for optimizing the acquisition time in terms of the number of filters, the PLL bandwidths, the PN sequence length, the SNR, etc. This should be a principal objective of future SMS data collection system studies.

Table V-19

PN Acquisition Parameters

Acquisition Bandwidth	75 Hz
SNR in 75 Hz Bandwidth	12.5 db
Probability of detection	99%
Probability of false alarm for individual filter	.001
Number of filters	100
System false alarm probability	0.1
Number of chips searched	2047
Maximum number of false alarms	200
Detection verification time	20 msec
Acquisition time with no noise	20 sec
Acquisition time at 13 db SNR	24 sec

4.2.2.4 Data Transmission—To be sure there are many techniques available for interfacing the 75 bps data with the DCP-PN communication link. The three principle techniques that might be considered may be listed as:

1. Sequence inversion modulation of the PN code with the 75 bps binary data. This results in a phase reversal modulation (PRK) at the correlator output of the PN receiver.
2. Sequence inversion using a high frequency duty ratio modulated signal. This will result in an on-off keyed AM signal at the correlator output.
3. PN clock phase modulation. This will also result in an on-off keyed AM signal at the correlator output.

This list could be carried on endlessly but for purposes of this discussion will be limited to those mentioned.

The data bit error probability as a function of SNR in a matched filter bandwidth for various modulation techniques is shown in Figure V-33. Initial indications point to the use of either coherent or differential coherent PSK which can be simply generated by a sequence inversion of the PN code at the DCP. This is shown in Figure V-34 as a direct modulo-2 addition of the data bit stream with the PN sequence. A critical problem, however, exists at the PN receiver in attempting to demodulate this type of signal if the PSK signal is transmitted without carrier. If a carrier is transmitted with the signal some loss will be incurred in the available SNR for bit error rate estimates. This loss can very easily be 3 db or greater. An additional problem lies in the short term stability of the DCP RF reference which must be well contained in a bandwidth much less than the data bit rate. In the case of 75 bps data the required short term stability of the 2 GHz DCP must be such that the phase noise on the carrier is well contained within the 10 Hz region around the carrier. This is a most difficult specification for the proposed TCXO frequency standard of the DCP.

In light of the problems involved with both short term frequency stability and mechanization which can result in 3 db or more loss over theoretical, it appears that some form of AM on-off keyed modulation structure might be a more logical choice. From the standpoint of short term frequency stability the spectrum now need only be contained within the data acquisition bandwidth and no problem is involved with carrier reference at the PN receiver.

AM carrier keyed modulation can be realized in two ways. First by modulo-2 adding a high pulse repetition frequency signal with the PN sequence

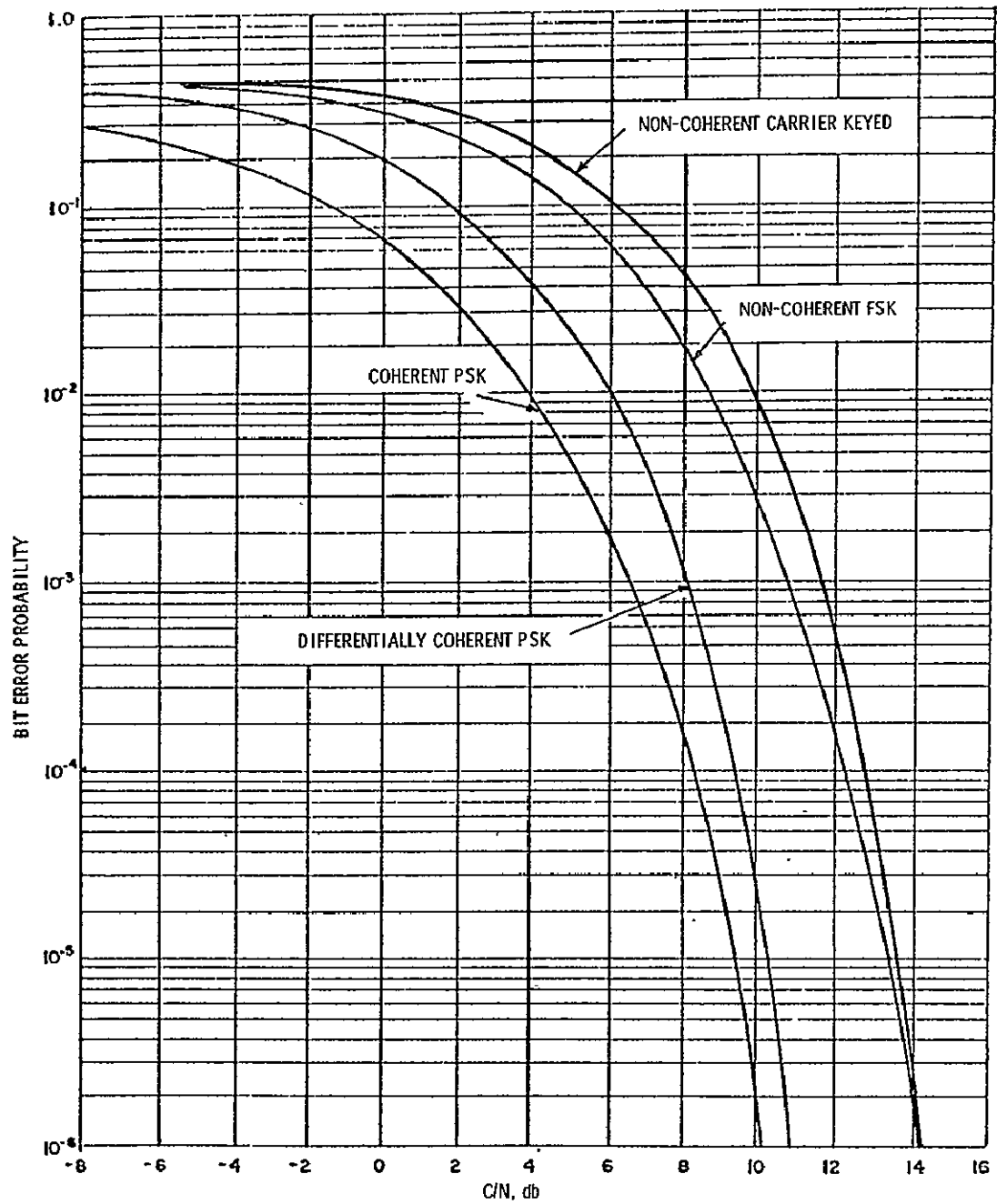


Figure V-33. Binary Error Probability vs. Carrier to Noise Ratio in a Matched Filter Bandwidth

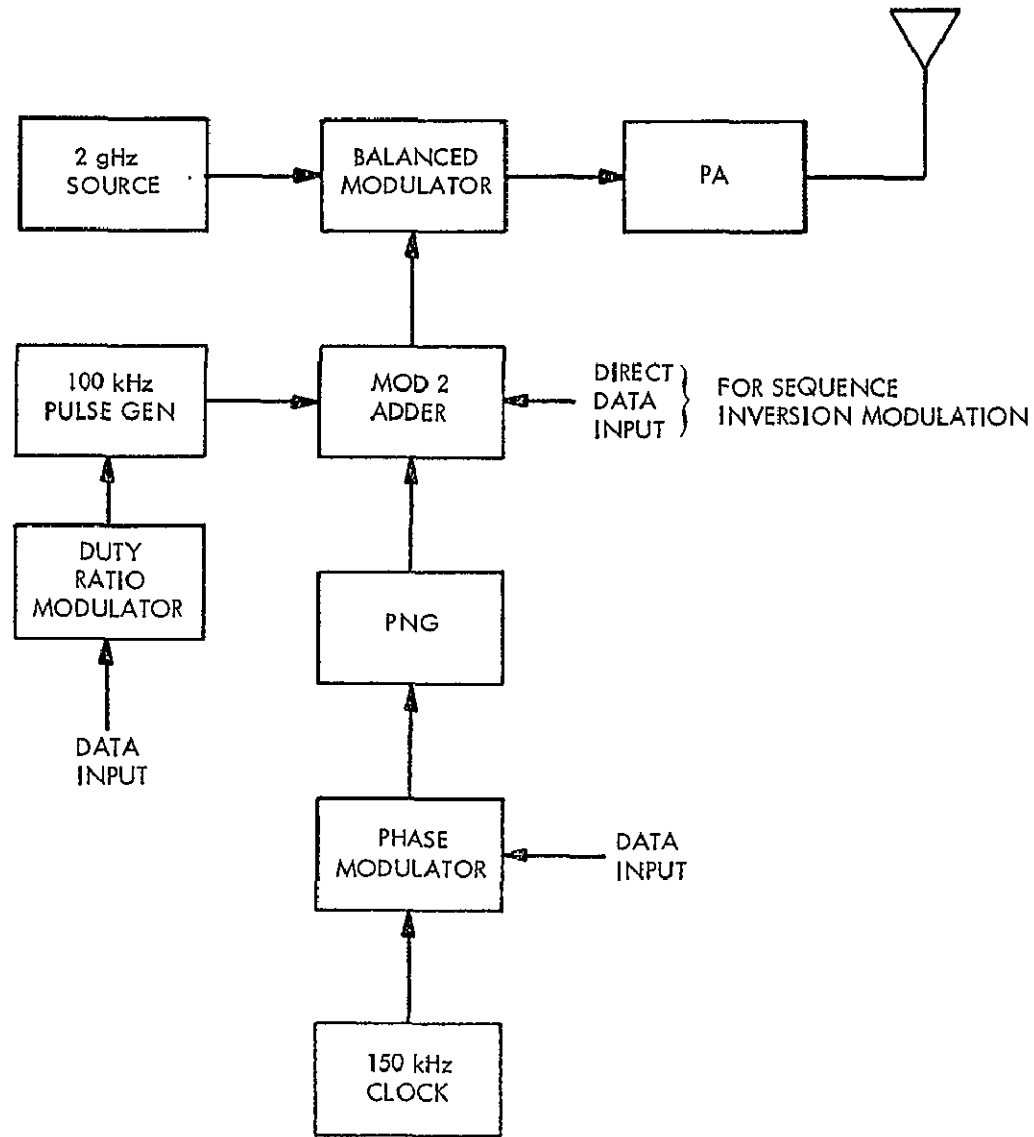


Figure V-34. Possible Techniques For Data Modulation of PN Signal

a PSK modulation of the correlated carrier is accomplished at the PN receiver. If the PRF of the generator is selected greater than the 40 kHz filter bank bandwidth of the $\sin x/x$ pulse sidebands are rejected and only the carrier component of the pulsed signal remains in band. Now if a 0 to 50% duty ratio modulation of the pulse generator is accomplished in accordance with the data input, an on-off keyed carrier will appear at the correlator output of the PN receiver. Referring to Figure V-30, the demodulated data video will appear at the PLL cosine output.

A second method for achieving an AM carrier keyed signal is by phase modulation of the DCP-PN clock oscillator. This results in an amplitude modulation of the correlation peak and the demodulated output will appear at the clock tracking loop phase detector output as indicated in Figure V-31.

With either of these two AM carrier keyed techniques, referring to Figure V-33, it should be possible to realize a 10^{-5} bit error probability with the expected 13.5 db SNR in the 75 Hz matched filter bandwidth.

4.2.2.5 Provision for Continuous and Interrogated DCP—The pseudo-noise data collection system that has been discussed thus far is structured to handle 10,000 DCPs on a semi-synchronous, non-interrogatable time plan. There is however the additional need for some DCPs to be read on command from the CDA station. Also a limited number of DCP stations will operate on a continuous basis over the 6 hour synoptic period. These requirements will be discussed in the paragraphs that follow.

4.2.2.5.1 Provision for Interrogation—Interrogation can be provided in several ways, but regardless of the technique employed, a receiver capability must be provided at the remote DCP. As a ground rule it will be assumed that the DCP will be structured with a receiving antenna system similar to that considered earlier. This will have a 3-db ground receive antenna gain at the 1.7-GHz downlink frequency at the 5° El point.

A reasonable method that can be effectively employed for transmission of the interrogation command would be to send a coded command for a short interval, perhaps 30 milliseconds just after the 30 millisecond wideband camera transmission and before the 480 millisecond stretch data transmission. In this manner, the full spacecraft EIRP of +55.0 dbm will be available for transmission of the interrogation command.*

The DCP down link power budget is presented in Table V-20. As seen, there is about an 8.5 db difference between the 5° elevation point and the sub-satellite link. Based on a 500 Hz matched filter bandwidth the E/N_0 will be 14.5 db and

Table V-20

DCP Interrogation Down-Link Power Budget

	<u>5° El</u>	<u>Sub-Satellite</u>
S/C Transmitter Power (dbm)	+ 43.0	+ 43.0
S/C Transmit Loss (db)	- 1.5	- 1.5
S/C Off Beam Center (db)	- 4.5	.0
S/C Antenna Gain (db)	+ 18.0	+ 18.0
S/C EIRP (dbm)	<u>+ 55.0</u>	<u>+ 59.5</u>
Free Space Loss (db)	-190.0	-189.0
DCP Off Beam Center (db)	- 3.0	.0
DCP Receive Loss (db)	- 0.5	- 0.5
DCP Antenna Gain (db)	+ 6.0	+ 6.0
DCP Ground Received Level (dbm)	<u>-132.5</u>	<u>-124.0</u>
DCP Ground Receiver Noise Density Based on 300°K Temp (dbm/Hz)	-174.0	-174.0
Total DCP Down-Link SNR _o (db-Hz)	+ 41.5	+ 50.0
E/No in 500 Hz Bandwidth (db)	+ 14.5	+ 23.0

23 db respectively which will give a bit error probability of better than 1×10^{-5} regardless of the modulation that might be used. Based on a 30-msec. time, therefore, as much as a 15 bit command can be transmitted to the DCP to be interrogated. This should be more than adequate to provide a unique command for each interrogatable DCP.

Referring to Figure V-35 it will be assumed for purposes of the present discussion that the DCPs to be interrogated will be structured within the 10,000 allotted for the total DCS.

As previously shown in section 2.2.2.1 the total PN-DCS will be divided into 25 independent frequency slots. It is certainly possible therefore to assign a certain number of these slots to the interrogatable DCPs. This can be readily accomplished provided the interrogatable DCP data requirements are not significantly different than those assumed for the non-interrogation system.

*This is based on a 4.5 db S/C off-beam center allowance for DCPs at the earth fringe. At the sub-satellite point the S/C EIRP will be +59.5 dbm.

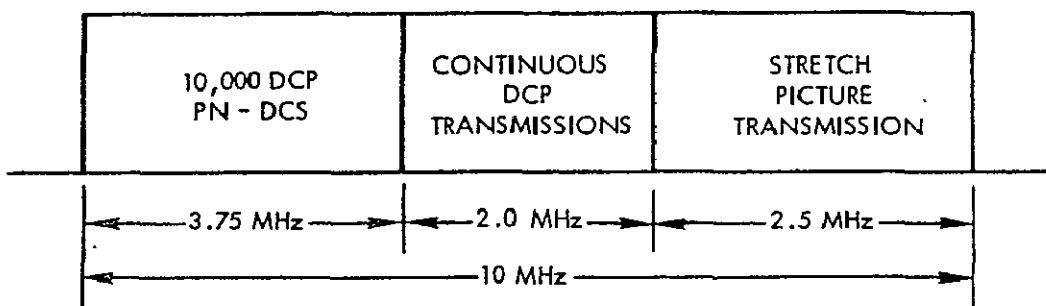


Figure V-35. DCP Bandwidth Allocation

Therefore up to 400 DCPs can be interrogated and read out in one 150 kHz frequency slot within a 6 hour synoptic interval. This again would be based on the use of 75 bps data and an average DCP capacity of about 2000 bits.

4.2.2.5.2 Provision for Continuous DCP Transmission—Referring to Figure V-35, 2.0 MHz of transmission bandwidth will be provided for multiplexing a number of continuous DCP transmissions. Since transmission is continuous the need for interrogation in this case is most likely not required. If therefore the continuous DCP is built without a receive capability multiplexing must be accomplished either by frequency division or some form of random access modulation structure such as pseudo-noise spread spectrum.

The optimum choice here again will be largely constrained by the DCP frequency stability which will ultimately limit the number of channels to be transmitted.

If pure frequency division were employed the number of continuous DCPs will be

$$N_c = \frac{B_c}{2 (f_b + f_o S)} \quad (71)$$

where B_c is the available transmission bandwidth for the continuous DCP's = 2.0 MHz

f_b is the matched filter data bandwidth.

f_o is the up link RF frequency = 2 GHz

S is the long term frequency stability = 1×10^{-5} /yr

Based on an ESSA requirement for a continuous bit rate $f_b = 500$ bps, from equation 71, about 49 DCP transmissions could be provided.

If a pseudo-noise technique is used the number of continuous DCPs will be given by equation 72 (from solving 65 for $N-1$) as

$$N_c = \frac{RL}{SPNR(L+R)} \quad (72)$$

where SPNR is the spread spectrum cross correlation noise. In this case however where acquisition time is less important the sequence length L can be increased to 8192 chips = $2^{13}-1$ or even higher perhaps.

Equation 72 can therefore be approximated as

$$N_c = \frac{f_c}{f_b SPNR} \begin{cases} L \gg R \\ N_c \gg 1 \end{cases} \quad (73)$$

where f_c is the PN chip rate which is about equal to the channel bandwidth $B_c = 2.00$ MHz.

And for an SPNR = 17 db the number of continuous PN-DCP will be about 80.

It is interesting to note that if the DCP frequency stability is increased to 1×10^{-6} , frequency division appears to be a much more feasible method. In that case from equation 71 N_c will be 400 continuous non-overlapping channels.

The up link calculation for the continuous DCP link is essentially the same as in Table V-17 except the DCP ground transmitter power must be increased by about 8 db because of the higher data bit requirements (500 bps in lieu of 75 bps).

4.2.2.6 Pseudo-Noise Ranging—The SMS system will also provide real-time simultaneous ranging information from a single master station via the S-band transponder back to itself (station A) and to two ground transponders at locations B and C as shown in Figure V-36. Since the CDA master station ground receiver will already be provided with pseudo-noise correlation detection circuits, it is a relatively simple matter to use one unique PN code for ranging to each station. PN ranging has the following advantages:

- a. No additional spacecraft equipment is required.
- b. Ranging can be done simultaneously with other communications with no interference.
- c. By using long PN sequences (only for ranging) virtually unambiguous range can be determined with no loss in range resolution using a single high-frequency clock tone.
- d. Continuous range readout and update is provided.
- e. Can use hard limited S/C repeater.

The basic concept of PN ranging can be readily understood from Figure V-37. A PN sequence of length (2^n-1) is transmitted first through the spacecraft back to the master station where it is correlated with an identical PN sequence in receiver No. 1. A unique point in the sequence is established as a reference point which will be interpreted as a start point. The same logic is used in the ground receiver to establish this reference point. The two-way range between the spacecraft and ground station is then readily determined from the time delay between these start and stop pulses. A conceptual block diagram of the CDA implementation is shown in Figure V-38. The turn-around ranging station concept is presented in Figure V-39.

It can be seen that the range measurement is unambiguous within one range element, ΔR , which is given by

$$\Delta R = \frac{2^n - 1}{f_c} \times C \quad (74)$$

where $C = 3 \times 10^8$ meters per second

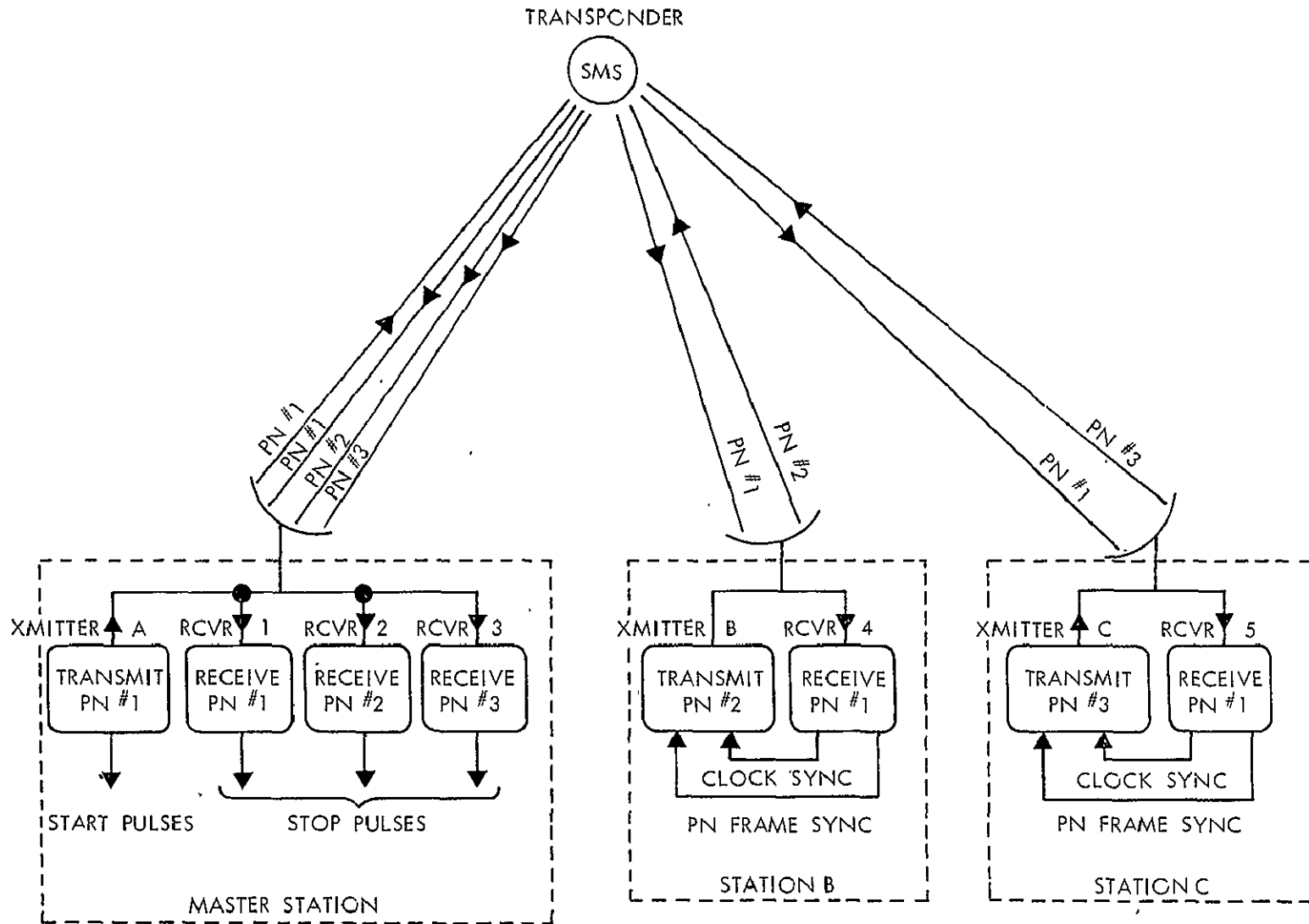


Figure V-36. SMS PN Ranging Concept

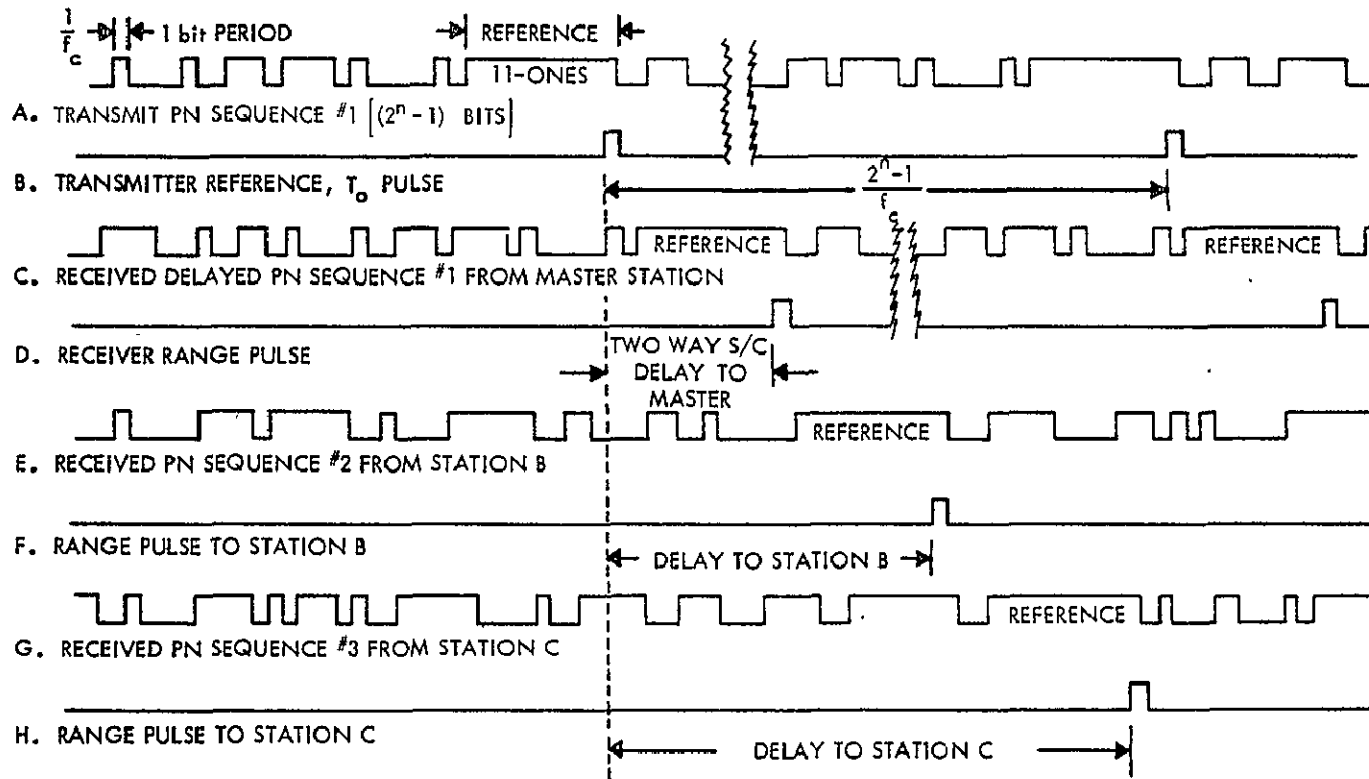


Figure V-37. Ranging Timing Diagram

V-147

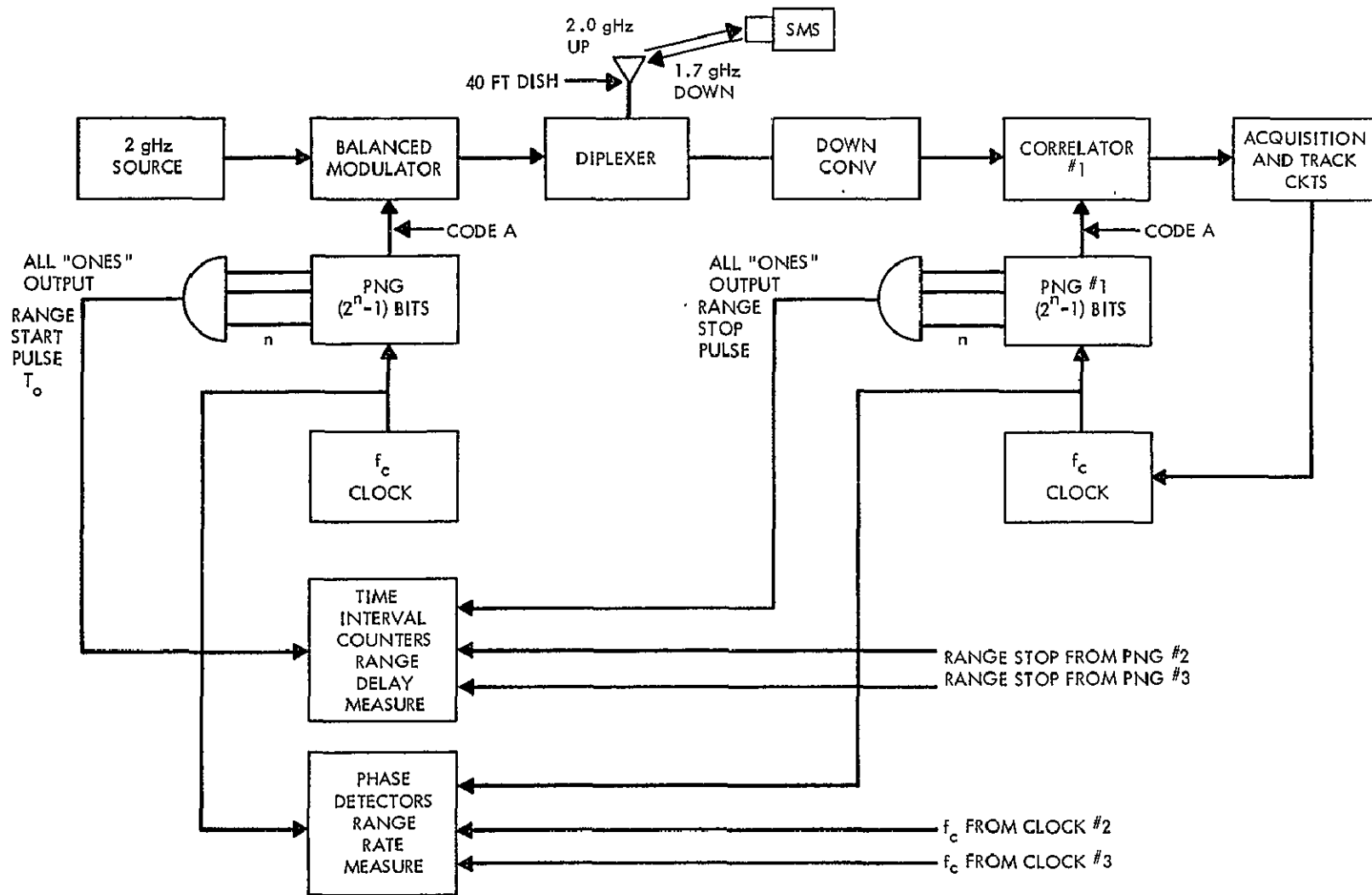


Figure V-38. Conceptual Block Diagram of CDA Station PN Ranging Requirements

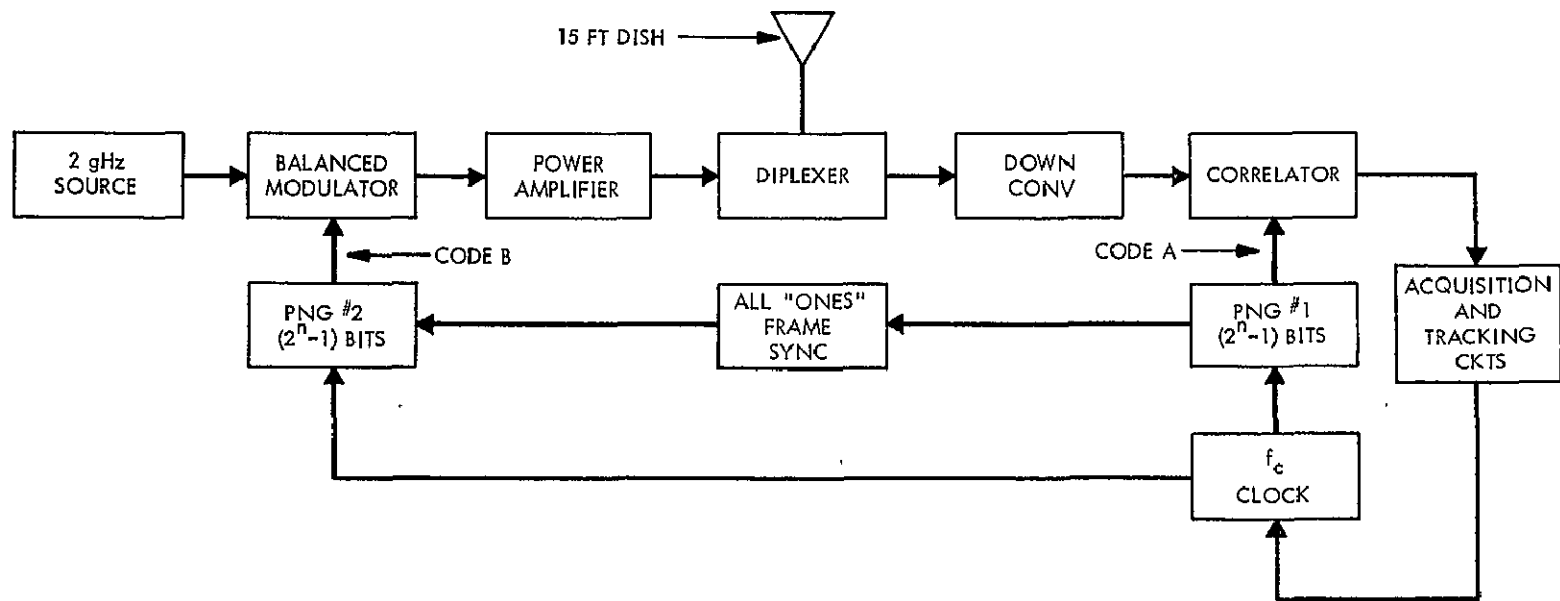


Figure V-39. PN-Turn Around Ranging Station Block Diagram

f_c = clock frequency or chip rate of the PN sequence

n = number of shift register stages in the PN coder

The range accuracy will depend ultimately on the attainable frequency stability of the clock oscillators in both the transmitter and receivers. Determination of range accuracy can be broken down basically into three problems:

- a. The ability to accurately measure the relative phase position between the transmitter and receiver clocks in the presence of receiver noise.
- b. The ability to measure absolute range will be limited by the relative drift or change in the system clocks during the actual range interval, in this case about 0.26 seconds.
- c. The accuracy in determination of the relative range change (range rate) will also depend on the relative short term stability of the system clocks during the PN range element time.

A useful method for expressing the range interval time jitter in terms of the system clock frequency and the RMS phase noise σ_n is presented in Figure V-40. Also in the case of a phase-lock loop operating well above threshold

$$\sigma_n = (\text{SNR})^{-1/2} \quad (75)$$

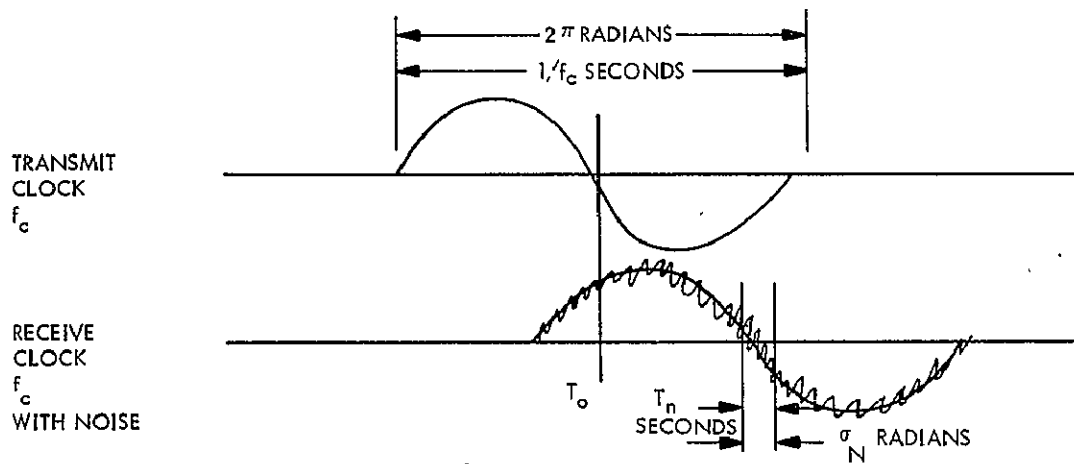
substituting this into the equation shown in Figure V-40 and expressing the range error, R_e , in meters yields

$$R_e = \frac{C}{2 \pi f_c \sqrt{\text{SNR}}} \quad (76)$$

It is proposed here that the three station PN ranging be accomplished using three of the 2.0 MHz bandwidth continuous PN channels. It should be pointed out that this could also be accomplished in this same band even if that spectrum were structured as an FDM system because of the low PN noise density across the entire 2.0 MHz channel.

It will be recognized that the SNR of equation 76 is the net result of four separate link calculations:

- a. 2.1 GHz up-link from CDA stations to SMS
- b. 1.7 GHz down-link from SMS to turn-around ranging stations (TRS)
- c. 2.1 GHz up-link from TRS to SMS
- d. 1.7 GHz down-link from SMS to CDA station



$$2\pi : 1/f_c = \sigma_N : T_n$$

$$T_n = \frac{\sigma_n}{2\pi f_c}$$

WHERE σ_N IS THE RMS PHASE NOISE

T_n IS THE RMS TIME JITTER DUE TO NOISE

Figure V-40. Development of Range Equation

As a design goal the range resolution, R_e , will be specified at about 1 meter. Solving equation 76 for $f_c = 2.00$ MHz, the required composite system SNR will be about 27.6 db. The individual up and down links therefore must each be much better than this.

Assuming that ranging may be done simultaneous with the stretch radio-meter transmission and also assuming a power shared hard limited spacecraft repeater the basic up and down link calculations for the DCS as given in Tables V-17 and V-18 will hold except for the antenna gains and required transmitter power levels. A summary of the up and down link turn around ranging are presented in Tables V-21 and V-22 respectively. The up and down links to the CDA will be non-critical and can be readily set to +34 db. Based on these figures the total link will be about 28.4 db in a 1 Hz bandwidth. A list of the salient features for the SMS PN turn-around ranging system are presented in Table V-23.

If ranging is done continuously, as mentioned previously, PN acquisition time is not a problem and a long sequence length can be employed. It should be mentioned that the non-ambiguous range element ΔR need only be long enough to resolve the maximum range variation with the synchronous SMS. Experience with ATS has indicated this to be less than 1,000 miles. From equation 74 with $(2^n - 1) = 32,767$ for $n = 15$ stages, ΔR will be over 3000 miles.

With regard to short term clock stability requirements, it is necessary that the clock time drift not produce a range error greater than 1 meter over the total 1/2 second two-way range interval. This can be expressed as

$$R_e = CSt_1 \quad (77)$$

where $C = 3 \times 10^8$ meters/sec

S is the required frequency

stability and

t_1 is the total two-way range interval

Therefore from equation 77 the required short-term stability will be 3×10^{-9} for 0.5 seconds. This is a requirement for both the CDA and TRS clock oscillators. This stability should also be consistent with the necessary 1 Hz PLL noise bandwidth constraints.

Table V-21

Up-Link to SMS From TRS for PN Turn Around Ranging 2.1 GHz

Total Losses (from Table V-16) (db) (Worst case based on 5° EI at TRS)	-201.5
S/C Antenna Gain (db)	+18.5
15' Antenna Gain (db)	<u>+35.7</u>
Net Losses (db)	-147.3
S/C Received Signal Level (dbm)	-137.0
TRS Transmitter Power (dbm)	+10.3
S/C Noise Density (dbm/Hz)	-171.0
TRS Up-Link (SNR) _o (db-Hz)	+34.0

Table V-22

Down-Link to 15' Turn Around Ranging Station 1.7 GHz

Total Losses (from Table V-17) (db)	-193.5
S/C Antenna Gain (db)	+18.0
15' Antenna Gain (db)	<u>+35.7</u>
Net Losses (db)	-139.8
S/C Transmitter Power for PN Ranging (dbm)	-3.0
Ground Received Signal Level (dbm)	-142.8
Receiver Noise Density (dbm/Hz) (Based on 100° K noise temp.)	-178.6
Total Down-Link (SNR) _o (db-Hz)	+35.8

Table V-23

Overall PN Ranging Link Summary

CDA to SMS Up-Link SNR (db)	34.0
SMS to TRS Down-Link SNR (db)	35.8
TRS to SMS Up-Link SNR (db)	34.0
SMS to CDA Down-Link SNR (db)	<u>34.0</u>
Total Link SNR (db)	28.4
System Noise Bandwidth (Hz)	1.0
Range Accuracy (meters) (From Eq. 77)	< 1.0
PN Clock Frequency (MHz)	2.0
Sequency Length Chips (n = 13)	32,768
Unambiguous Range Element (miles)	3,040
Frequency Stability	$3 \times 10^{-9}/0.5 \text{ sec}$

4.2.2.7 Data Loss Due to Camera Transmission—If a single transponder is used for the SMS mission there will be a 30 millisecond loss of data from the data collection system during the 30 millisecond wideband camera signal transmission. This represents a 5% loss of data based on the total 600 millisecond spin period, which is a loss of 2.25 bits assuming a 75 bps data rate. If a 7 bit data error detecting code is used, at most two consecutive words or characters will be omitted. It might be pointed out that the CDA station can indeed gate out the 30 millisecond slots by using the spacecraft camera 30 millisecond burst pulse. In this sense then at least one knows positively which data is in error even if an error detecting code were not used. A possible solution to this problem, other than using a separate transmitter for the DCS as discussed earlier, would be to use a form of error detecting code. This, however, would require the use of a longer code which also results in a reduction of the net DCP data capacity.

4.2.2.8 Data Collection Platforms—A detailed block diagram of the 2 GHz non-interrogatable DCP is shown in Figure V-41. From a circuit design and system cost analysis standpoint the major subsystems to be considered are listed in Table V-22. These cost figures are realistic estimates based on present technology. The 10 watt DCP is considered only; however, it should be pointed out that a much cheaper DCP could be built for the sub-satellite case where the required EIRP will be reduced by some 10 db. It is seen from Table V-24 that almost half the DCP cost is involved in the 10 watt power amplifier and the circularly polarized antenna. For example a linearly polarized antenna will cost only about \$20.00 with an effective gain loss of only 3 db relative to the circularly polarized antenna. Similarly a 2-watt power amplifier might reduce this cost to \$100. Therefore the sub-satellite DCP cost would be reduced to about \$800.

With regard to DCP power consumption the principal power drain will be that associated with the power amplifier itself. Assuming the PA to be 50 percent efficient, as much as 20 watts must be provided for that function alone. The remainder of the DCP will most likely use large scale integrated circuit techniques with low power drain MOS logic. The composite power drain of this circuitry will be under one watt. The only devices which will remain on continuously are the TCXO station standard and the associated count down logic. This may be on the order of 0.1 watts.

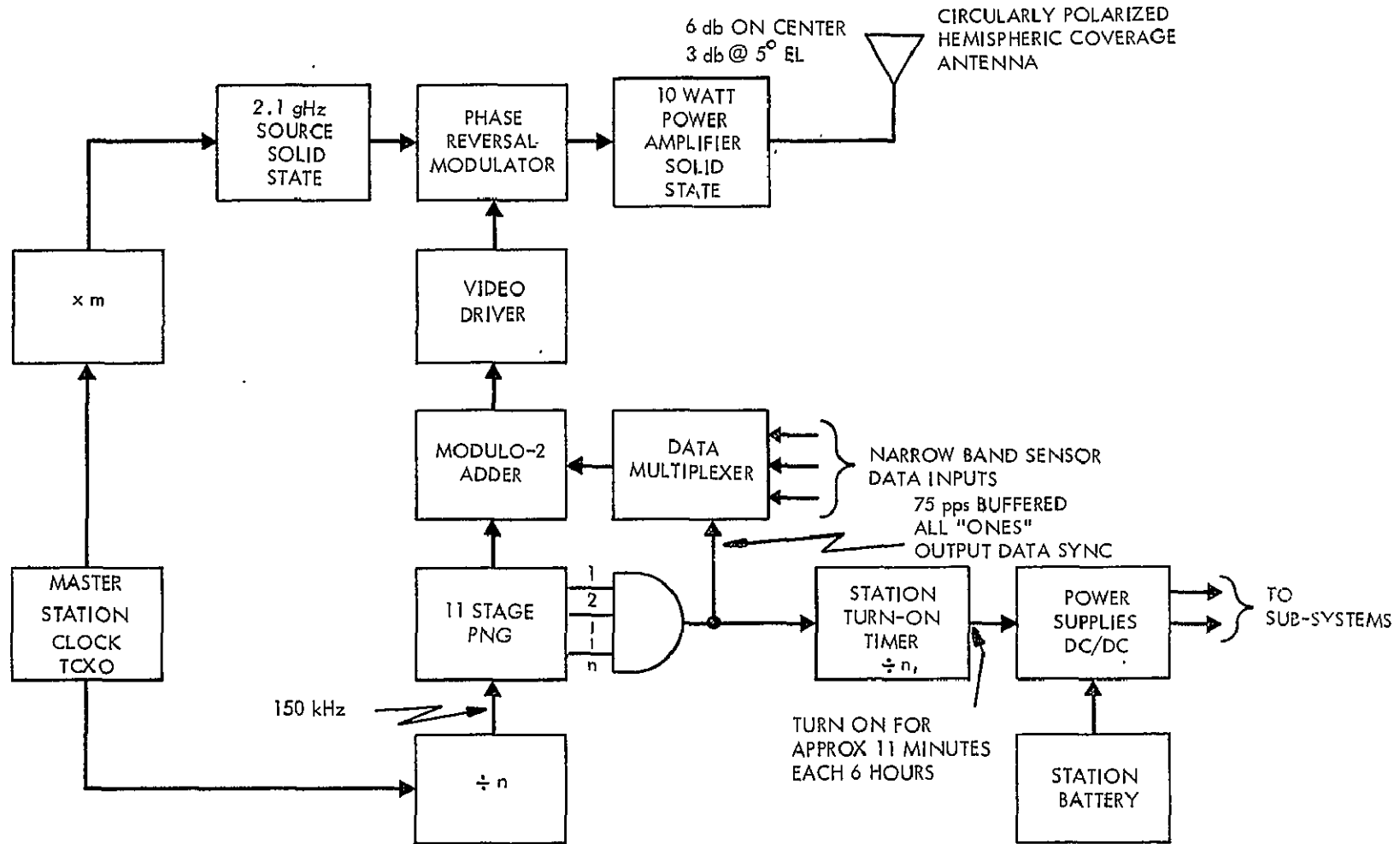


Figure V-41. PN-DCP Transmitter Block Diagram

Table V-24

Pseudo-noise DCP Subsystem
and Estimated Cost* Breakdown

Subsystem	Estimated Cost
10 Watt 2 GHz Power Amp	\$ 335
Circularly Polarized Ant	200
Phase Reversal Modulator and Video Driver	40
11-Stage PNG and Misc. Logic (Mod-2 Added, All-ones Buffering, etc)	50
Data Multiplexer	30
Station Master TCXO Clock 1×10^{-5} /yr Stability	35
2 GHz Multiplexer Chain (xm)	100
Clock Divider ($\div n$)	10
Station Timer and Countdown Logic	100
DC/DC Converter Power Supplies	70
Batteries	75
Assembly/Wire/Testing/Structure etc.	150
Total Approximate Cost	\$1,195

*Based on Quantities of 1000 or more

The primary battery energy, E_o , requirement can be expressed as

$$E_o = t \left(P_I + \frac{P_{DCP}T}{6} \right) \text{ watt-hours} \quad (78)$$

where P_I is the continuous idle power requirement in watts
 t is the time between battery replacement in hours
 P_{DCP} is the peak power requirement of the DCP
 T is the DCP turn on time in hours

Equation 78 is developed on the basis that the DCP will be on for a period T only 4 times each 24 hours, or once each 6 hours synoptic period. For the power estimates given above for the 10-watt DCP, an on time of 686 seconds, and assuming a single 400-watt-hour battery from Equation 78 the time between replacement will be about 22 days. For a DCP at the sub-satellite point where the peak primary power drain drops to perhaps 5-watts, the replacement time will be increased to about 64 days.

It is also of interest to briefly examine the effect of the DCP frequency stability on the battery replacement interval. Recalling the dependence of stability on the DCP on time as discussed earlier, if a 1×10^{-6} clock were used in lieu of the 1×10^{-5} , the DCP on time will drop to about 116 seconds, or a factor of almost 6 to 1. Therefore, from Equation 78, t will increase to 78 days or 130 days respectively for the fringe and sub-satellite DCP. The significance of this exercise is to show that ultimately a point is reached where the battery power drain will be almost totally a function of the idle power requirements. For example, based on the 0.1 watt idle power requirement alone, the battery will drain in 165 days. If the additional idle power requirements of an interrogatable DCP were added this time could well be reduced to 80 days or less.

4.2.2.9 Areas For Additional Study—It has been the intent of Section 4.2.2 to present a comprehensive plan for implementation of a pseudo-noise data collection system for the SMS. It is believed that sufficient information and analysis has been performed herein to show that the PN system at S-Band is indeed feasible and can be structured to yield sufficiently high reliability to fulfill the overall ESSA requirements. This is not to say that PN is the optimum or best selection for the DCS task, for indeed the many governing system constraints have not, as yet, been sufficiently developed to perform such an optimization trade-off.

In the event that PN is selected as the SMS-DCS modulation structure certain areas are still worthy of additional investigation. These might be listed as follows:

- a. Further investigation of the PN acquisition sequence to arrive at an optimum trade-off between filter bank size, PLL bandwidth, detection and false alarm probabilities, E/N_0 etc., with the objective of minimizing the PN acquisition time.
- b. Detail design and cost analysis of the data collection platforms—both interrogation and non-interrogation.
- c. Detail design and cost analysis of the CDA station correlation receivers.
- d. A more detailed examination of data modulation techniques with the purpose of optimizing the data error rate probability.
- e. Computer and/or laboratory simulation of the cross-correlation PN properties to confirm the E/N_0 estimates.

REFERENCES AND BIBLIOGRAPHY

1. Judge, W. J., "Multiplexing Using Quasiorthogonal Binary Functions," AIEE, Communication and Electronics, May 1962, pp. 80-83.
2. Martel, R. J., "System Design Consideration for a Satellite Spread Spectrum Random Access Communication Experiment, "Westinghouse ATS System Technical Memorandum No. 2, June 7, 1968.
3. Jones, J. J., "Hard-Limiting of Two Signals in Random Noise," IEEE Transactions on Information Theory, January 1963, pp. 34-42.
4. Schwartz, J. W.; Aein, J. M.; and Kaiser, J., "Modulation Techniques for Multiple Access to a Hard-Limiting Satellite Repeater, " Proceedings of the IEEE, May 1966, pp. 763-777.
5. Wittman, J. H., "Categorization of Multiple Access/Random Access Modulation Techniques," IEEE Transactions on Communication Technology, October 1967, pp. 724-725.
6. Golomb, et al., "Digital Communication With Space Applications," Prentice Hall, New Jersey, 1964.
7. Davenport, W. D., Jr., "Signal-to-Noise Ratios in Band-Pass Limiters," Journal of Applied Physics, Vol. 24, No. 6, June 1953, pp. 720-727.
8. Zegers, L. E., "Common Bandwidth Transmission of Information Signals and Pseudonoise Synchronization Waveforms," IEEE Transactions on Communication Technology, December 1968.
9. Blasbalg, et al., "Air-Ground, Ground-Air Communication Using Pseudonoise Through a Satellite," IEEE Transactions on Aerospace and Electronic Systems, September 1968.
10. Aein, J. M., "Multiple Access to a Hard-Limiting Communication Satellite Repeater," IEEE Transactions on Space Electronics and Telemetry, December 1964.
11. Ward, R. B., "Acquisition of Pseudonoise Signals by Sequential Estimation," IEEE Transactions on Communication Technology, December 1965.

12. Golomb, et al., "Synchronization," IEEE Transactions on Communication Systems, December 1963.
13. Anderson, D. R., and Wintz, P. A., "Analysis of a Spread Spectrum Multiple Access System With a Hard Limiter," IEEE Transactions on Communication Technology, April 1969.
14. Golomb, "Shift Register Sequences," Holden-Day, 1967.
15. Gold, R., and Kopitzke, E., "Study of Correlation Properties of Binary Sequences," Interim Report No. 1, Volume III, Magnavox Research Labs, Torrance, California, prepared for Air Force Avionics Laboratory RTD/AFSC, Wright-Patterson Air Force Base, Ohio.
16. Anderson, D. R., and Harper, W. R., "SMS Data Collection System Direct Sequence Multiple Access Analysis," Special TRW Report, July 1969.
17. Berkowitz, R. S., "Modern Radar," John Wiley & Sons, Inc., New York, 1965, pp. 274-313.
18. Gold, R., "Optimal Binary Sequences for Spread Spectrum Multiplexing," IEEE Transactions on Information Theory, Volume IT-13, 1967, pp. 619-621.
19. Aein, J. M., "Normal Approximation to the Error Rate for Hard Limited Correlators," IEEE Transactions on Communication Technology, February 1967.
20. Ward, R. B., "Digital Communication on a Pseudo Noise Tracking Loop Using Sequence Inversion Modulation," IEEE Transactions on Communication Technology, February 1967.
21. Skolnik, Merrill, I., "Introduction to Radar Systems," McGraw Hill Book Company, New York, 1962, p. 34.
22. Ewanus W. and Burkitt F. J., "Rapid Acquisition of Doppler Frequencies," 1962 IRE International Convention.

4.2.3 Random Access Data Collection System:

A recent memorandum on the data collection system* has suggested the use of a random access system as a feasible type of non-interrogated DCP (of course the system is compatible for use with a number of DCP's which can be interrogated). The random access system is based on the fact that each DCP message occupies a very small time-bandwidth cell compared to that available for the whole system. In fact all 10,000 DCP's occupy only a small fraction of the available system time-bandwidth. This being the case, the system time (T_0) frequency (W) plane is only sparsely filled by the DCP messages which are randomly and more or less uniformly distributed over the plane. This relative emptiness makes the probability of "collisions" between messages low. Moreover, the messages are repeated several times during T_0 and since the probability of message collisions are independent, the repetition almost results in a certainty of at least one message being received without interference.

Assume that each DCP transmits a report of duration τ at bit rate r and repeats approximately every T seconds but there is no synchronism whatever between the DCP's. Then the probability that a particular DCP report is overlapped in time by any other particular DCP report is

$$P_t = \frac{2\tau}{T} \quad (79)$$

If the DCP spectral width is Δf , the total available bandwidth W and the DCP's center frequencies uniformly distributed over W , the probability that a particular DCP report is overlapped in frequency by any other particular DCP is

$$P_f = \frac{2\Delta f}{W} \quad (80)$$

Now in order for interference between two DCP's to occur they must overlap in both time and frequency. Thus the probability of interference is -

$$P_i = P_t P_f = \frac{4\Delta f \tau}{WT} \quad (81)$$

*"An Evaluation of the SMS DCP Communications System Concept" October 1969 by Communications and Systems, Inc. Falls Church, Virginia.

If there are a large number of active users, M , the probability that a particular DCP will not be interfered with by any other is

$$P_c = (1 - P_i)^M = \left[1 - (4\Delta f \tau / WT) \right]^M \quad (82)$$

Now during a total system time frame T_o , each DCP will report $n = T_o/T$ times. Thus the probability of failing to receive at least one report from a particular DCP without interference is

$$P_f = [1 - P_c]^n = \left[1 - (1 - P_i)^M \right]^n = \left\{ 1 - \left[1 - (4\Delta f \tau / WT) \right]^M \right\}^{T_o/T} \quad (83)$$

For large M , $(1 - a)^M \approx e^{-Ma}$ thus (83) can be expressed in the more convenient form,

$$P_f = \left[1 - e^{-\frac{4\Delta f \tau M}{WT}} \right]^{T_o/T} \quad (84)$$

Sommer* has shown that this function is minimized for an optimum value of T ,

$$T_{opt} = \frac{4M\Delta f \tau}{W \ln 2} \quad (85)$$

in which case,

$$P_{f \min} = 2^{-(WT_{opt} \ln 2) / 4M\Delta f \tau} \quad (86)$$

It is of interest to plot equations (85) and (86) for the DCP system where it is assumed that the minimum frequency separation between users for negligible interference is $\Delta f = 200$ Hz, $M =$ number of users $= 10^4$, $\tau =$ average message length $=$ total system traffic (2×10^6 bits) \div system bit rate (75 bits/sec) \div number of users (10^4) $= 2.67$ seconds. Of course, $T_o =$ synoptic interval of 6 hours $= 21,600$ sec. Substituting these values into (85) and (86) yields

$$T_{opt} \text{ (minutes)} = 0.51 \times 10^3 / W \text{ (kHz)} \quad (87)$$

*Sommer, R. C. "On the optimization of Random Access Discrete Address Communications," *PIEEE* Oct. 1964.

and

$$P_{f \min} = 2^{-0.70 W(\text{kHz})} \quad (88)$$

which are plotted in Figures V-42 and V-43 respectively. The bandwidth W is at least the bandwidth determined by the long term stability of the DCP oscillators,

$$W(\text{kHz})/\text{min} = 2 f_0 S \quad (89)$$

where f_0 = DCP carrier center frequency (kHz)

s = DCP stability

To insure that the DCP's uniformly occupy the bandwidth, the DCP nominal center frequencies must be selected to an accuracy equal to a fraction of the bandwidth and will thus require W to be larger than $(2 f_0 S)$ to achieve a proper distribution. For example with a carrier frequency of 400 MHz and $S = \pm 10^{-6}$, the bandwidth due to stability is 800 Hz therefore W must be at least 800 Hz and, to obtain a good frequency distribution, W should probably be at least 8 kHz. Using 8 kHz in Figure V-42 it is seen that $P_{f \min} = .02$ and the optimum T is found to be approximately 65 minutes from Figure V-43. Using these values a basic block diagram of a random access data collection system might be as shown in Figure V-44 where the DCP is shown to be a very simple device in which the timer having relatively crude accuracy is used to turn the DCP on and off at the approximate time intervals and has no deliberate synchronization with any other DCP timer.

The real problem for this type of data collection system may occur in mechanizing the data utilization system. A random access system is explicitly that, each transmitter reports on command of its internal timer and it is the burden of the data utilization system to process the reports which come in at a frequency and time which are unpredictable by the data "consumer".

Since the DCP's are also distributed randomly in frequency over the bandwidth it will be necessary to have a filter bank to segregate transmissions which may overlap in time but are on different frequencies. It can be shown that in order to ensure that every transmission falls entirely within at least one filter for a finite number of filters the width of each overlapping filter must be $2\Delta f$ which in the example considered above is about 200 Hz.

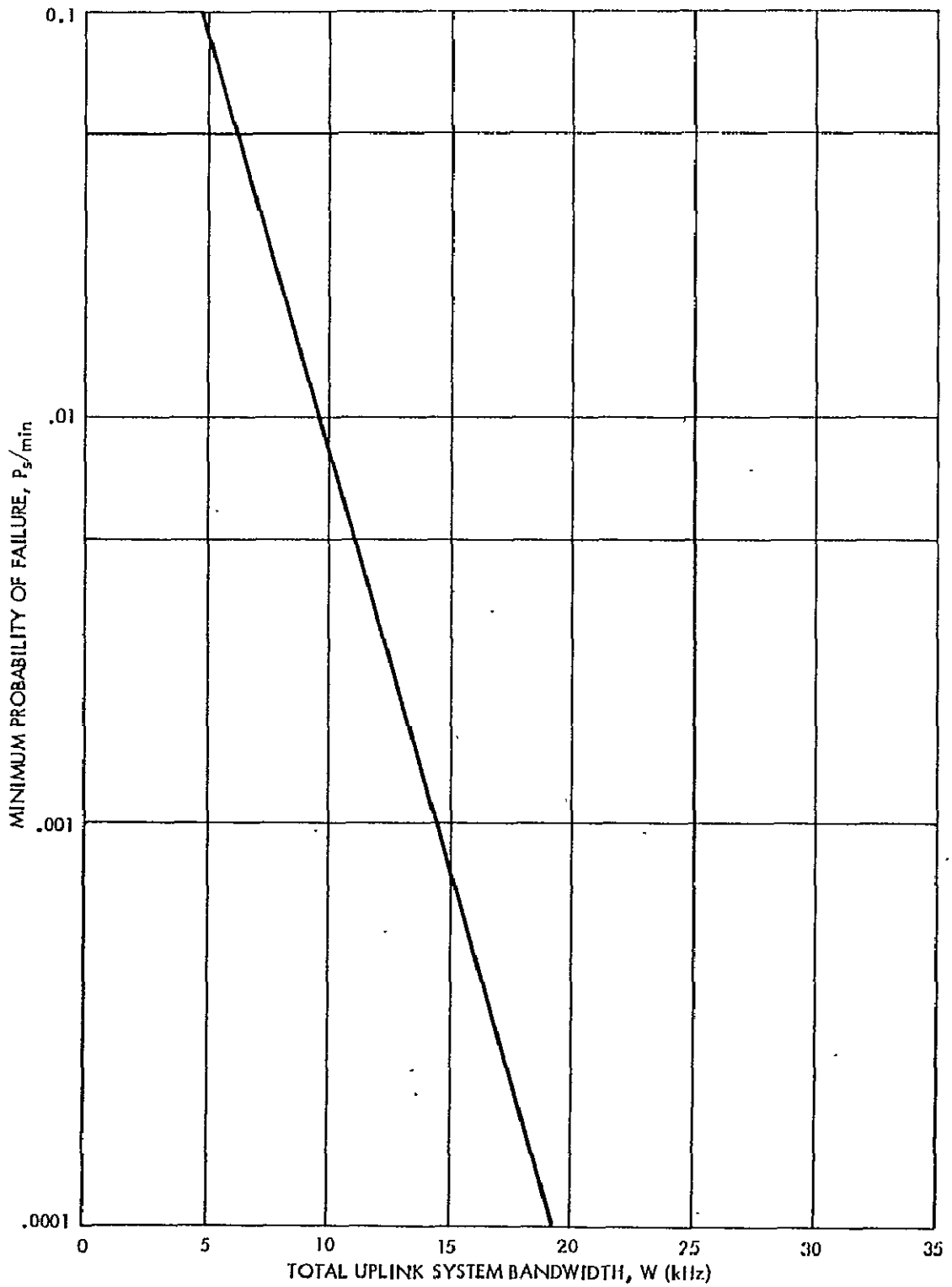


Figure V-42. Minimum Probability of Failure Versus Systems Bandwidth

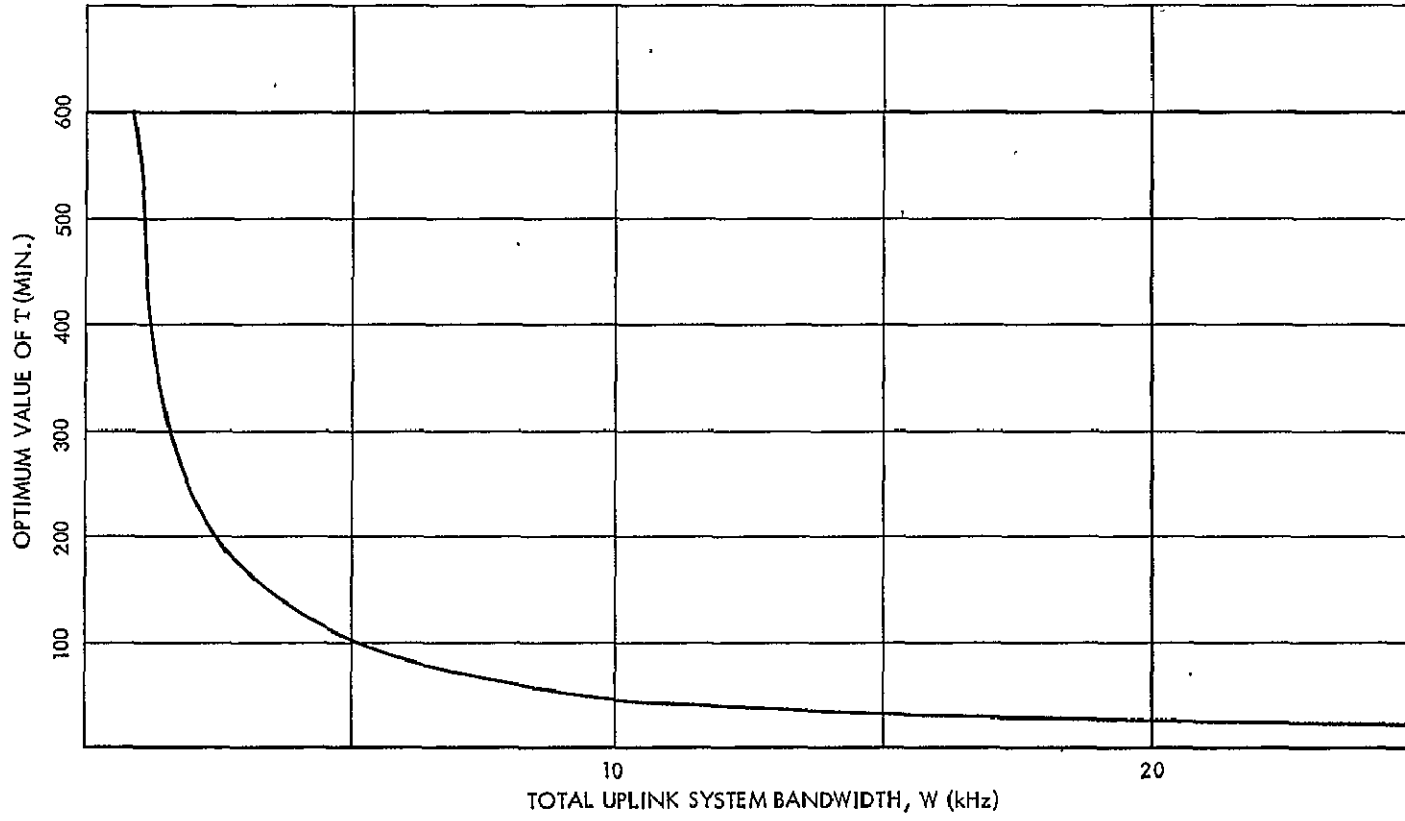
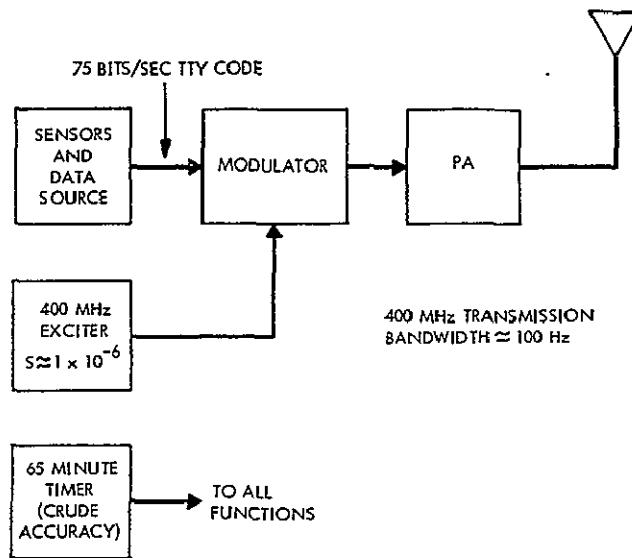
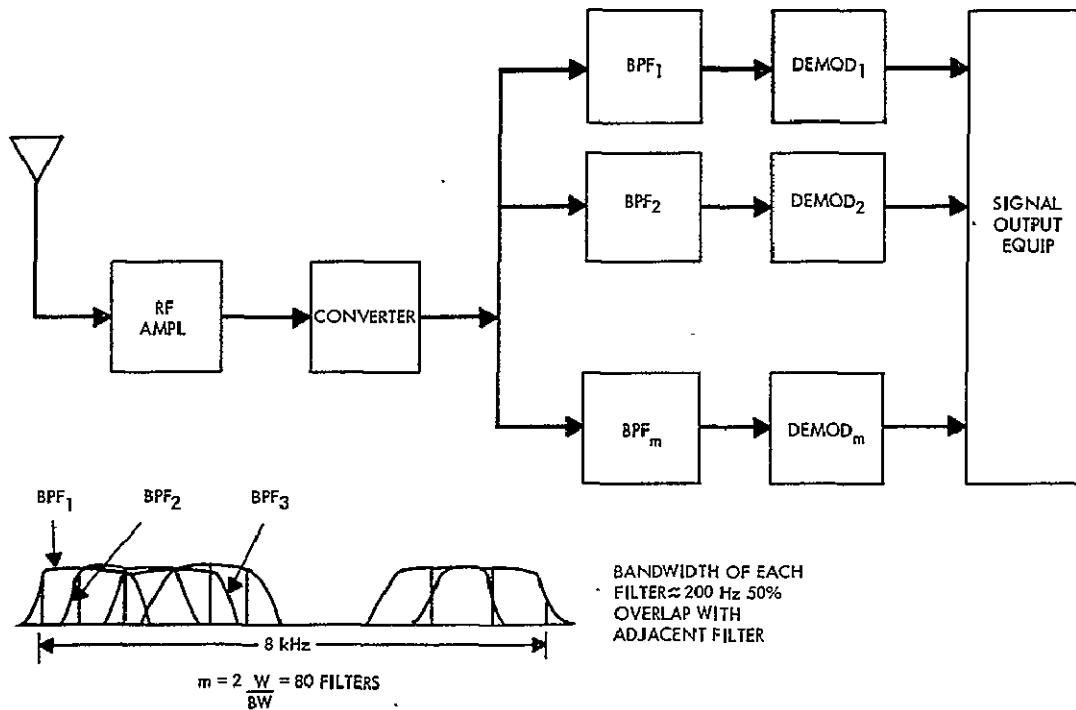


Figure V-43. Optimum Value of T Versus System Bandwidth



a. DCP TRANSMITTER



b. RECEIVER AT CDA STATION

Figure V-44. Random Access Data Collection System

Other forms of random access system should be investigated during phase C such as those employing discrete addresses through time-frequency modulation.

Random access systems will probably be found to result in considerable simplification of the DCP at the expense of a more complex CDA station receiver and possibly inconvenience to the data user.

4.3 SUMMARY OF DATA COLLECTION SYSTEM TECHNIQUES

In the previous paragraphs three methods of implementing the SMS Data Collection System have been analyzed. As is only to be expected each has its own advantages and disadvantages and these have been listed in Table V-25.

Table V-25

Comparison of Data Collection Systems

System	Advantages	Disadvantages
Interrogatable UHF or VHF	<ol style="list-style-type: none"> 1. Data can be read on command from CDA 2. More margin in Links than at S-Band 3. Frequency stability of DCP less critical at UHF than at S-Band 4. Transmission bandwidth requirements much less than a noninterrogatable system 	<ol style="list-style-type: none"> 1. Requires two S/C transponders and antenna systems 2. Multipath fading more serious than at S-Band 3. Requires a receiver on the DCP
Pseudo-Noise (PN) Spread Spectrum at S-Band	<ol style="list-style-type: none"> 1. Compatible with single S-Band S/C transponder 2. No receiver required on DCP 3. Automatic ranging provision for sub-satellite point determination 4. Offers discrimination against multipath and RFI interference 	<ol style="list-style-type: none"> 1. Largest bandwidth requirements 2. S-Band up-link power budget has least margin 3. Requires more expensive correlation receiver at CDA station 4. Relatively high DCP power drain due to higher transmitter duty cycle than interrogatable system
Random Access	<ol style="list-style-type: none"> 1. Could be compatible with single transponder 2. No receiver required on DCP 3. Requires no acquisition by correlation receiver at CDA 4. Requires less bandwidth than PN 5. Least complex DCP 	<ol style="list-style-type: none"> 1. Data return at CDA station is random over the 6 hour synoptic period 2. Power drain at the DCP is greater than would be required for an interrogatable system 3. Bandwidth required greater than interrogatable system 4. Excessive data flow and identification problem due to multiple transmissions in one 6 hour period

4.4 FINAL SELECTION OF DATA COLLECTION SYSTEM; PLAN FOR PHASE C STUDY

General - The purpose of the Phase C program with respect to the data collection system will be to review the system constraints and variables, analyze the alternatives from the aspects of both cost and practicality and recommend an optimum system. While the effort will be primarily analytical, it is probable that certain key areas of hardware feasibility will need to be checked experimentally.

The study will be performed in a logical sequence of five tasks as follows:

- 1) Survey users of data
- 2) Confirm or establish constraints
- 3) Determine those factors previously defined as variables
- 4) Trade-off analysis of candidate systems
- 5) Recommendation for final adoption

During each task the consideration of total system cost and reliability will be considered and in the trade-off analysis they will be considered among the explicit parameters upon which the final choice is based.

Survey of Users - It is deemed desirable to perform a new survey among the potential users of the meteorological and hydrological data similar to that performed during the GOES study of 1967. The survey will result in a more realistic estimate of the present traffic and system growth requirements than is presently available. It should also provide the requirements and preferences of the users with regard to the most practical and convenient method of disseminating the information collected. An example of this will be the desirability of retaining or replacing the ASCII code which has been assumed throughout the discussion of the data collection system. That is, it may be desirable to use a more easily generated code at the DCP's and convert to ASCII at the CDA stations before transmission to the users. On the other hand this would entail an additional complication at the CDA station and possibly precludes real time relay to the user which could be required by certain data customers.

Confirm or Establish Constraints - The data collection system constraints listed previously are at best tentative and reflect only an estimate available at the time of writing this report. The function of this task in Phase C will be to establish the actual state-of-the-art constraints on critical items such as frequency stability, receiver noise temperature, battery capacity and transmitter efficiency. This will be accomplished by contact with equipment manufacturers and/or by performing the appropriate tests as part of this task. All doubt with respect to state-of-the-art and cost of key items should be resolved at this stage.

Determination of Variables - Here the major system variables need to be determined. As discussed before, these items include the number of transponders (and transmitters) in the spacecraft, the method of timing the DCP reports and the frequency band(s) to be used. In most cases these variables are interdependent. The user requirements and constraints determined in the first two tasks serve to limit the scope of this investigation. For example if high stability oscillators on the order of one part in 10^8 were available (with suitably low power consumption) there may be no advantage of considering an "all interrogated" data collection system since autonomous reporting might provide a highly efficient utilization of time-bandwidth product. On the other hand if it was found that a stability of only one part in 10^5 was feasible, either a random access, spread spectrum or all interrogation system would be required.

Final Trade-Off Analysis - Those competing techniques which survived the determination of variables stage will be examined in detail here. Among the factors included in the trade-off analysis will be channel efficiency, operational reliability, maintainability and total system cost. The latter will be influenced by both the initial spacecraft and data collection system cost as well as maintenance costs of the DCPs and the operation of the CDA station and data distribution system.

Conclusions - The final task will be to infer from the trade-off analysis the parameters of that system which, by virtue of its combination of desirable attributes viz. economy, reliability etc., constitutes an optimum choice. A detailed block diagram of the complete data collection system will then be prepared. The specification of any blocks in the final configuration which might be considered "risk items" will be supported by test data and schematic diagrams. The data collection system will thus be defined to the point where the individual blocks could be engineered independently.

5. WEFAX

5.1 GENERAL

Weather facsimile (WEFAX) pictures will be sent from the CDA station via the spacecraft transponder to all APT stations within the area of coverage of the spacecraft. This is an operational procedure that has been proven feasible in the ATS experiment. In that experiment, gridded cloud pictures have been transmitted on a scheduled basis to meteorological customers. These pictures were generated from cameras on board the synchronous satellites (ATS) and the polar orbiting (ESSA Operational) satellites.

5.2 MODULATION TECHNIQUE

The modulation scheme for the link begins with a video signal occupying the band from about zero to 1.6 kHz. The video amplitude modulates a 2.4 kHz subcarrier which is applied as frequency modulation to the VHF transmitter. The peak frequency deviation due to the subcarrier is 9.0 kHz. The bandwidth occupied by the FM signal is approximated by Carson's rule to be 26.0 kHz. The output signal-to-noise ratio can then be found from the following formula:

$$S/N = (3/2) \frac{B \Delta F^2}{f_U^3 - f_L^3} (C/N) \quad (90)$$

where

S/N = output signal-to-noise ratio from discriminator

C/N = input carrier-to-noise ratio = 10 db

B = the FM receiver bandwidth = 30.0 kHz

ΔF = peak deviation = 9.0 kHz

f_U = highest FM baseband frequency = 4.0 kHz

f_L = lowest FM baseband frequency = 0.8 kHz

Substituting into equation 90 obtains $S/N = 28$ db which is the output signal-to-noise of the discriminator and the input signal-to-noise ratio to the AM detector.

The output of the AM demodulator is reduced by a factor of M^2 over the input where M = percentage amplitude modulation = 80%. Thus,

$$S/N \text{ output} = 26 \text{ db}$$

Since it has been estimated that at video a 13 db RMS signal-to-noise ratio provides an adequate FAX picture, it appears that the 10 db carrier-to-noise ratio is ample for this application.

5.3 S-BAND UP-LINK

Since the CDA station will be equipped with an S-band transmitter (for stretched data transmissions) it will be most economical to arrange for the WEFAX transmissions to be time shared with the stretched data transmissions and therefore utilize the full power of the ground transmitter and nearly the full power of the spacecraft transmitter. The transponder will operate as a saturated frequency translating repeater with the up-link frequency at 2.0 GHz. The up-link calculation is shown in Table V-26.

5.4 S-BAND DOWN-LINK

The present ATS WEFAX and ESSA and NIMBUS APT transmissions are in the VHF band and consequently APT stations are mechanized for VHF. Inspection of the down-link calculations in Table V-26 shows that the VHF band is indeed very attractive for SMS WEFAX in that it requires only a modest antenna at the APT station where low cost is usually a major consideration. However, the provision of a VHF transponder on the SMS spacecraft would pose severe power and weight problems (particularly the antenna) and it is not proposed therefore that the S/C have a VHF transmission capability. Thus it is likely that the WEFAX transmissions from SMS will be either at UHF, 400 MHz or S-band (1.7 GHz) and conversion of all present APT stations to one of these bands will be required for reception of SMS WEFAX.

5.5 CONVERSION OF APT STATIONS

A conceptual block diagram of 1.7 GHz Converter is shown in Figure V-15. If the antenna is equipped with a circularly polarized feed matched to the S/C antenna, the diameter of a parabolic antenna required for 25 db gain would be 4.5 feet. On the other hand, the use of a less expensive linearly polarized feed would incur a 3 db polarization loss requiring either an increase in the antenna

Table V-26

WEFAX Links

CDA - to - S/C Link (2025 MHz)

Ground Transmitter Power	40.0 dbm
Ground Antenna Gain	45.5 db
Free Space Loss	-190.7 db
Margin	<u>-3.0 db</u>
Received Carrier Power at S/C	-92.7 dbm
S/C Receiver Noise Temperature	27.7 db-°K
Boltzmann's Constant	<u>-198.6 dbm/Hz-°K</u>
S/C Noise Power Density	-170.9 dbm/Hz
Up-Link Carrier-to-Noise Density	78.2 db-Hz

S/C - to - APT Stations Link

	<u>136 MHz</u>	<u>402 MHz</u>	<u>1.70 GHz</u>
Ground Receiver Noise Figure	7.0	7.0	7.5 db
Ground Receiver Noise Temp.	30.7	30.7	31.2 db-°K
Boltzmann's Constant	-198.6	-198.6	-198.6 dbm/Hz-°K
Ground Rec. Noise Power Density	-167.9	-167.9	-167.4 dbm/Hz
Required Carrier-to-Noise Ratio	10	10	10 db
System Margin	3	3	3 db
<u>Overall Carrier-to-Noise Ratio</u>	<u>13</u>	<u>13</u>	<u>13 db</u>
Bandwidth (30 kHz)	44.8	44.8	44.8 db-Hz
Overall Carrier-to-Noise Density (Both Links)	57.8	57.8	57.8 db-Hz
Required Down-Link Carrier-to-Noise Density	57.8	57.8	57.8 db-Hz
Required Down-Link Carrier Power	-110.1	-110.1	-109.6 dbm
S/C Transmitter Power	43.0	43.0	43.0 dbm
S/C Antenna Gain (at 5° El. Point)	10.5	10.5	11.5 db
Free Space Loss (at Max. Range)	167.6	177.0	189.4 db
Minimum Required Ground Antenna Gain	4.0	13.4	25.3 db

diameter to 6.5 feet or an acceptance of a link with zero margin (rather than the 3 db in Table V-26) with the 4.5 foot dish. Where economy is the paramount consideration, the latter course would likely be adopted. The converter shown in Figure V-45 could be readily constructed from commercially available components at a cost of approximately \$100, while the cost of the antenna might approach \$1500 from commercial sources. The total S-band conversion would thus cost on the order of \$1600. If the WEFAX down-link is at UHF rather than S-band, the conversion cost can be expected to be considerably less than the above estimate, since the required antenna gain, now only 13 db, can be realized with a relatively inexpensive yagi or helical antenna.

V-175

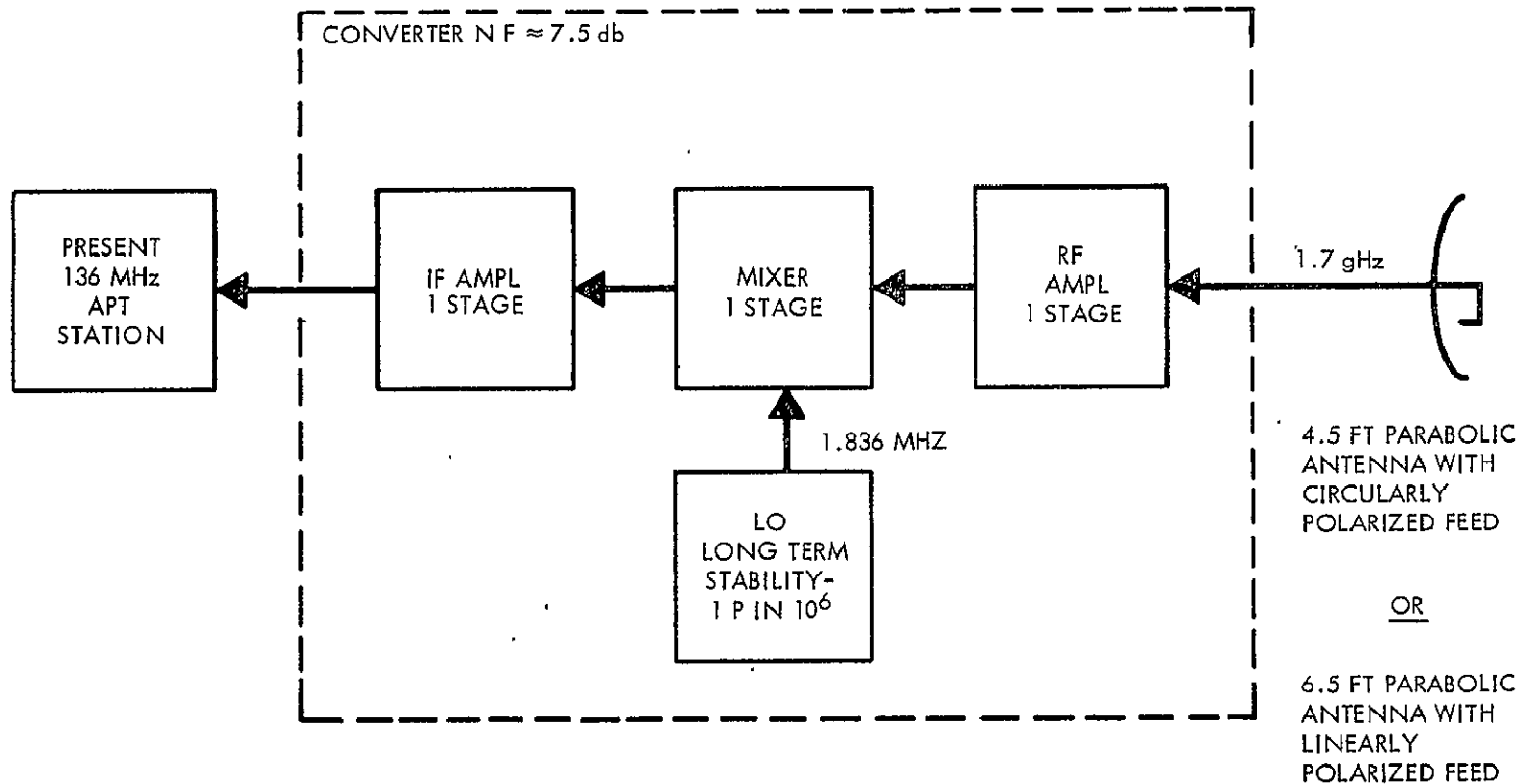


Figure V-45. Block Diagram of APT S-Band Conversion

6. SPACE ENVIRONMENT MONITORING SUBSYSTEM

Space for selected space environment monitoring sensors is available on the SMS spacecraft. The flight of all sensors, unless mandatory for spacecraft basic systems performance, is contingent upon their availability at the time of launch.

The Boulder Laboratories of the Environmental Science Services Administration have long been concerned with the relationships between solar disturbances and effects on the earth's near space environment. These relationships were originally recognized in the field of ionospheric radio communications where solar disturbances can create immediate and, at high latitudes, complete disruption of ionospheric radio communications. In recent years, a knowledge of solar disturbances and their effects has assumed even greater importance as it became recognized that the larger solar energetic particle event could pose significant radiation hazards for man in space and also become a constraint on the flight of supersonic transport aircraft operating at the fringes of the earth's atmosphere. A component of ESSA Research Laboratories in Boulder, the Space Disturbances Laboratory, is charged with carrying out research towards the better understanding of the interactions between solar and terrestrial phenomena and attempts to meet recognized national needs for current data on solar events and their effects by operating the Space Disturbances Forecast Center in Boulder. The Space Environment Monitor Subsystem is designed to provide direct measurements of important effects of solar activity in such a manner that the data will be available continuously in real time for use in the generation of advisory or warning messages. The data will also be used as an input to forecasting and operational research, and will be made available externally through the medium of the weekly preliminary reports from the Forecast Center and, on a longer time scale, through World Data Center A in Boulder.

6.1 SOLAR ENERGETIC PARTICLE MONITOR

Solar particle radiation constitutes the major radiation hazard to manned spaceflight activities. It also presents an operational problem to SST flights at high latitudes and is responsible for major high altitude communication blackouts. Major solar particle events are relatively infrequent, perhaps ten may occur over a sunspot maximum period.

Present knowledge of solar particles production and propagation is unsatisfactory for prediction purposes at present. The operational need exists for providing a warning of the onset of an event and sufficient immediate quantitative description of the flux to enable actual radiation hazards and communication

effects to be calculated. The first need can be met by ground-based ionospheric measurements within the polar cap regions (i. e., the regions having essentially zero magnetic cutoffs for solar particles). There are difficulties in maintaining adequate sensitivity with the variation in solar zenith angles and also considerable communications problems, particularly if, as would be desirable, the southern polar cap were to be instrumented. The second objective cannot be met by ground-based measurements except for the limited direct measurement of communication effects because of ambiguities in the relationship between atmospheric ionization and incoming flux, unless assumptions are made about the spectrum.

The direct measurement of the energetic particle flux by satellite is therefore necessary. The technology for such measurements is well established and space tested.

Low orbiting satellites can only make flux measurements when they are in the polar cap regions and therefore not shielded from the particles by the earth's field. Thus, although very useful as an addition to a ground-based warning system to provide direct particle flux and energy measurements the mechanics of the orbit and data transmission impose unavoidable losses in immediacy.

Geostationary satellites have great advantages for operation monitoring because of the possibility of continuous real time transmission of data to the ground. Their position at 6.6 earth radii imposes some problems of magnetic shielding for lower energy particles.

Early consideration of energetic particle monitoring from geostationary orbit based on simple magnetic cutoff theory suggested that the cutoff value would be at least 100 Mev for protons at local noon. It was known that the simple theory gave values much higher than those observed in many situations. Data from ATS 1 taken during the 28 January 1967 event show that protons with energies greater than 20 Mev have essentially free access to a geostationary satellite. Those in the 5 - 20 Mev range show about a 3:1 local time modulation with essentially free access at local midnight. An empirical correction for this modulation will be adequate for most operational purposes. Data from ATS 1 has recently been made available in real time to the Forecast Center in Boulder and current experience confirms the earlier observation.

The data required for radiation hazard calculations in the Manned Spaceflight program have been defined as at least 4 points in the spectrum between 15 and 100 Mev for protons and for alpha particles in the range 60 - 400 Mev. The percentage of alpha particles in a solar energetic particle event is normally quite low but their radiation damage capability is disproportionately high. The

SST problem demands a knowledge of higher energies than 100 Mev because the shielding effects of the atmosphere. The upper limit of interest is set by the rapidly decreasing numbers of protons at very high energies in a typical event. The data presently available make this a difficult limit to define. There is also the practical difficulty of providing energy resolution for very high energy particles within the limitations of satellite space and weight. The requirements for prediction of communication effects are primarily for information on proton fluxes below 50 Mev where the high latitude fluxes and ionospheric effects are large. Thus, our requirements must be defined within the limitations set on the one hand at low energies by the validity of measurements in geostationary orbit and at the other by the difficulties of providing energy resolution at proton energies above 500 Mev.

The outline specification, evolved from the foregoing considerations, is therefore to monitor proton energies in at least six ranges between 5 and >500 Mev and alpha particles in at least six ranges between 20 - >400 Mev. The dynamic range should accommodate both the galactic cosmic ray background and the largest known events. In addition to the proton and alpha particle channels, a single channel for energetic electrons ≤ 500 Kev is required to monitor the environment which might affect the X-ray detection system.

This need will be met by the solar energetic particle monitor which comprises a maximum of four small, solid-state detector units which are either in a "telescope" configuration or under a hemispherical shell.

Positioning of the detectors on the spacecraft skin is not critical except for a requirement that the hemispherical type should project sufficiently to have a clear 2π angle of view. Small obstructions can be tolerated.

The detector electronics consists of quantitative evaluation and data handling circuits which occupy a volume of 100 cubic inches, require 1.0 watts and weigh four pounds.

6.2 SOLAR X-RAY MONITOR

The soft X-ray emission centered in the range $0.5 - 16 \text{ \AA}$ associated with optically observed solar flare events is extremely variable both in intensity and spectral characteristics and shows little correlation with optical characteristics. The energy released as X-rays can be a very significant part of the total energy of an event and must therefore form an important part of any description of a flare which claims to be complete.

The X-ray emission is the direct cause of the immediate ionospheric effects associated with solar flares, i. e., height of reflection changes and changes in absorption of VLF, LF, and HF radio paths. These effects can be calculated from quantitative X-ray measurements and used as an operational input to the control of radio communication systems.

Many scientific experiments in both satellite and ground-based units are specifically designed to investigate flare-induced effects. The Boulder Forecast Center provides real time warnings of flare commences to experimenters on request and these can greatly assist the productivity of such experiments. An excellent future example of this need is the operation of the Apollo Telescope Mount (ATM) mission where real time prediction and control from the ground will be essential in obtaining maximum value from the high resolution spacecraft experiments. Studies for the ATM mission have also shown that direct satellite measurements of solar X-ray events can be perhaps an order of magnitude more sensitive for the detection of onset and confirmation of small events than is possible using the only ground-based alternative, observation of ionospheric effects using radio propagation, and should not suffer from the problem of false alarms.

The background level of X-ray radiation from the quiet sun is an excellent general indicator of solar activity and there is a good deal of evidence to suggest that most flares are preceded by a gradual buildup in background level over the preceding 10 - 30 minutes known as a precursor.

From the foregoing, the Space Disturbances Laboratory's operational requirements for solar X-ray data can be summarized:

- a. Background data for evaluation of solar activity trends and for precursor detection.
- b. Immediate detection of the onset of an X-ray event for warning purposes.
- c. Quantitative description and time history of the event.

In all cases, except for long term background data, a great deal of operational value is lost if the data are not available in essentially real time.

Objective b. can be met using the ground-based monitoring of ionospheric effects of solar X-rays, but direct methods are more sensitive and have a lower false alarm rate. Objectives a. and c. can only be met using direct measurements from a satellite. The basic satellite technology required is well established, however, there are problems in designing the sensor to avoid

unacceptable interference to the X-ray measurements by the energetic electron environment in geostationary orbit. For this reason, it is recommended that the X-ray monitor for the initial SMS should be of the simple type employing ion chamber or Geiger-Muller detectors covering the ranges 0.5 - 3 Å and 1 - 8 Å. The minimum useful threshold sensitivity would be 10^{-4} ergs cm^{-2} sec^{-1} (1 - 8 Å) and 10^{-6} ergs cm^{-2} sec^{-1} (0.5 - 3 Å) with a dynamic range of at least 10^3 . Better sensitivity and dynamic range would be desirable but may be impossible to achieve in the electron environment. It is recognized that this type of detector is incapable of giving the spectral information necessary for the calculation of ionospheric effects but will nevertheless meet the other requirements satisfactorily.

One possible realization of the solar X-ray monitor which has been studied comprises two detector units whose viewing direction will be perpendicular to the spin axis at 180° to each other. The units will consist of an ion chamber of a Geiger-Muller detector with highly asymmetric collimation (perhaps $45 \times 1^\circ$). The opening required in the spacecraft skin must have its long axis parallel to the spin axis and will have maximum dimensions of 10" x 1". The assembly will include one or two permanent magnets for electron shielding. The depth of the assembly, which will be a thin triangular form, may be up to 10".

The sensor electronics will occupy 100 cubic inches, require 2.0 watts, and weigh 8 pounds.

6.3 SYNCHRONOUS SATELLITE MAGNETOMETER

The geostationary series of satellites has opened a new perspective of magnetospheric measurement. The field lines at the geostationary position change slightly with local time and are considerably distorted by the solar-terrestrial disturbances. The tilt of the earth's dipole field axis with respect to the geographic axis means that a longitudinal change in the satellite's fixed location will move it to field lines associated with different geomagnetic latitudes.

Data from a nonstationary satellite gives the observer some difficulty in resolving spatial from temporal changes particularly for phenomena expected to have "rapid" variations. The geomagnetic fluctuations are in this problem area. The geostationary satellites are particularly useful, then, for the temporal change monitoring of the geomagnetic field within the magnetosphere. By remaining close to one field line the geostationary satellites are also unique for observations of field line guiding of waves and particles.

The magnetospheric outer boundary varies from about 8 to 12 earth radii in the noon meridian to much more than the 60 earth radii moon distance, as a tail, in the midnight meridian. The magnetosphere is a dynamic region whose magnetic field variations define, in many ways, the motions of the plasma of charged particles contained within its boundaries or guided to the earth's surface. These are the particles responsible for auroral radiowave absorption, polar communications blackouts, radiation hazards for space flight, etc. These fields have been studied by using the ground observatories. However, the scientific community has learned that this surface field is a complex mixture of the solid earth sources, magnetospheric perturbations, ionospheric currents, induced surface effects, and miscellaneous other contributions which are not easily measured. Satellite field determinations allow the separation of the space from the surface and ionospheric effects. Explorer and VELA type satellites circling the earth give us news of the solar wind region and magnetospheric boundary movement. Elliptical orbits of such satellites bring them rapidly through the magnetosphere presenting some difficulty in separating spatial from temporal changes. The geostationary satellite has an especially important monitoring value because continuous field measurements can be made in conjunction with the charged particle sensing at a fixed spatial position. For monitoring purposes, the significant question is not only to determine the quantity of energetic charged particles which have arrived within our earth's magnetosphere but what will be their route to the earth. An example of the need for concurrent particle and field measurements is seen in the series of articles in the *J. Geophys. Res.*, 73, Sept. 1, 1968, where the January 14, 1967 compression of the magnetopause past the geostationary satellite ATS 1 is discussed. During this period the magnetospheric field strength varied from 165 gamma just before the first boundary crossing to 210 gamma just after the last. This compares to an average value of 124 gamma on quiet days. The estimated velocity of the boundary at the time it crossed the satellite was 60 km/sec.

The magnetic field measurements coupled with the energetic particle determinations showed that the satellite on January 14, 1967, had sampled a region of space with characteristics quite different from the magnetospheric trapping region. A low particle count rate and radically different energy distribution could be reconciled with an intrusion of the magnetopause inside the satellite orbit. The particle observations without the field measurements would present an interpretation problem.

The space disturbance forecasting use of a geostationary satellite particle monitor concerns both the particle flux coming into the earth as well as on what "railroad track" this flux is moving. Day to day variations of the particles must be identified with the region of the magnetosphere and its field. The equatorward extent of the polar region ionospheric absorption events are defined by both the particle characteristics and the compressed earth's field.

The program for monitoring use of the SMS magnetometer would be effected in three stages. First, the field direction and magnitudes in a range of 10 to 500 gamma would be used immediately to warn of magnetospheric boundary compressions past the satellite position. Second, model earth fields would be fitted to the range of SMS field determinations to give the disturbance forecasting center predicted trajectories for the observed energetic particles. Third, comparison of earth surface and satellite field changes would be investigated with the view toward developing better techniques for projecting the earth observatory data into the space environment. The data from the Great Whale River, Jicamarca, and Byrd observatories operated for or in conjunction with ERL will be particularly valuable for this investigation.

Two research applications are immediately envisioned for the SMS magnetometer. First will be to investigate the currents within the magnetosphere. There is strong evidence for a ring current belt which may be particularly strong in the midnight hemisphere. The second study would involve the field micropulsations observed at SMS. Following a rapid compression of the magnetospheric field the power in the rapid fluctuations has been found to increase by about 10 times for ATS 1 observations. Measurements of the satellite concurrent with those near the feet of the principal field line at Great Whale River, Canada, and Byrd Station, Antarctica, will permit studies of propagation velocity, absorption and dispersion determinations for the hm waves.

The magnetometer instrument proposed is generally similar to that already operating on the ATS 1 satellite. Two flux gate sensors are used in conjunction with the spacecraft spin to define three orthogonal components of the ambient field. Additional offset generators and associated logic will enable measurements to be made over the range $\pm 250\gamma$ without saturation and with an instrument resolution of 0.1γ . It is not proposed that any attempt be made to make SMS a clean spacecraft magnetically, but that with reasonable care in siting the magnetometer, it will be possible, as in ATS 1, to make after the fact corrections for changes in spacecraft configuration. The real time resolution will probably be limited under these conditions to $\pm 10\gamma$, but this is adequate for the use proposed.

The instrument is anticipated to weigh about 1.1 lb, consume 750 mW, and occupy about 80 ins³.

6.4 SEMS DATA TRANSMISSION

It is desired that the SEMS data should be continuously available in Boulder for online reduction and display in the Space Disturbances Forecast Center.

This can be achieved either by direct reception of the Spacecraft telemetry in Boulder or by line transmission from the CDA station at Wallops. The former alternative is generally preferred providing that the S/C telemetry can be received with the 24' antenna which is anticipated to be available both for this purpose and for the reception of stretched video data. This arrangement both eliminates long line data transmission and simplifies the liaison required for maintenance of satisfactory performance.

7. SPACECRAFT DESCRIPTION

7.1 GENERAL

The following sections describe the basic SMS spacecraft and its sub-systems. The spacecraft is designed to support the sensors and subsystems required to meet the program objectives. No advances in basic spacecraft technology are anticipated. Therefore, the spacecraft and the housekeeping sub-systems design will be based on the flight proven designs of ATS III and INTEL-SAT III. The spacecraft weight at launch, including sensors and apogee motor will be approximately 1000 lbs. The available electric power will be a minimum of 120 watts at the end of 5 years. The telescope/radiometer will be capable of both day and night operation with the exception of the eclipse period.

7.2 STRUCTURE SUBSYSTEM

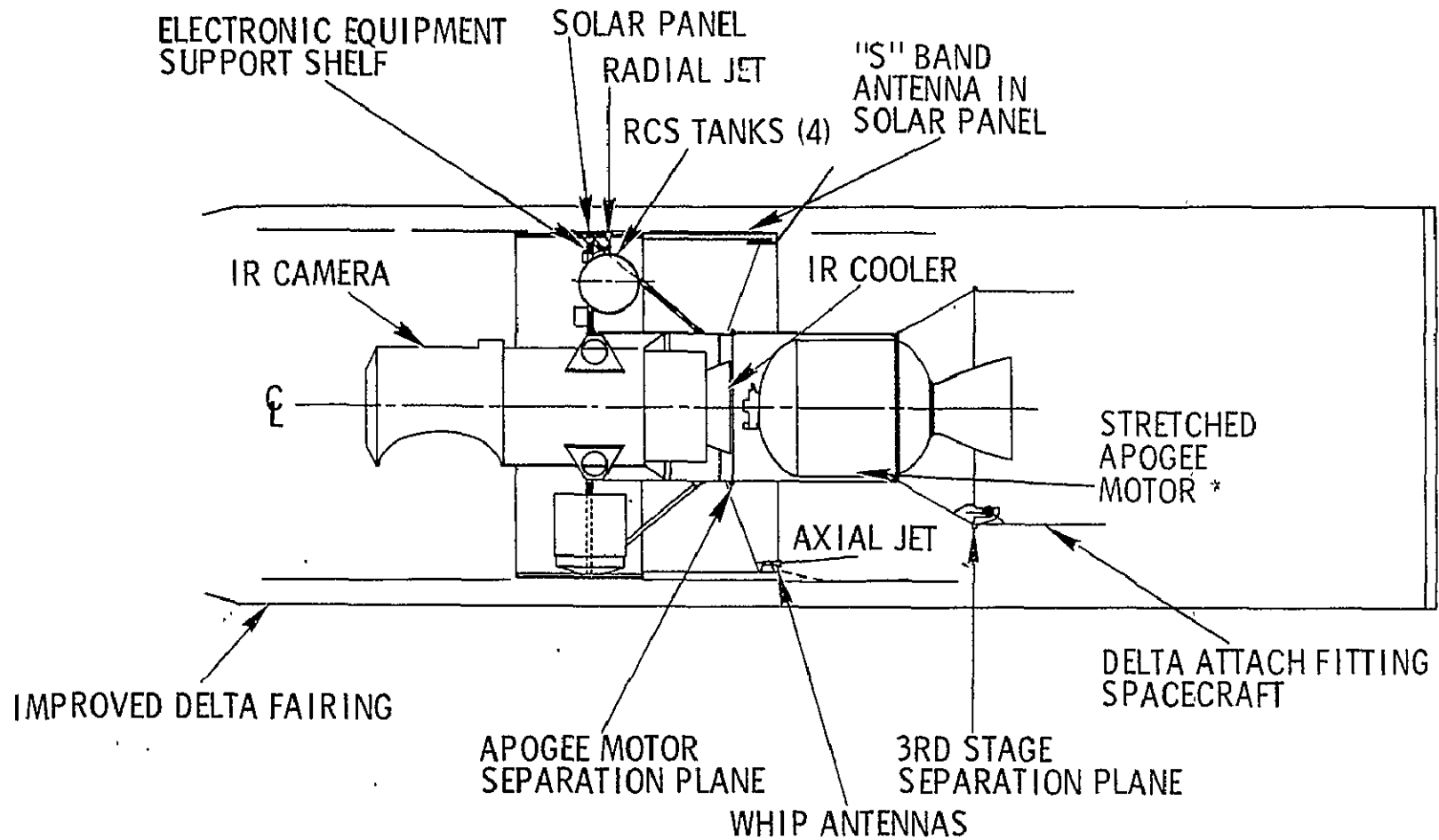
7.2.1 Structure Description

The spacecraft structure will be cylindrical in overall shape as shown in the conceptual drawing in Figure V-46. Its overall dimensions are 56 in. dia. x 65 in. long which is compatible with the standard Delta shroud. The primary structural member is a thrust tube located in the center of the cylinder. The radiometer/telescope is mounted in and structurally supported by the thrust tube. The radiometer/telescope instrument runs the length of the spacecraft. Looking out at one end is the scanning mirror. It requires a clear field of view of the earth. On the other end of the instrument is mounted the radiation cooler. This cooler requires a clear view of space with no sun impingement over the entire operational lifetime. The apogee motor is mounted to the thrust tube, covering the radiation cooler during the launch phase. Once orbit is achieved, the apogee motor is ejected, thus exposing the radiation cooler.

Support structure extends radially from the thrust tube to support the cylindrical solar panels which form the outer walls of the spacecraft. The annulus between the thrust tube and the solar panels will be thermally controlled and will contain the spacecraft electronics packages, the stationkeeping and attitude control equipment, batteries, most of the SEMS and ATS type spin scan camera (if required). Additional space is available for equipment that might be required by ESSA on future flights. The entire spacecraft including apogee motor will be mounted to the launch vehicle by means of a standard Delta adapter.

7.2.2 Antenna Structure

The despun S-band antenna affects the structural design depending on whether the electrically despun or the mechanically despun technique is used.



*** STRETCHING IS ACCOMPLISHED BY ADDING A CYLINDRICAL INSERT TO THE SPHERICAL PROPELLANT TANK**

Figure V-46. Conceptual Drawing of SMS Spacecraft

Present configuration calls for the use of an electrically despun antenna although the final decision will not be made until after the spacecraft contractor has had an opportunity to conduct a study on the subject.

If a mechanically despun antenna is selected it must be located in such a way as to have a clear field of view of the earth and must be out of the field of view of the sensors and radiation cooler. The most likely location would be above the radiometer/telescope scanning mirror.

7.2.3 Spacecraft Weights

The spacecraft weight breakdown is given in the following table.

SMS WEIGHT BREAKDOWN (pounds)

Radiometer/Telescope		135
SEMS		15
Structure		55
Thermal Control		5
Telemetry and Command Electronics		11
S-Band Electronics and Antennas		80
Ranging Unit		7
Stabilization		45
Electronics	10	
Reaction Control	25	
Pulsed Plasma	10	
Solar Power		55
Array	35	
Battery and Electronics	20	
Harness		20

Nutation Damping	15
	<hr/>
	438
Fuel	40
	<hr/>
	478
Apogee Motor and Adapter	<u>522</u>
Total	1000

7.3 THERMAL CONTROL

Thermal control of the SMS spacecraft will depend on passive energy balance techniques. Appropriate thermal coatings and insulation will be applied to all spacecraft parts based on a thermal design to be conducted by the prime contractor. Based on ATS experience, the temperature of the solar array is expected to vary from 55 to 85° F during normal orbital operation. During the maximum eclipse period, the solar array temperature is expected to reach a minimum of -80° F. The temperature range in the electronics equipment area at major equipment mounting areas is expected to be 70 ± 30° F during normal orbital operations. The thermal interface between the telescope/radiometer and the spacecraft will be studied by the spacecraft contractor during the early phases of the design. Special care will be taken to optimize the thermal exchange between the spacecraft and the instrument to minimize thermal gradients of the instrument. The thermal profile in the area of the apogee motor interface (after burn) will be studied. Special emphasis will be placed on the effect of the high motor case temperature (500 - 700° F) on nearby equipment, especially the radiation cooler. Use of special protective covers will be examined.

7.4 ELECTRICAL POWER SUBSYSTEM

Spacecraft electrical power will be supplied from solar cells. The system is designed such that the normal operation plus battery charging is supplied by the solar array output. During eclipse periods, nickel-cadmium batteries are provided to operate those subsystems essential for spacecraft survival. No operational data will be provided during this period. To provide operational capability during the eclipse period would require batteries in excess of the present weight allocation.

The capacity of the solar array will be sufficient to compensate for orbital degradation over the design life of 5 years. Accordingly, the array output will

be 160 watts at start of life and 120 watts at the end of 5 years. The system has an unregulated bus designed to provide a minimum of 24.5 volts to spacecraft subsystems. Each spacecraft subsystem is provided with an individual voltage regulator. The system is illustrated in simplified block diagram in Figure V-47. As indicated the main array feeds the unregulated bus. A voltage limiter limits the voltage on the unregulated bus from exceeding 32 volts. This limiter is required for the period immediately following the eclipse when the solar array temperature is at its extreme low. The battery is merely sized to provide for the essential loads during the eclipse period. It is charged from a separate section of the solar array appropriately sized to provide a constant, safe level of charge. The battery discharges into the unregulated bus through a discharge regulator to maintain the low voltage limit. Redundancy in the power system will be provided with the degree of redundancy to be determined during the early design phases. The power requirements of the major components are given in the following table. No attempt is made to determine duty cycles at this early stage of the program.

SMS POWER REQUIREMENTS

S-Band Electronics	75 watts
Telescope/Radiometer	23 watts
Telemetry and Command	18 watts
SEMS	12 watts

7.5 SPACECRAFT COMMUNICATION SUBSYSTEM

The fundamental requirements for the SMS spacecraft communication system will be based on the overall constraints imposed by the camera and data collection systems. These have already been discussed in some detail in sections 2.0, 3.0, and 4.0. The most important question that must be resolved with regard to the design of the S/C communication system lies in the use of one hard limited SHF transponder and/or a separate transponder for the data collection system. And if a separate transponder is used for the DCS, shall it be at S-band, UHF or VHF?

Actually three alternatives are available. Figure V-48 is the single hard limited S-band transponder which will certainly represent the least expensive S/C design. This of course has the principle disadvantage of power sharing the single 20 watt transmitter with the DCS and the stretch camera link. Also the DCS is compelled to live with the 30 msec data loss during the wideband camera downlink transmission.

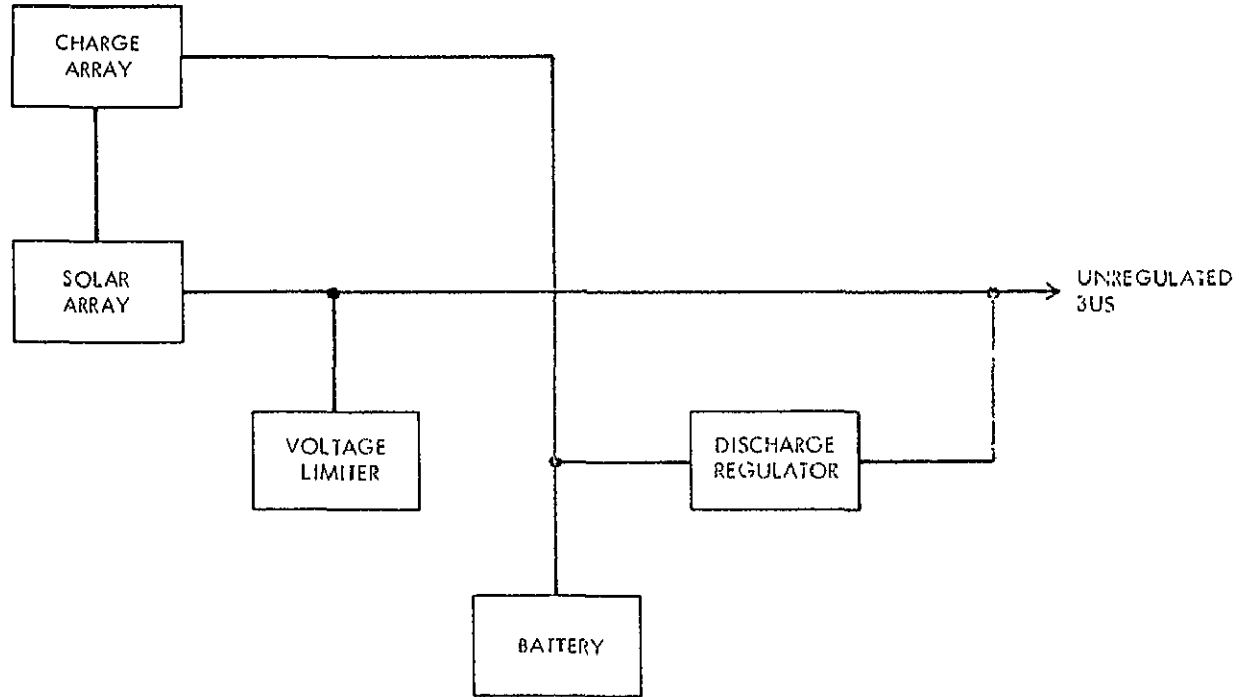


Figure V-47. Electric Power System Block Diagram

The second alternative is shown in Figure V-49. This is also an all S-band design; however, a 1 watt linear transmitter is added for exclusive operation with the DCS. This avoids the power sharing problem. An additional advantage is the added down-link DCS EIRP which will permit operation with smaller ground stations. Its principal disadvantage is that it is not compatible with a VHF or UHF DCS if that approach should be adopted, and the cost will be higher than the one transmitter system of alternative 1.

The third choice would involve the addition of a separate and complete UHF or VHF transponder for the DCS. This would be in addition to the S-band transponder as shown in Figure V-48, which of course would be devoted to the camera links. The advantages of this approach are essentially the same as those listed for the 1 watt linear S-band-DCS addition of alternative 2. The principal disadvantage would lie in the additional S/C cost of another transponder and UHF or VHF antenna system. A table listing and principal advantages and disadvantages of the alternatives discussed are presented in Table V-27.

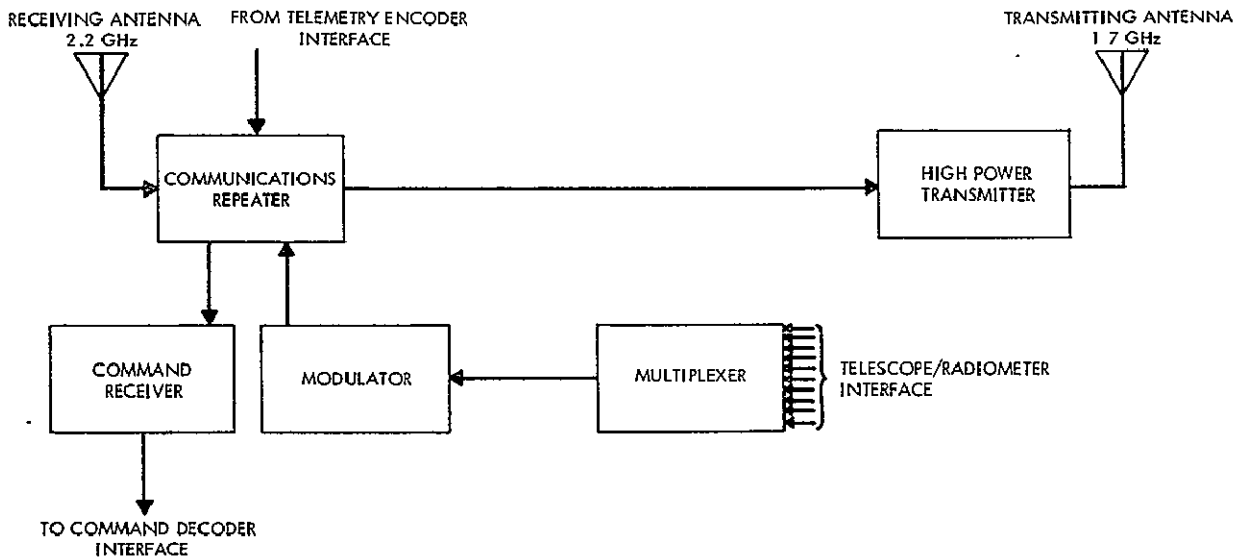
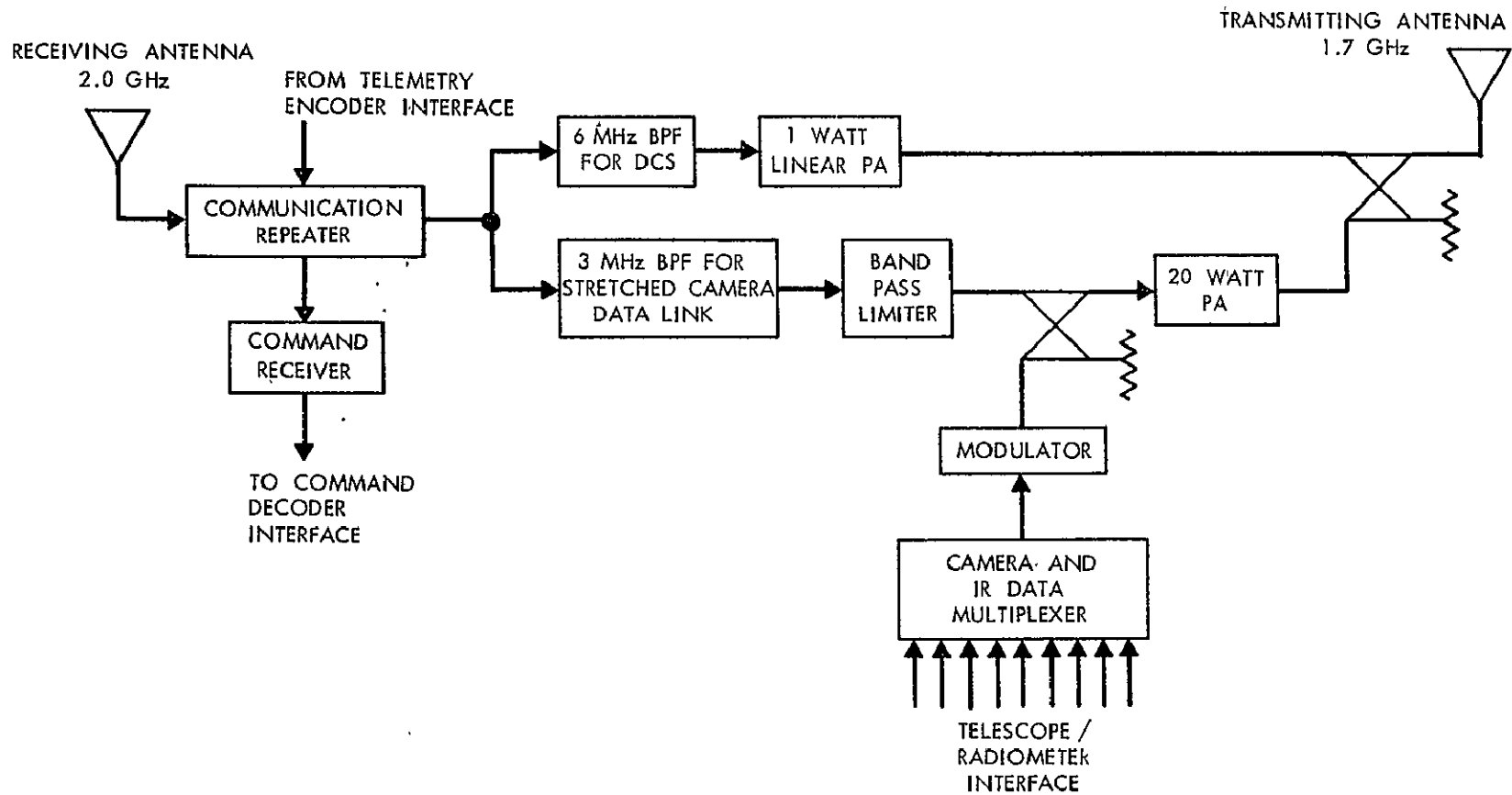


Figure V-48. Block Diagram of Spacecraft Communication Subsystem With Single S-band Transponder For DCS



V-192

Figure V-49. Block Diagram of All S-band Communication Transponder with Linear DCS Transmitter

Table V-27

SMS—Spacecraft Communication System Design Alternatives

S/C Design Approach	Advantages	Disadvantages
<p>Single-hard limited S-band transponder for both DCS and camera links</p>	<ol style="list-style-type: none"> 1. Cost is minimal 2. S/C primary power requirements minimal 3. Overall reliability maximized 4. Weight minimal 	<ol style="list-style-type: none"> 1. S/C EIRP is power shared between DCS and camera link 2. DCS SNR is degraded by at least 3db due to hard limited transponder 3. Not compatible with FDM multiplex techniques for DCS because of intermodulation due to hard limiting 4. 5% data loss due to 30 msec wideband camera transmission
<p>Single S-band transponder with separate 1 watt linear SHF transmitter for DCS</p>	<ol style="list-style-type: none"> 1. No hard limiter signal suppression 2. Increased DCS EIRP to permit operation with smaller ground stations 3. Compatible with other DCS modulation techniques such as FDMA. 1. } Same as above for 2. } alternative 2 3. } 	<ol style="list-style-type: none"> 1. Cost, weight and reliability all slightly worse than single transmitter SHF system 2. Not compatible with VHF or UHF DCS 3. 5% data loss due to 30 msec. wideband radiometer transmission
<p>Two transponder system: S-band for camera links VHF and/or UHF for DCS</p>	<ol style="list-style-type: none"> 4. From an overall DCS communications point of view this may yield the greatest channel capacity for a given system stability, EIRP, bandwidth, etc. 5. No data loss during 30 msec. camera transmission. 	<ol style="list-style-type: none"> 1. Cost, weight and reliability worst of the three alternatives considered

7.6 TELEMETRY AND COMMAND SUBSYSTEM

The telemetry and command (T&C) subsystem will be configured to operate in two different frequency bands, namely VHF and S-band. The VHF band will be utilized during the launch phase and the S-band when the spacecraft has attained synchronous orbit. The link calculations for the T&C subsystem are given in Tables V-28 and V-29 respectively.

7.6.1 Functions

In both frequency bands the T&C subsystem will perform the following functions:

- a. Receive, decode and enable execution of commands from ground stations.
- b. Encode and transmit data from spacecraft and space environment monitor subsystems.
- c. Radiate an unmodulated RF signal for tracking purposes.

In addition to the above the T&C subsystem will provide a transponder in the VHF band suitable for operation with Goddard Range and Range Rate systems as installed at STADAN tracking stations.

7.6.2 Channel Requirements

In order to provide the above functions the following channels will be required:

- a. Redundant telemetry transmission channels at both VHF and S-bands.
- b. Redundant command reception channels at both VHF and S-bands.
- c. Redundant ranging channels at VHF.

7.6.3 Equipment Required

The T&C subsystem will comprise the following redundant units:

- a. S-band receivers.
- b. VHF receivers.

Table V-28

Telemetry Subsystem Link Calculation

Frequency	<u>136.47 MHz</u>	<u>1700 MHz</u>
S/C Transmitter Power	33.0 dbm	*13.0 dbm
Diplexer and Line Losses	-4.0 db	-1.0
S/C Antenna Gain	-5.0 db	17.0
Path Loss	-167.5 db	-192.0 db
Ground Receiver Ant. Gain	18.0 db	44.5 db
Ground Receiver Losses	<u>-2.0 db</u>	<u>-1.0 db</u>
Received Carrier Power	-127.5 dbm	-119.5 dbm
Receiver Noise Temperature	435° K	25° K
Sidelobe Noise Temperature	65° K	75° K
Galactic Noise Temperature	<u>1200° K</u>	<u>--</u>
Total Receiving System Noise Temp.	1700° K	100° K
Total Receiving System Noise Temp.	32.3 db-°K	20.0 db-°K
Boltzmann's Constant	-198.6 dbm/Hz-°K	-198.6 dbm/Hz-°K
Noise Power Density	-166.3 dbm/Hz	-178.6 dbm/Hz
Carrier to Noise Density	38.8 db-Hz	59.1 db-Hz
Carrier to Noise Density at Threshold (SCO TLM)	<u>**38.0 db-Hz</u>	<u>38.0 db-Hz</u>
Margin	+0.8 db	+21.1 db
Carrier to Noise Density at Threshold (PCM TLM)	<u>35.0 db-Hz</u>	35.0 db-Hz
Margin	3.8 db	24.1 db

*Telemetry on beacon which is 30 db below full power output

**Telemetry Modes: PCM/PM Threshold at 35.0 db-Hz for error rate of 10^{-5} or less; FM/PM Threshold at 38 db-Hz for proper operation of ATS synchronous controller

***As indicated from the link calculations, real time SCO TLM is extremely marginal utilizing the VHF link and therefore will not be usable.

Table V-29

Command Subsystem Link Calculation

Frequency	<u>148.26 MHz</u>	<u>2000 MHz</u>
Transmitter Power	57.0 dbm	37.5 dbm
Transmitter Ant. Gain	11.0 db	44.5 db
Path Attenuation	-168.0 db	-192.0 db
S/C Antenna Gain	-5.0 db	+16.0 db
Passive Element Loss	-2.0 db	0.0 db
Polarization Loss	-3.0 db	0.0 db
System Operating Margin	<u>-3.0 db</u>	<u>-3.0 db</u>
Received Carrier Power	-113.0 dbm	-97.0 dbm
S/C Receiver Noise Temp.	29.3 db-°K	27.6 db-°K
Boltzmann's Constant	-198.6 dbm/Hz-°K	-198.6 dbm/Hz-°K
Bandwidth (19.7 kHz)	43.0 db-Hz	43.0 db-Hz
Received Noise Power	-126.3 dbm	-128.0 dbm
Command Receiver Threshold	-118.0 dbm	-119.7 dbm
Signal Margin Over Threshold	5.0 db	22.7 db
Carrier To Noise Ratio	13.3 db	31.0 db

Modulation	FSK/AM/AM
Frequency	7.4 kHz - Binary 0 8.6 kHz - Binary 1 5.79 kHz - Execute Tone
Bit Rate	128 BPS

For Error Rate of 10^{-5} , $\frac{E_o}{N_o} \simeq \frac{C_o}{N_o} = 13.4 \text{ db}$

- c. S-band transmitters.
- d. VHF transmitters.
- e. Telemetry encoders.
- f. Command decoders.
- g. Ranging interconnection units.
- h. VHF antenna unit.
- i. S-band antenna unit.

7.6.4 Configurations Required

The need to provide the functions listed above with a high degree of reliability leads to the following required configurations:

- a. Either telemetry encoder to either VHF and S-band transmitter.
- b. Either command decoder to either VHF and S-band receiver
- c. Each VHF receiver to a VHF transmitter.

7.6.5 T and C Ground Communication Link

A ground communications link is required which will enable real-time interchange of commands and PCM telemetry data between the ESSA Satellite Operations Control Center and the CDA station. This will provide the means for automation of the display and verification of command functions which are presently performed manually in the ATS system. Also PCM housekeeping telemetry can be processed more thoroughly in real-time with the data processing capability currently available at the central data processing facility.

7.6.6 S-Band T and C Equipment

The S-band command will be transmitted from the CDA station utilizing the same modulation and code format as the VHF command. The signal will be received at a nominal 4.9 MHz above the main up-link carrier and will be demodulated in a separate command receiver although it may share the S-band antenna and RF amplifier with the stretch signals (and interrogation and report signals if only one transponder is used).

The (nominal) 1700 MHz telemetry signal will be transmitted at the lower end of the down-link transmission spectrum. The level of the telemetry carrier will be 30 db below the full output of the transmitter. A 10.5 kHz sub-carrier oscillator (SCO) will phase modulate the telemetry carrier for the purpose of transmitting sun pulses, jet firings, apogee motor squib firing, execute tone pulses as well as other data. The telemetry carrier will be derived from an independent oscillator and summed into the antenna.

7.6.7 General Specifications

The following paragraphs delineate the specifications of the spacecraft telemetry and command system encoder and decoder. Tables V-28 and V-29 give the RF link requirements for the telemetry and command systems. As indicated, the VHF system is close to being marginal whereas the SHF system would be much more reliable.

7.6.7.1 Telemetry Encoders—The two redundant telemetry encoders will each consist of the following units:

- a. One 64 channel main multiplexer
- b. One 64 channel submultiplexer
- c. One 32 channel submultiplexer
- d. One subcarrier oscillator (SCO)
- e. One stable-voltage reference
- f. One PCM processor

Main Multiplexer. The 64 9-bit channels will be allocated as follows:

<u>Allocation</u>	<u>No. of Channels</u>
Frame Synchronization	3
Encoder Mode Identification	1
Submultiplexer Position Identification	1
Calibration Reference	1
64 Word Submultiplexer	1
32 Word Submultiplexer	1
Analog and Digital Data	57

PCM Processor - The PCM processor will contain a bit frequency oscillator, an analog-to-digital converter, and digital input gates. Analog data will be quantized to nine bits. Manchester coding will be utilized.

Bit Rate	194.18 bits/second
Word Length	9 bits
Frame Synchronization	27 bits
000 110 010 011 111 000 101 011 010	
Word Synchronization	Not Used
Output	Split Phase (Manchester Coding) (Binary zero equals 0,1 and binary one equals 1, 0)

Subcarrier Oscillator (SCO) - The subcarrier oscillator will operate at a frequency of $10.5 \text{ kHz} \pm 7.5\%$ (IRIG Channel 12). The SCO will provide capability for transmitting the following real time spacecraft data:

- a. Sun pulses (two groups)
- b. Jet firings (two groups)
- c. Apogee motor squib firing
- d. Execute tone pulse
- e. Other spacecraft data to be specified

Since the jet firings and apogee motor firing will occur at widely separate times, the frequency chosen for the apogee motor firing may be within the frequency band assigned to the jet firings.

Encoder Output Switching Unit - A switching unit will be provided to switch the outputs of the telemetry encoder (PCM and SCO) to either of the VHF transmitters or the S-band transmitters by ground command.

7.6.7.2 Command Decoders

Two redundant command decoders will be provided. Either decoder will receive the audio output signal of any of four command receivers (VHF and S-band) and generate command signals to all required circuitry.

Operating Mode - The command decoder will operate in a shift mode (shifting bits received serially into the command register). This mode will operate from a non-return-to-zero (NRZ) format, frequency-shift keyed (FSK) digital wave train. The bit synch, which will 50 percent amplitude modulate the "zero" or "one" tones, will be a 128 Hz sine wave, whose 0° crossing will be the transition between data bits.

Input Signals - The command system will be designed for data bit frequencies of 7400 cps for a "0" bit and 8600 cps for a "1" bit and an execute frequency of 5790 cps ± 0.2 percent.

Format - The command system will be designed for a command format consisting of the following major subdivisions:

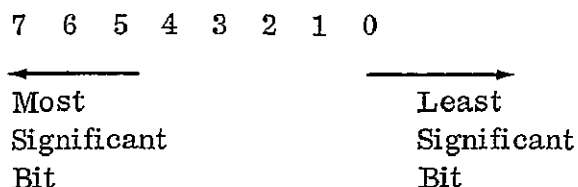
- a. Introduction
- b. Word Sync
- c. Address
- d. Command Number

The address and command will each be an 8-bit word.

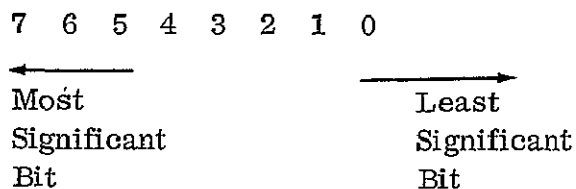
(a) Introduction. The purpose of the Introduction is to provide time to select and prepare the decoder for operation. The Introduction will be at least 27 bit times of "zero" or "one" tone.

(b) Word Sync. A Word Sync will be used to define the start time for the command that follows. The Word Sync will be a "one" followed by a "zero."

(c) Address. After the Word Sync, the next 8 bits of the command message will address a spacecraft and a specific command decoder. The format will be as follows:



(d) Command Number.- The second group of 8 bits of the command message will consist of the command number. The format will be defined as follows:



Operating Constraints

Execute. The execute tone will be processed in real time.

Inoperative. The execute channel will be held inoperative by a continuous "zero" tone.

Decoder Input Cross-Connecting Unit. A unit will be provided with cross-connecting facilities which will ensure that any receiver (VHF and S-band) is able to activate either decoder.

NOTE: The accent in the design of this will be on maximum reliability. Switching will not be utilized in this unit.

7.7 STABILIZATION & CONTROL

The stabilization and control system is used for active nutation control; injection velocity correction; coarse attitude control; station acquisition; station keeping (East-West and North-South, if required); station changing; spin-speed control; fine attitude control; and passive nutation damping.

7.7.1 Propulsion System

The propulsion system is used for the above listed functions. It is similar to the ATS system and will consist of two separate independent, essentially identical, systems using neat hydrazine as a propellant and nitrogen as a pressurant.

Each system has two valve-controlled thrusters that use Shell 405 catalysts to convert the hydrazine to gas at the nozzle. Their maximum thrust is 5 pounds. Each of the two systems has the capacity to hold approximately 36 lbs of hydrazine to give a minimum total impulse of 8000 lb-seconds at an Ips of 222 seconds. The total impulse of both systems is therefore at least 16,000 lb-seconds.

Each hydrazine reaction control system consists of the following components:

- a. Two spherical pressurized propellant tanks mounted 180 degrees apart.
- b. One nitrogen charge and vent fitting.
- c. One hydrazine fill and drain fitting.
- d. One low thrust hydrazine thrust chamber (with integral heat barrier tube and propellant control valve) thrusting parallel to the spacecraft spin axis.
- e. One low thrust hydrazine thrust chamber (with integral heat barrier tube and propellant control valve) thrusting normal to the spin axis and through the spacecraft center of gravity.
- f. One pressure transducer.
- g. Two redundant thermistors sensing propellant tank temperature of one of the tanks.

- h. Propellant filters as necessary.
- i. Associated manifolding and mounting clamps as required.

The system components, except for the thrust chambers, are welded together as an integral system to minimize leakage. The thrust chambers are downstream of the propellant control valves and, therefore, have no effect on system leakage.

For simplicity, light weight, and reliability, the propellant feed is designed to operate at an unregulated pressure as a blowdown system. The tanks are bladderless, since expulsion of the propellants and gas separation are aided by the centrifugal force created by the spacecraft spin. All components that can contact the contained hydrazine shall be of materials that will not contaminate the hydrazine or suffer corrosion by hydrazine or water or carbon dioxide combined with the hydrazine for a period of 5 years.

Before operation, each system is loaded with about 36 pounds of hydrazine. The tanks approximately 65 percent full, are pressurized with nitrogen to 200 psia. The mission operating sequence is as follows:

- a. The system will be armed as soon as the tanks are pressurized with nitrogen.
- b. The desired thrust chamber will be actuated by a command signal from ground control equipment.
- c. Continuous or pulse mode operation of either thrust chamber will be actuated by either a continuous or a pulsed command signal for the desired period of time.
- d. Cessation of electrical power to the propellant on-off valves will result in closure of the valves and shutdown of the thrust chambers.

At the completion of the sequence, the control system will remain in a pressurized and ready state.

The allotment of the 16, 000 lb-sec available total impulse will be as follows for a 550 lb S/C.

- a. Adjustment of Delta injection velocity errors, 75 ft/sec 1,275 lb-sec

b. 180° S/C reorientation, 100 rpm, 60 ft/sec	1,170 lb-sec
c. E-W Stationkeeping, 5 year, 7 ft/sec/yr	595 lb-sec
d. Automatic Nutation control to orbit 6 apogees; 55 hrs; 20-6 sec pulses/hr	3,300 lb-sec
e. Station relocation, twice, 30 ft/sec	1,020 lb-sec
f. Attitude trim. 5 years	250 lbs-sec
g. North-South Stationkeeping, 2.8 year 175 Ft/Sec/Yr	<u>8,390 lb-sec</u> 16,000 lb-sec

It should be noted that the weight available will determine the exact amount of fuel loaded on the spacecraft. This amount in turn will determine how long north-south station keeping will be possible.

7.7.2 Active Nutation Control

During the transfer orbit, prior to apogee motor ejection, the spacecraft spins about an axis of minimum moment of inertia and thus does not have long term spin-axis stability. Passive energy dissipation, as in nutation damping, fuel sloshing, and structural damping, results in a buildup of nutation in order to conserve angular momentum. To hold down the rate of nutation buildup, the primary source of energy dissipation (the mercury nutation damper) is caged during the transfer orbit. With the caged damper, many hours are required for the dissipation of sufficient energy to cause the large nutation angles; although without control, the nutation angle could build up to an objectionable value (2 to 4 degrees) at apogee engine firing. In order to ensure an adequately small nutation angle throughout the transfer orbit phase of the mission, active nutation control capability has been included to remove nutation by ground command whenever required.

Insofar as the spacecraft subsystems are concerned, active nutation control capability is implemented by providing an accelerometer (two for redundancy) which measures axial acceleration (acceleration parallel to the spin axis) resulting from spacecraft nutation. Nutation may be described as a "coning" or wobble of the spin axis around the inertially fixed angular momentum vector.

The nutational motion gives rise to a sinusoidally varying axial acceleration which can be readily sensed by a linear accelerometer mounted near the

outer periphery of the spacecraft. The accelerometer output is telemetered to the ground station and defines the transverse component of angular momentum at any instant. With this knowledge, properly phased axial jet pulses may be commanded to remove the transverse component of angular momentum, thus reducing the satellite motion to one of simple spin about the spin axis.

Operation of the active nutation control system is summarized below. The telemetered accelerometer output is tracked in the ground station. The required time delay between accelerometer descending zero crossing and jet command is manually introduced. A series of axial jet pulses is then commanded, each pulse having spin period duration and being separated from the preceding pulse by the nutation period. Each pulse reduces the transverse angular momentum by given increment until the nutation (accelerometer output) becomes suitably small. Only about six pulses are required to reduce 2 degrees of nutation angle to less than 0.1 degree.

This system may also be activated by an onboard feedback system that is set to trigger axial jet pulses at the proper phase relation to drive the accelerometer back to zero when the output of the accelerometer exceeds a pre-set level.

7.7.3 Passive Nutation Damper

This unit consists of a gas filled tube approximately one inch in diameter and two feet long. Attached to it is a small reservoir containing about 1.5 lbs of mercury. The mercury is retained in the reservoir by a pyrotechnic valve. The tube is located parallel to the spin axis, outboard on the spacecraft. The reservoir is located inboard.

When it is desired to uncage the damper the pyrotechnic valve is fired by ground command, the mercury runs into the tube to fill it about 25% and damping is produced by sloshing and surface waves. Damping can be optimized by tuning the damper dimensions to spacecraft size and spin rate.

7.7.4 Spacecraft Spin Control

Spin control on SMS will be effected simply by giving all on-board orbital velocity control jets a fixed misalignment bias such that their alignment bias given to each jet will be in the range of 0.5 degree. With such a despin bias in jet alignment, spin control is accomplished, when required, by inducing an appropriate amount of nutation which, upon being damped out by the passive nutation damper, results in an increase in spin. This spin increase is due to the fact that, in the process of damping the energy of nutation while conserving

angular momentum, a significant portion of the nutational angular momentum is transferred to spin axis angular momentum.

The process of inducing nutation (or "wobble", as it is sometimes called) is quite simple. A train of axial jet pulses is sent by ground control, each pulse being one spin period in duration and separated from the preceding pulse by the nutation period. The effect of such a series of pulses is to induce or create transverse angular velocity in an optimum fashion so that the spacecraft nutates or wobbles. In this process, transverse angular momentum has been increased while spin axis angular momentum remains unchanged. The spin axis is now generating a cone whose axis is the original angular momentum vector. Now as the nutation is damped, the spin axis finally coincides (very closely) with its original attitude, and the spin has increased to correspond to the higher total angular momentum.

Thus, with an effective means available for spin increase, it remains to provide assurance that the spin cannot become too great. (Nutation spin control is unidirectional; despin cannot be effected through nutation.) Such assurance is provided by giving the jets a despin alignment bias so that a worst-case situation of misalignment tolerances will not result in excessive spin. The spin is therefore bounded by some upper limit fixed by the bias and by any lower limit desired.

7.7.5 Fine Attitude Control

The attitude of the spacecraft spin axis relative to the orbit plane can be controlled by the hydrazine jets to a maximum precision of .05 degree (180 arc seconds). It is necessary to have a fine attitude control system with much finer pulse increments. The spacecraft attitude requirements as a function of picture resolution are given in Table V-30.

An acceptable fine propulsion system is a pulsed plasma jet using teflon or other fuel. Such a system was flown successfully on the LES-6 spacecraft. For SMS, two pulse plasma thruster units would be required, placed 180° apart on the spacecraft. Each unit should contain .2 lb of fuel, which will give 60 lb-sec of impulse at a specific impulse of 300 seconds. Power to each unit should not exceed 3.0 watts while pulsing once every other revolution. Weight of each unit should not exceed 4 pounds, including fuel and power conditioning. Each unit should produce at least 6 micro-pound-seconds of impulse with each pulse. 280 of these pulses would precess the spacecraft spin axis by one arc-second. The pulse centroid is highly repeatable.

Table V-30

SMS Spacecraft Attitude Requirements versus Resolution

	1/2 n. m.	1 n. m.	2 n. m.
S/C Position, maximum distance from selected nominal sub-satellite point, orbit degree	±0.1	±0.1	+0.1
S/C Position, maximum deviation of perpendicularity of spin axis to orbit plane, (line tilt of earth image shall be no greater than 1/2 line width) arc second	±15	±30	±60
Change of S/C sub-satellite position, maximum rate per day, orbital degrees	.012	.025	.050
Change of spin axis position, maximum rate per day, arc seconds (ATS I uncorrected rate = 10 sec per day)	2.5	5	10
Nutation and Jitter of S/C During one picture period. (Telescope allowed equal amount additional) arc seconds	0.8	1.6	3.3

7.7.6 Stabilization and Control General

The stationkeeping and attitude control maneuvers will be pre-calculated at the ESSA Satellite Operations Control Center and commanded from the CDA station. This will require that considerable ranging data be made available to the central data processing facility at Suitland. Historical maneuvering data will also have to be considered in maneuver planning. The frequency of these maneuvers will not be known until after the launch of the spacecraft. Thus, the impact on data processing capability is unknown, but it could be considerable.

7.8 APOGEE MOTOR

The apogee motor will be a "stretched" version of an existing qualified apogee motor. Stretching is accomplished by adding a cylindrical insert to the spherical propellant storage tank. This provides an increased fuel carrying capability without major motor redesign. The fuel loading will be determined by launch vehicle capability and by spacecraft weight. When proper orbit is achieved the apogee motor will be jettisoned from the spacecraft.

7.9 SPACECRAFT INTEGRATION AND TEST

The sensors and spacecraft subsystems will be integrated and tested according to techniques established on the ATS and other programs.

The integrated spacecraft weight, including apogee motor and adapter, will be approximately 1000 lb of which 120 lb is allocated for the radiometer/telescope.

The objectives of the test program are to prove the ability of the spacecraft design to meet all performance requirements, and to demonstrate the dependability of the flight hardware. The performance requirements will be demonstrated by system tests performed according to approved system test procedures. A quality assurance and reliability program together with flight hardware acceptance testing will assure the dependability of the flight hardware.

8. LAUNCH REQUIREMENTS

8.1 LAUNCH VEHICLE

The SMS spacecraft will be launched by a long tank Delta M-6 launch vehicle. The three-stage launch vehicle has an overall length of approximately 106 feet and a maximum body diameter of 8 feet. The nominal launch weight is 231,000 pounds. The Delta launch vehicle is a reliable, low-cost vehicle with a success-to-launch ratio of over 90 percent for the past 7 years. A brief description of the vehicle's major characteristics follows. (See Figure V-50.)

8.1.1 First Stage

The first stage is a McDonnell Douglas Astronautics Company (MDAC) modified Thor (DSV-2L-1B) booster incorporating either six Castor II (TX33-52 solid-fuel) rocket motors. The booster is powered by an MB3, Block III, Rocketdyne engine using liquid oxygen (lox) and liquid hydrocarbon propellants. The main engine is gimbal-mounted to provide pitch and yaw control from lift-off to main engine cutoff (MECO). Two liquid-propellant vernier (XLR-101-NA-11) engines provide roll control throughout first-stage operation and pitch and yaw control from MECO to first stage separation.

8.1.2 Second Stage

The second stage (DSV-3E-4) is powered by an Aerojet General Corporation AJ10-118-E liquid-fuel, pressure-fed engine employing inhibited red fuming nitric acid (IRFNA) and unsymmetrical dimethylhydrazine (UDMH) propellants. The second-stage main engine is also gimbal-mounted to provide pitch and yaw control through second-stage burn. A nitrogen gas system using eight fixed nozzles provides roll control during powered and coast flight as well as pitch and yaw control after second-stage cutoff (SECO). Two fixed nozzles fed by the propellant tank helium pressurization system provide retrothrust after third-stage separation.

8.1.3 Third Stage

The third stage is the TE-364-4 spin-stabilized solid-propellant motor manufactured by the Thiokol Chemical Corporation (TCC). The third-stage motor is secured in a spin table mounted to the second stage. The firing of two to eight solid propellant rockets fixed to spin table accomplishes spinup of the third-stage assembly.

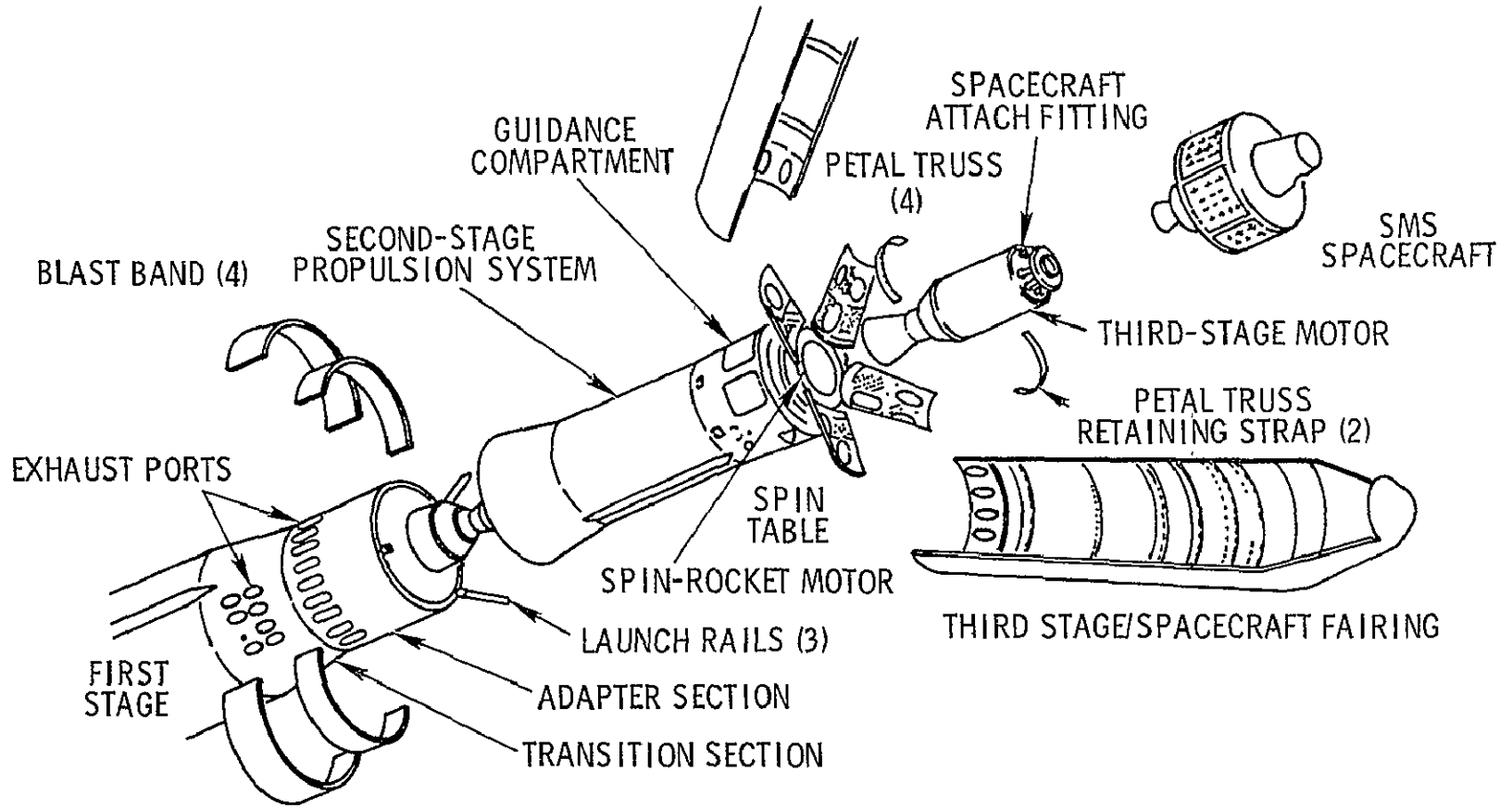


Figure V-50. Delta M-6 Launch Vehicle-Spacecraft Separation Schematic

8.1.4 Attach Fitting

The SMS spacecraft is attached to the launch vehicle by means of the 8 × 9 conical attach fitting, which in turn is secured to the spin-table assembly mounted to the second stage. The firing of from two to eight solid-propellant rockets fixed to the spin table accomplishes spin-up before spacecraft separation.

8.1.5 Fairing

The standard Delta fairing (DSV-3E-7) will be used. It is 224 inches long and 65 inches in diameter and is attached to the forward face of the second stage. This fairing, which protects the spacecraft from aerodynamic heating during the boost flight, is jettisoned as soon as the vehicle leaves the sensible atmosphere shortly after second-stage ignition.

8.1.6 Guidance and Control

Preprogrammed autopilots control the vehicle and the sequence of operations from lift-off to third-stage separation. The autopilots supply discrete steering commands and flight-sequence signals. Between second-stage ignition and third-stage separation, up to three pitch rates and two yaw rates can be obtained by the five steering commands. Third-stage attitude is effected by second-stage pitch and yaw maneuvers during the coast period.

A Western Electric Company (WECO) ground radio-command guidance system is used to correct trajectory deviation from about 90 seconds after lift-off until the tracking radar horizon is reached. Before ground guidance is terminated, an integrating accelerometer on the second stage is actuated to command SECO.

8.2 LAUNCH OPERATIONS

GSFC Operations Control (OPSCON) will conduct ground communications operations for launch. The SMS project manager will direct all mission operations from the GSFC Mission Control Room (MCR) in GSFC building 14.

8.2.1 Launch Site

All launchings will proceed from the Eastern Test Range (ETR) facility at Cape Kennedy.

8.2.2 ETR Launch Facilities

The ETR, formerly called the Atlantic Missile Range, contains the John F. Kennedy Space Center (KSC). The Unmanned Launch Operations (ULO) Directorate of KSC provides NASA management for ETR launches and represents the project in all dealings with the range manager. The Air Force Missile Test Center (AFMTC), headquartered at Patrick Air Force Base (PAFC), operates the ETR and is the Air Force Agency responsible for providing and coordinating the services needed to support ETR launches.

The ETR facilities used for a Delta launch include the spacecraft laboratory, launch complex 17, and range tracking facilities. The spacecraft laboratory includes receiving spacecraft storage, spacecraft laboratory rooms, spacecraft telemetry laboratory, and engineering offices. A line-of-sight antenna tower is interconnected with receivers and recorders in the lab. Launch complex 17 consists of launch pads 17A and 17B, gantries, a blockhouse, and an administration and engineering building used by DAC, Aerojet, and NASA personnel concerned with launch operations.

8.2.3 Range Support Office

The range support office (RSO) provides contact with NASA elements for range user functions and relationships, and provides coordination for NASA elements in common areas of range support. The RSO receives and distributes all range processed test data, and represents the project in all pre- and post-operation briefings, debriefings and critiques related to range support.

8.2.4 NASA Project Office

Each NASA element, resident or nonresident, conducting activities that involve the ranges may either establish a project or mission office in the RSO, with personnel detailed to the office; or delegate the responsibility to ETRO. Project office personnel detailed to the RSO will represent their projects or missions in all negotiations with the range. These range contacts will be subject to basic RSO policy constraints.

8.2.5 Delta Operations Branch

The Delta Operations Branch provides vehicle technical management of the NASA Delta launch programs, verifying that vehicle systems and supporting aerospace ground equipment are acceptable to NASA launch standards. The Delta Operations Branch reviews all vehicle test procedures and related documents for conformance to system specifications and monitors all testing to

ensure compliance with accepted test and safety procedures. In addition, the branch technically reviews any failure or compromise of system or component integrity to determine the best resolution of the problem. This resolution is coordinated with the vehicle contractor. After launch, the branch reduces and analyzes flight performance data for the flight report.

8.3 GO/NO-GO VAN

In addition to the fixed facilities at the ranges, a go/no-go van will be used for prelaunch and launch checkout of the spacecraft.

8.4 LAUNCH PARAMETERS

The SMS will be launched from ETR (Cape Kennedy) at a launch azimuth of approximately 90 degrees. The launch window will be selected when all parameters affecting the launch are defined.

8.5 LAUNCH AND TRAJECTORY

The modified Thor booster burn and DSV-3E-4 second stage burn place the spacecraft in a trajectory for the short coast to the first equatorial crossing at a nominal 100 nautical mile altitude in a plane inclined 33 degrees to the equatorial plane. Immediately prior to third stage ignition and second stage separation at the first equatorial crossing, solid rocket motors attached to the adapter section spin up the combined third stage, apogee motor and spacecraft to approximately 100 rpm.

Third stage burn results in spacecraft injection into a transfer orbit with an apogee of 19,350 nautical miles and an inclination of 33 degrees.

Following injection into transfer orbit, a spring-ejecting mechanism separates the spacecraft and apogee motor from the third stage. Spin-stabilization will maintain the spacecraft attitude during the coast-to-second-apogee period.

During the coast phase, accelerometers will provide nutation sensing. Sun sensors and RF polarization will provide attitude information. Hydrazine thrusters will provide active nutation damping and attitude corrections. The coast period is sufficient to obtain orbital data and make necessary vernier attitude corrections before apogee-motor ignition.

The apogee motor is fired at second apogee to provide the necessary plane change and circularize the orbit.

APPENDIX A

LINK CALCULATIONS FOR VARIOUS SOMS/GOES DATA COLLECTION CONFIGURATIONS

The five feasible configurations of the SOMS/GOES DCS which are shown in Figure A-1 are:

- a) Single transponder—VHF
- b) Single transponder—UHF
- c) Single transponder—S-band
- d) Cross-strapped transponder—S-band/VHF
- e) Cross-strapped transponder—S-band/UHF

The following parameters will be assumed in the link calculations provided in Tables A-1 through A-10:

Path Lengths:

CDA (Wallops Island, 7.3° off beam center)—23,800 s.mi.

S/C to DCP (8.5° off beam center)—25,700 s.mi.

CDA Station:

S-band: Antenna—40' diameter parabola
Net Gain at 2.0 GHz—45.5 db
Net Gain at 1.7 GHz—44.1 db
Transmitter—1 watt
Receiver noise temperature—100°K (20 db-°K)

UHF: Antenna—net gain 24.2 db
Transmitter—10 watts
Receiver noise temperature—200°K (23 db-°K)

VHF: Antenna—net gain 14.0 db
Transmitter—10 watts
Receiver noise temperature—1250°K (31 db-°K)

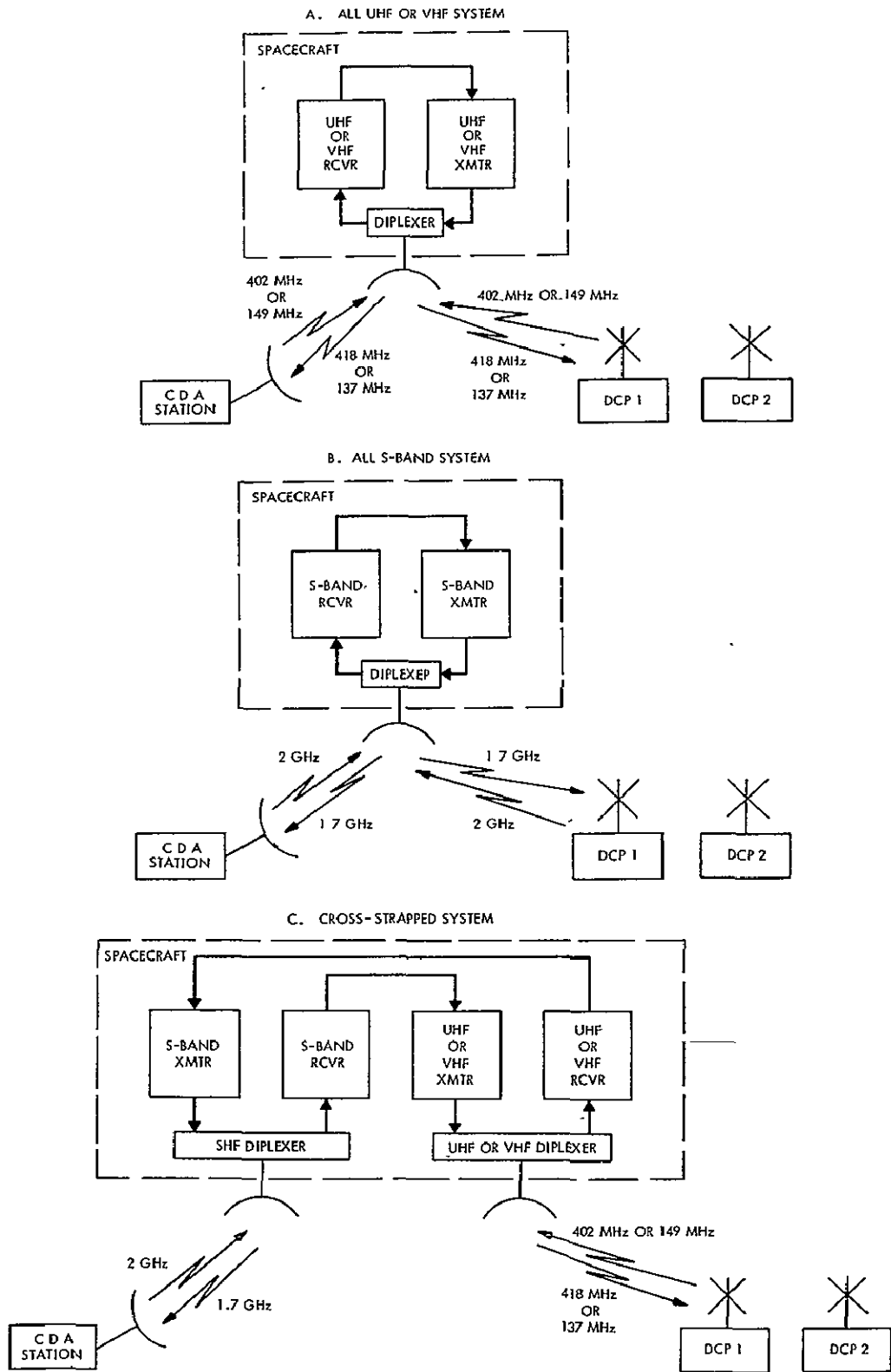


Figure A-1. Alternative Configurations of Data Collection Systems Considered in SOMS and GOES Studies

DCP:

Antenna—net gain 3.0 db (all bands)

Transmitter—10 watts (all bands)

Receiver noise temperatures—UHF 380°K (25.8 db-°K)
VHF 500°K (27.0 db-°K)
S-band 610°K (27.8 db-°K)

Spacecraft:

Total transmitter power—20 watts

Antenna:

VHF and UHF—net gain 10.5 db

1700 MHz—

gain = 18.0 db

losses = 1.5 db

off-beam center loss (Wallops Island) = 3.0 db

off-beam center loss (8.5° off beam) = 4.5 db

net gain at CDA Station (Wallops Island) = 13.5 db

net gain at DCP = 12.0 db

2000 MHz—

gain = 18.5 db

loss = 1.0 db

off-beam center loss (Wallops Island) = 3.0 db

off-beam center loss (8.5° off beam) = 6.0 db

net gain at CDA station (Wallops Island) = 14.5 db

net gain at DCP = 11.5 db

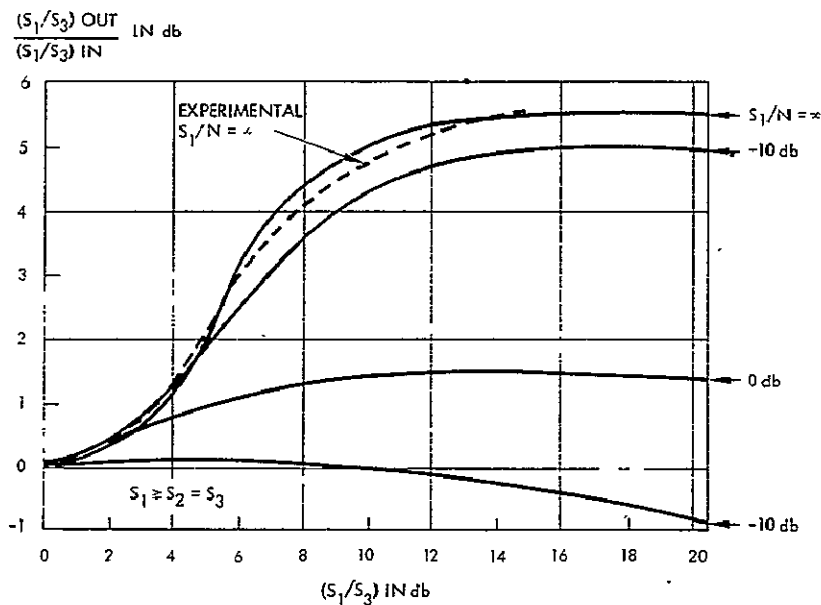
Receiver noise temperatures—UHF 690°K (28.4 db-°K)
VHF 1250°K (31.0 db-°K)
S-band 590°K (27.7 db-°K)

Communications Channels:

The interrogation signal is assumed to be transmitted from the CDA station as a DSBSC signal as discussed in Section 4.2.1. As indicated in the traffic analysis Section, 4.1.1, two interrogations and two reports must be relayed simultaneously by the spacecraft in order to clear all the traffic at the desired bit rate. In the single-band systems three carriers, one interrogation and two

reports, share the power of the hard-limited transponder. The presence of the larger interrogation signal will cause a suppression of each of the smaller signals with respect to the amplitude ratios at the input. The amount of signal suppression can be read off the curves in Figure A-2. In the case of the cross-strapped systems the interrogation and reporting signals are segregated and the limiter suppression occurs between the two reporting signals. However, by assuming a maximum margin of -3db in the level of the DCP signal at the spacecraft, the maximum disparity between the two DCP signals entering the repeater is also fixed at 3db. Jones¹ has shown that for large signal-to-noise ratios, the 3db power disparity at the input results in a maximum small signal suppression of 4.1 db at the output of the limiter.

In all cases the output signal-to-noise ratio is computed in a 100 Hz bandwidth (75bps) and a 3db modulation loss is incurred in the interrogation links due to each DCP processing only one of the two pairs of sidebands. The required carrier-to-noise ratio is 9.5 db which corresponds to a 10^{-5} probability of error for coherent PSK modulation.



(From Shaft, P.D. "Limiting of Several Signals and its Effect on Communication System Performance")

Figure A-2. Three Signal Suppression

¹J. J. Jones, "Hard-Limiting of Two Signals in Random Noise," IEEE Transactions on Info. Theory, Jan. 1963.

Table A-1

All UHF System

CDA-to-S/C Link 402 MHz

Ground Transmitter Power	40.0	dbm
Ground Antenna Gain	14.0	db
Free Space Loss	-176.7	db
Spacecraft Antenna Gain	10.5	db
Margin	<u>- 3.0</u>	db
Received Carrier Power at S/C	-115.2	dbm
S/C Receiver Noise Temperature	28.4	db-°K
Boltzmann's Constant	<u>-198.6</u>	dbm/Hz-°K
S/C Noise Power Density	-170.2	dbm/Hz
Up-link Carrier-to-Noise Density	55.0	db-Hz

S/C-to-DCP Link 418 MHz

S/C Transmitter Power	43.0	dbm
S/C Antenna Gain	10.5	db
Free Space Loss	-177.3	db
Ground Receiver Antenna Gain	3.0	db
Modulation Loss	<u>- 3.0</u>	db
Received Carrier Power	-123.8	dbm
Ground Receiver Noise Temperature	25.8	db-°K
Boltzmann's Constant	<u>-198.6</u>	dbm/Hz-°K
Ground Receiver Noise Power Density	-172.8	dbm/Hz
Down-link Carrier-to-Noise Density	49.0	db-Hz
Overall Carrier-to-Noise Density	48.0	db-Hz
Bandwidth	20.0	db-Hz
Overall Carrier-to-Noise Ratio	28.0	db
Required Carrier-to-Noise Ratio	9.5	db
System Margin	18.5	db

Table A-2

All UHF System

DCP-to-S/C Link 402 MHz

Ground Transmitter Power	40.0	dbm
Ground Antenna Gain	3.0	db
Free Space Loss	-177.0	db
Spacecraft Antenna Gain	10.5	db
Margin	<u>- 3.0</u>	db
Received Carrier Power at S/C	-126.5	dbm
S/C Receiver Noise Temperature	28.4	db-°K
Boltzmann's Constant	<u>-198.6</u>	dbm/Hz-°K
S/C Noise Power Density	-170.2	dbm/Hz-°K
Up-link Carrier-to-Noise Density	43.7	db-Hz

S/C-to-CDA Link 418 MHz

S/C Transmitter Power	43.0	dbm
Loss due to limiter suppression	- 5.0	db
Power disparity between interrogation and reporting signals	- 11.5	db
Radiated Power for each DCP	26.5	dbm
S/C Antenna Gain	10.5	db
Free Space Loss	-177.0	db
Ground Receiver Antenna Gain	<u>24.2</u>	db
Received Carrier Power	-115.8	dbm
Ground Receiver Noise Temperature	23.0	db-°K
Boltzmann's Constant	<u>-198.6</u>	dbm/Hz-°K
Ground Receiver Noise Power Density	-175.6	dbm/Hz
Down-link Carrier-to-Noise Density	59.8	db-Hz
Overall Carrier-to-Noise Density	43.6	db-Hz
Bandwidth	20.0	db-Hz
Overall Carrier-to-Noise Ratio	23.6	db
Required Carrier-to-Noise Ratio	9.5	db
System Margin	14.1	db

Table A-3

All VHF System

CDA-to-S/C Link 149 MHz

Ground Transmitter Power	40.0	dbm
Ground Antenna Gain	14.0	db
Free Space Loss	-168.0	db
Spacecraft Antenna Gain	10.5	db
Margin	<u>- 3.0</u>	db
Received Carrier Power at S/C	-106.5	dbm
S/C Receiver Noise Temperature	31.0	db-°K
Boltzmann's Constant	<u>-198.6</u>	dbm/Hz-°K
S/C Noise Power Density	-167.6	dbm/Hz
Up-link Carrier-to-Noise Density	61.1	db-Hz

S/C-to-DCP Link 137 MHz

S/C Transmitter Power	43.0	dbm
S/C Antenna Gain	10.5	db
Free Space Loss	-167.6	db
Ground Receiver Antenna Gain	3.0	db
Modulation Loss	<u>- 3.0</u>	db
Received Carrier Power	-114.1	dbm
Ground Receiver Noise Temperature	27.0	db-°K
Boltzmann's Constant	<u>-198.6</u>	dbm/Hz-°K
Ground Receiver Noise Power Density	-171.6	dbm/Hz
Down-link Carrier-to-Noise Density	57.5	db-Hz
Overall Carrier-to-Noise Density	55.9	db-Hz
Bandwidth	20.0	db-Hz
Overall Carrier-to-Noise Ratio	35.9	db
Required Carrier-to-Noise Ratio	9.5	db
System Margin	26.4	db

Table A-4

All VHF System

DCP-to-S/C Link 149 MHz

Ground Transmitter Power	40.0	dbm
Ground Antenna Gain	3.0	db
Free Space Loss	-168.3	db
Spacecraft Antenna Gain	10.5	db
Margin	- 3.0	db
Received Carrier Power at S/C	-117.8	dbm
S/C Receiver Noise Temperature	31.0	db- °K
Boltzmann's Constant	-198.6	dbm/Hz- °K
S/C Noise Power Density	-167.6	dbm/Hz- °K
Up-link Carrier-to-Noise Density	49.8	db-Hz

S/C-to-CDA Link 137 MHz

S/C Transmitter Power	43.0	dbm
Loss due to limiter suppression	- 5.0	db
Power Disparity between interrogation and reporting signals	- 11.3	
Radiated Power for each DCP	26.7	dbm
S/C Antenna Gain	10.5	db
Free Space Loss	-167.3	db
Ground Receiver Antenna Gain	14.0	db
Received Carrier Power	-116.1	dbm
Ground Receiver Noise Temperature	31.0	db- °K
Boltzmann's Constant	-198.6	dbm/Hz- °K
Ground Receiver Noise Power Density	-167.6	dbm/Hz
Down-link Carrier-to-Noise Density	51.5	db-Hz
Overall Carrier-to-Noise Density	47.6	db-Hz
Bandwidth	20.0	db-Hz
Overall Carrier-to-Noise Ratio	27.6	db
Required Carrier-to-Noise Ratio	9.5	db
System Margin	18.1	db

Table A-5

All S-Band System

CDA-to-S/C Link 2.0 GHz

Ground Transmitter Power	30.0	dbm
Ground Antenna Gain	45.5	db
Free Space Loss	-190.7	db
Spacecraft Antenna Gain	14.5	db
Margin	<u>- 3.0</u>	db
Received Carrier Power at S/C	-103.7	dbm
S/C Receiver Noise Temperature	27.7	db- °K
Boltzmann's Constant	<u>-198.6</u>	dbm/Hz- °K
S/C Noise Power Density	-170.9	dbm/Hz
Up-link Carrier-to-Noise Density	67.2	db-Hz

S/C-to-DCP Link 1.7 GHz

S/C Transmitter Power	43.0	dbm
S/C Antenna Gain	12.0	db
Free Space Loss	-189.4	db
Ground Receiver Antenna Gain	3.0	db
Modulation Loss	<u>- 3.0</u>	db
Received Carrier Power	-134.4	dbm
Ground Receiver Noise Temperature	27.8	db- °K
Boltzmann's Constant	<u>-198.6</u>	dbm/Hz- °K
Ground Receiver Noise Power Density	-170.8	dbm/Hz
Down-link Carrier-to-Noise Density	36.4	db-Hz
Overall Carrier-to-Noise Density	36.4	db-Hz
Bandwidth	20.0	db-Hz
Overall Carrier-to-Noise Ratio	16.4	db
Required Carrier-to-Noise Ratio	9.5	db
System Margin	6.9	db

Table A-6

All S-Band Link

DCP-to-S/C Link 2.0 GHz

Ground Transmitter Power	40.0	dbm
Ground Antenna Gain	3.0	db
Free Space Loss	-191.0	db
Spacecraft Antenna Gain	11.5	db
Margin	<u>- 3.0</u>	db
Received Carrier Power at S/C	-139.5	dbm
S/C Receiver Noise Temperature	27.7	db-°K
Boltzmann's Constant	<u>-198.6</u>	dbm/Hz-°K
S/C Noise Power Density	-170.9	dbm/Hz-°K
Up-link Carrier-to-Noise Density	31.4	db-Hz

S/C-to-CDA Link 1.7 GHz

S/C Transmitter Power	43.0	dbm
Loss due to limiter suppression	- 5.5	db
Power disparity between interrogation and reporting signals	- 35.8	db
Radiated Power for each DCP	- 1.7	dbm
S/C Antenna Gain	13.5	db
Free Space Loss	-189.1	db
Ground Receiver Antenna Gain	<u>44.1</u>	db
Received Carrier Power	-129.8	dbm
Ground Receiver Noise Temperature	20.0	db-°K
Boltzmann's Constant	<u>-198.6</u>	dbm/Hz-°K
Ground Receiver Noise Power Density	-178.6	dbm/Hz
Down-link Carrier-to-Noise Density	48.8	db-Hz
Overall Carrier-to-Noise Density	31.3	db-Hz
Bandwidth	20.0	db-Hz
Overall Carrier-to-Noise Ratio	11.3	db
Required Carrier-to-Noise Ratio	9.5	db
System Margin	1.8	db

Table A-7

S-Band/UHF Cross-Strapped System

CDA-to-S/C Link 2.0 GHz

Ground Transmitter Power	30.0	dbm
Ground Antenna Gain	45.5	db
Free Space Loss	-190.7	db
Spacecraft Antenna Gain	14.5	db
Margin	<u>- 3.0</u>	db
Received Carrier Power at S/C	-103.7	dbm
S/C Receiver Noise Temperature	27.7	db-°K
Boltzmann's Constant	<u>-198.6</u>	dbm/Hz-°K
S/C Noise Power Density	-170.9	dbm/Hz
Up-link Carrier-to-Noise Density	67.2	db-Hz

S/C-to-DCP Link 418 MHz

S/C Transmitter Power	40.0	dbm
S/C Antenna Gain	10.5	db
Free Space Loss	-177.3	db
Ground Receiver Antenna Gain	3.0	db
Modulation Loss	<u>- 3.0</u>	db
Received Carrier Power	-126.8	dbm
Ground Receiver Noise Temperature	25.8	db-°K
Boltzmann's Constant	<u>-198.6</u>	dbm/Hz-°K
Ground Receiver Noise Power Density	-172.8	dbm/Hz
Down-link Carrier-to-Noise Density	46.0	db-Hz
Overall Carrier-to-Noise Density	46.0	db-Hz
Bandwidth	20.0	db-Hz
Overall Carrier-to-Noise Ratio	26.0	db
Required Carrier-to-Noise Ratio	9.5	db
System Margin	16.5	db

Table A-8

S-Band/UHF Cross-Strapped System

DCP-to-S/C Link 402 MHz

Ground Transmitter Power	40.0	dbm
Ground Antenna Gain	3.0	db
Free Space Loss	-177.0	db
Spacecraft Antenna Gain	10.5	db
Margin	<u>- 3.0</u>	db
Received Carrier Power at S/C	-126.5	dbm
S/C Receiver Noise Temperature	28.4	db-°K
Boltzmann's Constant	<u>-198.6</u>	dbm/Hz-°K
S/C Noise Power Density	-170.2	dbm/Hz-°K
Up-link Carrier-to-Noise Density	43.7	db-Hz

S/C-to-CDA Link 1.7 GHz

S/C Transmitter Power	40.0	dbm
Loss due to limiter suppression (maximum)	- 4.1	db
Power disparity (maximum)	- 3.0	db
Radiated Power for each DCP	32.9	dbm
S/C Antenna Gain	13.5	db
Free Space Loss	-189.1	db
Ground Receiver Antenna Gain	<u>44.1</u>	db
Received Carrier Power	- 98.6	dbm
Ground Receiver Noise Temperature	20.0	db-°K
Boltzmann's Constant	<u>-198.6</u>	dbm/Hz-°K
Ground Receiver Noise Power Density	-178.6	dbm/Hz
Down-link Carrier-to-Noise Density	80.0	db-Hz
Overall Carrier-to-Noise Density	43.7	db-Hz
Bandwidth	20.0	db-Hz
Overall Carrier-to-Noise Ratio	23.7	db
Required Carrier-to-Noise Ratio	9.5	db
System Margin	14.2	db

Table A-9

S-Band/VHF Cross-Strapped System

CDA-to-S/C Link 2.0 GHz

Ground Transmitter Power	30.0	dbm
Ground Antenna Gain	45.5	db
Free Space Loss	-190.7	db
Spacecraft Antenna Gain	14.5	db
Margin	- 3.0	db
Received Carrier Power at S/C	-103.7	dbm
S/C Receiver Noise Temperature	27.7	db-°K
Boltzmann's Constant	-198.6	db/Hz-°K
S/C Noise Power Density	-170.9	dbm/Hz
Up-link Carrier-to-Noise Density	67.2	db-Hz

S/C-to-DCP Link 137 MHz

S/C Transmitter Power	40.0	dbm
S/C Antenna Gain	10.5	db
Free Space Loss	-167.6	db
Ground Receiver Antenna Gain	3.0	db
Modulation Loss	- 3.0	db
Received Carrier Power	-117.1	dbm
Ground Receiver Noise Temperature	27.0	db-°K
Boltzmann's Constant	-198.6	dbm/Hz-°K
Ground Receiver Noise Power Density	-171.6	dbm/Hz
Down-link Carrier-to-Noise Density	54.5	db-Hz
Overall Carrier-to-Noise Density	54.3	db-Hz
Bandwidth	20.0	db-Hz
Overall Carrier-to-Noise Ratio	34.3	db
Required Carrier-to-Noise Ratio	9.5	db
System Margin	24.8	db

Table A-10

S-Band/VHF Cross-Strapped System

DCP-to-S/C Link 149 MHz

Ground Transmitter Power	40.0	dbm
Ground Antenna Gain	3.0	db
Free Space Loss	-168.3	db
Spacecraft Antenna Gain	10.5	db
Margin	- 3.0	db
Received Carrier Power at S/C	-117.8	dbm
S/C Receiver Noise Temperature	31.0	db-°K
Boltzmann's Constant	-198.6	dbm/Hz-°K
S/C Noise Power Density	-167.6	dbm/Hz-°K
Up-link Carrier-to-Noise Density	49.8	db-Hz

S/C-to-CDA Link 1.7 GHz

S/C Transmitter Power	40.0	dbm
Loss Due to Limiter Suppression (maximum)	- 4.1	db
Power Disparity (maximum)	- 3.0	db
Radiated Power for each DCP	32.9	dbm
S/C Antenna Gain	13.5	db
Free Space Loss	-189.1	db
Ground Receiver Antenna Gain	44.1	db
Received Carrier Power	- 90.5	dbm
Ground Receiver Noise Temperature	20.0	db-°K
Boltzmann's Constant	-198.6	dbm/Hz-°K
Ground Receiver Noise Power Density	-178.6	dbm/Hz
Down-link Carrier-to-Noise Density	88.1	db-Hz
Overall Carrier-to-Noise Density	49.8	db-Hz
Bandwidth	20.0	db-Hz
Overall Carrier-to-Noise Ratio	29.8	db
Required Carrier-to-Noise Ratio	9.5	db
System Margin	20.3	db

APPENDIX B

CONTRIBUTION OF THE EARTH TO DCP ANTENNA NOISE

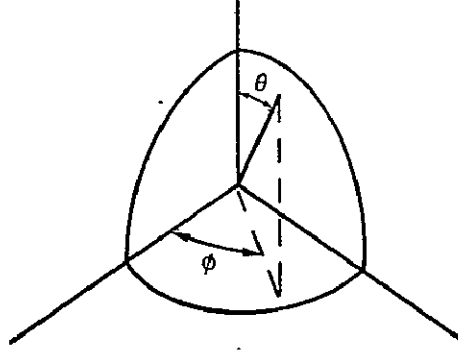


Figure B-1 Antenna Coordinate System

It is assumed that the DCP antenna is nominally hemispherical in coverage with a gain of 2. It is also assumed that the earth is seen by the antenna up to an elevation of 45° , $\pi/4 \leq \theta \leq \pi/2$. This takes into account the possibility of the DCP site being located in a valley or on a pitching bouy and should be a conservative estimate of the worse case.

Skolink* gives an expression for the antenna temperature as:

$$T_a = \frac{\iint T_s(\theta, \phi) G(\theta, \phi) \sin \theta \, d\theta d\phi}{\iint G(\theta, \phi) \sin \theta \, d\theta d\phi}$$

where $T_s(\theta, \phi)$ is the antenna noise temperature as a function of θ and ϕ shown below and $G(\theta, \phi)$ is the relative gain as a function of θ and ϕ .

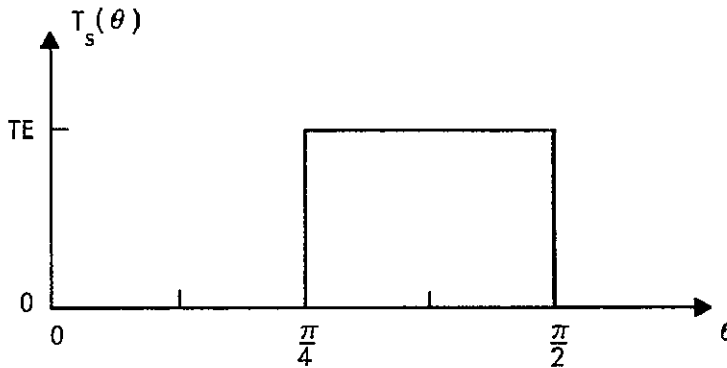


Figure B-2 $T_s(\theta, \phi) = T_s(\theta)$ vs. θ

*M. I. Skolink, Introduction to Radar Systems McGraw Hill 1962, P. 372

Thus,

$$T_a = \frac{\int_0^{2\pi} d\phi \int_{\pi/4}^{\pi/2} 2T_E \sin \theta d\theta}{\int_0^{2\pi} d\phi \int_0^{\pi/2} 2 \sin \theta d\theta} = \frac{1}{\sqrt{2}} T_E$$

for $T_E = 290^\circ \text{ K}$ = temperature of earth
 $T_a = 205^\circ \text{ K}$

APPENDIX C

SMS FIELD INTENSITY CALCULATIONS

It will be necessary to determine the ground power density at the sub-satellite point due to the S-band transmission from the SMS.

Now power density may be calculated from:

$$P \text{ (power density)} = \frac{\text{EIRP (of S/C)}}{4\pi R^2} \quad (1)$$

where R is the range to the S/C.

$$\begin{aligned} \text{Therefore, for } R &= 22.3 \times 10^3 \text{ s. miles} \\ P &= (\text{EIRP} - 162.1) \text{ dbw/meter}^2 \end{aligned} \quad (2)$$

For the case of the SMS - 1.7 GHz, 20 watt downlink transmitter with an 18 db antenna gain and 1.5 db feed losses, the S/C maximum EIRP will be +29.5 dbw (+59.5 dbm) and P (maximum) will be -132.6 dbw/meter². This full S/C EIRP will be transmitted to the ground for the 25 MHz wideband radiometer link to the CDA station, the 3 MHz stretched data transmission link to DUS's, the narrowband (less than 4 kHz) interrogation link to DCP's, and the 26 kHz WEFAX link to APT stations. The respective field intensities for these downlinks are given in the following table:

	(dbw/meter ² /4kHz)
25MHz radiometer data downlink	-170.6
3MHz stretched data downlink	-161.2
Interrogation link	-132.6
WEFAX link	-140.8

The ITU has established a restriction on field intensity, in shared bands, of -152 dbw/meter²/4kHz. However, this restriction does not apply in the 1690 - 1700 MHz band since this band is allocated solely for meteorological use.

Therefore, as long as the interrogation and WEFAX links are placed in the above band, there will be no contravention of the ITU requirements.